Mechanistic studies of cholesterol lipotoxicity pertinent to NASH

by

Lay Theng Gan
MBBS (Hons) FRACP

A thesis submitted for the degree of Doctor of Philosophy of The Australian National University

© Copyright by Lay Theng Gan
All Rights Reserved

September 19

Preface

The research detailed in this thesis was performed at the Australian National University (ANU) Medical School Liver Research laboratory between July 2011 and January 2015 under the supervision of Professor Geoff C. Farrell.

Any collaborative research detailed herein clearly describes the candidate's contribution and appropriately credits the work of others. With the exception of published data, this research has not been submitted to any other Institution or University.

Lay Theng Gan

September 19

Abstract

Non-alcoholic fatty liver disease (NAFLD) affects ~30% of the world population with similar or higher prevalence in Australia. The pathology of NAFLD ranges from benign simple steatosis (SS) to non-alcoholic steatohepatitis (NASH), with fibrosis that can progress to cirrhosis. Understanding the pathogenesis of NASH remains a challenge. In both humans and mice, obesity, diabetes and metabolic syndrome are associated with NAFLD, but free cholesterol (FC) accumulates in livers showing NASH but not in those with SS. Such cholesterol-loaded livers are sensitised to cytokine-mediated mitochondrial injury. However, at the time this research was conducted, there was no direct evidence that linked FC lipotoxicity to hepatocyte cell death or inflammatory recruitment.

In this thesis, primary murine hepatocytes were loaded with FC by exposing them to human low-density lipoprotein (LDL), and these cells were used to characterise the mechanisms of hepatocellular injury and cell death (apoptosis and necrosis). In particular we tested the hypothesis that *c*-Jun *N*-terminal kinase (JNK) activation and mitochondrial injury are essential steps in FC hepatocellular lipotoxicity. We also examined how FC-injured hepatocytes could promote activation of Kupffer cells (KC), which is a key feature of liver inflammation in NASH.

The background to NAFLD and NASH as an important public health problem, and as a liver disease is introduced in Chapter 1. Concepts about NASH pathogenesis are discussed in light of available knowledge up to the start of this PhD in 2011. The common research materials and methods are discussed in Chapter 2.

In Chapter 3, the novel *in vitro* model of FC-loaded primary murine hepatocytes is described. Briefly, primary murine hepatocytes (C57B6/J wild type [WT]) were incubated with LDL (0–40 μM), and shown to be loaded with FC. The subcellular sites of primary hepatocyte FC were determined by co-localising filipin fluorescence with organelle markers. The results were compared with the intracellular distribution of FC seen in atherogenic diet-fed *foz/foz* mouse livers, an *in vivo* model of NASH. In mice with NASH, FC co-localised to plasma membrane (PM), mitochondria and

endoplasmic reticulum (ER) compartments. This pattern was replicated in hepatocytes incubated with LDL to dose-dependently increase hepatocyte FC. Further, FC loading reduced PM fluidity and caused cell surface blebbing, with release of extracellular vesicles (EVs), as evident on scanning and transmission electron microscopy (EM).

In Chapter 4, the role of JNK1 in FC-mediated hepatocellular injury was explored using primary hepatocytes from WT, *Jnk1*$^{-/-}$and *Jnk2*$^{-/-}$ mice. These cells were incubated with LDL (0–40 μM), and molecular pathways of FC-mediated cell death determined by western blot and immunofluorescence. Separate experiments were performed with chemical specific JNK1 inhibitors (CC-401, CC-930 and CC-003) in WT hepatocytes. Supernatant was collected from FC-loaded WT, *Jnk1*$^{-/-}$ and *Jnk2*$^{-/-}$ hepatocyte experiments and assayed for high mobility group box 1 (HMGB1) and EVs. Supernatant or EVs from WT FC-injured primary hepatocytes were added to primary KC cultures from WT and *Tlr4*$^{-/-}$ mice. Ultrastructural changes were assessed by electron microscopy (EM), while TNF and IL-1β release into the supernatant was quantified by enzyme-linked immunosorbent assay (ELISA).

FC loading caused dose-dependent LDH leakage, apoptosis, necrosis and HMGB1 release. At 40 μM LDL, hepatocellular cell death was associated with JNK1 activation, *c*-Jun phosphorylation, mitochondrial membrane pore transition, cellular oxidative stress (increased GSSG with reciprocal decrease in GSH concentration) and ATP depletion. Administration of JNK inhibitors (CC-401, CC-930 and CC-003) ameliorated hepatocellular apoptosis and necrosis, while *Jnk1*$^{-/-}$ hepatocytes were refractory to FC-induced injury. Cyclosporine A (inhibits mitochondrial membrane permeability transition [MPT] pore opening) and caspase-3 inhibitors abrogated FC-mediated hepatocellular cell death. Importantly, there was no increase of ER stress proteins *in vitro* or *in vivo*, while inhibitors of ER stress-mediated cell death, 4-phenylbutyric acid failed to protect FC-loaded hepatocytes.

In Chapter 5, the supernatant and EVs isolated from pervious experiments were studied, in particular their ability to active KCs and proinflammatory pathways. Addition of HMGB1-enriched culture medium from FC-loaded hepatocytes activated KCs, as assessed by increased nuclear NF-κB (p65) fluorescence, release

of IL-1β and TNF-α, and ultrastructural changes. These effects were mitigated by administration of HMGB1-neutralising antibody, and were absent in *Myd88*$^{-/-}$ knockout hepatocytes. As mentioned above, deposition of FC within the PM of hepatocytes also released EVs and these were shown here to contain HMGB1. The results allowed us to conclude that FC loading of hepatocytes stimulates HMGB1 secretion and release of PM-derived EVs. In turn, HMGB1 activates KCs through a TLR4-MyD88 dependent process.

In Chapter 6 we sought to characterise EVs from both human and experimental NASH, with a particular focus on their cell-of-origin and protein composition. To achieve this, EVs were isolated from healthy human controls, NAFLD patients with simple SS, NASH but with no or mild-moderate fibrosis (F0-F2), and NAFLD with advanced fibrosis (F3-F4), as well as atherogenic diet-fed *foz/foz* mice with NASH and wildtype (WT) mice with SS. Composition of EVs harvested from the circulation was studied using a combination of western blotting and flow cytometry. EVs were found to circulate in both experimental and human NAFLD, with significantly higher levels in patients with clinical NASH and advanced fibrosis compared with healthy controls or those with SS. Furthermore, these EVs were highly enriched with HMGB1 and TLR4, in addition to CD4-, CD8-, CD36- and CD147-positive markers. A significant proportion of circulating EVs were hepatocellular in origin, as shown by their "tags" of asialoglycoprotein receptor 1 (ASGRP1) and solute carrier family 10 member 1 (SCL10A1). Chapter 7 summarises the key experimental findings from Chapters 3 to 6 in a broader context, and proposes several important directions for future research.

Collectively, the research findings presented here demonstrate that FC deposition in mitochondria and PM causes hepatocyte cell death, confirm the role of JNK1 activation as an important pathway for hepatocyte lipotoxic injury and reveal a link between HMGB1 and EVs with lipotoxicity and engagement of KC activation in a TLR4-dependent manner. It is proposed that this is a likely causal link in the transition from steatosis to NASH. Additionally, in both human and experimental NASH, distinct EV populations circulate, and this provides a potential for development of novel non-invasive diagnostic tests, as well as molecular targets.

Acknowledgements

Completion of this thesis would not have been possible without the hard work and support of many people. I would like to take this opportunity to express my sincerest gratitude to the following individuals and organisations, all of whom have contributed to this project in one way or another.

Professor Geoffery Farrell, for being my primary supervisor. Without your excellent supervision and support this PhD would not have been possible. This is in particular during my post PhD write-up time when I was hospitalised with my twins due to obstetrics complication and also when I was struggling to juggle high clinical workload and completing the PhD. I am very grateful for your patience and understanding all this time.

Professor Shivakumar Chitturi for his generous co-supervision and advice.

Professor Narci Teoh, for her valuable scientific input over the last few years.

Dr Harpreet Vohra (flow cytometry specialist, John Curtin School of Medical Research, ANU) for her expertise and guidance with the flow cytometry experiments (Chapter 6).

Fellow members of the ANU Liver Research Laboratory for their friendship and academic input into this PhD, especially Dr Deborah Heydet, Dr Sharon Pok, Teddy Dywer, Dr Evi Arfianti, Heng Jian Wong and Vanessa Barn. I would like to especially acknowledge Dr Derrick Van Rooyen, who helped me through one of the toughest times in my research career and for his ongoing friendship.

Associate professor Matthew Yeh for generously spending hours reporting the liver histopathology detailed in Chapter 6.

ANU Bioscience Research Facility Animal Services Division (Canberra) for kindly providing Wildtype (WT) and *MyD88*$^{-/-}$ mice (C57B/6J strain). Dr David Nikolic-

Paterson (Department of Nephrology, Monash Medical Centre, Clayton Victoria) for donating the *Jnk1*$^{-/-}$ and *Jnk2*$^{-/-}$ knockout mice, and Shaun Summers from Monash Medical Centre Animal Facilities (Clayton Victoria) for providing the *Tlr2*$^{-/-}$ and *Tlr4*$^{-/-}$ knockout mice.

Daryl Webb and Frank Brink, as well as the staff at the ANU Advanced Microscopy Unit, for providing advice and guidance with light, fluorescent and electron microscopy.

Brydan Bennett from Celgene (San Diego, CA) for supplying specific JNK inhibitors (CC-401, CC-930 and CC-003) used in Chapter 5.

Professor Jun Yu and Eagle Chu (Department of Medicine and Therapeutics at The Chinese University of Hong Kong) for kindly performing the Bio-Rad Bioplex ™ assays (Bio-Rad, Hercules, CA).

The Australian National Health and Medical Research Council (NHMRC) for funding this research project (grants APP418101 and APP585411) and kindly awarding me a PhD scholarship (1017886).

A very special thanks goes to my family:
My husband, Chik Chuan Foo for putting up with my multiple mood swings, the move across 2 states, my career and our beautiful daughters Alice and Clarice Foo.
My parents Teck Chuan Gan and Chai Geok Lee and brother, Dr Eng Kooi Gan for constantly believing in me and never wavering in their support of my completing this PhD.

List of tables

List of figures

Publications and presentations

PUBLICATIONS:

- **Gan, L. T., Van Rooyen, D. M., Koina, M., McCuskey, R. S., Teoh, N. C., Farrell, G. C.** (2014). Hepatocyte free cholesterol lipotoxicity results from JNK1-mediated mitochondrial injury and is HMGB1 and TLR4-dependent. *J. Hepatol.* 61(6):1376-84.
- **Van Rooyen, D. M., Gan, L., Yeh, M., Haigh, G., Ioannou, G., Teoh, N., Farrell, G. C.** (2013). Pharmacological cholesterol lowering reverses fibrotic NASH in obese, diabetic mice with metabolic syndrome. *J. Hepatol.* 59(1):144-52.
- **Farrell, GC, van Rooyen, DM, Gan, L, Chitturi, S** (2012). NASH is an inflammatory disorder: pathogenic, prognostic and therapeutic implications. *Gut Liver*. **6** : 149–171
- **Gan, L, Chitturi, S, Farrell, GC** (2011). Mechanisms and implications of age-related changes in the liver: Non-alcoholic fatty liver disease in the elderly. *Curr Geront and Geriatric Res.* **2011**: 831536

PRESENTATIONS:

- **Gan, L. T., Shadbolt, B., Wong, V., Adams, L., Dwyer, T., Chan, H., Teoh, N., Chitturi, S., Farrell, G. C.** (2014). Improved prediction of liver fibrosis and probability of NASH in patients with NAFLD by combining liver stiffness with clinicopathological and biomarker measurements. Poster presentation at *Australian Gastroenterology Week*, Surfer's Paradise, Goldcoast, Qld.
- **Gan, L. T., Van Rooyen, D. M., Cooper, M., Robertson, A., Teoh, N., Farrell, G. C..** What causes Kupffer Cell activation in NAFLD? HMGB1, TLR4, Crystals and NLRP3 inflammsomes link free cholesterol pro-inflamamtory pathways in NASH. Poster presentation at *Australian Gastroenterology Week*, Surfer's Paradise, Goldcoast, Qld.
- **Gan, L. T., Van Rooyen, D. M., Cooper, M., Robertson, A., Teoh, N. C., Farrell, G. C.** (2014). Cholesterol crystals and enriched media from lipotoxic hepatocytes interact with the NRLP3 inflammasome via TLR4 to

activate Kupffer cells: a novel, blockable pro-inflammatory pathway linking lipotoxic liver injury to the pathogenesis of NASH. Poster presentation at *Australian Gastroenterology Week*, Surfer's Paradise, Goldcoast, Qld.

- **Gan, L. T., Van Rooyen, D. M., Farrell, G. C.** (2013). Free cholesterol-induced lipotoxic injury to hepatocytes is mediated by JNK activation and mitochondrial injury. Oral presentation at *Canberra Health Annual Research Meeting (CHARM)*, Canberra, ACT.
- **Gan, L. T., Van Rooyen, D. M., Koina, M., McCuskey, R. S., Teoh, N. C., Farrell, G. C.** (2013). Free cholesterol causes hepatocyte cell death via JNK-mediated mitochondrial injury, and triggers release of hepatocyte-derived extracellular vesicles to activate Kupffer cells in the pathogenesis of NASH. *Australian Gastroenterology Week*, Surfer's Paradise, Goldcoast, Qld.
- **Gan, L. T., Van Rooyen, D. M., Koina, M., McCuskey, R. S., Teoh, N. C., Farrell, G. C.** (2013). A lipotoxic mechanism of NASH: Free cholesterol causes hepatocyte apoptosis and necrosis by JNK-mediated mitochondrial injury, and resultant release of hepatocyte-derived HMGB1 and extracellular vesicles activate Kupffer cells. Oral presentation at *Australian Liver Association (ALA)*, Broadbeach, Goldcoast, Qld.
- **Gan, L. T., Van Rooyen, D. M., Heydet, D., Barn, V., Farrell, G. C.** (2012). Free cholesterol (FC) loading causes both apoptosis and necrosis in murine primary hepatocytes, while FC lipotoxicity predisposes hepatocytes to free-fatty acid-mediated cellular injury. Poster presentation at *Australian Gastroenterology Week*, Adelaide, SA.
- **Gan, L. T., Van Rooyen, D. M., Heydet, D., Barn, V., Farrell, G. C.** (2012). Cholesterol-loading in murine primary hepatocytes activates JNK and increases cellular apoptosis and necrosis. Poster presentation at *Australian Gastroenterology Week*, Adelaide, SA.
- **Gan, L. T., Ajamieh, H., Heydet, D., Dwyer, T., Evers, M., Cribb, J., Teoh, N., Chitturi, S., Farrell, G. C.** (2012). Use of non-invasive biomarkers to assess disease severity in non-alcoholic fatty liver disease

(NAFLD). Oral presentation at *Canberra Health Annual Research Meeting (CHARM)*, Canberra, ACT.

List of abbreviations

ΔΨmt	mitochondrial membrane potential
ΔpH	electrochemical concentration gradient
ABCA1	ATP-binding cassette, sub-family A, member 1
ABCG5	ATP-binding cassette, sub-family G, member 5
ABCG8	ATP-binding cassette, sub-family G, member 8
ACAT	acyl-CoA:cholesterol acyltransferase
AIM2	absent in melanoma 2 inflammasome
ALT	alanine aminotransferase
ANOVA	analysis of variance
AP-1	activator protein-1
ASC	apoptosis-associated speck-like protein
ASGPR	asialoglycoprotein receptor
ASP	apoptosis-associated speck-like protein
Ath	atherogenic
ATP	adenosine-5'-triphosphate
BA	bile acid
BiP	binding immunoglobulin protein
BMI	body mass index
BSA	bovine serum albumin
Bsep	bile salt exporter protein
CARD	caspase-recruitment domain
CD	cluster of differentiation
cDNA	complementary DNA
CE	cholesterol esters
CM	chylomicron
COX-IV	cytochrome C oxidase-IV
CR	chylomicron remnant
CTPI	carnitine palmitoyltransferase I
Cyp	cytochrome P450
Cyp27a1	sterol 27-hydroxylase
Cyp7a1	sterol 7α-hydroxylase

Cyp7b1	oxysterol 7α-hydroxylase
Cyp8b1	sterol 12α-hydroxylase
CytC	cytochrome *c*
Da	Dalton, $1.660\ 54 \times 10^{-24}$ gram
DAG	diacylglycerol
DAMP	damage-associated molecular pattern
DEPC	diethylpyrocarbonate
DIC	decarboxylate carrier
dNTP	deoxynucleotide
EGF	epidermal growth factor
ELISA	enzyme linked immunosorbent assay
EM	electron microscopy
EMMPRIN	extracellular matrix metalloproteinase inducer
ER	endoplasmic reticulum
ETC	electron transport chain
EV	extracellular vesicle
F4/80	a 160 kDa glycoprotein expressed by murine macrophages
FC	free cholesterol
FCT	forward cholesterol transport
Foz/*foz*	Fat-Aussie (*ALMS1* mutant) mice
FXR	farnesoid-X receptor
g	gravitational acceleration (measured in factors of 9.80665 m/s^2)
GSH	glutathione
GSSG	glutathione disulfide
h	hours
HA	hyaluronic acid
HBA1c	glycated hemoglobin, marker for 3 month plasma glucose level
HBSS	Hank's buffered salt solution
HCC	hepatocellular carcinoma
HDL	high-density lipoprotein
HF	high-fat

HMGB1	high-mobility-group-box-1 protein
HMGR	3-hydroxy-3-methylglutaryl-CoA reductase
HNF	hepatocyte nuclear factor
HOMA	homeostasis model assessment
HPLC	high-performance liquid chromatography
Ig	immunoglobulin
IκB	inhibitor of nuclear factor-kappa B
IKK	IκB kinase
IL	interleukin
IRS	insulin receptor substrate
IVC	inferior vena cava
JNK	*c*-Jun *N*-terminal kinase
LDH	lactate dehydrogenase
LDL	low-density lipoprotein
LDLR	low-density lipoprotein receptor
LE	late endosome
LOX1	lectin-like oxidised low-density lipoprotein receptor-1
LPC	lysophosphatidylcholines
LPS	lipopolysaccharide
LRH1	liver receptor homolog-1
LRR	leucine-rich repeat
LXR	liver-X receptor
Ly	lysosome
M30	caspase cleaved cytokeratin CK-18 fragment antigen, apoptosis marker
M65	both cleaved and uncleaved CK-18, necrosis and apoptosis marker
MAMPs	microbial-associated molecular patterns
MAP	mitogen-activated protein
MAPK	mitogen-activated protein kinase
MCD	methionine choline-deficient diet
MCP-1	monocyte chemoattractant protein-1
MDP	muramyl dipeptide
MEKK	MAPK kinase kinase

min	minutes
miR	microRNA
mL	millilitre
MLN64	metastatic lymph node 64 protein
MMP	matrix metalloproteinase
mRNA	messenger ribonucleic acid
MS	metabolic syndrome
MTT	methyl tetrazolium
MyD88	myeloid differentiation primary response gene 8
NACHT	neuronal apoptosis inhibitor protein, MHC class 2 transcription activator, incompatibility locus protein from *Podospora anserina* and telomerase-associated protein
NADPH	nicotinamide adenine dinucleotide phosphate
NAFLD	non-alcoholic fatty liver disease
NASH	non-alcoholic steatohepatitis
NEMO	NF-κB essential modifier
NF-κB	nuclear factor-kappa B
NPC	Niemann Pick disease Type C
NPC1L1	Niemann Pick C1-like-1 protein
NRF	nuclear factor erythroid 2-related factor
NRLP3	NOD-like receptor inflammasome 3
NS	non-significant (P>0.05)
OGC	2-oxoglutarate carrier
ORP	OSBP-related proteins
OSBP	oxysterol-binding protein
P2X7	P2X purinoceptor 7
PA	palmitic acid
PAMP	pathogen-associated molecular pattern
PAT	perilipin, adipose differentiation-related protein tail-interacting protein of 47 kDa proteins
PCR	polymerase chain reaction
PE	phosphatidylethanolamine
PFP	platelet free plasma

PI	propidium iodide
PL	phospholipid
PM	plasma membrane
PPAR	peroxisome proliferator-activated receptor
PRP	platelet rich plasma
PRR	pattern recognition receptor protein
PuFA	polyunsaturated fatty acid
PUMA	p53 upregulated modulator of apoptosis
PV	portal vein
PYD	pyrin domain
qPCR	quantitative real-time PCR
RCT	reverse cholesterol transport
RHD	Rel-homology domain
RIPA	radio immunoprecipitation assay buffer
RISC	RNA-inducing silencing complexes
ROS	reactive oxygen species
RT	room temperature
RT-PCR	reverse transcription-PCR
SCL10A1	solute carrier family 10 member 1
SD	standard deviation
SEM	standard error of the mean
sFFA	saturated free fatty acid
siRNA	small interfering ribonucleic acid
SNP	single nucleotide polymorphism
SR-B1	scavenger receptor-B1
SREBP	sterol regulatory element binding protein
SS	simple steatosis
SSD	sterol-sensing domain
StAR	steroidogenic acute regulatory protein
T2D	type 2 diabetes
TAK	transforming growth factor-β activated kinase
TBE	trypan blue exclusion
TBP	TATA box-binding protein
TG	triglyceride

Th	helper T-cell
TIR	toll-interleukin-1 receptor
TLR	toll-like-receptor
TNF	tumour necrosis factor
TNFR	tumour necrosis factor receptor
UQ	ubiquinone
VCAM-1	vascular cell adhesion protein 1
WEM	William’s E media
WB	western blot
WT	wild-type

Table of contents

CHAPTER 1

Introduction

1.1 Overview of non-alcoholic fatty liver disease (NAFLD)

In 1986 Schaffner and Thaler introduced the term "non-alcoholic fatty liver disease (NAFLD)" (1986), for the spectrum of liver pathology associated with steatosis when it occurred in men or women without other cause (viral, toxic, known genetic metabolic disease), in persons consuming non-toxic levels of alcohol. The "barrier" definition for alcohol intake per day was taken as <20 grams for men and <10 grams for woman (McCullough 2004, Farrell *et al.* 2007). NAFLD is now the most prevalent liver disease worldwide. It affects 15-45% of the population in modern (westernised) societies, including Australia, and is closely related to over-nutrition, sedentary lifestyle and the obesity and type 2 diabetes (T2D) pandemics (Gan *et al.* 2011). The term NAFLD includes a wide spectrum of pathology, ranging from: simple steatosis (SS; fat accumulation within hepatocytes, in which total hepatic triglyceride [TG] content exceeds 5% of total liver weight), but without accompanying hepatitis or steatonecrosis, to non-alcoholic steatohepatitis (NASH), a more severe form of NAFLD defined below, to cirrhosis (Angulo 2002, World Gastroenterology Organisation Global Guidelines 2012).

The term NASH was actually six years prior to the term NAFLD, by Jurgen Ludwig and colleagues in 1980 working at the Mayo Clinic. They noted 20 cases of steatohepatitis in non-alcoholic patients (most obese tea-totallers with diabetes) between 1970 and 1980 (Ludwig *et al.* 1980). Others had noticed similar cases in Japan and the United States, particularly in obese woman with diabetes, but the existence of a "non-alcoholic" form of steatohepatitis was controversial until Ludwig's article. Driven by the increasing global prevalence of obesity (Figure 1.2A,B), NAFLD is commonplace today and is the most common cause of abnormal liver function (Sattar *et al.* 2014). Not only does NAFLD affect more affluent, nutritionally abundant countries like America, Europe and Australia, but is now very common in the Asia-Pacific region (Fan and

Farrell, 2009, Williams *et al.*, 2011, Younossi *et al.*, 2011, Armstrong *et al.*, 2012) (See Figure 1.2C) and South America.

Table 1.1 Association between body mass index (BMI) and prevalence of NAFLD.

Body mass index	Classification	NAFLD prevalence
<24.9	Normal	~25%
25-29.9	Overweight	67%
>30	Obese	94%

Data adapted from the Italian Dionysos study (Bedogni *et al.* 2007).

Approximately 25% of patients with NAFLD have NASH (Ong *et al.* 2005, Lam and Younossi 2010, Williams *et al.* 2011). The pathology characterised by steatosis, hepatocellular injury and cell death, lobular inflammation, Mallory hyaline (aggregated cytoskeleton [cytokeratins] proteins) and progressive peri-sinusoidal fibrosis (type I collagen deposition) (Brunt 2002). Left untreated, 10-20% of NASH patients develop progressive fibrosis and cirrhosis, at a rate of approximately 9-20% over a 5-10 year period (Figure 1.1). NASH and cirrhosis predispose patients to hepatocellular carcinoma (HCC), with neoplastic transformation occurring at a cumulative rate ranging between 2.4-12.8% per year in cirrhotic patients (White *et al.* 2012, Cholankeril *et al.* 2017). Given its high prevalence and prolonged natural history, NASH has become the leading indication for liver transplantation recently (Wong *et al.* 2014).

In addition to its importance as a liver disease, NASH is associated with increased risk of death from cardiovascular diseases (coronary heart disease, cerebrovascular disease) and common cancers (reviewed by Farrell and Larter [2006], Gan *et al.* [2011], Farrell [2014]). Several of the likely pathogenic involved are discussed below.

1.2 Pathogenic mechanisms of NASH

In 1998 Day and James proposed a "two-hit" hypothesis of NASH pathogenesis (Day and James 1998). In this first "model" for the disease, they ascribed steatosis to be the first "hit", with steatosis predisposing the liver to a second, injurious insult (cytokines or oxidative stress, for example) triggering hepatocellular damage, inflammation and possible development of fibrosis. Many now view this model as an over-simplification

of NASH pathogenesis. For example, NASH is associated with more profound metabolic disorder (prediabetes, arterial hypertension, metabolic syndrome) than SS which is better explained by a metabolic pathogenesis of NASH. Others have noted a multitude of other pathogenic steps, not just two (Tilg and Moschen 2010, Peverill *et al.* 2014).

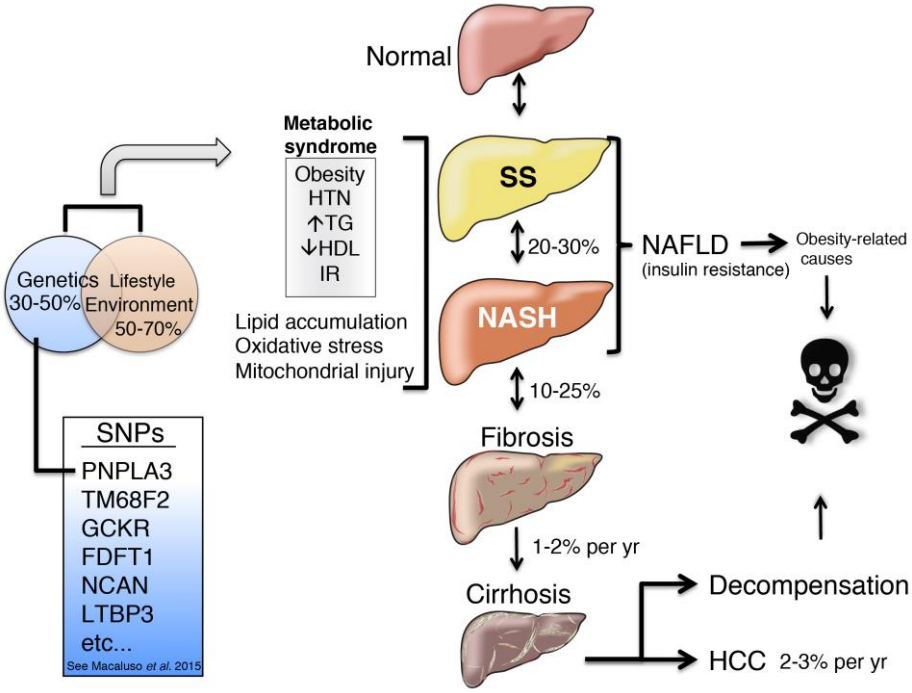

Figure 1.1 Natural history of NAFLD.

Genetic (30-50%) and environmental/lifestyle factors (50-70%) contribute to the prevalence of NAFLD Macaluso *et al.* (2015). Several single nucleotide polymorphisms (SNPs) predispose to NAFLD, including PNPLA3, TM68F2, among others. SNPs associated with NAFLD have been extensively reviewed by Macaluso *et al.* (2015). NAFLD is the hepatic manifestation of metabolic syndrome and covers a continuum of pathology from simple steatosis (SS) to non-alcoholic steatohepatitis (NASH) and cirrhosis. Image adapted from Macaluso *et al.* (2015).

Abbreviations: CVD, cardiovascular disease, HCC, hepatocellular carcinoma; HDL, high-density lipoprotein; HTN, hypertension; IR, insulin-resistance; NAFLD, non-alcoholic fatty liver disease; NASH, non-alcoholic steatohepatitis; PNPLA3, Patatin-like phospholipase domain-containing protein 3; SNP, single nucleotide polymorphism; SS, simple steatosis; TG, triglyceride.

As a result the model has evolved to a "multiple parallel hits" hypothesis that implicates several concurrent insults (see Table 1.2 for summary of several mechanisms of liver injury implicated in NASH pathogenesis). These include mitochondrial dysfunction, oxidative stress, and adipose dysfunction to name a few. The progression of NAFLD pathways from SS to NASH likely involves a complex interaction between environmental and genetic factors (Figure 1.3) (reviewed by Farrell and Larter, 2006,

Cusi, 2012, Farrell *et al.*, 2012). The primary focus of this thesis is the mechanisms of NAFLD progression, with specific focus on the role of cholesterol.

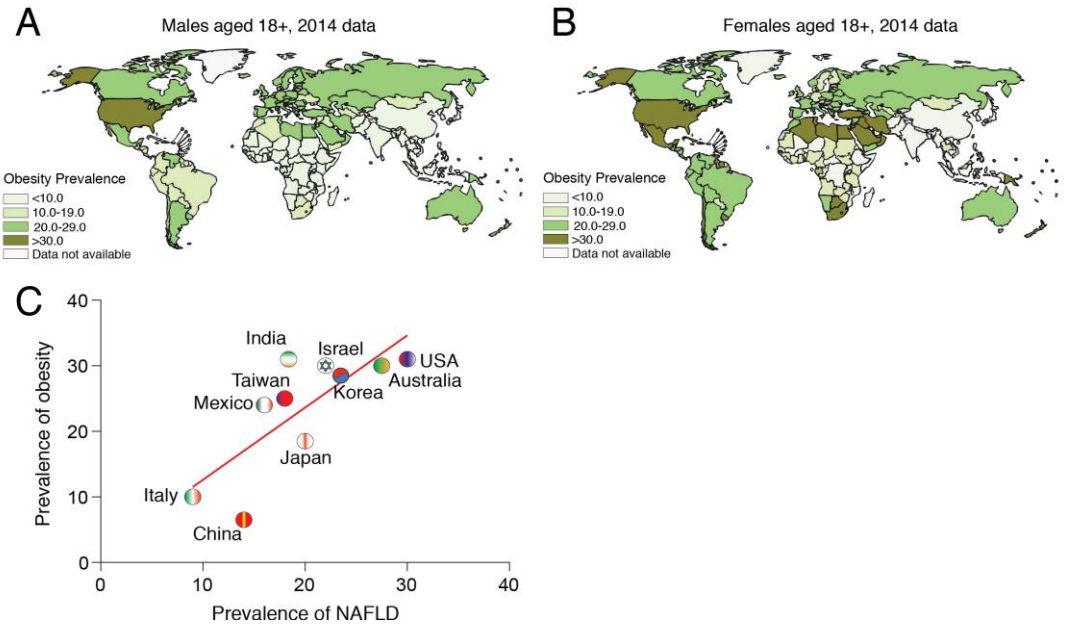

Figure 1.2 Global prevalence of obesity and relationship to NAFLD prevalence.

Standardised population estimates for global prevalence of obesity (BMI>30.0 kg/m2) for (**A**) males and (**B**) females older than 18 years of age sex based on 2014 World Health Organisation (WHO) data (World Health Organization 2015). (**C**) The relationship between obesity and NAFLD prevalence from several countries, including Australia. The linear regression for this correlation is represented by the red curve (R^2 = 0.592). Panels A and B, were adapted from World Health Organisation Global Health Data Repository (World Health Organization 2015). Panel C was adapted from Loomba and Sanyal (2013) to included Australian obesity and NAFLD data from Australian Bureau of Statistics (2015) and Farrell *et al.* (2012).

1.3 Lipotoxicity

The term *lipotoxicity* was first proposed by Roger Unger to describe the mechanism by which accumulated free fatty acids (FFA) cause pancreatic beta-cell destruction in the pathogenesis of T2D (Lee *et al.* 1994, Unger 1995). This term describes cellular injury and death (often with resultant inflammation), caused by saturated FFA (sFFA) and their metabolites, including diacylglycerol (DAG), ceramide and TG (Unger and Zhou 2001). In NASH, the accumulation of toxic lipid molecules has been proposed as a direct cause of hepatocellular damage and recruitment of inflammation (Neuschwander-Tetri, 2010), and in 2012 Ken Cusi coined the term 'liver lipotoxicity' for NASH. Evidence for the lipotoxic role of FFA, TG and cholesterol and other lipid molecules is now described.

Table 1.2 Models of NAFLD progression and mechanisms of hepatocellular injury implicated in the pathogenesis of NASH.

Model	Primary factor	Secondary factor	References
"Two hit" hypothesis	Steatosis (metabolic, obesity, diabetes etc…)	Injury – oxidative stress, cytokines	Day and James 1998
Metabolic injury hypothesis	Insulin resistance	Hyperinsulinaemia	Chitturi *et al.* 2002, Malaguarnera *et al.* 2009, Montesi et al. 2013, Yu *et al.* 2013
	Mitochondrial dysfunction	Reduced ATP synthesis	Cortez-Pinto *et al.* 1999, Kojima *et al.* 2007
		Reduced GSH pool	Mari *et al.* 2006, Mari *et al.* 2008
	Oxidative stress		Sakaida and Okita 2005, Kojima *et al.* 2007, Neuschwander-Tetri 2010, Sumida *et al.* 2013
	Lipotoxicity	Free fatty acids (Saturated)	Malhi *et al.* 2006, Neuschwander-Tetri 2010, Leamy *et al.* 2013
		Free cholesterol	Mari *et al.* 2006, Puri *et al.* 2007, Mari *et al.* 2008, Caballero *et al.* 2009, Van Rooyen and Farrell 2011, Van Rooyen et al. 2011, Van Rooyen *et al.* 2013
		Oxidised cholesterol (oxysterols)	Subramanian *et al.* 2011, Walenbergh *et al.* 2013
		Lysophosphatidylcholine	Han *et al.* 2008
		Diacylglycerides	Puri *et al.* 2007, Gorden *et al.* 2011
		Ceramides	Pagadala *et al.* 2012, Garcia-Ruiz *et al.* 2015, Kasumov *et al.* 2015
	ER stress	Unfolded protein response (unlikely involved; (Leclercq *et al.* 2011)	Dara *et al.* 2011, Malhi and Kaufman 2011, Lake *et al.* 2014, Zhang *et al.* 2014
	Adipose dysfunction	Altered adipokine expression (hypoadiponectin, etc…)	Baranova and Younossi 2007, Tsochatzis *et al.* 2008, Tsochatzis *et al.* 2009, Wolfs *et al.* 2015
	Hypoxia and reduced hepatic blood flow, sleep apnoea		Byrne 2010, El-Azeem I and Saraya 2012, Nath and Szabo 2012, Suzuki *et al.* 2014

It should be noted that this list of potential mechanisms of liver injury in NASH is not exhaustive.
Abbreviations: ATP, adenosine triphosphate; ER, endoplasmic reticulum; GSH, glutathione.

1.3.1 TGs and FFAs

FFAs are composed of a carboxylic acid and long-chain hydrocarbon side group. Table 1.3 lists some common mammalian saturated and unsaturated FFA. Saturated FFAs have no double bonds, whereas unsaturated FFAs contain two or, in the case of polyunsaturated FFAs more than two. The extent of desaturation determines the physical characteristics of the FFA (flexibility, melting temperature, packing space). FFA with 14-20 carbon atoms are the most common in animals (Voet and Voet 2004). Importantly, FFAs rarely exist in the "free" (unesterified) state in the body; they are usually esterified to other lipid molecules, such as DAGs and TGs, cholesterol esters, glycerophospholipids, and sphingolipids (Voet and Voet 2004). Increased blood and tissue FFAs levels are associated with several diseases, including: insulin-resistance, diabetes, NAFLD (Browning and Horton 2004, Meshkani and Adeli 2009, Zhang *et al.* 2014).

TGs are the most abundant esterified lipid species in animals (Mahley 2002). They are composed of three fatty acid chains esterified to a glycerol backbone (Haagsman and Van Golde 1984, Voet and Voet 2004). Along with DAG and/or other esterifed sterols (oxysterols, cholesterol esters), TG aggregate within the cell cytoplasm to form lipid droplets that are coated with a monolayer of proteins, collectively termed PAT proteins (perilipin, adipose differentiation-related protein [ADRP] tail-interacting protein of 47 kDa proteins) (Murphy 2001, Bickel *et al.* 2009). Lipid droplets are found in all cells but are most common within adipocytes, a cell tasked with TG storage or mobilisation in times of need (Angel and Sheldon 1965, Angel 1970, Angel and Farkas 1970, Farkas *et al.* 1973). They are also abundant in liver, particularly in fatty liver disorders.

Deposition of TG in non-adipose tissues, such as the liver, tends to occur in situations of lipid excess and with metabolic dysregulation, as in T2D and metabolic syndrome (Kawano and Cohen 2013). In skeletal myocytes, TG deposition induces insulin-resistance through fatty acyl-CoA, DAG, or ceramide intermediates. These molecules are capable of activating serine/threonine kinases that, in turn, phosphorylate insulin receptor substrate (IRS) proteins to cause impaired receptor signalling (Kwak 2013) thereby causing physiologic insulin resistance, a fundamental mechanism in the development of metabolic syndrome and NASH.

Within the liver, large TG deposits were originally thought to be the primary lipid species responsible for NAFLD progression to NASH (Boustiere and Gauthier 1985, Marchesini *et al.* 2001). This "TG-centric" hypothesis was supported by the strong correlation between NAFLD severity and level of TG formation (steatosis) (Ogawa *et al.* 2013). However, the view that *TGs contribute to NAFLD progression* has been challenged by several studies demonstrating the safety of this lipid species within hepatocytes (Liao *et al.* 2003, Flowers *et al.* 2006, Monetti *et al.* 2007, Li *et al.* 2009). In fact, it has been proposed that TG accumulation may actually be a protective mechanism that counters lipotoxicity (Flowers *et al.* 2006, Li *et al.* 2009, Neuschwander-Tetri 2010, Peverill *et al.* 2014). Accordingly, focus has now shifted to sFFAs, their metabolites (ceramide, DAG, lipophosphatidylcholine [LPC]) and free cholesterol (Neuschwander-Tetri, 2010)(Arteel 2012). The potential role of FFAs in NAFLD has been extensively reviewed by others (Feldstein *et al.* 2004, Malhi *et al.* 2006, Alkhouri *et al.* 2009) and the evidence summarised in Table 1.3. Further discussion is beyond the scope of this thesis.

Table 1.3 Saturated and unsaturated FFAs that are comon in man.

Common name	IUPAC Name	Formula	Double bond number	Double bond position	Lipotoxicity to hepatocytes	Refs
Capric	Decanoic	$C_9H_{19}COOH$	0	N/A	Protective – decreases steatosis in hepatocytes	Wang *et al.* 2017
Lauric	Dodecanoic	$C_{11}H_{23}COOH$	0	N/A	Protective – decreases steatosis in hepatocytes	Wang *et al.* 2017
Myristic	Tetradecanoic	$C_{13}H_{27}COOH$	0	N/A	Increases palmitic acid; induces hepatocyte apoptosis	Martinez *et al.* 2015
Palmitic	Hexadecanoic	$C_{15}H_{31}COOH$	0	N/A	Lipotoxic; TNF-α, IL-6, -8 release; apoptosis; mitochondrial dysfunction	Feldstein *et al.* 2004, Malhi *et al.* 2006, Chavez-Tapia *et al.* 2012
Stearic	Octadecanoic	$C_{17}H_{35}COOH$	0	N/A	Apoptosis; mitochondrial dysfunction; JNK activation	Malhi *et al.* 2007; Zhang 2011
Palmitoleic	*cis*-9-hexadecenoic	$C_{15}H_{29}COOH$	1	9	Protects against palmitic acid-induced cell death	Listenberger *et al.* 2003
Oleic	*cis*-9-octadecnoic	$C_{17}H_{33}COOH$	1	9	Lipotoxic; TNF-α, IL-6, -8 release; lipid peroxidation; increased caspase-9 dependent apoptosis	Feldstein *et al.* 2004, Cui *et al.* 2010, Chavez-Tapia *et al.* 2012
Linoleic	All *cis*-9,12-octadecadienoic	$C_{17}H_{33}COOH$	2	9, 12	Protects against palmitic acid-induced cell death; reduces ER stress	Zhang *et al.* 2011
α-Linolenic	All *cis*-9,12,15-octadecatrienoic	$C_{17}H_{31}COOH$	3	9, 12, 15	Protects against stearic acid-induced ER stress	Zhang *et al.* 2011
Arachidonic	All *cis*-5,8,11,14-octadecatrienoic	$C_{19}H_{31}COOH$	4	5, 8, 11, 14	Protects against palmitic acid-induced cell death	Cheon *et al.* 2014
Eicosapentaenoic acid	All *cis*-5,8,11,14,17-icosapentaenoic acid	$C_{19}H_{29}COOH$	5	5,8,11,14,17	Protects against palmitic acid-induced cell death	Sakamoto *et al.* 2017
Docosahexaenoic acid	All-*cis*-docosa-4,7,10,13,16,19-hexa-enoic acid	$C_{21}H_{31}COOH$	6	4,7,10,13,16,19	Protects against palmitic acid-induced cell death	

Abbreviations: FFA, free fatty acids

1.3.2 Cholesterol as a mediator of liver injury

Cholesterol is an essential sterol required for various cellular processes including: steroidogenesis, management of normal cellular membrane function and fluidity, electrical insulation of nerve fibres, bile salt and vitamin D synthesis, and bile-

associated fat and fat-soluble vitamin absorption (Miller and Bose 2011, Yu *et al.* 2014). Within the body, cholesterol exists in two predominant forms, free cholesterol (FC) and cholesterol esters (CEs) (see Figure 1.6A, B).

Studies investigating the tissue distribution of tissue lipid species in NAFLD are limited due to the ethical and logistic constraints of acquiring liver samples from patients and healthy individuals. Nonetheless, Puri *et al.* (2007) performed a small (*n*=9 per group) lipidomic analysis of liver samples from control, NAFL (a term they prefer to simple steatosis), and NASH patients. Several differences were observed between the disease phenotypes. Levels of DAGs and TGs were significantly increased in livers showing NAFL and NASH compared with control livers. These increases in all patients with NAFLD were accompanied by significant reductions in both free- and esterified polyunsaturated FFAs. On the other hand, there was a striking stepwise increase in FC between groups, the lowest levels being in controls, intermediate levels in NAFL and the highest in NASH livers (Puri *et al.* 2007).

Two years later, a Spanish research group, Caballero and colleagues (2009), expanded on this research by staining NAFLD and health livers for FC using filipin, a highly fluorescent macrolide antibiotic with high binding affinity for FC. The authors simultaneously investigated the transcriptional expression of several cholesterol regulatory genes in the liver samples, including the transcription factor sterol-regulating element binding protein (SREBP)-2 expression (Caballero *et al.* 2009). SREBP2 was significantly elevated in diseased livers. SREBP2 regulates both hepatic cholesterol uptake via LDL receptor (LDLR), a PM-bound receptor responsible for LDL uptake, and FC biosynthesis through the transcriptional induction of HMG-CoA reductase (HMGR) (Edwards *et al.* 2000, Osborne 2000, Miserez *et al.* 2002). SREBP2 also regulates pathways of FC disposition, such as biotransformation into bile acids (BS), thereby reducing hepatic FC levels (Edwards *et al.* 2000). These data combined with more recent human data (Min *et al.* 2012) and experimental (murine) NASH studies (Xu *et al.* 2010, Van Rooyen *et al.* 2011, Chan *et al.* 2012, Van Rooyen *et al.* 2013) implicate FC in NASH pathogenesis.

In vitro experiments in primary hepatocytes by Van Rooyen *et al.* (2011) showed that SREBP2 is responsive to insulin stimulation. Thus the hyperinsulinaemia observed in

patients with IR (secondary to excess caloric intake with subsequent adipose inflammation) may account for increased hepatic SREBP2 expression in NASH (Caballero *et al.* 2009, Van Rooyen and Farrell 2011) (see Figure 1.3).

Ioannou *et al.* (2013) have demonstrated the presence of birefringent cholesterol crystals (stained using filipin) in the livers of humans and mice with NASH. Diseased livers produced unique "Crown-like" structures, which reflect pro-inflammatory Kupffer cell (KC; resident liver macrophages) scavenging of necrotic parenchymal cells (Itoh *et al.* 2013). Similar crown-like structures have been observed in chronically inflamed fatty white adipose tissue (WAT) of humans and mice (Cinti *et al.* 2005). Whether in liver or WAT, crown-like structures are comprised of classically activated (M1) macrophages characterised by cluster of differentiation 11c (CD11c) (Cinti *et al.* 2005, Itoh *et al.* 2013). Further details about different macrophage subpopulations (M1 classical *versus* M2 alternative) are described in Chapter 5.

Mari and colleagues (2006) identified mitochondrial dysfunction as a potential mechanism of FC-induced liver injury. In this study, hepatic cholesterol loading was achieved using dietary strategies and was shown to cause mitochondrial loading with FC. Such FC-loaded primary hepatocytes were sensitised to cytokine-mediated cell death (Mari *et al.* 2006). Caballero and colleagues (2009), observed that the increase in hepatocyte FC levels in NASH were associated with a 7-15-fold increase in steroidogenic acute regulatory protein (StAR) mRNA expression. StAR is a mitochondrial protein responsible for transport of FC into the mitochondria, where it is required for steroidogenesis (Estabrook and Rainey 1996, Jefcoate 2002, English 2010, Miller and Bose 2011, Korytowski *et al.* 2013). Together, these data are consistent with the proposal that FC lipotoxicity may cause mitochondrial dysfunction in NASH, and that FC may play a crucial role in progression from SS to NASH.

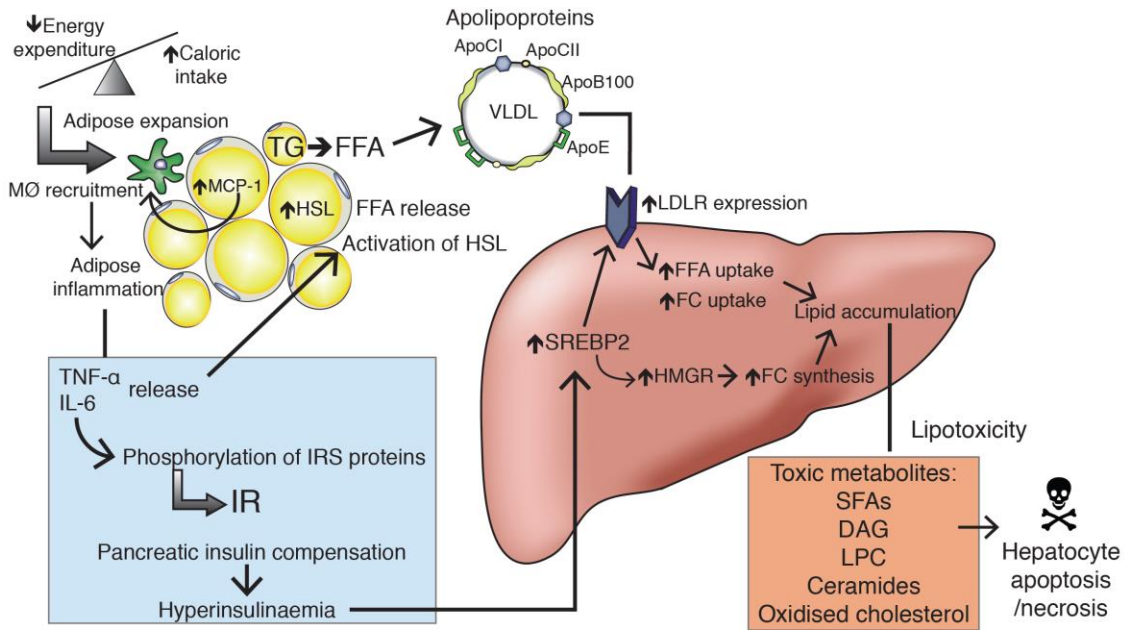

Figure 1.3 Relationship between adipose inflammation, insulin resistance and hepatic lipid accumulation in NASH.

The combination of reduced energy expenditure and increased caloric intake results in adipose tissue expansion and development of adipocyte cell injury and monocyte chemoattractant protein (MCP)-1 release. Macrophages are recruited to inflamed adipose tissue and secrete a number of cytokines, including TNF-α. Cytokine secretion, inflammation and concomitant sympathetic stimulation (as a result of obesity-associated hyperleptinaemia) up-regulates hormone sensitive lipase (HSL), in turn liberating free fatty acids (FFA) from TG stores. FFAs are transported within the intravascular compartment by very low-density lipoproteins (VLDL). Inflammatory cytokines are also capable of phosphorylating insulin receptor substrate (IRS) proteins to cause insulin-resistance (IR); this leads to pancreatic compensation and resistant hyperinsulinaemia. High levels of circulating insulin and glucose promote the expression of sterol-responsive element binding protein-2 (SREBP2) and downstream HMG-CoA reductase (HMGR; the rate-limiting step in cholesterol biosynthesis and target of statin drugs) activity and LDL receptor (LDLR) expression. These factors cause increased hepatic free cholesterol (FC) biosynthesis and uptake. Similarly, increased VLDL uptake, via LDLR, causes accumulation of FFAs and toxic metabolic products including saturated FFAs (SFAs), diacylglycerides (DAG), lysophosphatidylcholine (LPC), ceramides, and oxidised cholesterol products. All these molecules could contribute to hepatocellular injury.

1.4 Mitochondrial involvement in NASH

Mitochondria are small (0.5 – 10 μm) cellular organelles tasked with generating adenosine triphosphate (ATP) from carbohydrate, lipid, and protein precursors. Structurally, mitochondria have three distinct compartments, an outer and inner membrane and an intermembrane space. The inner mitochondrial membrane partitions the mitochondrial matrix and contains mitochondrial DNA, ribosomes and various

proteins tasked with cellular respiration. The integrity of these membranes is critical to the formation of a mitochondrial membrane potential ($\Delta\Psi mt$), which generates a proton gradient, as described below.

Glycolysis and the citric acid cycle (also known as the Krebs or tricarboxylic acid cycle) have been extensively described. They will not be discussed here, except to mention the generation of reduced NADH and $FADH_2$ as electron carriers. These molecules are utilised by the electron transport chain (ETC), specifically complexed I (NADPH dehydrogenase) and II (succinate dehydrogenase), to generate a hydrogen proton (H^+) gradient across the inner mitochondrial membrane, and to transfer two electrons to ubiquinone (UQ; also known as coenzyme Q10). UQ is a lipid soluble electron chaperone. It transfers the received electrons to water-soluble cytochrome *c* (CytC) via complex III (cytochrome bc1) (Figure 1.4A). In the process, two H^+ are actively pumped from the mitochondrial matrix into the intermembrane space against a electrochemical concentration gradient (ΔpH).

The fourth complex involves cytochrome *c* oxidase, an enzyme complex, which transfers electrons from CytC, in turn, reducing diatomic oxygen to form H_2O while pumping additional H^+ into the intermembrane space. The high concentration of H^+ serves as the driving force for ATP synthase (complex V). Thus, as H^+ ions pass through complex V, adenosine diphosphate is phosphorylated to the higher energy form of ATP (Figure 1.4A).

Experimental and human studies of NASH livers have revealed multiple mitochondrial changes in hepatocytes, as has been extensively reviewed by Pessayre and Fromenty (2005). The salient points will be discussed here.

As determined by counting mitochondrial number in liver sections, as well as by quantifying hepatic mitochondrial DNA content, the number of mitochondria in human NASH livers is significantly decreased. The remaining mitochondria become rounded and swollen (megamitochondria) and have a reduced number of cristae. Linear "para-crystalline" inclusions are also observed within mitochondria of hepatocytes from NASH patients but are not found with SS (Caldwell *et al.* 1999, Sanyal *et al.* 2001) (Figure 1.4B). These ultra-structural changes are accompanied by respiratory chain

dysfunction (Caldwell *et al.* 1999) and increased mitochondrial membrane permeability (Koek *et al.* 2011, Gan *et al.* 2014). The latter results in cytochrome *c* leakage from the mitochondria, and causes decoupling of ETC complexes III and IV (Figure 1.4B). Hepatic steatosis stimulates mitochondrial β-oxidation, which in turn increases NADH and $FADH_2$ levels, thereby increasing the pool of mitochondrial electrons and the generation of reactive oxygen species (ROS) (Figure 1.4Bi).

ROS identified in mammalian systems include singlet oxygen, superoxide, hydrogen peroxide and hydroxy ions. These reactive molecules can further damage the mitochondria by promoting lipid peroxidation of polyunsatured fatty acids (PuFA), protein oxidation and mitochondrial DNA damage. ROS are also able to leak into the adjacent cytoplasm, inflicting similar oxidative damage to cellular lipids, proteins and DNA. This results in expression of pro-inflammatory markers such as tumor necrosis factor (TNF)-α, tumour growth factor (TGF)-β, interleukin (IL)-8, and Fas ligand (FasL) (Figure 1.4Bii).

In addition to electron transport chain dysfunction, hepatic expression of ATP synthase is significantly reduced in NASH patients. Collectively, all these changes result in a reduced in ATP output. Hepatic ATP levels also inversely correlate with serum TNF-α, BMI and IR values in patients with NASH (Perez-Carreras *et al.* 2003).

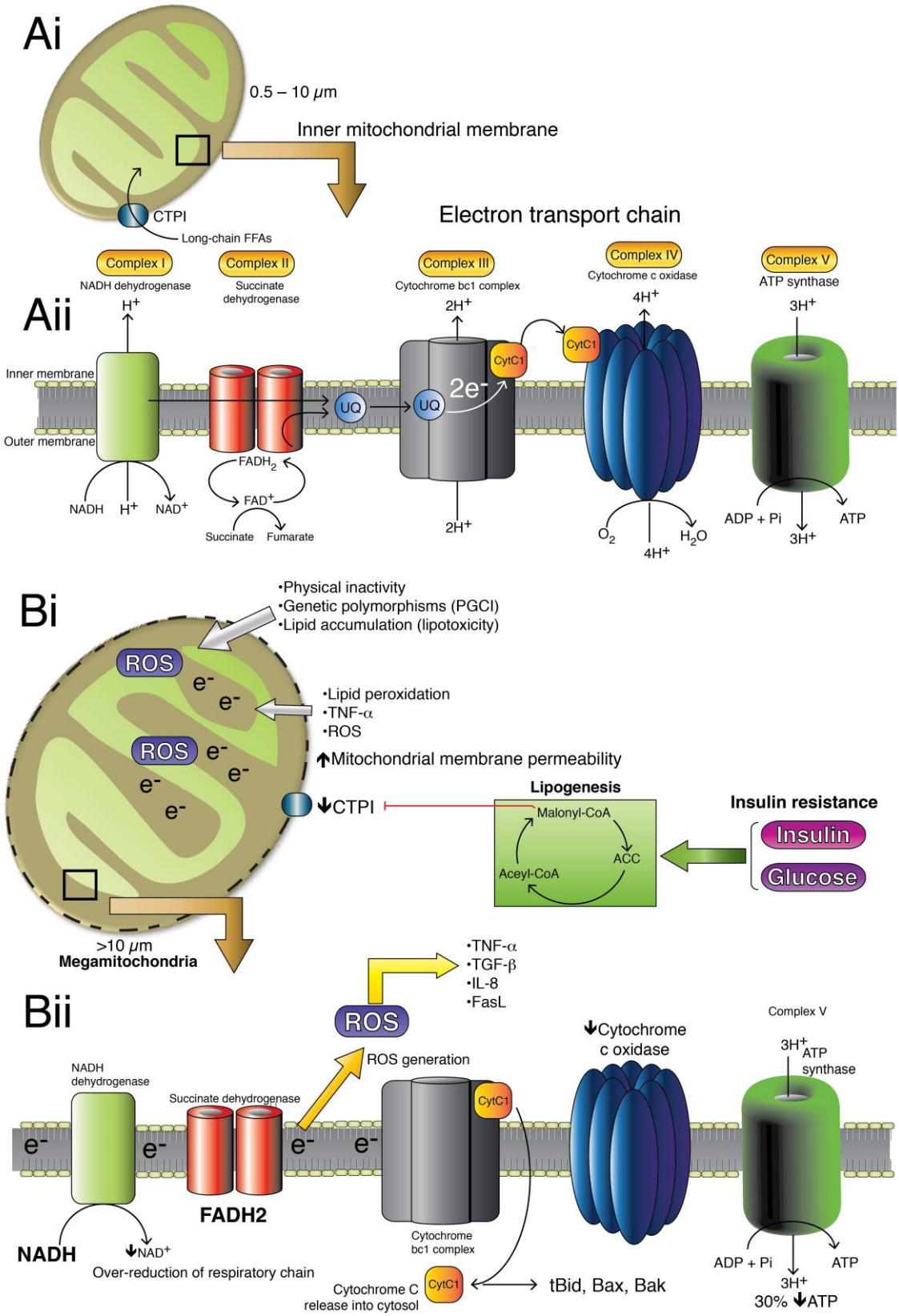

Figure 1.4 Schematic of mitochondrial electron transport chain function and pattern of dysfunction observed in NASH.

Legend for Figure 1.4 (**Ai**) Electron transport chain (ETC) is the terminal phase of aerobic respiration and involves five protein complexes within the inner mitochondrial membrane. (**Aii**) Complex I (NADH dehydrogenase) couples NADH oxidation to transmembrane pumping of a hydrogen proton (H^+). Complex II (succinate dehydrogenase) generates electrons (e^-), which are chaperoned by ubiquinone (UQ) to complex III (cytochrome bc1) and transferred to cytochrome *c* (CytC). CytC then transfers the electrons to complex IV (cytochrome *c* oxidase) where they react with diatomic oxygen molecule to form water. H^+ ions within the inter-mitochondrial membrane space flow through complex V (ATP synthase), phosphorylating ADP to ATP. (**Bi**) In NAFLD, physical inactivity, genetic polymorphisms (including peroxisome proliferator-activated receptor gamma coactivator-1 [PGCI]) and lipotoxicity culminate in mitochondrial dysfunction. (**Bii**) Insulin resistance causes hyperglycaemia and hyperinsulinaemia, which drive hepatic lipogenesis and formation of malonyl-CoA, which inhibits mitochondrial carnitine palmitoyltransferase I (CTPI), resulting in reduced long-chain FFA trafficking into the mitochondria. Excess caloric intake and insulin resistance leads to generation of excess NADH and $FADH_{2,}$ which accumulate within the inner mitochondrial membrane, contributing to the reactive oxygen species (ROS) that lead to the increased mitochondrial permeability, and CytC leakage, inducing inflammatory cytokine expression (TNF-α, TGF-β, IL-8 and FasL).

Abbreviations for Figure 1.4: ACC, Acetyl-CoA carboxylase; ADP, adenosine diphosphate; ATP, adenosine triphosphate; e^-, free electron; $FADH_2$, reduced flavin adenine dinucleotide; NAD^+, oxidised nicotinamide adenine dinucleotide; NADH, reduced nicotinamide adenine dinucleotide; ROS, reactive oxygen species; UQ, ubiquinone.

1.4.1 Glutathione antioxidant pathway

Reduced glutathione (GSH) is a powerful antioxidant and the most abundant intracellular thiol molecule in mammals (Persson *et al.* 2002, Circu and Yee Aw 2008). It is synthesised exclusively in the cytosol from three precursor amino acids, namely: cysteine, glycine and glutamate (Gushima *et al.* 1983, Beutler and Gelbart 1986, Ribas *et al.* 2014) (the synthesis of GSH is described in Figure 1.5A). Cysteine provides the oxidisable thiol (R-SH) moiety. Following synthesis, GSH distributes to various cellular organelles, including the mitochondria. There are two mitochondrial surface transporters, 2-oxoglutarate carrier (OGC) and dicarboxylate carrier (DIC) (Figure 1.5B) (the concentration of which in the mitochondrial matrix is equivalent to the cytoplasmic concentration (Chen and Lash 1998, Ribas *et al.* 2014).

Within the mitochondrial GSH functions as a protective agent against:

1. **ROS** generated during ETC (see above, Section 1.4, Figure 1.4)
2. **Lipid peroxidation**, and
3. **Electrophiles**, which included electrophilic FFAs (Schopfer *et al.* 2011).

In the presence of ROS or other strong electrophiles, GSH is converted to glutathione disulphide (GSSG), a step catalysed by GSH peroxidase (Jocelyn 1970, Sies and Summer 1975). Two GSH molecules are consumed to form one GSSG molecule. Reduced glutathione is recovered by glutathione reductase, which uses nicotinamide adenine dinucleotide phosphate (NADPH) as the reducing agent in this reaction. Oxidised NADP is then recycled back to NADPH via glucose-6-phosphate dehydrogenase (G6PD) (Mareni and Gaetani 1976, Cheng *et al.* 1983, Watanabe and Nagashima 1983) (see Figure 1.5C).

1.5 Cholesterol regulation and homeostasis

The various pathways of cholesterol homeostasis have been extensively reviewed elsewhere (Charlton-Menys and Durrington 2008, Van Rooyen 2012, van der Wulp *et al.* 2013). Since the majority of this thesis focus on the lipotoxic role of cholesterol in hepatocytes, the major mechanisms of cholesterol homeostasis and the intracellular trafficking of FC will be briefly mentioned here.

1.5.1 Dietary absorption, intravascular transport and hepatic homeostasis

Cholesterol homeostasis within the body is intricately regulated at all stages of absorption, biosynthesis, biotransformation to bile salts, as well as excretion (Ikonen 2008, Moore *et al.* 2010). Excess cholesterol is associated with cardiometabolic disorders (atherosclerosis), T2D, metabolic syndrome and Alzheimer's disease (Ledesma and Dotti 2005, Huang 2009, Rottiers and Näär 2012). Conversely, insufficient cholesterol uptake, *de novo* biosynthesis and/or impaired trafficking has been linked to neurodegenerative disorders (Peake and Vance 2012).

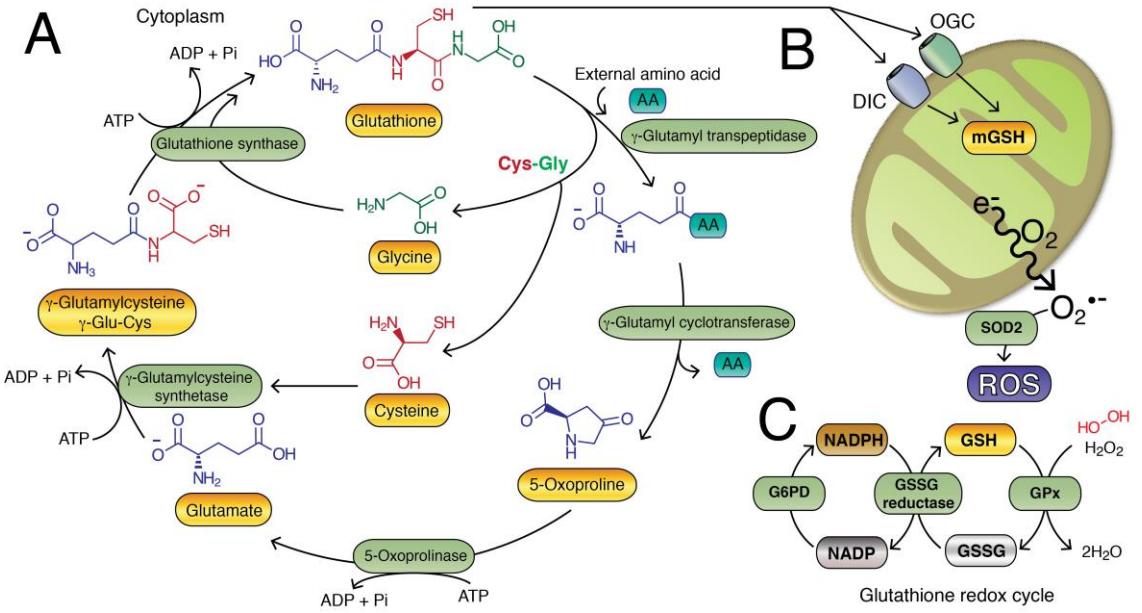

Figure 1.5 Glutathione synthesis, mitochondrial trafficking and role as a mitochondrial antioxidant.

(**A**) Glutathione (GSH) is synthesised from glycine, cysteine and glutamate amino acid precursors in a series steps involving five enzymes. In the first rate limiting step, cysteine and glutamate are conjugated, catalysed by γ-glutamylcysteine synthetase to form γ-glutamylcysteine (γ-Glu-Cys). Glutathione synthase then bonds glycine to γ-Glu-Cys, forming GSH. These enzymatic steps are ATP-dependent. (**B**) Cytoplasmic GSH is transported across the mitochondrial membrane by two transporters, 2-oxoglutarate carrier (OGC) and dicarboxylate carrier (DIC). Mitochondrial GSH (mGSH) is an anti-oxidant protecting the cell from reactive oxygen species (ROS) generated during cellular respiration. Superoxide ($O_2^{\bullet-}$) ions, generated in the electron transport chain, are acted upon by superoxide dismutase (SOD)-2, forming hydrogen peroxide (H_2O_2), another ROS. (**C**) ROS are converted to biologically safe water by GSH peroxidase, which oxidises GSH to glutathione disulfide (GSSG). Two molecules of GSH are recovered from one GSSG molecule by glutathione reductase, with NADPH oxidised to NADP in the process. In turn, NADP is reduced to NADPH via glucose-6-phosphate dehydrogenase (G6PD).

Abbreviations: AA, amino acid; ADP, adenonsine diphosphate; ATP, adenosine triphosphate.

The major portion of bodily cholesterol (~70%) is derived from *de novo* biosynthesis and reclamation from bile. Biosynthesis occurs within several tissues, including the liver and steroidogenic tissues (adrenals and gonads). In this process, the entire 27-carbon structure of cholesterol is enzymatically constructed from simple acetyl-CoA precursor molecules, in a three-stage process (Berg *et al.* 2002, Voet and Voet 2004). Dietary cholesterol, however, contributes 30% to the total body cholesterol pool (Hylemon *et al.* 2001). The FC in food is absorbed directly by Niemann Pick-C1-like-1 transporters expressed on enterocytes of the proximal jejunum (Garcia-Calvo *et al.*

2005, Xie *et al.* 2012). On the other hand, dietary CEs can either undergo hydrolysis to FC (by pancreatic lipases and cholesterol ester hydrolase [CEH]) or be absorbed directly by cluster of differentiation-36 (CD36) and scavenger receptor-B1 (Hauser *et al.* 1998, Schulthess *et al.* 2000, Cai *et al.* 2004, Nassir *et al.* 2007). Importantly, CD36 is also important for FFA absorption (Goldberg *et al.* 2009, Pepino *et al.* 2014).

Once inside the enterocyte, FC is esterified to CEs by ER-bound acyl-CoA:cholesterol acyltransferase (ACAT)-1 or -2 and stored along with TG as a lipid droplet vesicle (Nguyen *et al.* 2012) (Figure 1.7C and Figure 1.8). Since CEs, as well as TG, are hydrophobic, they require packaging with Apo to form water-soluble lipoprotein complexes prior to intravascular transport. Enterocytes synthesize ApoB-48, C-I, C-III and E, which all combine in the ER and golgi apparatus to form chylomicron (CM) micelles (Cartwright *et al.* 2000, Hesse *et al.* 2013). CMs contain phospholipids, a small amount of surface FC and a central core of neutral lipids (CEs and TGs) (Ockner *et al.* 1969, Björkegren *et al.* 1998). Nascent CMs are then secreted into villus lacteals and transported through the lymphatic system, entering the systemic venous circulation via the thoracic duct (Ockner *et al.* 1969).

As CM complexes flow through the intravascular space, lipoprotein lipases (LPL) present on the luminal surface of capillary endothelial cells hydrolyse CM TGs to release FFAs (Nakajima *et al.* 2011). These FFA are rapidly taken up by cells via CD36 (also known as scavenger receptor B; see Table 1.4). CD36 is expressed on the surface of multiple cell types, including: adipocytes, skeletal myocytes and hepatocytes (Masuda *et al.* 2009). Absorbed FFA can then be stored intracellularly in the form of esterified lipid (TG or CE) or transported into mitochondria via carnitine palmitoyltransferase I (CTPI) (see Figure 1.5) for β-oxidation (Goldberg *et al.* 2009, Pepino *et al.* 2014).

TG-depleted CMs are referred to as chylomicron remnants (CRs) (Nordestgaard and Tybjærg-Hansen 1992) (Figures 1.6 and 1.7). These particles are endocytosed by hepatocytes via LDL receptor (LDLR), a surface receptor responsible for the recognition of ApoB-48 on CMs/CRs and ApoB-100 proteins found on VLDL, IDL, and LDL particles. CRs bind to LDLR and are cleared from the circulation through

receptor-mediated endocytosis (Figure 1.8). Endocytosed LDL-cholesterol is then distributed intracellularly.

1.5.2 Intracellular cholesterol trafficking – from LDL to organelles

The exact mechanisms of intracellular cholesterol trafficking have been subject to conjecture. However, studies in Niemann Pick disease Type C (NPC), a rare and fatal autosomal recessive disorder characterised by progressive neurological deterioration have provided a working model (Roff *et al.* 1992, Ikonen 2006). This has been summarised by Yu *et al.* (2014), and is briefly described here.

The pathognomonic features of NPC are cholesterol depletion of myelin sheaths and progressive neuronal dysfunction (Infante *et al.* 2008). The clinical manifestions include psychosis, cerebellar ataxia, dystonia, dysarthria and dysphagia, in addition to supranuclear gaze palsy (Josephs *et al.* 2003, Sévin *et al.* 2007, Walterfang *et al.* 2012). Approximately 95% of NPC cases are caused by mutations in the *NPC1* gene, while the remaining 5% of cases are attributable to *NPC2* gene mutations (Vanier 2010). These mutations result in loss-of-function of the NPC1 or NPC2 proteins and cause an accumulation of FC within the late endosome (LE) and/or lysosomal compartment(s), as well as FC depletion in other subcellular sites. The latter include the plasma membrane (PM), ER and mitochondria (Bi and Liao 2010, Rodriguez-Pascau *et al.* 2012, Tamura and Yui 2014).

NPC1 is a ~140 kDa (1278 amino acid) protein capable of binding and trafficking FC and oxysterols (Garver *et al.* 2008). Its structure includes 13 transmembrane regions, three highly conserved luminal loop regions, and a sterol-sensing domain (SSD). The latter has a shared sequence homology with other sterol-sensing proteins, that regulate cholesterol homeostasis, including HMG-CoA reductase, NPC1-like protein 1 (NPC1L1) and SREBP2 (Ioannou 2000, Scott and Ioannou 2004, Subramanian and Balch 2008). The loop 1 portion adjacent to the *N*-terminal domain contains a hydrophobic pocket capable of "capturing" the cholesterol perhydrocyclopentanophenanthrene ring. This enables insoluble cholesterol to be trafficked and negates the need for an aqueous cholesterol phase (Abi-Mosleh *et al.* 2009). Interestingly, NPC1 is found specifically in LE/lysosomes after LDLR-facilitated

uptake of LDL, and is usually absent from cholesterol-depleted LE/lysosomal vesicles (Blom *et al.* 2003, Zhang *et al.* 2003).

Unlike NPC1, NPC2 is a small 16 kDa lysosomal protein ubiquitously expressed in most lysosomes (Blom *et al.* 2003). This protein possesses two β-sheets, which arrange to form a small hydrophobic pocket and this expands in the presence of oxysterols to accommodate the cholesterol hydrocarbon motif (Xu *et al.* 2007).

Following receptor-mediated endocytosis of LDL-bound CE, the LE/early lysosome is acidified by the action of proton-ATPase pumps (Mindell 2012). The fall in pH activates lysosomal lipases, which in turn hydrolyse CE to FC. NPC2 rapidly binds lysosomal FC in a 1:1 stoichiometric ratio and chaperones it to NPC1 present on the lysosomal membrane surface (Vanier and Millat 2004) (Okamura *et al.* 1999). The NPC1-FC complex then buds off the LE/lysosome and fuses with the ER and/or PM (Yu *et al.* 2014). Alternatively, oxysterol-binding protein (OSBP) and OSBP-related proteins (ORP)-5 and -8 are capable of delivering cholesterol from LE/lysosomal NPC1 to different subcellular sites (Figure 1.8) (Du *et al.* 2011, Zhou *et al.* 2011, Du and Yang 2013, Olkkonen and Li 2013, Yu *et al.* 2014). These ORP proteins are recycled to the LE/lysosome by vacuolar protein sorting 4/ suppressor of potassium transport growth defect-1 (VPS4/SKD1) proteins (Ikonen 2006, Ikonen 2008, Du *et al.* 2011, Yu *et al.* 2014).

On average, FC makes up between 40–50% of the total PM lipid content (Ray *et al.* 1969, Lange *et al.* 1989, van Meer *et al.* 2008). In all, the PM contains approximately 60–90% of total cellular cholesterol (de Duve 1971, Lange *et al.* 1989, Liscum and Munn 1999). In contrast, FC contributes only ~5% to the total ER lipid content; collectively ER compartments contain <1% of total cellular FC (Lange and Steck 1997).

Recently, Das and colleagues (2014) have identified three distinct PM FC pools using perfringolysin O, a bacterial toxin that binds to cholesterol-rich membranes. These separate pools of PM FC are maintained by sphingomyelin sequestration after LE/lysosomal trafficking, and are important to the overall regulation of intracellular cholesterol homeostasis (Das *et al.* 2014).

Another transmembrane protein present in the LE/lysosome, metastatic lymph node 64 protein (MLN64), is responsible for trafficking of FC to the outer mitochondrial membrane (Figure 1.8) (Zhang *et al.* 2002, Rigotti *et al.* 2010). This process can occur without NPC1 involvement; however, NPC1 is required to prevent excess FC deposition in the mitochondria (Charman *et al.* 2010). As mentioned earlier (Section 1.5.2), StAR is a small 30 kDa protein present on the outer mitochondrial membrane and is tasked with moving FC across the mitochondrial membrane (Arakane *et al.* 1996, Lo *et al.* 1998, Rigotti *et al.* 2010). This "bilayer movement" of cholesterol is essential for the synthesis of steroid molecules (King *et al.* 2002).

The expression of LDLR, HMGR, NPC1, NPC1L1 and are all transcriptionally controlled by SREBP2 (Miserez *et al.* 2002, Pramfalk *et al.* 2010, Xiao and Song 2013). The sterol-response of SREBP2 and it's transcriptional role in the regulation of cholesterol homeostasis is described elsewhere (Van Rooyen *et al.* 2011). To the author's knowledge no studies have investigated the intracellular localisation and trafficking of hepatocyte FC in NAFLD (a "future direction" discussed in Chapter 7).

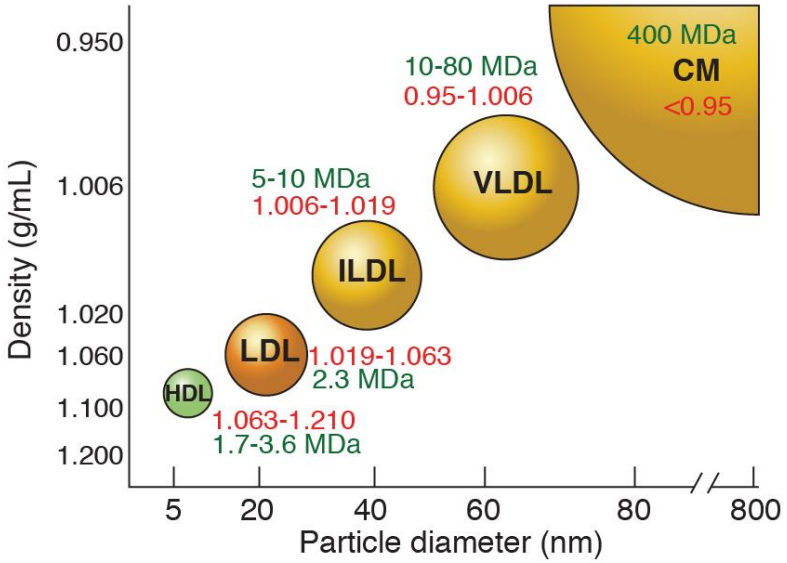

Figure 1.6 Lipoprotein size and density characteristics.

Size (protein size in mega-Daltons [MDa] is shown in green) and density (red text) characteristics for the major lipoprotein classes. Panel is adapted from published data (Voet and Voet 2004, Lieberman and Marks 2005, Suchy 2012).

1.5.3 Hepatic forward and reverse cholesterol transport: the counter-balance between LDL and HDL.

Forward cholesterol transport (FCT) involves the hepatic synthesis and secretion of VLDL particles into the systemic circulation. These particles are characterised by ApoB100, ApoC and ApoE apolipoproteins and contain high amounts of TG (56%), CEs (15%) and FC (8%) (see Figure 1.7) (Mann and Skeaff 1998, Gotto 2003). FCT allows TGs and FC to be delivered to peripheral tissues for utilization and/or storage. As with CMs, TGs are hydrolysed by capillary LPLs to FFAs (Gomez-Coronado *et al.* 1993, Jokinen *et al.* 1994). As the TG content of VLDL decreases, the particle density increases (see Figure 1.7D) and VLDL particles transition to IDLs and eventually to LDL particles. LDL has the highest FC and CE content (Figure 1.7).

Circulating LDL can accumulate within arterial intima and is atherogenic (Havel 1998, Kellner-Weibel *et al.* 1999, Kellner-Weibel *et al.* 1999, Vine *et al.* 2008). This process is accelerated by oxidant stress, which results in LDL lipid peroxidation and Schiff-base reactions to the lysine residues of ApoB100 (Figure 1.9). Unlike native, unmodified LDL, oxidised LDL is immunogenic. It may complex with IgG or IgM, in turn triggering the classical complement cascade and immunological responses. Furthermore, LDL is also susceptible to glycation and enzymatic degradation of ApoB100 (Figure 1.9). Unfortunately, modified LDL invariably involves ApoB100 damage. This prevents physiological uptake and removal of these particles by LDLR. Instead, modified LDL is recognised by the scavenger-receptor family of membrane transporters (see Table 1.4 for details).

Oxidised LDL can be taken up by SR-B1 on macrophages, resulting in formation of foam cells. FC and/or oxidised FC species accumulate within foam cells and trigger necroinflammation. While the exact mechanisms responsible for foam cell death and inflammation in atherosclerosis are ill-defined, there is increasing evidence that pattern recognition receptors (PRRs), especially toll-like receptors are activated by pathogen-associated molecular patterns (PAMPs) and danger-associated molecular patterns (DAMPs) (Angelovich *et al.* 2015). The NOD-like receptor inflammasome 3 (NLRP3) has also been implicated, particularly activated by cholesterol crystals (Section 1.6). TLR receptors and sterile inflammation pathways are detailed later in this chapter (Section 1.7.1).

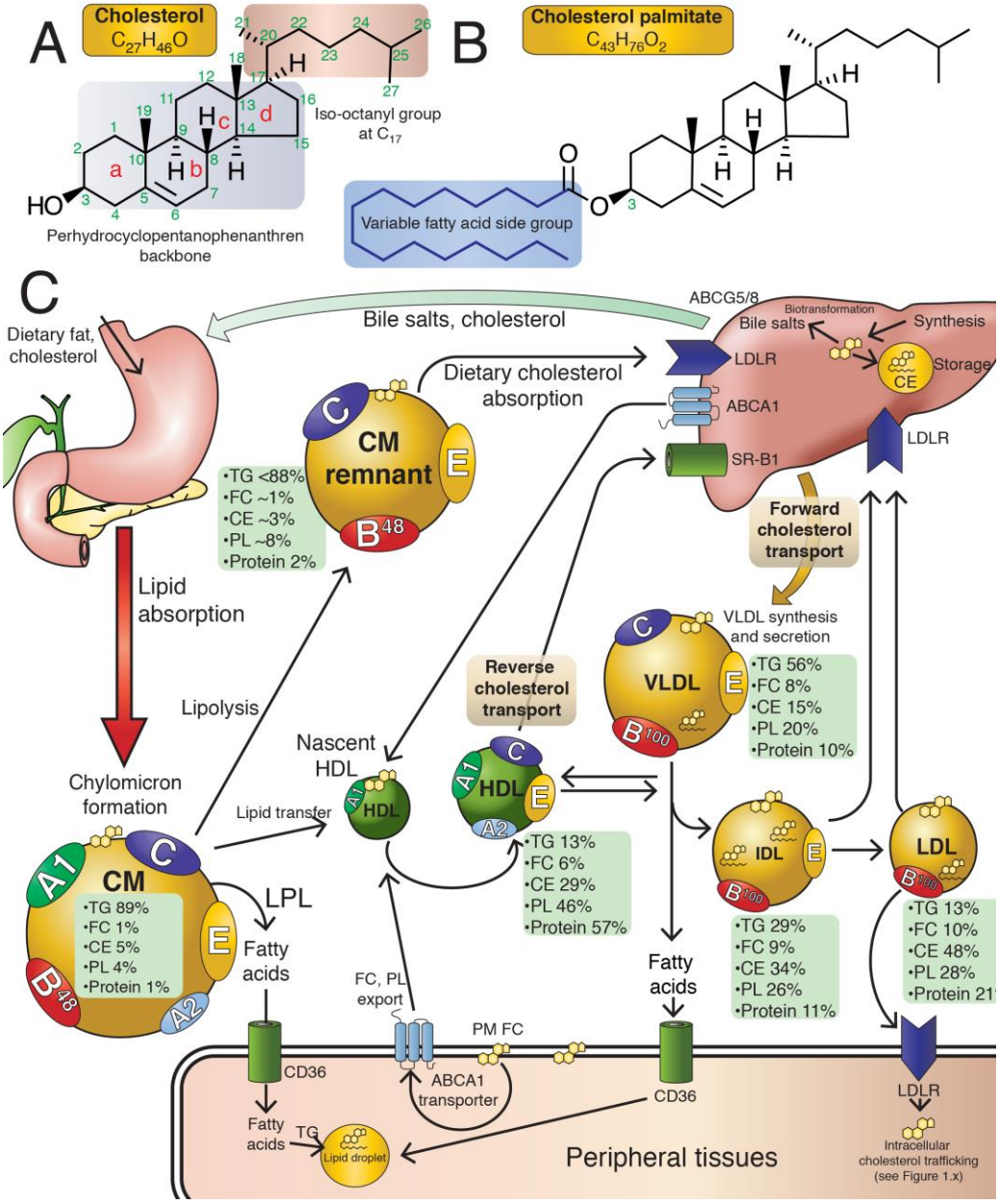

Figure 1.7 Molecular structures of free cholesterol (FC) and a cholesterol ester (CE) (cholesterol palmitate), as well as the lipoprotein transport and metabolic pathways responsible for trafficking these lipid species.

(**A**) FC is a 27-carbon molecule with a four-ring perhydrocyclopentanophenanthrene nucleus (labelled a-d in red text) and an iso-octanyl group conjugated to carbon 17. (**B**) CEs contain a variable fatty acid moiety (palmitate is used as an example here) are attached by an ester bond to the cholesterol hydroxyl group of carbon 3. (**C**) Cholesterol trafficking within various lipoproteins (see text for details). Green text boxes detail the protein and lipid composition of the various lipoprotein species. Lipoproteins A1, A2, B48, B100 and C define the different populations of lipoproteins (CMs, VLDL, IDL, LDL and HDL). Panel C is adapted from and Mann and Skeaff (1998) and Lusis *et al.* (2004).

Abbreviations for Figure 1.7: ABCA1, ATP-binding cassette protein-A1; CD, cluster of differentiation CM, chylomicron; FC, free cholesterol; LDL, low-density lipoprotein; LDLR, LDL receptor; LPL, Lipoprotein lipase; PL, phospholipid; SR-B1, scavenger receptor-B1; TG, triglyceride.

The pro-atherosclerotic nature of LDL is counteracted in the body by HDL, which participates in reverse cholesterol transport (RCT). RCT is a process controlled by ATP-binding cassette protein A1 (ABCA1), a 254 kDa membrane-bound protein that facilitates the formation of HDL (Sahoo *et al.* 2004, Zarubica *et al.* 2007). HDL are comprised of small, dense particles containing apo proteins A-I, A-II, C, and E, among others. It is capable of docking with ABCA1 via apoA-I on the surface of peripheral tissue cells (Oram 2003, Oram and Heinecke 2005). This interaction facilitates FC efflux from the cell via two independent processes. First, intracellular FC is trafficked to ABCA1 by OSBP, ORP8, and NPC1 (Figure 1.8) (Choi *et al.* 2003, Bowden and Ridgway 2008, Yan *et al.* 2008, Rodriguez-Rodriguez *et al.* 2010). Second, apoA-I acts as a lipid translocase and facilitates FC and PL translocation across the PM and into the HDL particle (Denis *et al.* 2004, Denis *et al.* 2004, Vedhachalam *et al.* 2007). It should also be noted that HDL can acquire lipids from other lipoprotein species during intravascular exchange.

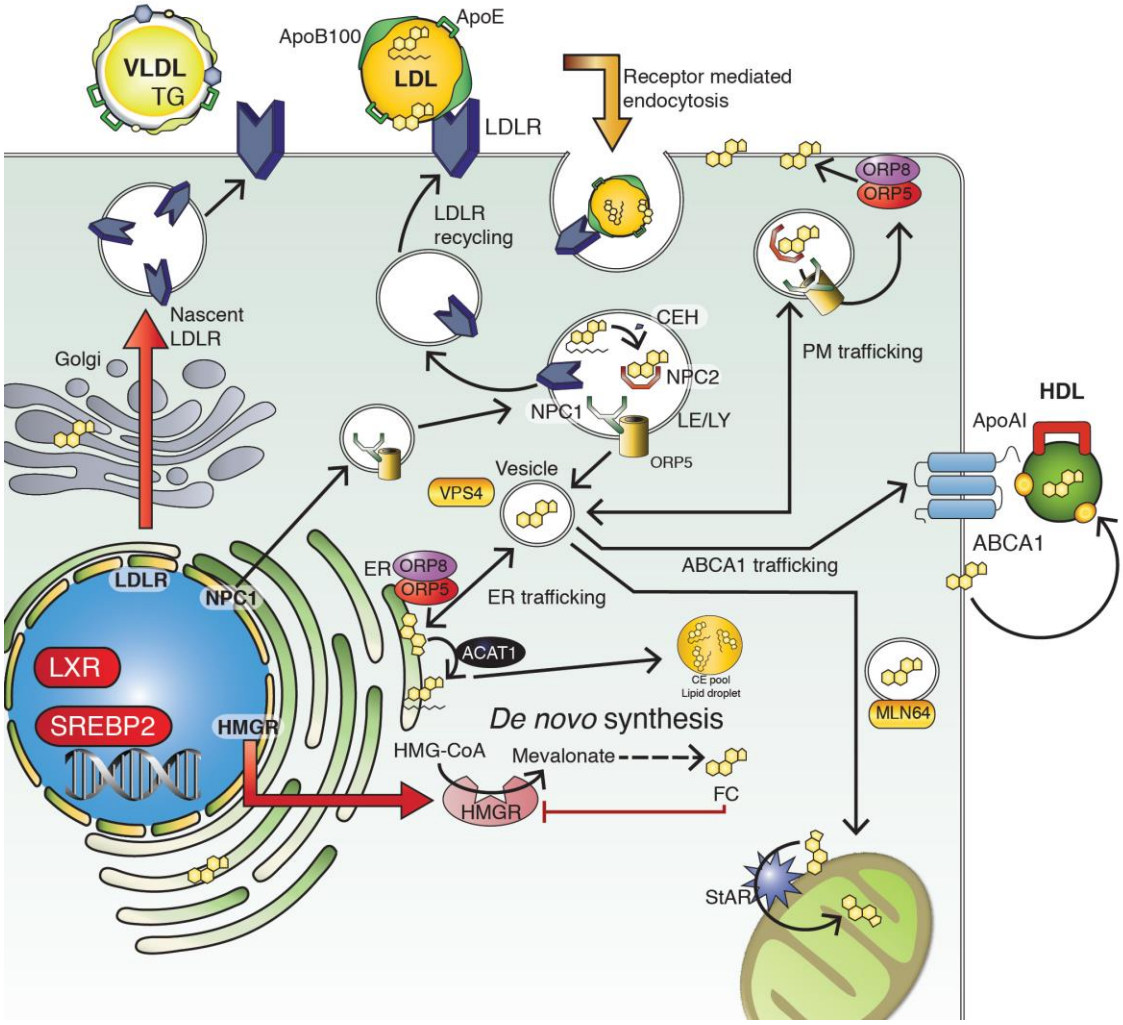

Figure 1.8 Intracellular cholesterol trafficking pathways.

After ApoB100 binds to the LDL receptor (LDLR), LDL and VLDL undergo receptor-mediated endocytosis. Phagocytosed early endosomes mature to late endosomes (LE) / lysosomes (Ly); this allows vesicular sorting and LDLR recycling to the cell surface. Simultaneously, CEs are hydrolysed to FC by cholesterol ester hydrolase (CEH) and lysosomal acid lipase. Niemann-Pick disease type C2 protein (NPC2) chaperones FC to Niemann-Pick disease type C1 (NPC1), a transmembrane protein involved in trafficking FC to PM, ER and the mitochondrial compartments. PM and ER trafficking also involves oxysterol-binding protein (OSBP) and OSBP-related proteins (ORP)-5 and -8 (see text, Section 1.5.2). NPC1-FC transport to the outer mitochondrial membrane requires metastatic lymph node 64-protein (MLN64). StAR then translocates FC across the mitochondrial membrane leaflet (see Section 1.5.2).

Other abbreviations: ABCA1, ATP-binding cassette protein A1; Apo, apolipoprotein; ER, endoplasmic reticulum; HDL, high-density lipoprotein; HMGR, HMG-CoA reductase; LXR, liver X receptor; SREBP2, sterol-regulatory element-binding protein-2.

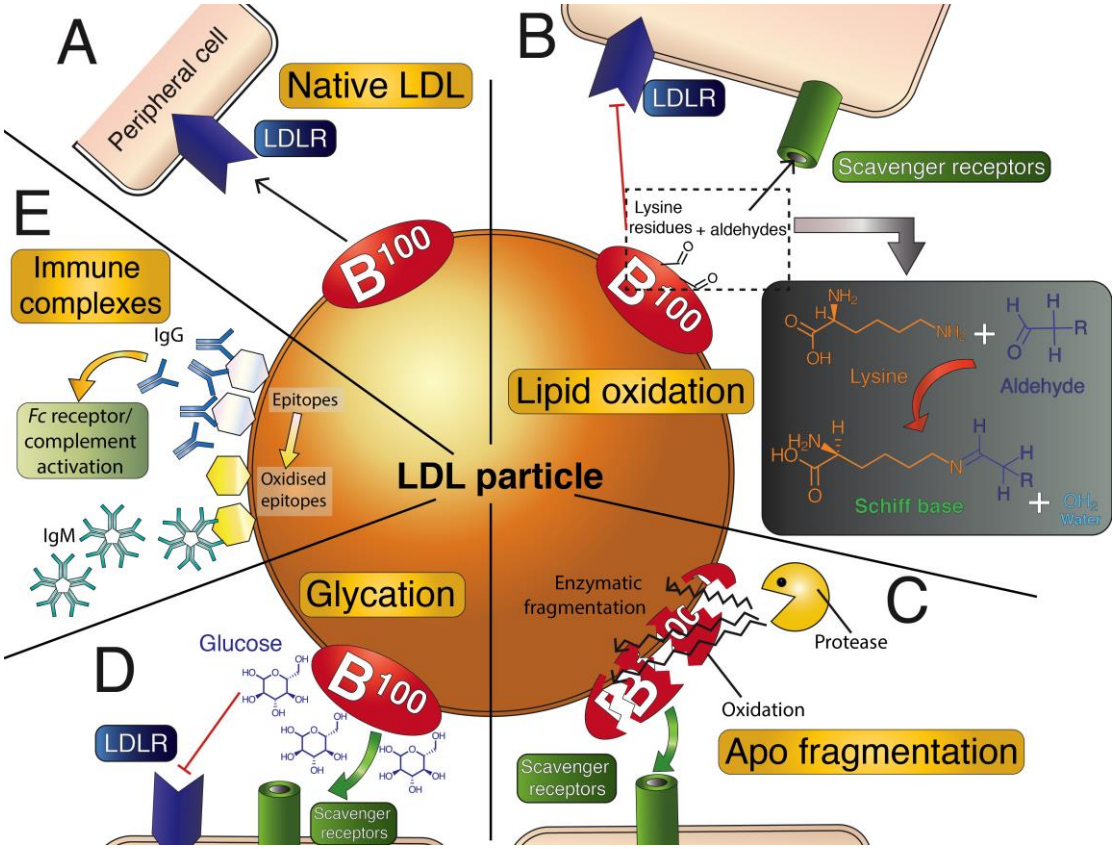

Figure 1.9 Possible LDL modifications and their effects on LDLR binding.

(**A**) Native (unmodified) LDL is recognised by LDLR, which binds ApoB100 (B100) and triggers receptor-mediated endocytosis. (**B**) Oxidation of LDL can occur in the presence of copper salts or lipoxygenases, which are expressed by many cell types, including endothelial cells, monocytes, macrophages and smooth muscle cells. Oxidation results in the conjugation of aldehyde groups to the lysine residues of ApoB100. This modification prevents LDL from binding to LDLR. (**C**) As a result, oxidised LDL is no longer recognised by LDLR. Instead, it is exclusively transported by the scavenger receptor family of transporters (see Table 1.4). Oxidised LDL is also susceptible to enzymatic degradation. (**D**) Glycation (non-enzymatic conjugation of glucose molecules to Apo proteins) is another common modification that inhibits LDLR recognition of LDL. (**E**) Immunogenic epitopes generated by LDL oxidation can result in immunoglobulin (Ig) binding on the LDL particle surface. In turn, this contributes to inflammatory responses. Image adapted from Gleissner and colleagues (2007).

Note: In this figure *Fc* refers to the fragment crystallisable component of immunoglobulin, not free cholesterol.

Table 1.4 Classes and ligand specificity of the scavenger receptors.

Class	Name	Ligand	Reference
A	**SR-AI**	Modified LDL (oxidation, acetylation)	Suzuki *et al.* 1997
	SR-AII		
B	**CD36**	Oxidised LDL, long-chain FFAs, oxidised phospholipids	Nicholson *et al.* 1995, Febbraio *et al.* 2000, Kunjathoor *et al.* 2002, Podrez *et al.* 2002
D	**CD68**	Oxidised LDL	Lougheed *et al.* 1997, Yoshida *et al.* 1998, Lougheed *et al.* 1999, Song *et al.* 2011
E	**LOX1**	Oxidised LDL	Oka *et al.* 1998
G	**CXCL16**	PS, oxidised lipoproteins	Wagsater *et al.* 2004

Abbreviations: CD, cluster of differentiation; CXCL16, chemokine (C-X-C motif) ligand 16; FFA, free fatty acids; LDL, low-density lipoprotein; LOX1, lectin-like oxidised low-density lipoprotein (LDL) receptor-1; PS, phosphatidyl serine; SR, scavenger receptor.

1.6 The inflammasome: an essential component of the innate immune response

NAFLD disease progression seems likely to involve all innate immune system cells, including: neutrophils, natural killer cells, dendritic cells, and natural killer T-cells, as well as macrophages (Peverill *et al.* 2014). The majority of macrophages identified in liver biopsies are resident macrophages or KCs (Zhan and An 2010). Activation of these cells is an important source of inflammation responsible for activation of neighbouring hepatic stellate cells (HSC), thereby facilitating downstream liver fibrosis (Zhan and An 2010, Meli *et al.* 2014).

One pro-inflammatory mechanism utilised by the innate immune involves inflammasomes, a family of macro-molecular complexes that consist of several intracellular pattern recognition receptors (PRRs) proteins. These PRRs patrol the cell and respond to pathogen-associated molecular patterns (PAMPs), as well as danger-associated molecular patterns (DAMPs) (Shaw *et al.* 2011, Guo *et al.* 2015). In more recent years, a metabolic stress-sensing inflammasome involved in metabolic diseases such as obesity and T2D has been described (termed the "metabolic inflammasome") (Dagenais *et al.* 2012, Wen *et al.* 2012), although this remains controversial.

The inflammasome complex assembles in the cytosol in response to a series of two PAMP and DAMP signals (see Figure 1.11) (endotoxin is a common Signal 1). The target of activated inflammasomes is pro-caspase 1, which dimerises to release cleaved active caspase 1. In turn this leads to:

1. Caspase-1-dependent post-translational regulation of pro-IL-1β and pro-IL-18 (Mariathasan and Monack 2007), and cleaving both proteins to generate the active cytokines.
2. Activation of caspase-1-dependent cell death, termed pyroptosis (Schroder and Tschopp 2010, Eitel *et al.* 2011), which has some characteristics of apoptosis and others of necrosis and necroptosis.

Cellular secretion of active IL-1β and IL-18 increases significantly after inflammasome activation (Sollberger *et al.* 2014). These interleukins promote innate cell maturation and activation (especially monocytes) and possibly neutrophils, as well as recruitment and activation of cellular immunity (helper T-cells [Th1 and Th2]) (Jander and Stoll 1998, Mencacci *et al.* 2000, Netea *et al.* 2000, Chen *et al.* 2011).

PAMPs include a wide range of microbial-associated molecular patterns (MAMPs) found on bacteria, fungi, and viruses. They are detected by several receptors, including TLRs, C-type lectin Receptors (CLRs, which includes dectin-1; see Figure 1.10), receptor kinases, and intracellular PRRs (these include the various NOD-like receptors [NLRs]). Once activated, many PRRs trigger formation of the inflammasome cascade, which starts with the recruitment of several proteins containing a caspase-recruitment domain (CARD). Importantly, pro-caspase-1 possesses a CARD domain, which facilitates complex formation with other CARD domain-containing proteins. In turn, these interact with apoptosis-associated speck-like protein (ASC), a small 22 kDa adaptor protein (Sutterwala *et al.* 2006, Fernandes-Alnemri *et al.* 2007, Mariathasan and Monack 2007, Willingham *et al.* 2007). In the absence of PRR stimulation, the NLR and AIM2 inflammasome components exist as monomers (McIlwain *et al.* 2013). Several other protein domains are involved in inflammasome assembly. They include:

1. The "*neuronal apoptosis inhibitor protein, MHC class 2 transcription activator, incompatibility locus protein from Podospora anserina and telomerase-associated protein*" (NACHT).
2. Leucine-rich repeat (LRR) NRL domain

3. NACHT, LRR and PYD (NALP) associated domain (NAD)
4. A non-NRL PRR, termed “hematopoietic interferon-inducible nuclear antigens with 200 amino acid repeats”, or HIN-200 domain.

The varying inflammasomes (see Figure 1.10 for structures) are classified according to the component PRR domains listed above, and the presence of adapter CARD, ASC and pyrin (PYD). Three inflammasomes possess nucleotide-binding oligomerisation domain NLR PRR components. A fourth, the *absent in melanoma 2* (AIM2) inflammasome, contains the non-NRL HIN-200 domain (see above). This too is a caspase-1 inflammasome but is activated by foreign cytoplasmic dsDNA (Fernandes-Alnemri *et al.* 2009, Hornung *et al.* 2009) (Figure 1.11). For the NRL inflammasomes:

1. **NLRP1** includes NACHT, LRR and PYD domains-containing protein 1 components and detects muramyl dipeptide (MDP), a peptidoglycan motif present in the cell wall of gram-positive and negative bacteria (Chamaillard *et al.* 2003, Franchi *et al.* 2009, Faustin and Reed 2013).

2. **NLRP3** contains LRR, NAD and NACHT domains, in addition to CARD, ASC and PYD domains-containing protein 3 (Franchi *et al.* 2009) (see Figure 1.10). This complex is activated in the methionine/choline-deficient mouse model (MCD) of NASH (Csak *et al.* 2011), as well as in *foz/foz* mice with NASH, as used in this thesis (Mridha *et al.* 2017). Wree *et al.* (2014) have also shown that NLRP3 activation is associated with fibrosis in experimental NASH. Of particular importance to the work described in this thesis, NLRP3 activation is often linked to mitochondrial stress, damage and the presence of excess ROS (Zhou *et al.* 2011).

3. **NLRC4** contains CARD domain-containing protein 4 and is activated by bacterial components. This inflammasome complex is also responsible for pyroptosis (McCoy *et al.* 2010, Miao *et al.* 2010).

1.6.1 NLRP3-specific triggers

Activation of inflammasomes and down-stream IL-1 and IL-18 secretion is an important step in the innate immune response. However, inflammasomes have also been implicated in the pathogenesis of multiple autoimmune and inflammatory diseases, including: adult-onset Still’s disease (Gerfaud-Valentin *et al.* 2014) and gout (Shaw *et al.* 2011, Guo *et al.* 2015). As previously mentioned, activation of the NLRP3 inflammasome is particular relevant to NAFLD research.

Inflammasome complex activation requires two signals (two-signal model). The first signal is usual a PAMP and primes the complex for activation. The second (activation) signal, which can be either a PAMP or DAMP, then activates the complex (He *et al.*). PAMPs and DAMPs involved are summarised in Figure 1.11. PAMPs include bacterial, fungal and viral components, which are detected by TLRs, NODs, CLRs, and other PRRs. These activated receptors, in turn initiate the expression of pro-inflammatory transcription factors like NF-κB p65 (discussed later) and instigate assembly of the NLRP3 inflammasome complex (Grishman *et al.* 2012).

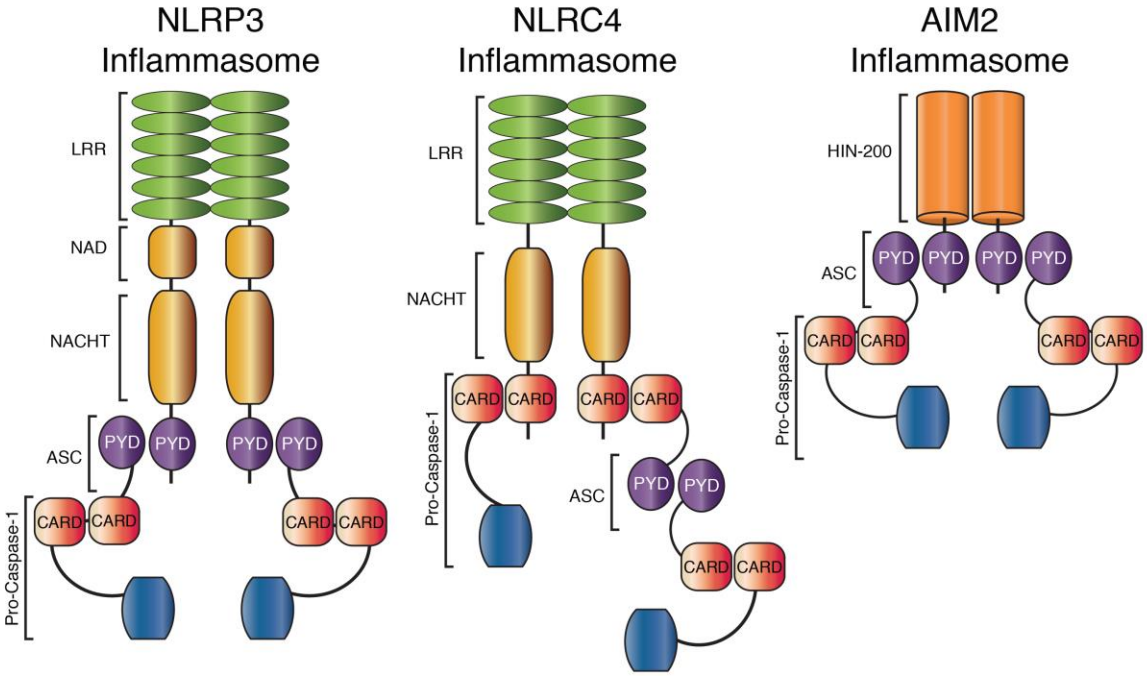

Figure 1.10 Structure of some major inflammasome complexes.

Component structures of the NACHT, LRR and PYD domains-containing protein-3 (NLRP3), NLR Family, CARD Domain Containing 4 (NLRC4) and the absent in melanoma-2 (AIM-2) inflammasome complexes. Image are adapted from Eitel *et al.* (2010).

Abbreviations: ASC, apoptosis-associated speck-like protein containing a CARD; CARD, caspase recruitment domain CPPD; HIN-200, hematopoietic interferon-inducible nuclear antigens with 200 amino acid repeats; LRR, *C*-terminal leucine-rich repeat; NACHT, NOD or NBD – nucleotide-binding domain; NAD, NACHT-associated domain.

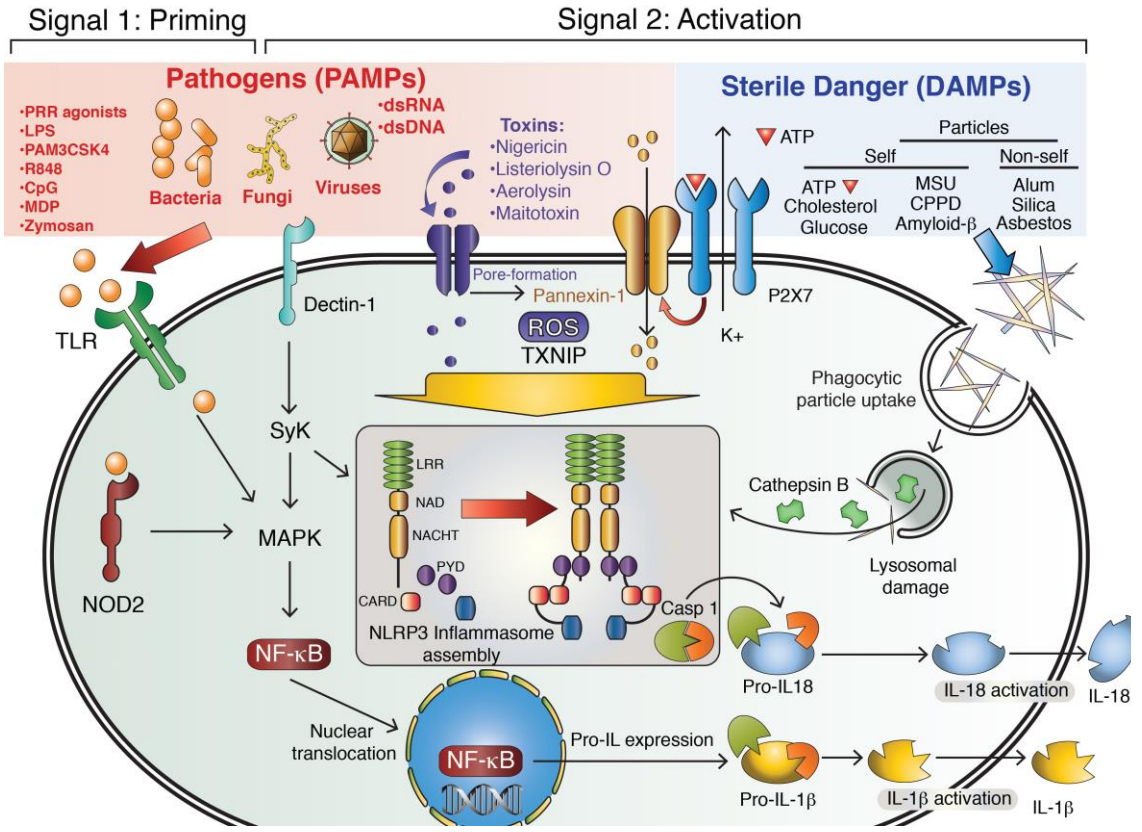

Figure 1.11 How different pathogen- (PAMPs) and danger-associated molecular patterns (DAMPs) are involved in two-signal activation of NLRP3.

The two-signal activation pathway for the NLRP3 inflammasome (see text above for details). Image is adapted from Conforti-Andreoni *et al.* (2011).

Abbreviations: ATP, adenosine triphosphate; CpG, cytosine-phosphate-guanine motif/island; DAMPs, danger (or damage)-associated molecular patterns; dsDNA, double-stranded DNA; dsRNA, double stranded RNA; IL, interleukin; LPS, lipopolysaccharide; LRR, *C*-terminal leucine-rich repeat; MAPK, mitogen-activated protein kinase; MDP, muramyl dipeptide; MSU, mono-sodium urate; NF-κB, nuclear factor-kappa B; NACHT, NOD or NBD – nucleotide-binding domain; NOD2, nucleotide-binding oligomerization domain-2; P2X7, ligand-gated ion channel; PAM3CSK4, a synthetic triacylated lipopeptide TLR1/2 agonist; PAMPs, pathogen-associated molecular pattern; PRR, pattern-recognition receptors; PYD, pyrin domain; R848, resiquimod – a pro-inflammatory imidazoquinoline compound; ROS, reactive oxygen species; Syk, spleen tyrosine kinase; TLR, toll-like receptor; TXNIP, thioredoxin (TRX)-interacting protein.

Several DAMPs are also capable of inducing a NLRP3 inflammasome response following the first priming signal. These include:

1. **Extracellular ATP** – the presence of extracellular ATP activates purinergic ATP-gated P2X purinoceptor 7 (P2X7) receptor (P2X7R), a ligand-gated non-specific cation (K^+, Na^+, Ca^{2+}, and Mg^{2+}) channel that in turn depolarises the cell and activates the

NLRP3 inflammasome (Verhoef *et al.* 2004, Petrilli *et al.* 2007, Qu *et al.* 2007, Qu *et al.* 2009, Minkiewicz *et al.* 2013, Gicquel *et al.* 2014).

2. **FC crystals** – phagocytic uptake of FC crystals by macrophages causes lysosomal destabilisation, damage and cathepsin B release, which in turn induces NLRP3 inflammasome activation. This pathway is hypothesised to be involved in the pathogenesis of atherosclerosis (Duewell *et al.* 2010, Rajamaki *et al.* 2010, Janoudi *et al.* 2016).

3. **High mobility group box 1 protein (HMGB1)** – A non-histone nuclear protein called high mobility group box 1 (HMGB1) protein. Injured and damaged cells (usually necrotic) release HMGB1, which is able to activate TLR4 (discussed in Section 1.7.1). In turn, this activates several pro-inflammatory pathways, including the NLRP3 inflammasome (Lu *et al.* 2012, Wang *et al.* 2013). HMGB1 plays an important role in the pathways described in this thesis. Accordingly, this specific DAMP is further discussed below, and in Chapters 4 and 5.

1.7 HMGB1 and sterile inflammation

Necrosis results in release of HMGB1, which has dual functions depending on its subcellular localisation. Intracellularly, HMGB1 binds to DNA and acts as a transcriptional regulator (Bustin and Reeves 1996, Brickman *et al.* 1999, Agresti and Bianchi 2003, Bell *et al.* 2006). Outside the cell, however, HMGB1 serves as a cytokine and is also able to augment lipopysaccharide (LPS) signalling through TLR4 (Qin *et al.* 2009, Li *et al.* 2015). The cytokine activity of HMGB1 can only manifest when the protein translocates from the nucleus to the extracellular milieu (Bell *et al.*, 2006) (Andersson *et al.* 2002). This translocation may be facilitated by the formation of extracellular vesicles (EV), a process described further in Section 1.7.4 of this Chapter, and a key element of studies reported in Chapters 5 and 6.

The hallmarks of human NASH include activation of the *c*-Jun *N*-terminal kinases in hepatocytes (JNK, pathway described in Section 1.7.3), macrophage infiltration, oxidative stress, and apoptotic cell death. There is now increasing evidence for necrotic cell death in NASH (Joka *et al.*, 2011). Recently, Li and colleagues reported that FFAs activate hepatocytes (not KCs) via TLR4 mediated release of HMGB1 in mice as well as *in vitro* (palmitic acid [PA] lipotoxicity to primary hepatocytes). These authors emphasised this as being important in the early stages of NAFLD development (Li *et*

al., 2011). However, the potential role for HMGB1 release from necrotic hepatocytes in sustaining recruitment of inflammatory signals in NASH pathogenesis does not seem to have been explored previously. It will be addressed in Chapter 6.

HMGB1 has also been shown to activate hepatic stellate cells and to stimulate their proliferation, thereby inducing hepatic fibrosis (Kao *et al.* 2008). Kao *et al.* (2008) demonstrated that circulating HMGB1 down-regulates membrane metalloproteinase (MMP)-2, but not MMP-9, and this could contribute further to extracellular matrix deposition and fibrosis in NASH. Additionally, biological (antibody) neutralisation of circulating HMGB1 has been shown to ameliorate the development of atherosclerosis in vascular disease-prone ApoE-deficient mice. Specifically, anti-HMGB1 antibody treatment reduced expression of CD11c and CD83 (markers of total and mature dendritic cells, respectively) (Kanellakis *et al.* 2011). As previously mentioned, HMGB1 is an important TLR4 ligand. Downstream TLR activation pathways will now be described.

1.7.1 TLR activation pathways

TLRs are one family of PRRs (Akira *et al.* 2006, Kaisho and Akira 2006). They are expressed by cells of the innate immune system, which include: macrophages, monocytes, dendritic cells, neutrophils, and natural killer cells (Kadowaki *et al.* 2001, Hayashi *et al.* 2003, Takeda 2005, Takeda and Akira 2005). To date, 13 *TLR* genes have been identified for humans and mice; however, not all are operative across all species. In humans, only TLR1 to 10 are present, while mice lack TLR10 functionality (Deng *et al.* 2014).

Surveillance for extracellular PAMPs/DAMPs is performed by PM-bound TLRs-1, 2, 4, 5, 6, and 11. On the other hand, TLRs 3, 7, 8, 9, and 13 are found intracellularly in the endosomal/lysosomal system, allowing them to detect and respond to intracellular pathogens (bacteria and viruses) and danger signals (for example TLR9 responds to cytosine-phosphodiester linked guanine [CpG] DNA motifs and mitochondrial DNA) (Tohme and Manoury 2014). With the exception of TLRs 1, 2, and 6 and TLRs 7 and 8, each receptor responds to a specific trigger PAMP/DAMP; these are summarised in Figure 1.12. TLR4 is of particular importance to this thesis. It is activated by HMGB1 released from cells undergoing oxidative stress or necrosis, this allows TLR4 to

contribute to sterile inflammation (Andersson and Tracey 2011, Tsung *et al.* 2014, Zhang *et al.* 2015). The relevance of this to progression of fatty liver to NASH will be discussed in Chapters 4 and 5.

Once triggered, TLR receptors initiate a signalling cascade that involves various adaptor and signalling scaffold proteins. Toll-IL-1 receptor (TIR) is a universal adaptor protein, which along with myeloid differentiation primary response gene 8 (MyD88), MyD88-adapter-like (MAL), and/or TRIF-related adaptor molecule (TRAM) relay the TLR activation signal to a larger kinase scaffold complex (Takeuchi *et al.* 2000, Fitzgerald *et al.* 2001, Bannerman *et al.* 2002). TLR3 is the only TLR that does not signal through MyD88; instead, it relies solely on a TRIF adaptor protein (Figure 1.12) (Yamamoto *et al.* 2003).

The scaffolding complex stimulated by the TLR adaptor protein cascade includes IL-1R-associated kinase (IRAK)-1, -2, -4, and a TLR-specific TRAF protein. PM-bound TLRs signal through TRAF6, while the endosomal TLRs activate TRAF3 (see Figure 1.12) (Tseng *et al.* 2010, Kawasaki and Kawai 2014). TRAF6-containing scaffold complexes trigger a secondary down-stream protein complex containing transforming growth factor-β activated kinase (TAK)-1 and TAK1-binding protein (TAB)-2 and -3 (Inokuchi *et al.* 2010).

Downstream of the IRAK/TRAF complex, TLR stimulation eventually culminates in the activation of several pro-inflammatory and pro-apoptotic pathways. These include:

1. The canonical NF-κB pathway (Section 1.7.2)
2. The classical MEKK pathway to JNK activation (see Section 1.7.3 and Figure 1.12).

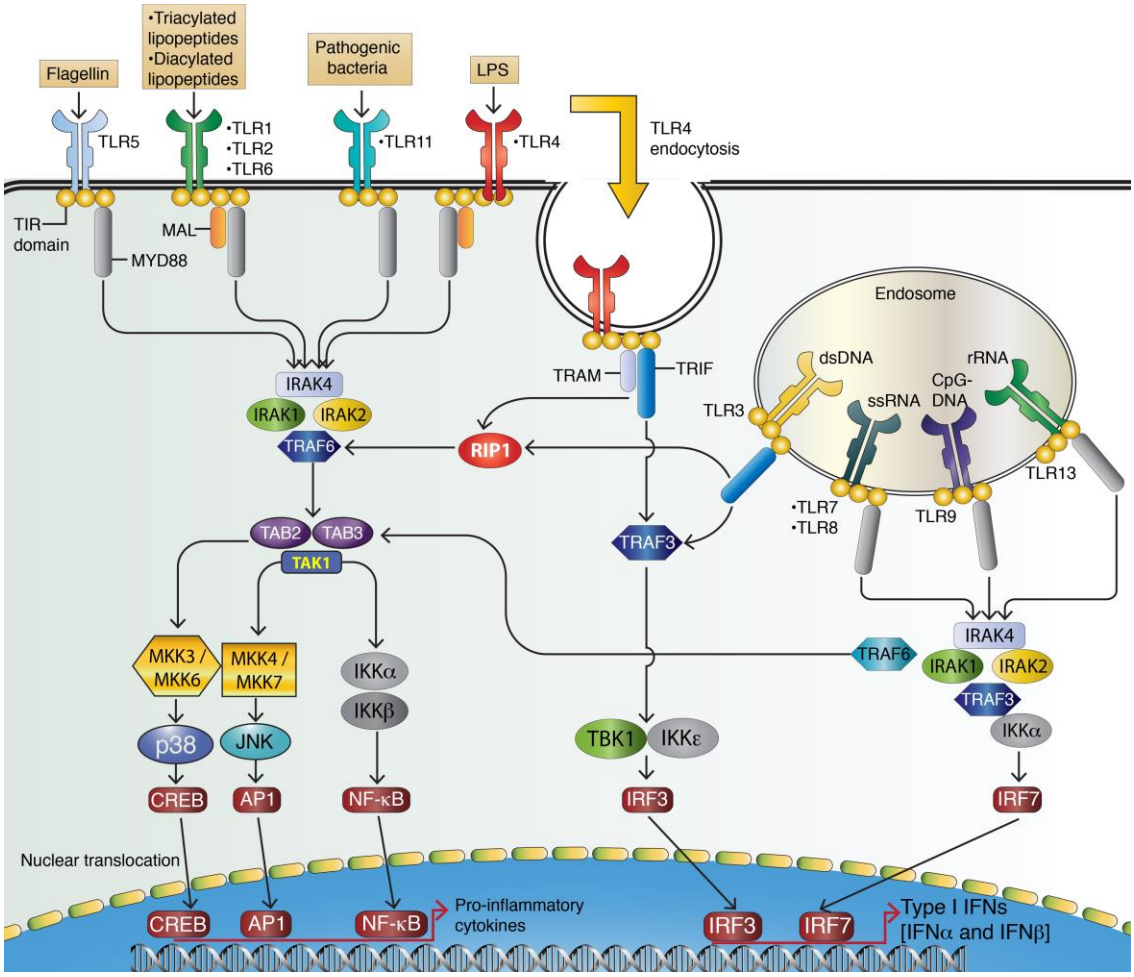

Figure 1.12 Toll-like receptor (TLR) activation pathways.

The signalling cascades involved in TLR activation are described in Section 1.7.1. This figure was adapted from O'Neill *et al.* (2013).

Abbreviations: AP-1, activator protein 1; CREB, cAMP response element-binding protein; dsDNA, double-stranded DNA; IKK, inhibitor of nuclear factor kappa-B kinase; IRAK, interleukin-1 receptor-associated kinase; JNK, *c*-Jun *N*-terminal kinases; LPS, lipopolysaccharide; MAL, MyD88-adapter-like; MKK, MAP kinase kinase; MyD88, myeloid differentiation primary response gene 8; RIP1, receptor-interacting protein kinase 1; rRNA, bacterial ribosomal RNA; TAB, TAK1-binding protein; TAK, TGF-β-activated kinase; TBK1, TANK-binding kinase 1; TIR, toll-IL-1 receptor; TLR, toll-like receptor; TRAF, TNF receptor-associated factor TRAM, TRIF-related adaptor molecule.

1.7.2 The NF-κB signalling pathway

NF-κB is a dimeric transcription factor involved in regulating inflammatory and immunological responses, as well as cell survival, adhesion and oncogenesis (Simeonidis *et al.* 1999, Perkins 2007). A significant degree of overlap exists between the JNK and NF-κB signalling pathways. For example TNF-α signalling is able to activate both MKK4/7 and the upstream NF-κB activation complex. NF-κB dimers are

comprised of five separate proteins, RelA (referred to from here on as NF-κB p65), RelB, c-Rel, NF-κB1 (p50/p105) and NF-κB2 (p52/p100) (details are listed in Table 1.5).

In NASH, NF-κB p65 has been shown to play an important role in the transition from SS to fibrotic steatohepatitis. Importantly, the degree of NF-κB p65 activity closely correlates with disease severity (Ribeiro *et al.* 2004, Tian *et al.* 2013) (Ban *et al.* 2007, Videla *et al.* 2009), while blocking NF-κB activation prevented liver inflammatory recruitment in the MCD model (Dela Pena *et al.* 2005).

Structurally, all NF-κB transcription factors contain a Rel-homology domain (RHD). This functions as a DNA binding site and allows for homodimeric or heterodimeric interaction between NF-κBs (Gilmore 2006). The transcriptional activity of NF-κB proteins is strictly controlled within the cell, where it is regulated by a number of additional proteins. In their latent (inactive) state, NF-κB transcription factors are sequestered in the cytoplasmic compartment by three small NF-κB inhibitor (IκB) proteins, IkBα, -β and ε (Huxford *et al.* 1998, Jacobs and Harrison 1998) (Figure 1.13). In this state, the NF-κB protein RHD domains are hidden by IκB proteins (Huxford *et al.* 1998, Jacobs and Harrison 1998).

Table 1.5 NF-κB family of transcription factors.

Gene	Protein	Class	Protein size (kDa)	Function	Reference
NFKB1	NF-κB1	I	105 50 processed	Inflammation, modulation of adaptive immune responses, B/T-cell cancer, cell proliferation and survival, cell stress responses	Meyer *et al.* 1991, Beinke and Ley 2004, Yu and Lin 2010
NFKB2	NF-κB2	I	100 / 52	Similar to NF-κB1	Beinke and Ley 2004, Yu *et al.* 2009
RELA	RelA (p65)	II	65	Inflammation, immune modulation, cell survival/apoptosis control, oncogenesis	Ivanov *et al.* 1995, Aoudjit *et al.* 1997, Li *et al.* 2002
RELB	RelB	II	70	Antigen presenting cell functioning, lymphoid development inflammation	Shih *et al.* 2012, Millet *et al.* 2013
REL	c-Rel	III	69	Lymphocyte maturation and development, inflammation, lymphocyte oncogenesis	Ruan *et al.* 2009, Gilmore and Gerondakis 2011, Shih *et al.* 2012, *Ramakrishnan et al.* 2013

Abbreviations: kDa, kiloDalton; NF-κB, nuclear factor-kappa B; REL, V-Rel avian reticuloendotheliosis viral oncogene homolog.

Several NF-κB activation pathways have been characterised, the most common of which is the classical (also termed canonical) pathway. Here, pro-inflammatory stimulation through TNFR, TLRs (for example LPS stimulation of TLR4), and T-cell receptor activation starts the assembly of an IκB kinase (IKK) complex. This complex comprised of three proteins: IKKα, IKKβ and NF-κB essential modifier (NEMO) (Yamaoka *et al.* 1998, Simeonidis *et al.* 1999, Karin and Ben-Neriah 2000, Perkins 2007). The IKK complex phosphorylates the IκB proteins, which retain the NF-κB transcription factors within the cytoplasm. As seen in Figure 1.13, the $Ser^{32/36}$ residues of IκBα is phosphorylated in this process. This allows for ubquitination and destruction of the IκB proteins by the 26S proteasome. In turn, this exposes the NF-κB protein RHD domains, allowing for heterodimeric and homodimeric complex formation and, most importantly, nuclear translocation (Gilmore 2006).

Less commonly, NF-κB activation can occur through the RelB non-canonical activation pathway (see Figure 1.13). Here, immunological signals such as the CD40 ligand, LPS, and latent membrane protein-1 can activate NF-κB inducing kinase (NIK), can lead to RelB transcriptional activity (Figure 1.13).

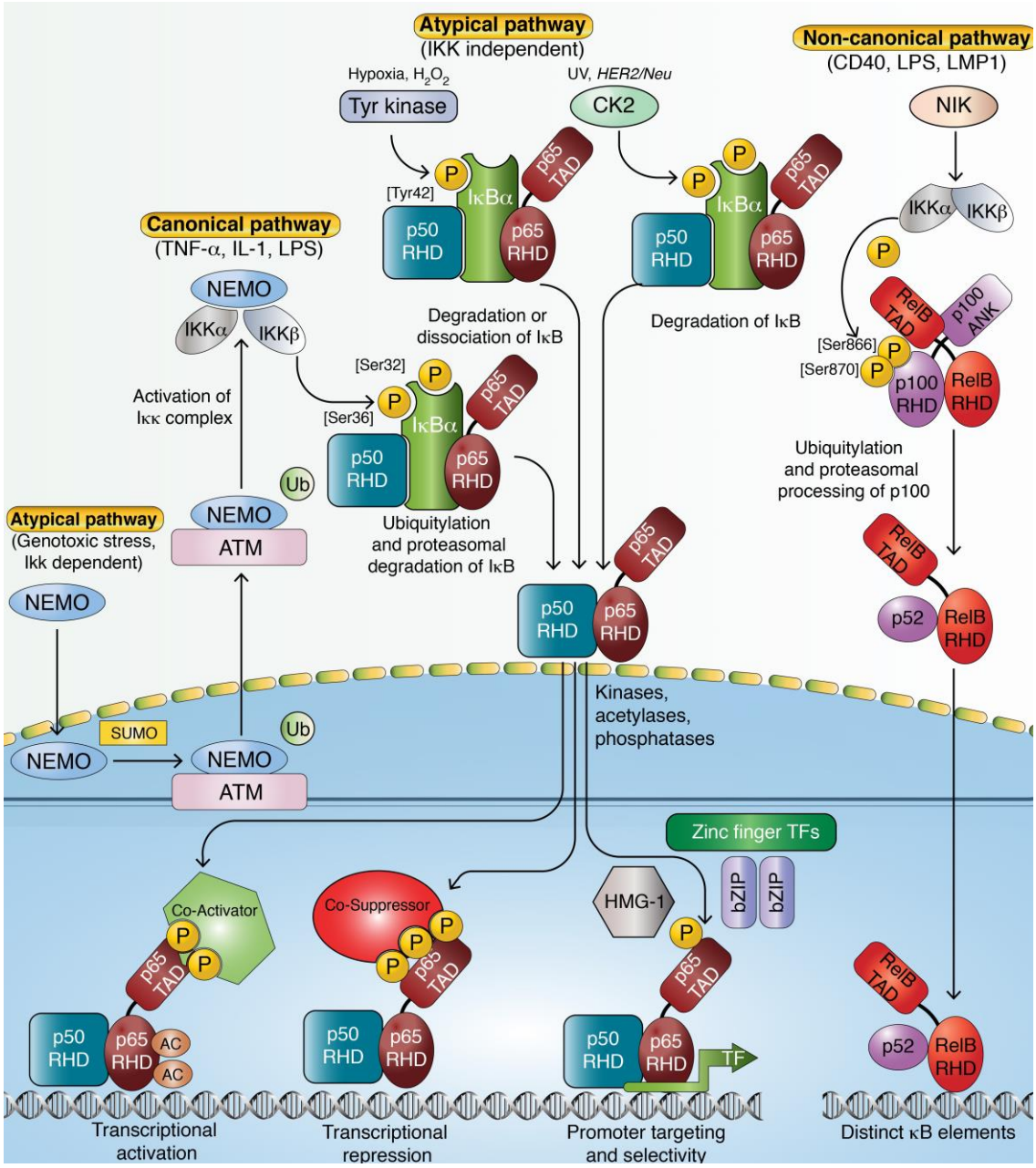

Figure 1.13 The canonical (classical), non-canonical and atypical pathways of NF-κB activation.

Details of this signalling pathway are provided in Section 1.7.2. Image adapted from Perkins (2007).

Abbreviations for Figure 1.13: AC, acetylation; ATM, ataxia telangiectasia mutated; bZIP, leucine-zipper-containing transcription factor; CD, cluster of differentiation; CK2, casein kinase 2; HER2/Neu, receptor tyrosine-protein kinase erbB-2; HMG1, high-mobility-group protein-I IκBα, inhibitor of κB alpha; IKK, IκB kinase; IL, interleukin; LMP1, latent membrane protein-1; LPS, lipopolysaccharide; NEMO, NF-κB essential modulator; NF-κB, nuclear factor-κB; SUMO, small ubiquitin-like modifier; RelB, V-Rel Avian reticuloendotheliosis viral oncogene homolog B; RHD, Rel-homology domain; TAD, transcriptional activation domain; TF, transcription factor; TNF, tumour necrosis factor; Ub, ubiquination; UV, ultra-violet.

1.7.3 *c*-Jun *N*-terminal kinases (JNKs)

The JNK proteins are a family of mitogen-activated protein kinases (MAPKs) activated by pro-inflammatory and cell stress signals. These kinases are tasked with the phosphorylation of *c-Jun* at $Ser^{63}/^{73}$ residues (Vlahopoulos and Zoumpourlis 2004). This allows *c*-Jun to complex with *c*-Fos to form a *c*-Jun-*c*-Fos heterodimer, known as activator protein 1 (AP-1). AP-1 serves as a transcription factor for numerous genes involved in inflammation (cytokines and chemokines), apoptosis (Fas ligand [FasL]), cellular proliferation and differentiation (nuclear factor of activated T-cells [NFAT}, TGF-α, -β, IL-2), and oncogenesis (cyclin-D, *E2F* genes) (Angel and Karin 1991, Jacobs-Helber *et al.* 1998, Shaulian and Karin 2002, Klein and Assoian 2008, Vartanian *et al.* 2011). It should be noted that other AP-1 heterodimer permutations exist; they are composed of Jun (*c*-Jun, JunB and JunD) and Fos (*c*-Fos, FosB, Fra1 and Fra2) components (Ameyar *et al.* 2003). Of interest to NASH, AP-1 and NF-κB are often activated by similar stimuli and there is much overlap with the genes they regulate.

There are three separate JNK genes, *JNK*-1, -2, and -3, and each expresses a number of isoforms (Alexandrov *et al.* 1999). JNK-1 and -2 each express four proteins, which are ubiquitously expressed in all tissue types. JNK-3, however, is selectively expressed in neurons and cardiac myocytes, and only produces two protein isoforms (JNK3α1 and JNK3α2; Figure 1.14A). Interestingly, all ten of these proteins weigh either 46- or 54-kDa, depending on their amino acid length (Coffey 2014). This coincidence makes for some technical challenges in separating them by western blot analysis, unless highly specific antibodies are available (see Chapter 2, Section 2.3).

A plethora of triggers activate JNK signalling. They include:

1. **Oxidative stress** (Wang *et al.* 2007, Wang *et al.* 2008, Son *et al.* 2011, Tang *et al.* 2013)

2. **Mitochondrial dysfunction** (Barateiro *et al.* 2012, Qi *et al.* 2015)
3. **TLR activation** (Matsuguchi *et al.* 2003, Thobe *et al.* 2007)
4. **Ultra-violet radiation** (Adler *et al.* 1995, Fritz and Kaina 1999, Wu *et al.* 2002)
5. **Inflammatory signals** (cytokines such as TNF and IL-1) (Lee *et al.* 1997, Tournier *et al.* 2001)
6. **Physical cell stress and heat shock responses** (Adler *et al.* 1995)
7. **The unfolded protein responses and ER stress** (Barateiro *et al.* 2012)

All the above signals activate JNK through a complex pathway involving several mitogen-activated protein kinase (MAPK) kinase kinases (MEKKs). These include dual leucine zipper bearing kinase (DLK), NCK-interacting protein kinase (TNIK), MEKK1, MEKK4, various mixed-lineage kinases (MLKs), apoptosis signal-regulating kinase 1 (ASK1), and thousand-and-one amino acid kinase 2 (TAOK2) (Figure 1.14B). Importantly, TNF is able to initiate a JNK response through TNF-receptors, which in turn activate TNF receptor-associated factor-2 (TRAF2), an adaptor protein involved in upstream JNK activation (Liu *et al.* 1996, Lee *et al.* 1997). TRAF2 then proceeds to interact with apoptosis signal-regulating kinase 1 (ASK1) (Liu *et al.* 2000).

Activated MEKKs then initiate MKK kinases -4 and/or -7. These MKKs activate JNK through phosphorylation at specific sites (Deacon and Blank 1997, Cuenda and Dorow 1998). MKK4 preferentially phosphorylates Tyr residues, while MKK7 tends to phosphorylate Thr amino acids (see Figure 1.14) (Tournier *et al.* 2001) (see Figure 1.14B). The important role of JNK in NASH is detailed in Chapter 4, where the specific role of JNK-1 and JNK-2 in FC-induced hepatocellular injury are investigated.

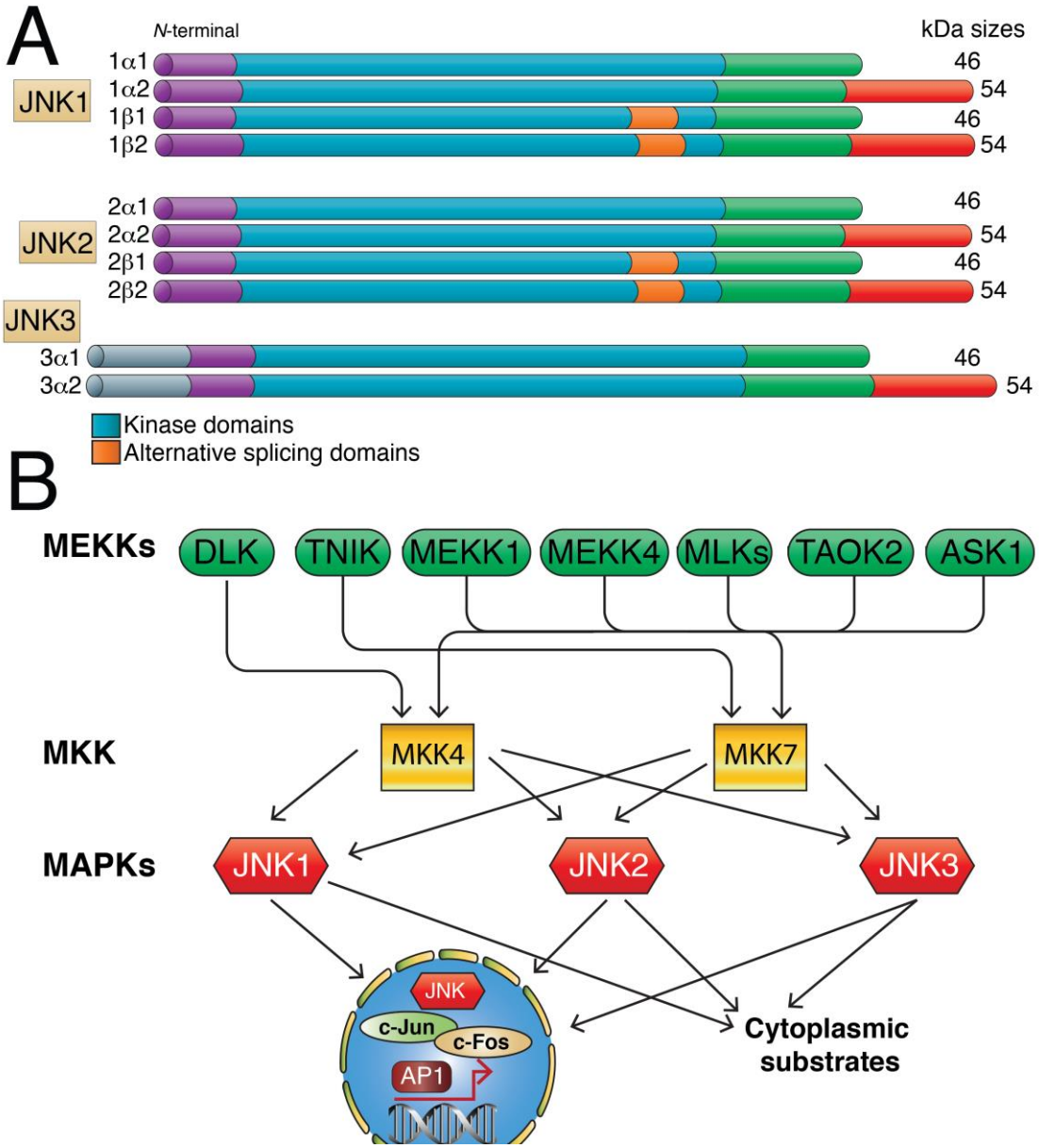

Figure 1.14 JNK proteins and isoforms and the JNK activation cascade.

(**A**) A total of 10 JNK proteins are expressed, four each for JNK1 and JNK2 and two for JNK3. Each of these JNK proteins, depending on amino acid length, weigh 46 or 54 kDa. (**B**) JNKs belong to the classical group of mitogen-activated protein kinases (MAPK) and are activated by MAPK kinases (MKKs), MKK4 and MKK7. Several upstream MKK kinase (MEKK) pathways are responsible for MKK activation, these include: dual leucine zipper bearing kinase (DLK), NCK-interacting protein kinase (TNIK), MEKK1, MEKK4, various mixed-lineage kinases (MLKs), apoptosis signal-regulating kinase 1 (ASK1), and thousand-and-one amino acid kinase 2 (TAOK2). Following activation, JNK can interact with various cytoplasmic substrates or activate *c*-Jun, which in turn forms heterodimers with *c*-Fos to form AP-1 (see text) and regulate gene transcription (Botteron and Dobbelaere 1998, Humar *et al.* 2007). Image adapted from Coffey *et al.* (2014).

1.7.4 Extracellular vesicles (EVs) as a potential paracrine mediator of hepatocellular damage

As described earlier, EVs may play a pathogenic role in cell-cell signalling and mediation of hepatocellular damage. EVs are small (≤1.5 μM) particles (See Figure 1.15 for details on size and mechanism of EV production) which are physiologically involved in normal cell to cell communication (Paolicelli *et al.* 2019). However, they arise from the PM of activated or damaged cells, and exhibit exposed anionic phospholipids, phosphatidylserine (PS) and phosphatidylethanolamine (PE) on their surface (Shet 2008). EVs also bear surface membrane antigens reflecting their cells of origin (see Table 1.6 for summary of some cell markers used to characterise EVs).

The process of EV release involves cleavage of the cell cytoskeleton and is mediated by caspase 3. Several groups, including studies from the host laboratory, have demonstrated that Ca^{2+} dependent proteases are involved in EV generation (Teoh *et al.* 2014, Ajamieh *et al.* 2015). These enzymes include calpain and gelsolin, both of which cleave actin filaments; this allows for activation of scramblase leading to cytoskeletal eversion. The changes to the cellular cytoskeleton also result in phospholipid reorganisation, with migration of PS and PE to the outer cellular surface, allowing EVs to bud off (Figure 1.15).

Within the last 10 years, the role of EVs has emerged as a complex one. It is now known that they are heterogenous particles, and potentially contain a multitude of biologically active macromolecules (see Figure 1.16). The exact composition of EVs is largely dependent on parental cell type and the mechanism for their formation. Not withstanding this, most EVs contain:

1. DNA, including mitochondrial DNA (Tatischeff *et al.* 1998)

2. RNAs (Eg: miRNA, coding mRNA, non-coding, as well as RNA-inducing silencing complexes (RISC) (Silva and Melo 2015, Iavello *et al.* 2016)

3. Proteins: heat shock proteins, growth factors, tetraspanins. The later includes a number of CD proteins listed in Table 1.6 (De Maio 2011, Chiasserini *et al.* 2014).

4. Lipid-enriched bilayer (compared with parent cell), comprised of FC, sphingomyelin, PS and bioactive eiconsanoids and prostaglandins, as well as lipid rafts (Koumangoye *et al.* 2011, Fais *et al.* 2016). Importantly, cholesterol plays an important role in EV release (Llorente *et al.* 2007) and uptake (Mulcahy *et al.* 2014).

Once taken-up by target cells, circulating EVs can participate in paracrine signalling (short-range intercellular signalling), as comprehensively reviewed by Mulcahy *et al.* (2014). This can occur through a number of routes, including: caveolin-mediated phagocytosis, lipid raft internalisation, and receptor-mediated uptake. Once internalised, the EV cargo (Figure 1.16) is released into the target cell where it can, depending on the exact cargo composition, induce a number of function effects, including hyper-inflammation (Szabo and Momen-Heravi 2017).

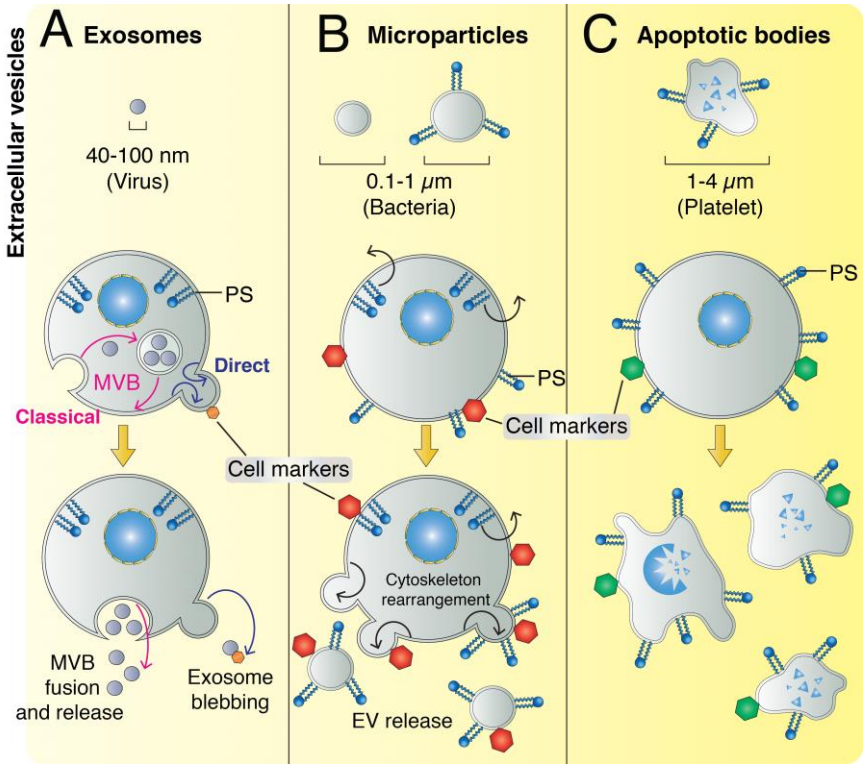

Figure 1.15 Types of extracellular vesicles (EVs) and mechanisms of their release.

(**A**) Exosomes, the smallest EVs, measure 40-100 nm (size of an average virus) and are generated by either the *classical* and/or *direct pathways*. The classical pathway (as represented by pink arrows) involves invagination of plasma membrane to form multivesicular bodies (MVBs). These coalesce within endosomal vesicles and fuse with the PM releasing extracellular exosomes. The direct pathway is simpler (blue arrows). Here exosomes bleb off the PM surfaces into the extracellular space. Importantly all EVs harbour markers of the cell of origin; this allows for qualitative analysis using assay techniques (see Table 1.6 for several examples of cell-specific markers). (**B**) Microparticles (MPs) are larger (0.1-1 µm; roughly the size of cocci bacteria) and are generated by phosphatidyl serine (PS) translocation from the inner to the outer PM surface. This reorganises the cytoskeleton causing MP release. (**C**) Apoptotic bodies are larger 1-4 µm EVs, formed from activation of apoptotic pathways (especially mitochondrial dysfunction and leakage). Here, DNA fragmentation, PM asymmetry, and disorganisation of cytoskeleton proteins generates the apoptotic fragments. Image adapted from Lemoinne *et al.* (2014).

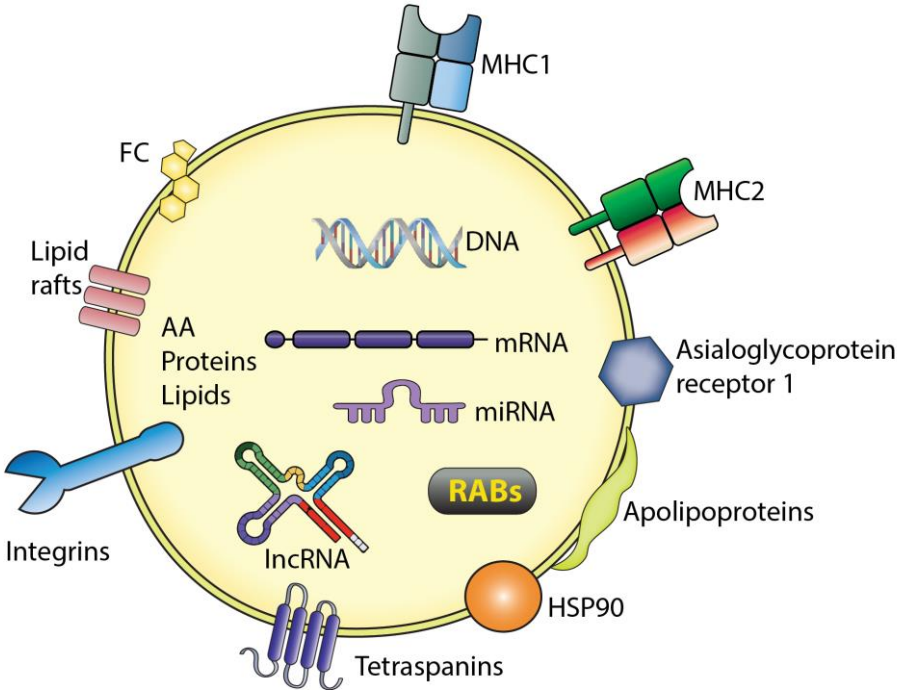

Figure 1.16 Typical extracellular vesicle composition.

Details of EV composition are described in Section 1.7.4, Szabo and Momen-Heravi (2017) recently published a review detailing EV involvement in viral and alcoholic liver disease, as well as NAFLD (image adapted from their review).

Abbreviations: AA, amino acids; DNA, deoxyribosnucleic acid; FC, free cholesterol, HSP90, heat shock protein 90; lncRNA, long noncoding RNA; MHC, major histocompatibility complex class; mRNA, messenger RNA; miRNA, microRNA; RABs, Ras-related proteins.

Exposing primary rat hepatocytes or HepG2 cells (a well-differentiated immortalised human hepatoma cell line) to palmitic or stearic acid results in EV release (Povero *et al.* 2013). Povero and colleagues (2013) subsequently demonstrated that these isolated EVs contain several microRNAs (miR) and can recruit, as well as activate HSCs. In their quiescent state, HSCs store vitamin A in the peri-sinusoid. This inactivated phenotype is governed by peroxisome proliferator-activated receptor (PPAR)-γ expression (Hazra *et al.* 2004). The EVs derived from FFA-damaged hepatocytes suppress HSC PPAR-γ expression, thereby activating HSC expression of pro-fibrotic genes, including collagen type-1 and alpha smooth muscle actin (Povero *et al.* 2013).

Importantly, to the author's knowledge, the relationship between cholesterol lipotoxicity in hepatocytes and EV formation has not been explored. It is a major strand of the research conducted in this thesis.

Table 1.6 Cellular protein markers used to identify source of circulating EVs.

Protein tag	Cell type of origin	Assay technique	References
Annexin V	All EV	FACS (Total)	Julich *et al.* 2014
Asialoglycoprotein receptor-ß	Hepatocytes	WB	Ise *et al.* 2001, Severgnini *et al.* 2012, Shi *et al.* 2013
VE-cadherin/CD144	Sinusoidal endothelia cells (SES)	FACS/WB	Lalor *et al.* 2006, Goldman *et al.* 2014
Vascular cell adhesion molecule	SES	WB	Holmen *et al.* 2005, Lalor *et al.* 2006
E-Selectin	SES	WB	Daneker *et al.* 1998, Holmen *et al.* 2005, Lalor *et al.* 2006
CD41	Platelets	FACS	Mitjavila-Garcia et al. 2002, Bagamery et al. 2005, van Velzen et al. 2012
Pselectin/CD62P	Activated platelets	FACS/WB	Murakami *et al.* 1996, Jy *et al.* 1999, Lu *et al.* 2011
Tissue factor/CD142	Activated platelets	FACS/WB	Panasiuk *et al.* 2007
CD1d tetramer	NK T cells	FACS	Miyagi *et al.* 2003, Stenstrom *et al.* 2005, Montoya *et al.* 2007
CD8	CD8 T cells	FACS	Storek *et al.* 1998, Ondoa *et al.* 2005
Ly6G	Neutrophils	FACS	Rose *et al.* 2012
CD15	Neutrophils	FACS	Pillay *et al.* 2013
F4/80	KC/macrophages	FACS	Zhang *et al.* 2008, Rose *et al.* 2012
CD14	Monocytes/macrophages/myeloid dendritic cells	FACS	Pillay *et al.* 2013

Abbreviations: CD, cluster of differentiation; EV, extracellular vesicles; FACS, fluorescence-activated cell sorting; KC, Kupffer cell; Ly6G, lymphocyte antigen 6 complex locus G6D; NK, natural killer cell; SES, sinusoidal endothelial cell; WB, western blot.

1.8 Recent conceptual changes in NASH

Following the completion of the research outlined in this thesis, there have been new and emerging concepts of regarding the pathogenesis and treatment of NASH. This short review will focus on two topics, namely contemporary research regarding the role

of the microbiome in NASH pathogenesis, and novel treatment options based on potential molecular targets in NASH.

1.8.1 The role of the intestinal microbiome in NASH pathogenesis

The gut microbiota of patients with NAFLD has been the subject of extensive investigation in recent year. Several studies have demonstrating microbial dysbiosis and small intestinal bacterial overgrowth in patients with NAFLD (including those with NASH) compared with healthy counterparts (Aragones *et al.* 2019, Dornas and Lagente 2019, Duarte *et al.* 2019, Martin Mateos and Allen 2019, Milosevic *et al.* 2019). More specifically, microbial metagenomic analysis and *16S* amplification sequencing have identified significant increases in certain intestinal bacterial phyla and species, such as *Bacteroides* and *Ruminococcus,* in NASH patients compared with non-NASH controls (Boursier *et al.* 2016). *Escherichia coli* and *Bacteroides vulgatus* intestinal colonisation has been observed in individuals with advanced liver fibrosis (Loomba *et al.* 2017, Caussy and Loomba 2018, Jayakumar and Loomba 2019). In fact, an associated between the abundance of Gram-negative gut bacteria and progression of liver fibrosis is now well established (Ilan 2012, Zhu *et al.* 2015, Ghoshal *et al.* 2017).

It has been hypothesised that high dietary sugar and saturated fat content, as well as increased antibiotic use, selectively favour certain intestinal bacterial species and reduce luminal microbial complexity (Friedman *et al.* 2018). In turn, this leads to dysbiosis. When coupled with reduced bacterial fermentation of non-digestible carbohydrates, the result can be impaired bacterial production of short chain fatty acids (ScFA) (Malik *et al.* 2010). ScFAs are used by enterocytes as a source of energy (Schonfeld and Wojtczak 2016). Further, a decreased supply of ScFAs within the intestine causes aberrant tight junction expression. This leads to increased intestinal permeability, which allows intestinal bacteria, fungi and associated pathogen-associated molecular patterns (PAMPs) to translocate the mucosa layer and enter the portal circulation (Hiippala *et al.* 2018). A consequence could be induction of hepatic inflammation via innate and adaptive immune responses, including activation of inflammasome pathways (Figure 1.17). As described in thesis Sections 1.3 and 1.7, these inflammatory pathways are at least partly responsible for hepatic injury, fibrosis and eventual cirrhosis in NASH.

Multiple animal studies have shown a significant beneficial effect of probiotic administration in NASH models; the findings are summarised in a review by Perumpail and colleagues (2019). Unfortunately, only a few human studies have investigated the effects of probiotics as a treatment for NASH. Ma *et al.* (2013) examined four randomised control trials involving 134 NAFLD/NASH patients and found that modulation of the gut microbiota using probiotic therapy not only significantly decreased hepatic injury, as measured by ALT and AST, but also reduced circulating total-cholesterol and TNFα. Notwithstanding the limitations of small cohort sizes and relatively short study duration (median 3.75 months), the results of these studies are promising.

1.8.2 Potential targets and future treatment strategies

Maintenance of a healthy diet, regular exercise and weight loss are the current mainstay of NAFLD treatment (Ok *et al.* 2018, Panera *et al.* 2018, Sporea *et al.* 2018, Brunner *et al.* 2019, Ratziu *et al.* 2019). However, poor patient compliance with these lifestyle interventions remains a significant barrier to treatment (Neuschwander-Tetri 2009). Coupled with the increasing prevalence and burden of disease, this makes treatment of NASH a pressing public health issue. At the time of writing (August 2019), there are currently no US Food and Drug Administration-approved treatments for NASH. Several Biotechnology and pharmaceutical companies are currently developing NASH-targeted therapies with numerous clinical trials currently planned or underway (see Table 1.7). Such agents or devices (eg Revita Duodenal Mucosal Resurfacing) generally target one of five pathways. These include, pathways involved in modulation of 1) oxidative metabolism of FAs, 2) *de novo* lipogenesis, 3) oxidative stress/inflammation, 4) apoptosis or 5) fibrosis (see Figure 1.18). Only two agents, obeticholic acid (OCA) and Elafibranor will be discussed since this area is beyond the scope of this thesis. OCA is discussed in detail in Chapter 7, Section 7.2.4. Elafibranor is discussed here.

1.8.2.1 Elafibranor

Elafibranor is a multipotent agent capable of activating PPARα, PPARγ, PPARδ with a preferential PPARα binding specificity. Modulation of these transcription factors alters the expression of genes involved in lipid metabolism, energy homeostasis and inflammation (Souza-Mello 2015). Elafibranor recently passed the phase IIa trial phase with 182 non-cirrhotic NASH patients given either 80 or 120 mg drug per day. After 12

months of treatment, patients receiving Elafibranor showed improved inflammatory markers, plasma lipids, glucose homeostasis and hepatic insulin resistance (Ratziu *et al.* 2016). This agent is currently in phase III trials (Table 1.7).

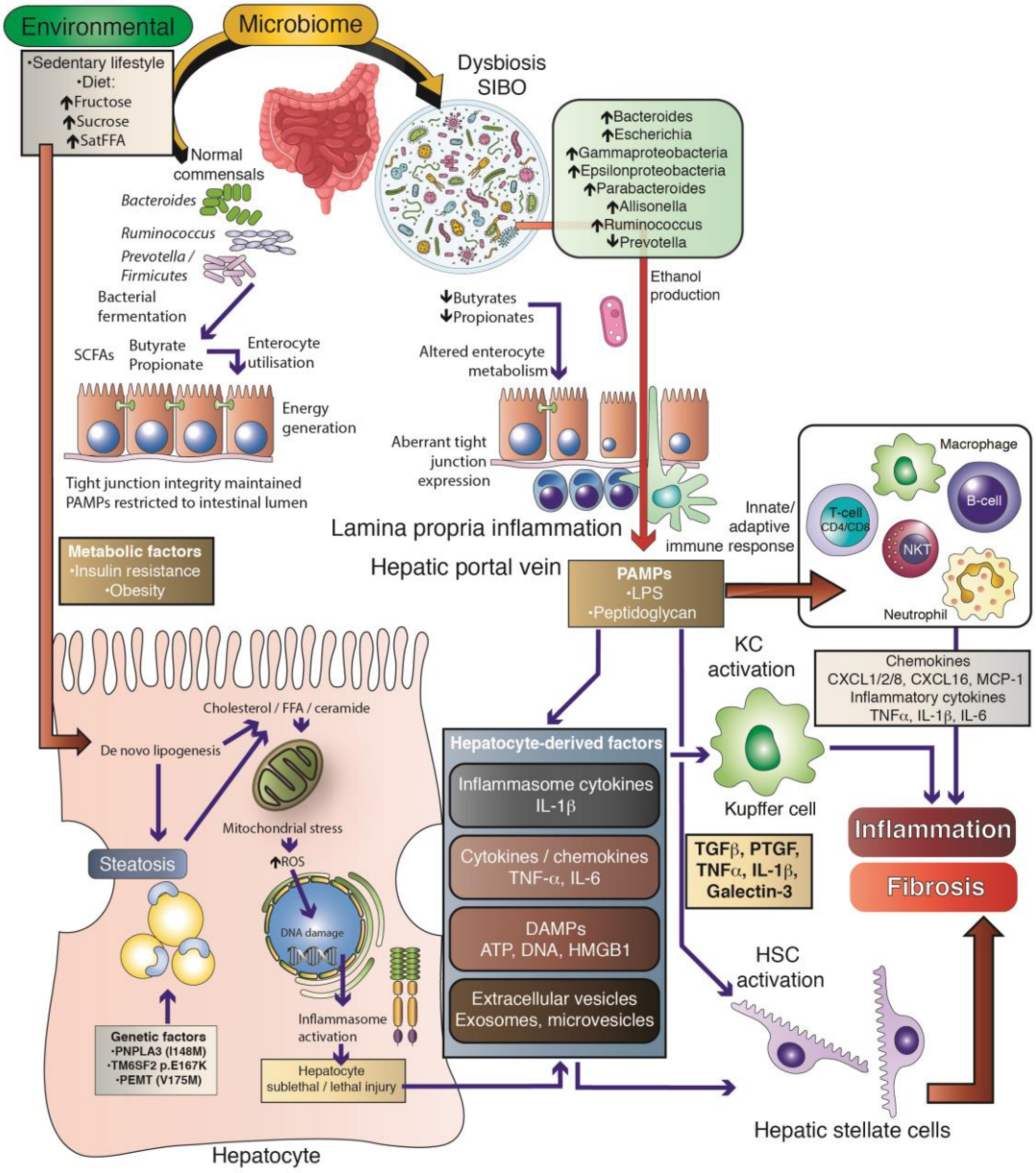

Figure 1.17 Integrated role of the dietary and microbial factors in the pathogenesis of lipid-mediated liver injury, inflammation and fibrosis.

See text for details.

Abbreviations: CXCL, chemokine ligand; FFA, free fatty acid; HSC, hepatic stellate cell; IL, interleukin; LPS, lipopolysaccharide; KC, Kupffer cell; MCP1, monocyte chemoattractant protein-1; NKT, natural killer T-cell; PAMP, pathogen-associated molecular patterns; PTGF, platelet-derived growth factor; ROS, reactive oxygen species; SatFFA, saturated fatty acid; SCFA, short chain fatty acid; SIBO, small intestine bacterial overgrowth; TGF-β, transforming growth factor beta; TNF-α, tumor necrosis factor alpha.

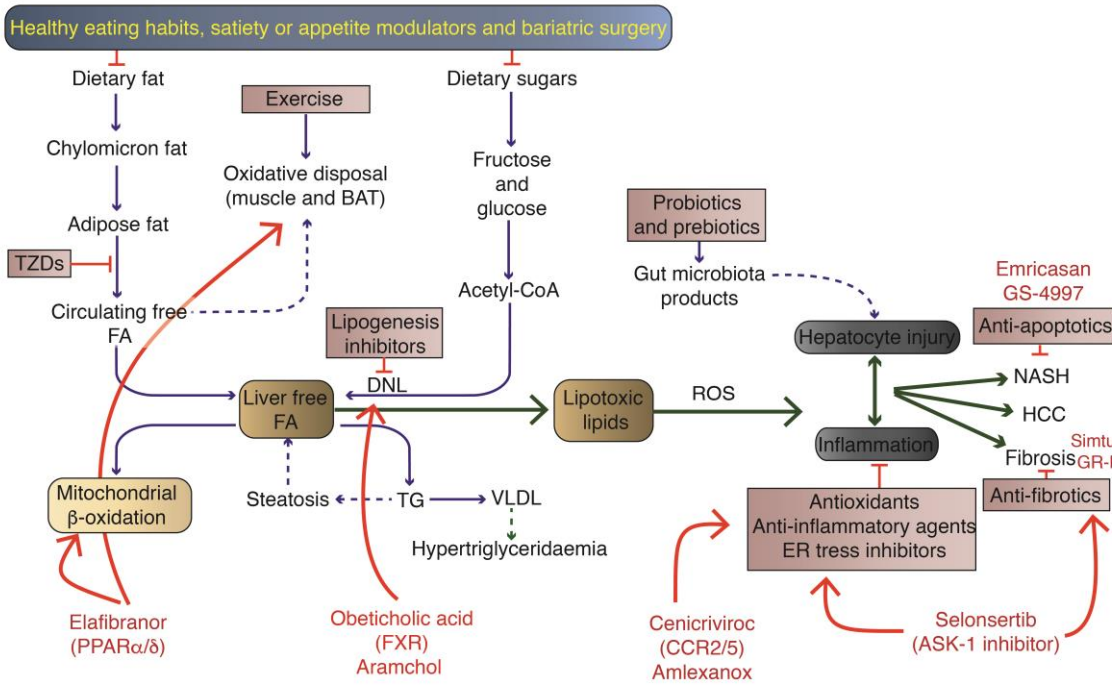

Figure 1.18 Potential therapeutic target points within the lipotoxic model of NASH.

As previously described (Section 1.3.1), lipids accumulate within the liver as a consequence of excessive fat and sugar intake which culminates in increased circulating free fatty acids (FA) and *de novo* lipogeneis (DNL). Sedentary lifestyle and insulin resistance also contribute to the FA pool by reducing mitochondrial β-oxidation. In turn, FA and cholesterol generate reactive oxygen species (ROS) through mitochondrial injury, in turn, causes hepatocyte injury and inflammation. These factors increase the risk of NASH, liver fibrosis and carcinogenesis. The pink boxes represent potential target sites in the pathway. Several phase III agents shown in red text (see Table 1.7 for additional agents). Image adapted from Brunt *et al.* (2015).

Abbreviations: BAT, brown adipose tissue; HCC, hepatocellular carcinoma; NASH, non-alcoholic steatohepatitis; TZDs, thiazolidinediones; VLDL, Very-low-density lipoprotein

Table 1.7 Current NASH treatment clinical trials.

Phase	Status	Clinicaltrials.gov identifier	Agent	Study	Mechanism	Study population - liver related inclusion criteria	Completion date
I	Recruiting	NCT02808312	**GS-9674**	Pharmacokinetics and pharmacodynamics of GS-9674 in adults with normal and impaired hepatic function.	**FXR agonist**	Three cohorts: mildly impaired and normal hepatic functin, moderate hepatic impairment and severe hepatic impairment.	Oct-18
I	Not yet recruiting	NCT02612662	**AZD4076**	A study to assess the safety and tolerability of single doses of AZD4076 in healthy male subjects.	**miR-103/-107 antagonist**	Normal liver function.	Dec-20
II	Recruiting	NCT02684591	**Aramchol**	Aramchol for HIV-associated NAFLD and lipodystrophy (ARRIVE).	**SCD inhibitor**	One or more risk factor for more severe liver disease	Feb-18
II	Recruiting	NCT02787304	**Volixibat**	Volixibat (SHP626) in the treatment of adults With NASH.	**ASBT inhibitor**	Histologic confirmation of NASH without cirrhosis (F0-F3)	Jul-18
II	Not yet recruiting	NCT03486899	**BMS-986036**	A study of experimental medication BMS-986036 in adults with NASH and stage 3 liver fibrosis (FALCON 1).	**FGF-21 analogue**	Histologically confirmed NASH with stage 3 liver fibrosis according to NASH CRN classification	Sep-21
II	Recruiting	NCT02443116	**NGM-282**	Study of NGM282 in patients with NASH.	**FGF-19 analogue**	Histologically confirmed NASH diagnosis	Sep-19
II	Not yet recruiting	NCT03375788	**Tesamorelin**	Growth Hormone Releasing Hormone Analog to Improve Nonalcoholic Fatty Liver Disease and Associated Cardiovascular Risk	**GHRH analogue**	Hepatic steatosis as demonstrated by either a) Grade 1+ steatosis on a liver biopsy performed within 12 months of the baseline visit, without >10% reduction in body weight or addition of medications to treat fatty liver, or b) liver fat fraction ≥5% on hydrogen-magnetic resonance spectroscopy (1H-MRS)	Oct-22
II	Not yet recruiting	NCT01792115	**Vitamin E**	Treatment for NAFLD with different doses of vitamin E.	**Anti-oxidant**	Clinical suspicion of NAFLD or elevated LFTs, steatosis on imaging,	Aug-19
II	Enrolling	NCT03059446	**Cenicriviroc**	Rollover study of Cenicriviroc for the treatment of liver fibrosis in participants with NASH.	**CCR2/CCR5 antagonist**	Successful completion of both Treatment Period 1 and Treatment Period 2, of the CENTAUR Study (652-2-203), including a Year 2 liver biopsy.	Jul-30
II	Recruiting	NCT03205345	**Emricasan**	Emricasan, a caspase inhibitor, for treatment of subjects with decompensated NASH cirrhosis (ENCORE-LF)	**Caspase inhibitors**	Cirrhosis due to NASH with exclusion of other causes of cirrhosis.	Aug-19
II	Recruiting	NCT03042767	**IMM-124e**	Anti-LPS antibody treatment for paediatric NAFLD.	**Anti-LPS IgG-rich bovine antibody (Paediatric NAFLD)**	Nonalcoholic fatty liver disease (NAFLD) diagnosis confirmed by liver biopsy or MRI.	May-19
II	Recruiting	NCT03061721	**Saroglitazar**	Saroglitazar magnesium in patients with NAFLD and/or NASH.	**PPARα/γ agonist**	Documented diagnosis of NAFLD	Nov-19
III	Recruiting	NCT02704403	**Elafibranor**	Phase 3 study to evaluate the efficacy and safety of Elafibranor vs placebo in patients with NASH (RESOLVE-IT).	**PPARα/δ agonist**	NASH with NAS score ≥4	Dec-21
III	Recruiting	NCT03439254	**Obeticholic acid**	Study evaluating the efficacy and safety of Obeticholic acid in subjects with compensated cirrhosis due to NASH (REVERSE)	**FXR agonist**	Subjects with a confirmed diagnosis of NASH and a fibrosis score of 4 based upon the NASH CRN scoring system.	Jul-21
III	Not yet recruiting	NCT03053050	**GS-4997**	Safety and efficacy of Selonsertib in adults with NASH and bridging (F3) fibrosis (STELLAR 3).	**ASK1 inhibitor**	Liver biopsy consistent with NASH and bridging (F3 fibrosis) according to the NASH CRN classification.	Feb-23
IV	Not yet recruiting	NCT03434613	**Rosuvastatin +/- ezetimibe**	A randomized, prospective, open label, active control, phase IV study to evaluate the effects of statin monotherapy or dtatin / Ezetimibe combination therapy on hepatic steatosis in patients with hyperlipidemia and NAFLD	**HMG-CoA reductase and NPC1L1 inhibitor**	Patients diagnosed with fatty liver by abdominal ultrasonography or liver fibroscan.	Jan-20

Abbreviations: ASBT, apical sodium-dependent bile acid transporter; ASK1, Apoptosis signal-regulating kinase 1; CCR, C-C chemokine receptor; CRN, Clinical Research Network; FGF, fibroblast growth factor; FXR, farnesoid X receptor; GHRH, growth hormone-releasing hormone; HIV, human immunodeficiency virus; LPS, lipopolysaccharide; miR, micro ribonucleic acid; MRI, magnetic resonance imaging; NAS, non-alcoholic fatty liver disease activity score; NASH, non-alcoholic steatohepatitis; NCT, ClinicalTrials.gov registry number , NPC1L1, Niemann-Pick C1-Like 1; PPAR, peroxisome proliferator-activated receptor; SCD, stearoyl-CoA desaturase 1.

1.9 Research aims and objectives

The major aims of the research described in this thesis are summarised below.

1. Develop an *in vitro* model for loading hepatocytes with FC in order to study the cellular mechanisms of lipotoxicity exerted by this lipid species in live cells (Chapter 3).
2. Test whether FC-mediated injury and cell death to hepatocytes is linked to mitochondrial damage and/or ER stress (Chapter 4).
3. Characterise the role of JNK-1 in FC-mediated lipotoxicity to hepatocytes (Chapter 4).
4. Examine whether FC-induced lipotoxicity liberates EVs from injured and apoptotic hepatocytes (Chapter 5).
5. Determine whether circulating EVs in experimental (murine) and human NASH contain markers of hepatocytes, as well as inflammatory cells and platelets (Chapter 6).

CHAPTER 2
General materials and methods

Techniques commonly used throughout the thesis are described in this chapter. Detailed procedures for more specialised methods will be included in the later relevant chapters.

2.1 Reagents and other research materials, including commercial assay kits

Reagents were obtained from the following providers:

Sigma Aldrich (St Louis, MO)

2'7'-Dichlorofluorescein diacetate, ammonium persulfate (APS), bovine serum albumin (BSA) (≥96% purity for tissue culture; ≥98% for western blot, and ≥99.9% for palmitic acid dissolution), cacodylic acid, 3-[(3-cholamidopropyl)-dimethylammoniol]-1-propanesulfonate (CHAPS), cyclosporine A, diethylpyrocarbonate (DEPC), dimethylsulphoxide (DMSO), ethylene glycol tetraacetic acid (EGTA), filipin III (from *Streptomyces filipines)*, 4-(2-hydroxyethyl)-1-piperazine ethanesulfonic acid (HEPES), Höechst 33342, hydrogen peroxide (H_2O_2), Igepal CA-630, metaphosphoric acid, human unmodified low density lipoprotein (LDL), NaCl, nicotinamide, Nile red, oil red O, palmitic acid, phosphatase inhibitor cocktail 1 & 2, ponceau S, 2-propanol, protease inhibitor cocktail, saponin, sodium bicarbonate, sodium deoxycholate, sodium dodecyl sulphate (SDS), sucrose, tetramethylrhodamine methyl ester percholate (TMRM), triethanolamine, TRI-reagent, triton X-100, trypan blue, tween-20, and 2-vinylpyridine.

Amresco (Solon, Ohio, USA)

Calcium chloride dihydrate, ethylenediaminetetraacetic acid (EDTA), phosphate buffer saline (PBS) tablets.

ProSciTech (Thuringowa, Qld, Australia)

Osmium tetroxide 4% aqueous solution, hexamethyldisilazane (HMDS), 11 mm plastic coverslips, parafomaldehyde 16% (v/v), glutaraldehyde 25% (v/v), uranyl acetate, digitonin ($C_{56}H_{92}O_{29}$), IM032 Crystal mount™, Hematoxylin Gill's No.2.

Life Technologies (Carlsbard, CA, USA)

William's E media (WEM), Hank's balanced salt solution (HBSS 1X and 10X), rat-tail collagen, RPMI 1640, dithiothreitol (DTT), ProLong® Gold antifade, penicillin and streptomycin, fetal calf serum, ATP determination kit, Superscript III, Annexin V-Alexa Fluoro® 350

Other

Arylamide/bis-acrylamide (30%, 29:1 ratio), iQ SYBR Green Supermix, Precision Plus™ Prestained Protein standards, qPCR reaction tubes and plate sealers were all purchased from Bio-Rad (Hercules, CA). Percoll™ and tetramethylethylenediamine (TEMED) were from GE Healthcare (Buckinghamshire, UK). Free cholesterol E (free cholesterol molarity determination) and NEFA C (fatty acid molarity determination) kits were purchased from Wako (Osaka, Japan). NE-PER nuclear:cytoplasmic extraction kits, SuperSignal West Pico and Femto enhanced chemiluminescence (ECL) substrate solution were purchased from ThermoScientific (Rockford, IL); Western Lightning Plus ECL (Cayman Chemicals, Ann Arbor, MI). Membrane fluidity kit was from Marker Gene Technology (Eugene, OR). Random and oligo (dT) primers and Cytotox 96© non-radioactive cytotoxicity assay were from Promega (Madison, WI). Ethanol, glycine, HCl, methanol, and Tris (tris-[hydroxymethyl] aminomethane) were purchased from Astral Scientific (Caringbah, NSW, Australia); polyvinylidene fluoride (PVDF), sterilising filters (22 µm) and deionised ultrapure water (d.H_2O) were obtained from a Milli-RO® water purification system from Millipore (Billerica, MA). Cell culture flasks (T_i 75) and dished (T_i 55), 6-, 24- and 96-well plates were from Iwaki Sterilin (Staffordshire, UK); Sterile 15 mL plastic screw top tubes used in cell culture were purchased from Sterilin Bibby (Staffordshire, UK); 50 mL plastic screw tops and 4-chamber plastic slides for cell culture were from Nunc (Roskilde, Denmark). Cell strainers (100 µm) were purchased from BD Biosciences (Franklin Lakes, NJ);

Centrifuge tubes 5 mL and 15 mL from Beckman Coulter (Brea, CA). ELISA kits for murine IL-6, IL1-β and TNF-α were purchased from R&D Systems (Minneapolis, MN), while murine serum IL-18 ELISA kits were from Medical & Biological Laboratories Co., Ltd. (Nagoya, Japan). Paraformaldehyde was obtained from Electron Microscopy Sciences (Hatfield, PA); ultra-pure water was from Baxter Healthcare (Toongabbie, NSW), and types 2 and 4 collagenase were purchased from Worthington (Lakewood, NJ). Ketamine hydrochloride and xylazil were from Troy Laboratories (Glendenning, NSW). Finally, skim milk powder (Diploma, Fonterra Foodservices, North Ryde, NSW) was purchased from a local food retailer.

ELISA kits for human hyaluronic acid (HA) were purchased from Echelon® (Utah, USA); hepatocyte-specific cytokeratin-18 markers M30 and M65 (EpiDeath65®) kits were purchased from Peviva (Broma Sweden); pro-collagen III *N*-terminal peptide (PIIINT) kits were from Cusabio (Wuhan, Hubei, China); EVs (MP) ELISA kits (based on annexin V analysis) were from Hypen BioMed (Neuville-Sur-Oise, France).

2.2 JNK inhibitors

Specific JNK inhibitors CC-401, CC-930 and CC-003 were from kindly provided by Celgene (San Diego, CA), courtesy of Brydan Bennett (see acknowledgements).

2.3 Antibodies

Antibodies were purchased from Abcam (Oxford, UK), Cell Signalling Technology (Danvers, MA), R&D Systems (Minneapolis, MN), Santa Cruz (Santa Cruz, CA), BD Pharmingen (Franlin Lakes, NJ), Life Technologies/ Invitrogen (Carlsbad, CA), BioLegend (San Diego, CA), eBioscience (San Diego, CA), AbD Serotec (Raleigh, NH), Polyscience (Warrington, PA) and Novus Biologicals (Littleton, CO). Primary and secondary antibody supplier details, catalogue numbers, and application details are shown in Tables 2.1 and 2.2, respectively.

Table 2.1 Primary antibodies used in this research

Antibodies	Host	Supplier	Catalogue number	Application	Dilution	Band (kDa)
ASGPR 1/2	Rabbit	Santa Cruz	sc-28977	WB	1:200	50, 95
β-actin	Mouse	Sigma-Aldrich	A5441	WB	1:5000	42
Bcl-xL	Rabbit	Cell Signaling	2764	WB	1:900	30
Bax	Rabbit	Santa Cruz	sc-6236	WB	1:200	23
Cathepsin B	Mouse	Abcam	ab58802	WB	1:750	38
c-Jun	Rabbit	Cell Signaling	9165	WB	1:900	48
Chop	Mouse	Cell Signaling	2895	WB	1:1000	27
Cytochrome C	Rabbit	Cell Signaling	4272	WB	1:1000	14
COX-IV	Rabbit	Cell Signaling	4844	WB	1:1000	17
COX-IV	Mouse	Abcam	ab14744	IF	1:500	16
F4/80	Rat	Abcam	MCA497R	IHC, IF	1:135, 1:40	160
GRP78	Rabbit	Abcam	ab21685	IF, WB	1:1400	78
HMGB1	Rabbit	Abcam	ab18256	IF, WB	1:80, 1:900	30
HNF-4α	Mouse	Abcam	ab41898	IF, WB	1:80, 1:500	52
HSP60	Rabbit	Cell Signaling	4870S	WB	1:1000	60
HSP90	Goat	R&D Systems	AF3775	WB	1:2000	90
ICAM-1	Goat	R&D Systems	AF796	WB	1:500	80
ICAM-1	Mouse	R&D Systems	BBA3	WB	1:500	80
SAPK/JNK	Rabbit	Cell Signaling	9258	WB	1:900	46, 54
TLR4	Rabbit	Cell Signaling	2219	IF	1:50	95-100
TLR4	Rabbit	Abcam	ab13556	WB	1:900	95-100
TLR9	Rabbit	Abcam	ab13928	WB	1:900	110
Lamin B1	Rabbit	Abcam	ab16048	IF	1:500	68
LAMP	Rat	Abcam	ab13524	IF	1:100	105
LDLR	Rabbit	Abcam	ab52818	IF, WB	1:200, 1:1700	140
Na/K-ATPase	Mouse	Abcam	Ab7671	IF	1:90	112
NFκB p65	Rabbit	Cell Signaling	4764	IF, WB	1:80, 1:2000	65
Phospho-cJun	Rabbit	Cell Signaling	3270	IF, WB	1:80, 1:750	48
Phospho-SAPK/JNK	Rabbit	Cell Signaling	4668	IF, WB	1:750	46, 54
Phospho-JNK1	Rabbit	Abcam	ab18680	IF, WB	1:40, 1:750	48
TBP	Mouse	Abcam	ab818	WB	1:2000	38
VCAM-1	Goat	R&D Systems	AF643	WB	1:500	85-110
VCAM-1	Mouse	R&D Systems	BBA5	WB	1:500	85-110

Abbreviations for Table 2.1: ASGPR, asialoglycoprotein receptor; Bcl-xL, B-cell lymphoma-extra large; Bax, bcl-2-like protein 4; Chop, C/EBP homologous protein; COX-IV, cytochrome c oxidase subunit; GRP78, glucose regulated protein-78; HMGB1, high mobility group box 1; HNF, hepatocyte nuclear factor; HSP90, heat shock protein-90; HSP60, heat shock protein-60; ICAM, inter-cellular adhesion molecule-1; JNK, c-Jun N-terminal kinase; TLR, toll-like receptor; LAMP, lysosome-associated membrane protein; LDLR, LDL receptor; Na/K-ATPase, sodium-potassium ATP-ase; NFκB p65, nuclear factor kappa-B protein 65; TBP, tata-box binding protein; VCAM-1, vascular cell adhesion protein 1; WB, western blot; IF, immunofluorescence. Antibodies were purchased from Abcam (Cambridge, UK), AbD Serotec (Oxford, UK), Cell Signalling (Danvers, MA), R&D Systems (Minneapolis, MN) and Santa Cruz Biotechnology, Inc (Santa Cruz, CA).

Table 2.2 Secondary antibodies used in this research

Antibody	Host	Supplier	Catalogue number	Conjugate	Application	Dilution
Goat	Rabbit	Santa Cruz	sc-2768	HRP	WB	1:10,000
Mouse	Goat	Santa Cruz	sc-2005	HRP	WB	1:10,000
Rabbit	Goat	Santa Cruz	sc-2004	HRP	WB	1:10,000
Rat	Goat	Santa Cruz	sc-2006	HRP	WB	1:10,000
Goat	Chicken	MP	A-21467	Alexa 488	IF	1:1,000
Mouse	Goat	Invitrogen	A-11001	Alexa 488	IF	1:1,000
Rabbit	Chicken	MP	A-21441	Alexa 488	IF	1:1,000
Rat	Chicken	MP	A-21470	Alexa 488	IF	1:,1000
Rabbit	Chicken	MP	A-21427	Alexa 555	IF	1:10,000

Abbreviations for Table 2.2: HRP, horseradish peroxidase; IF, immunofluorescence; WB, western blot. Antibodies were purchased from Invitrogen (Carlsbad, CA), Molecular Probes (Eugene, OR), and Santa Cruz Biotechnology, Inc (Santa Cruz, CA).

2.4 Animals and diets

All animal experimentation conformed to the high standards stipulated by NHMRC and international guidelines, and was approved by the ANU Animal experimentation Ethics Committee (protocol A2012/22). Only female mice were used. Mice used to obtain liver cells for primary hepatocytes and primary KC culture were C57B/6J strain. Wildtype (WT) and *Myd88*$^{-/-}$ mice (C57B/6J strain) were obtained from Animal Services Division, ANU Bioscience Research Facility (Canberra). *Tlr2*$^{-/-}$ and *Tlr4*$^{-/-}$ mice were kindly provided by Dr Shaun Summers from Monash Medical Centre Animal Facilities (Clayton Victoria), while *Jnk1*$^{-/-}$ and *Jnk2*$^{-/-}$ mice were obtained (by kind gift) from Dr David Nikolic-Paterson (Department of Nephrology, Monash Medical Centre, Clayton Victoria).

NOD.B10 strain (WT and *Alms1* mutant [*foz/foz*]) mice were used, as indicated, in relevant chapters pertinent to *in vivo* correlations with *in vitro* experiments. NOD.B10 strain mice were bred at The Canberra Hospital (TCH) animal facility.

All mice received food, water *ad libitum* and were maintained in a sterile animal facility under constant 12-hour light/dark cycle at 22°C, with relative humidity greater than 40%. Mice were housed (~4/cage) in individually ventilated cages (IVC) (Tecniplast, Philadelphia, PA). Cages were lined with sterile ALPHA-dri PLUS® (Sheppard Specialty Papers, Richland, MI). Unless otherwise indicated, mice were fed chow (5% fat, 67% carbohydrate, 19% protein, 0% cholesterol) from

weaning until sacrifice (age: 6–8 weeks). NODB.10 mice were either fed chow or atherogenic (Ath) diet (23% fat, 45% carbohydrate, 20% protein, 0.2% cholesterol) (SF03-020, Specialty Feeds, Glen Forrest, WA, Australia).

2.5 Primary hepatocyte isolation

Primary hepatocytes were isolated from mice as previously outlined (Berry *et al.* 1997, Van Rooyen *et al.* 2011). For each experiment, hepatocytes isolated from a minimum of 3–4 mice were pooled, prior to culturing on plates. Briefly, the procedure is outlined below:

2.5.1 Reagents

William's E media and 1X Hank's buffered salt solution (HBSS). Solutions were purchased commercially and required no additional preparation.

0.5 M EDTA stock solution. EDTA (18.61 g) was dissolved in distilled water (80 mL), pH corrected to 8.0 with NaOH, and final volume adjusted to 100 mL. Solution was sterile filtered (22 µm), aliquoted and stored at 4°C until ready for use.

1 M $CaCl_2$ stock solution. $CaCl_2$ (11.1 g) was dissolved in distilled water (100 mL). Solution was filter sterilised (22 µm), aliquoted, and stored at 4°C until ready for use.

Penicillin-streptomycin (pen-strep) antibacterial solution. Solution was purchased commercially (100X strength) and only required dilution prior to use.

Perfusion buffer stock solution (20 mM HEPES, 404 µM $NaHCO_3$, 1X pen-strep in HBSS, pH 7.4). HEPES (2.38 g) and $NaHCO_3$ (17 mg) were dissolved in HBSS (500 mL). Pen-strep (5 mL) was added, pH adjusted to 7.4, and filter sterilised (22 µm). Buffer was aliquoted into four sterile falcon tubes, as per Figure 2.1. Solutions were pre-warmed to 37°C in water bath prior to use. Perfusion solutions #2 and #4 received additional components as described below.

Perfusion buffer #2 (20 mM HEPES, 404 µM $NaHCO_3$ in HBSS, 0.5 mM EDTA, pH 7.4). EDTA (25 µL of 0.5 M stock) was added to the perfusion buffer solution (25 mL) and mixed thoroughly before use.

Perfusion buffer #4 (20 mM HEPES, 404 µM $NaHCO_3$ in HBSS, 1 M $CaCl_2$, 100 U/mL of type 2 collagenase, pH 7.4). $CaCl_2$ (250 µL of 1 M stock) and type 2 collagenase (Worthington, Lakewood, NJ) (~20 mg of 248 U/mg stock) were added to perfusion solution (50 mL). Collagenase was weighed out but (in order to preserve catalytic activity) not added to tube four until liver was being perfused by perfusion solution in tube two.

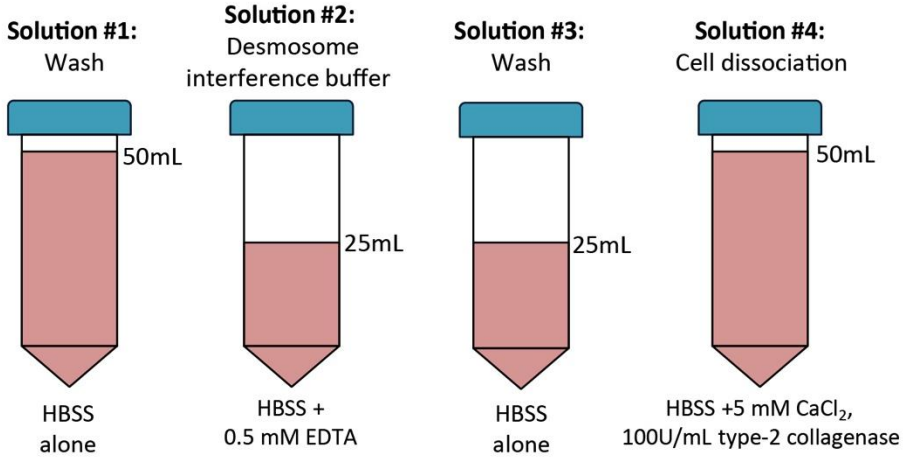

Figure 2.1 Schematic representation of perfusion buffer solutions.

Prepared perfusion buffer (50 mL) was aliquoted into tubes one and four, while 25 mL into tubes two and three. Tubes two and four were supplemented with 25 µL of 0.5 M EDTA and 250 µL of 1 M $CaCl_2$, respectively. Type 2 collagenase (100 U/mL) was added into tube four immediately before use.

Hepatocyte culture media (10 mM HEPES, 1% (m/v) BSA, 10 mM nicotinamide in William's E, pH 7.4). HEPES (2.38 g), BSA (10 g), and nicotinamide (1.21 g) were dissolved in William's E buffer (1 L), and pH adjusted to 7.4, before solution was filter sterilised (22 µm).

2.5.2 Procedure

Mice were anaesthetised by intraperitoneal injections of ketamine hydrochloride and xylazine (100 and 20 mg/kg body weight, respectively) prior to midline laparotomy. Intestines were displaced laterally to expose the portal vein (PV), before the mesentery was carefully blunt-dissected and a 22 gauge intravenous

catheter was used to cannulate the PV (this was secured in place by silk sutures). Pre-warmed buffer solutions (Figure 2.1) were infused at a rate of 8 mL/min through the catheter using a pre-calibrated peristaltic pump. Perfusion buffer solution (tube #1, 50 mL) was used to flush blood from the liver. At the onset of perfusion, the abdominal and thoracic inferior vena cavas (IVC) were severed to prevent hydrostatic pressure build-up. Cholecystectomy was performed, and evident bile (yellow) on liver surface was washed away with saline to prevent bile contamination of the liver.

Following the initial "wash-out", the liver was perfused with EDTA-containing buffer solution #2 (25 mL). This chelates ionic calcium, thereby allowing desmosome-cytoskeleton dissociation (Mattey and Garrod 1986, Berry *et al.* 1997). EDTA solution was flushed out by perfusion buffer solution #3 (25 mL). Finally, perfusion buffer #4 (50 mL) containing 100 U/mL of collagenase and $CaCl_2$ (to scavenge remaining EDTA), was perfused into the liver, causing matrix digestion so that the liver becomes soft and swollen.

Following collagenase digestion, the liver was excised and cells suspended in ice cold culture media. The final homogenate was then passed through a 100 µm cell sieve and centrifuged (100 x g, 2 min, 4°C) to pellet hepatocytes. Non-parenchymal cell fractions (present in the supernatant) were discarded and hepatocytes resuspended in ice-cold William's E buffer (50 mL). This step was repeated twice to purify parenchymal cell fractions. Cellular viability was quantified using trypan blue exclusion (TBE) (Strober 2001). Hepatocytes (>90% viability) were seeded onto rat-tail collagen coated plates (5 µg/cm^2) at a cell density of ~6.5 x 10^4 viable cells/cm^2 and cultured in WEM.

After 4 hours, non-adherent cells were washed off with sterile HBSS (37°C, pH 7.4), and the remaining adherent primary hepatocytes were loaded with free cholesterol (FC) by incubation with unmodified human low density lipoprotein (LDL) (20–40 µM) or control (no LDL) culture media (37°C, pH 7.4). Cells were grown for 24 hours (37°C, 5% CO_2), after which cells and supernatant were collected and stored at –80°C until use. Further specific experimental details are described in relevant Chapters (Chapters 4 and 5).

2.6 Collection and processing of mouse and human blood samples for extracellular vesicles analysis

Venous blood was collected from mice and humans subjects (patients with various liver diseases and health controls, see Chapter 6) for EV isolation. As described in later Chapters 5 and 6, EV fractions were assayed by ELISA, western blotting, and flow cytometry.

2.6.1 Mouse blood collection

For *in vivo* studies of circulating EVs in experimental NASH, NOD.B10 mice received diets identical to those used in earlier dietary experiments (Van Rooyen *et al.* 2011) (2.4). At experimental endpoints, mice were anaesthetised, as per Section 2.4.1 and blood was collected in citrate anticoagulant. Tubes were kept at room temperature, and were gently mixed (avoiding vigorous agitation) to prevent activation of blood EVs (Simak *et al.* 2006, Yuana *et al.* 2011). Collected blood samples were processed immediately (always ≤2 hours for mouse samples; though this was not always possible for human samples), initially centrifuged (1,500 x g, 15 min, RT) and pellet discarded. The supernatant, which constitute the platelet-rich plasma (PRP) fraction, was further centrifuged (13,000 x g, 2 min, RT) to remove platelet and cellular debris, resulting in a platelet-free plasma (PFP) fraction. This fraction was frozen at –80°C (Lacroix *et al.* 2012) and later used for EV isolation and characterisation by ELISA quantification, western blotting, and conduct of immunophenotyping by flow cytometry (described in detail, Section 2.7.1.2).

2.6.2 Human blood sample collection

Venous blood was taken from patients with NAFLD across the clinical spectrum (simple steatosis [SS], NASH and advanced fibrosis), those with other liver disease and healthy controls (recruitment details described in Chapter 6, Section 6.3). Blood was collected by certified phlebotomists at The Canberra Hospital Pathology Collection Centre into citrate-filled vacutainer tubes. Within 1–2 hours of collection, samples were centrifuged (1,500 x g, 15 min, RT) and pellet discarded. Thereafter, PRP supernatant was processed in an identical manner to mouse samples (see above, Section 2.6.1).

2.7 Extracellular vesicle isolation and analysis

Extracellular vesicle (EV)s (≤1.0 μm) were isolated from tissue culture supernatant (Section 2.5.1.1) and PFP (Section 2.6) by a previously reported method (Baj-Krzyworzeka *et al.* 2002, Orozco and Lewis 2010). Briefly, details are outlined below:

2.7.1 Procedure

2.7.1.1 EV isolation from primary hepatocyte supernatant

From *in vitro* experiments, conditioned media from primary hepatocytes treated with LDL (Section 2.5.1) was collected and centrifuged (500 x g, 5 min, RT, no brakes) to pellet cellular debris and fractionate residual lipid colloids. Further centrifugation (10,000 x g, 10 min, RT) was performed to remove mitochondrial and other subcellular organelles. Finally, to ensure the smaller EVs (0.03–0.1 μm) were pelleted, further ultracentrifugation (100,000 x g, 90 min, RT) (Baran *et al.* 2010, Baj-Krzyworzeka *et al.* 2012) was performed. Final EV pellets were processed separately according to purpose of use, as follows:

PS residues in supernatant (neat) and EV fractions (post-selective centrifugation at 10,000 x g and 100,000 x g) were quantified by ELISA (Hyphen BioMed, Neuville-Sur-Oise, France), conducted as per Manufacturer's instructions.

EV fractions for use in primary murine KC-stimulation experiments were resuspended in sterile WEM, and protein quantified by NanoDrop 1000 spectrophotometer (ThermoScientific, Wilmington, DE, USA). EV pellets were normalised to 10 μg protein/mL for use in experiments with primary KCs, as per Section 2.8. These fractions were stored at –80°C until use.

EV fractions for use in WB were resuspended in radio immunoprecipitation assay (RIPA) buffer containing protease and phosphatase inhibitors (Sigma Aldrich) prior to ultrasound sonication (60 sec) (Vasina *et al.* 2013). Homogenised protein was quantified using DC™ Protein Assay (BioRad, Hercules, CA), as per Manufacturer's instructions. These fractions were normalised to 6.25 mg protein/mL. Further details pertaining to WB are described in Section 2.13.

2.7.1.2 EV isolation from mice

For *in vivo* studies of circulating EVs in experimental NASH, NOD.B10 mice received diets identical to those used in earlier dietary experiments (Van Rooyen *et al.* 2011). In anaesthetised animals, venous blood was collected, as outlined in Section 2.6.1.

PS equivalents of EV fractions were quantified by commercially available ELISA (Hyphen BioMed, Neuville-Sur-Oise, France). PFP samples stored at –80°C were rapidly thawed at 37°C (to minimise ice crystals formation) (Orozco and Lewis 2010) before analysis of PS content.

Smaller EVs (0.03–0.1 μm) were pelleted, as described above (Section 2.7.1.2). EV fractions were prepared according to purpose of use, as follows.

EV fractions intended for flow cytometry were suspended in PBS and stored at –80°C until ready to use. Smaller EVs/ endosomes pelleted at 100,000 x g tend to have lower abundance of PS residues compared to larger sized EVs/ectosomes; the later tend to be associated with formation of lipid rafts, which are membrane regions containing higher levels of cholesterol and signalling molecules. Endosomes transport different cargo than the ectosomes originating from the same cell, showing more transporting selectivity for intracellular proteins and other molecules (Baj-Krzyworzeka *et al.* 2012). Detecting EVs that exhibit double-positive staining for annexin V and specific cell surface markers allow the cell of origin to be characterised. Bearing this in mind, EV populations were first identified in flow cytometry by positive annexin V staining (PS conjugate) (Becton Dickinson, San Jose, USA). Antibodies to different cell type-specific antigens were then used to identify the cellular origin of circulating EV preparations. For example, CD41 fluorescence was taken to represent cells originating from platelets, CD144 from endothelial cells, and F4/80 representing EV originating from murine macrophages (Simak and Gelderman 2006, Simak *et al.* 2006). A summary of the specific monoclonal antibodies used in identification of EV origin by flow cytometry is presented in Table 2.3 (Fuhrer *et al.* 1994, Stockert 1995, Hanna *et al.* 2003, Iacono *et al.* 2007, Lynch and Ludlam 2007, Shugarts and Benet 2009, Weidle *et al.* 2010, Guy *et al.* 2011, Padda *et al.* 2011).

To characterise the EV cargo of smaller ectosomes, WB techniques were used, as described above.

Table 2.3 Specificities of monoclonal antibodies used to identify cell types of origin of EVs

Subtypes	Antigen	Protein name	Mode of detection	Ref
Endothelial	CD31 (CD42–)	PECAM-1	Flow cytometry	1
	CD31 (CD41–)	PECAM-1	Flow cytometry	1
	CD62E	E-Selectin	Flow cytometry	1
	CD144	VE Cadherin	Flow cytometry, WB	1
	CD51avb3	Vitronectin	Flow cytometry	1
	CD146	MelCAM	Flow cytometry	1
	CD105	Endoglin	Flow cytometry	1
	CD54	ICAM-1	Flow cytometry	1
Platelet	CD42a	GPIX	Flow cytometry	1
	CD42b	GPIb	Flow cytometry	1
	CD42	CDIbIX	Flow cytometry	1
	CD41	GPIIbIIIa	Flow cytometry	1
	CD61	GPIIIa	Flow cytometry	1
	CD62P	P-selectin activation	Flow cytometry	1
Monocyte	CD14	Endotoxin receptor	Flow cytometry	1
Erythrocyte	CD235	Glycophorin A	Flow cytometry	1
Hepatocyte	ASGPR1/2	Endocytic transport receptor on the basolateral surface of hepatocytes	WB	2–4
	SCL10A1/NTCP	Primary carrier for conjugated bile salt uptake from portal blood, located on basolateral surface of	Flow cytometry	5,6
Others	CD282	Toll-like receptor 2	Flow cytometry	
	CD284	Toll-like receptor 4	Flow cytometry	
	CD147 (EMMPRIN, basigin)	matrix metalloproteinase induction, cell adhesion, T cell activation, embryonic development,	Flow cytometry, WB	7–9

References: (1) Lynch *et al* (2007), (2) Fuhrer *et al* (1994), (3) Shugarts and Benet (2009), (4) Guy *et al* (2011), (5) Stockert *et al* (1995), (6) Padda *et al* (2011), (7) Hanna *et al* (2003), (8) Iacono *et al* (2007), (9) Weidle *et al* (2010).

Abbreviations: ASGPR, asialoglycoprotein receptor; CD, cluster differentiation; EMMPRIN, extracellular matrix metalloproteinase inducer; GP, glycoprotein; ICAM, intracellular adhesion molecule; MelCAM, melanoma cell adhesion molecule; NTCP, sodium-taurocholate co-transporter; PECAM, platelet endothelial cell adhesion molecule; SLC10A, solute carrier protein 10A; WB, western blotting.

2.7.1.3 Extracellular vesicle isolation from human blood samples

Venous bloods samples were collected from volunteer healthy controls and patients with NAFLD or other liver disease, as described in Section 2.6.2. EV fractions were prepared, as described above, according to intended purpose of use (flow cytometry

or WB). Further details of antibody staining for flow cytometry analysis are detailed in relevant Chapters.

2.8 Primary Kupffer cell (KC) culture

Primary KCs were isolated from collagenase-perfused mouse livers using the methodology described by Froh *et al* (Froh *et al.* 2003). For each experiment, a minimum of 5–6 mice were used to obtain sufficient KCs (pooled). The procedure for isolation of KCs is briefly outlined below:

2.8.1 Reagents

See Section 2.5.1 for perfusion buffer solution recipes.

RPMI 1640 1X (4.5 g/L D-glucose, 2.3 g/L HEPES buffer, L-glutamine, 1.5 g/L sodium bicarbonate, 0.1 mg/L sodium pyruvate). Solution was purchased commercially, required no additional preparation.

HBSS 10X (138 mM NaCl, 5.4 mM KCL, 0.4 mM Na_2HPO_4, 5.6 mM dextrose, 0.8 mM $MgSO_4.7H_2O$, 1.26 mM $CaCl_2.7H_2O$, 4 mM $NaHCO_3$). Solution was purchased commercially, required no additional preparation.

Percoll solution 50% (Percoll™, 4 mM $NaHCO_3$, 10X HBSS, 1X pen-strep, pH 7.4, final density ~ 1.065 g/mL). $NaHCO_3$ (0.35 g) was dissolved in 400 mL distilled water and added to 500 mL of Percoll™ and 100 mL of 10X HBSS. The pH was adjusted to 7.4, before filter sterilisation (0.22 µm filter).

Percoll solution 25% (final density ~ 1.037 g/mL). For 20 mL, add 10 mL of 50% Percoll solution (prepared above), and 10 mL of 1X HBSS (containing red pH indicator).

Two-step Percoll gradient (50%/25%). Percoll (20 mL of 25%) was carefully layered over 20 mL of 50% Percoll in 50 mL tubes.

2.8.2 Procedure

Following liver perfusion, as per Section 2.5, liver homogenates were subjected to several rounds of centrifugation to purify KC cell fractions. Details are outline below (schematic representation of the centrifugation process is presented in Figure 2.2).

2.8.2.1 Centrifugation suspension

The filtered suspensions were centrifuge initially for 3 min, 35 x g, 4°C (maximum brake). (All steps between centrifugation were performed in 50 mL falcon tubes, cooled using ice). Supernatant fractions (fraction #1) were transferred to clean 50 mL tubes kept chilled. This supernatant fraction contains predominantly non-parenchymal cells, KCs, endothelial cells, lymphocytes and stellate cells, whilst the pellets contain hepatocytes. If hepatocytes needed to be collected, the pellets were used after subjection to the centrifugation protocol (Section 2.5). Otherwise, for further non-parenchymal cell isolation, the pellets were then resuspended in 50 mL with ice cold HBSS.

Following resuspension, pellets were again centrifuged (3 min, 25 x g, 4°C, maximum brake). The resultant supernatant fractions (fraction #2) were transferred to clean 50 mL tubes and stored on ice. Pellets were resuspended in chilled HBSS and centrifuged (3 min, 20 x g, 4°C, maximum brake). Pellets obtained at this stage were discarded and supernatants were transferred to clean 50 mL tubes (fraction #3).

Isolated fractions #1, 2, 3 were centrifuged (7 min, 650 x g, 4°C, maximal brake), thereby pelleting hepatic non-parenchymal cells; these pellets contain mostly KC, but also endothelial, stellate cells, leukocytes, cell debris, and a few swollen parenchymal cells. Supernatants obtained at this stage were discarded, while pellets in reconstituted in 10 mL HBSS. This homogenate was carefully layer onto a 50%/25% Percoll gradient (Figure 2.3.A), which was centrifuged (15 min, 1,800 x g, 4°C, no brake). The resultant uppermost layer was discarded (Figure 2.3.B), and the middle layers collected, pooled together, and centrifuged (7 min, 650 x g, 4°C, maximum brake). Pellets obtained at this stage were resuspended in 1 mL HBSS and subjected to TBE (Section 2.5.1). KC viability was routinely ≥99%.

Following isolation, KCs were seeded onto plastic coverslips or culture plates (0.5–1.0 x 10^6cells/cm^2). Cells were cultured in RPMI 1640 (10% FBS, pen-strep, 37°C). To obtain pure monolayer culture of KCs, an incubation time of 15 min (not more than 30 min) was chosen based on the selective adherence (i.e., attachments and spreading) of KCs to plastic surfaces. Non-adherent cells, which include sinusoidal endothelial cells, were removed by media change. After 4 hours, these KC cultures were exposed to either supernatant of conditioned media from FC-injured primary hepatocytes, or to isolated EV fractions from this supernatant. EV fractions used to treat KCs were standardised to 10 µg protein/mL of media (Section 2.7.1.2). Further experimental details are outlines in relevant Chapters.

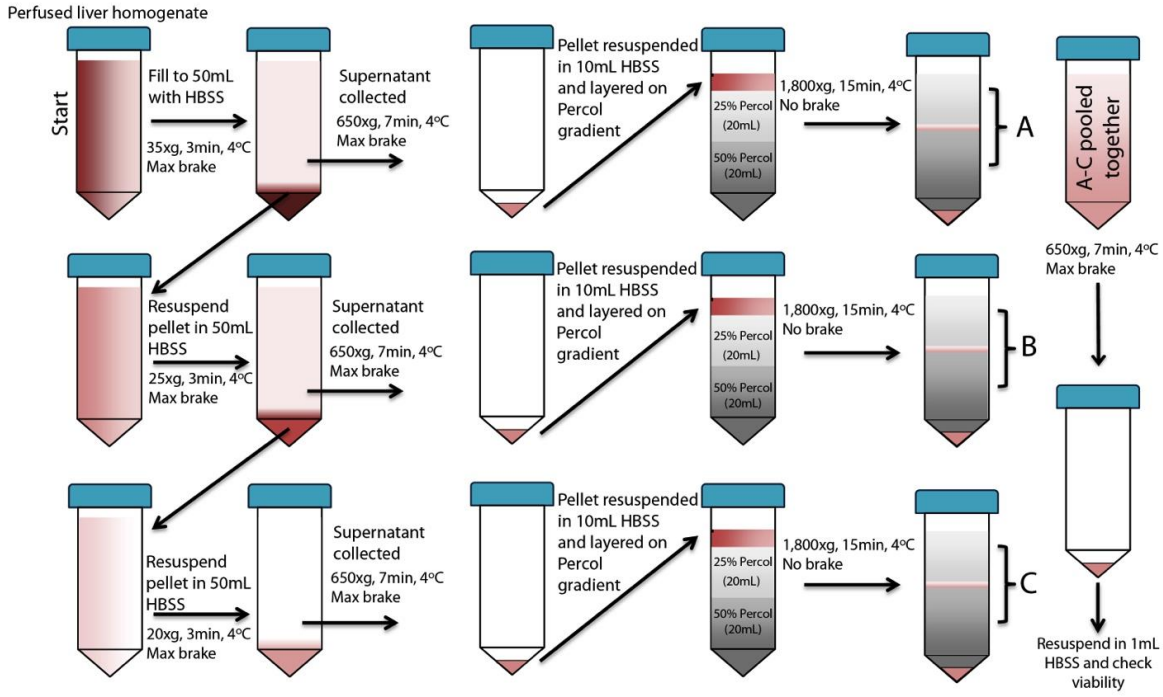

Figure 2.2 Schematic representation of the centrifugation step required for primary Kupffer cell isolation from murine livers.

2.9 Semi-quantitative analysis of gene expression

Gene expression as mRNA levels was assessed by real-time reverse transcriptase (RT)-PCR amplification of desired genes, using designed primers (Table 2.4). In order to assess mRNA expression in primary hepatocytes, cells were cultured on 55 cm^2 plates (n=3–5/group), then scraped off after 24 hours of treatment with indicated additions (Chapters 4 and 5). Complementary DNA (cDNA) was

subsequently synthesised, and real-time PCR performed. Details of methods relating to these steps are outlined below.

2.9.1 Ribonucleic acid (RNA) isolation

Total ribonucleic acid (RNA) was isolated from liver lysates or hepatocytes using the guanidinium thiocyanate-phenol-chloroform extraction method developed by Chomcyznski and Sacchi (2006).

2.9.1.1 Reagents

Diethylpyrocarbonate (DEPC)-treated water. DEPC (0.4 mL) was diluted in qPCR-grade d.H_2O (200 mL), the solution mixed thoroughly and incubated overnight (RT, fume hood) prior to liquid-cycle autoclaving.

Salt solution (5 M NaCl in DEPC-treated d.H_2O). NaCl (11.68 g) was dissolved in DEPC-treated d.H_2O (final volume 40 mL).

75% (v/v) Ethanol-DEPC. Ethanol (150 mL of >99% solution) was diluted with DEPC-treated d.H_2O (50 mL).

TRI reagent, isopropanol and chloroform were purchased commercially, and required no additional preparation prior to use.

2.9.1.2 Procedure

Following 24 hours incubation of primary hepatocytes, culture media was aspirated and stored at –80°C until further use. Hepatocytes were then washed with ice cold PBS, homogenised in TRI reagent (1 mL), and incubated at room temperature (10 min) before centrifugation (16,000 x g, 10 min 4°C). Pelleted cell debris was discarded and supernatants were transferred to sterile Eppendorf tubes. Chloroform (200 µL of 100% [v/v] stock) was added, and samples vortexed (15 sec), and incubated (15 min, RT) prior to centrifugation (16,000 x g, 15 min, 4°C). Clear upper phases containing total RNA were transferred to sterile Eppendorf tubes before addition of isopropanol (500 µL of 100%) and salt solution (20 µL, 5 M NaCl DEPC-treated stock). Samples were further incubated (5 min, RT), and centrifuged (16,000 x g, 15 min, 4°C) to pellet RNA. Supernatants were discarded

and pellets washed with 75% DEPC-treated ethanol (1 mL) prior to centrifugation (16,000 x g, 10 min, 4°C). Ethanol was subsequently aspirated and pellets resuspended in DEPC water (50 µL) before drying.

Purified RNA samples were quantified by spectophotometry (Nanodrop, Themo Scientific, Wilmington, DE). For cDNA synthesis, RNA samples were standardised to concentration of 1 µg DNA/µL in DEPC-treated d.H_2O and stored at –80°C.

2.9.2 cDNA synthesis

2.9.2.1 Reagents

10 mM deoxynucleotides (dNTPs), 1 µg/µL random hexamers, 0.1 M dithiothreitol (DTT), 5X first strand buffer, and Superscript® III reverse transcription (RT) enzyme (200 U/µL) were purchased from Invitrogen (Carlsbad, CA) and required no additional preparation before use.

Mastermix #1 (1.11 nM dNTPs, 0.11 µg/µL random hexamers in DEPC-treated d.H_2O). 10 mM dNTPs (1 µL), and DEPC-treated d.H_2O (7 µL) were combined for each RT-PCR reaction.

Mastermix #2 (17 nM DTT, 0.8X first strand buffer, 200 U Superscript® III). 0.1 M DTT (1 µL), 5X first strand buffer (4 µL), and Superscript® III (1 µL) were added for each RT-PCR reaction.

2.9.2.2 Procedure

RNA samples were diluted (1 µg RNA/µL) (Section 2.9.1.2) and subjected to reverse transcription using commercial reverse-transcription PCR (RT-PCR) kit (Invitrogen, Carlsbad, CA). Briefly, for each cDNA reaction, mastermix solution #1 (9 µL) was added to each tube, before incubation (65°C, 10 min), after which tubes were chilled on ice (1 min). PCR tubes containing mastermix #2 were prepared separately and heated (50°C, 2 min), after which mastermix #2 (6 µL) was added to tubes containing mastermix #1. Tubes were then incubated (50°C, 1 h), heated (70°C, 15 min) to inactivate Superscript® III, chilled on ice (5 min), and diluted by adding DEPC-treated PCR grade water (30 µL) to give stock cDNA concentration of approximately 0.1 µg/µL. Stock cDNA preparations were further diluted 1:50

(PCR-grade d.H_2O) prior to qPCR analysis. Individual experimental samples were subjected to RT-PCR simultaneously (in the same run) to negate inter-assay variation, commonly observed between separate cDNA synthesis reactions (Stahlberg *et al.* 2004, Stahlberg *et al.* 2004).

2.9.3 Real-time PCR

2.9.3.1 Reagents

PCR-grade d.H_2O, and iQ SYBR Green Supermix were purchased commercially. Primers were designed using Beacon Designer™ V7.0 (PREMIER Biosoft, Palo Alto, CA), ensuring amplicon products crossed at least 1 exon boundary. Sequences are summarised in Table 2.4. Designed primers were purchased from Geneworks (Thebarton, SA, Australia).

250 µM primer stocks. Primers were prepared to 250 µM stock concentrations by addition qPCR-grade d.H_2O (calculated from primer nmol weights).

Primer working solution (7.5 µmol in qPCR-grade d.H_2O). Primer stocks (6 µL of 250 µM stock) were diluted in qPCR-grade d.H_2O (194 µL), to yield 7.5 µmol working solutions.

cDNA standard solutions. Standard cDNA samples were made up by pooling cDNA, and serially diluting with PCR-grade d.H_2O to create 1:10, 1:40, 1:160, 1:640 and 1:2560 dilutions of pooled cDNA. Standards were included in each qPCR reaction, allowing relative gene expression to be calculated in relation to overall gene expression.

Master-mix solution (0.4 units of iQ SYBR Green Supermix, 150 nM forward and reverse primer, 32.5% PCR-grade d.H_2O). IQ SYBR Green Supermix (10 µL), forward and reverse primer (0.4 µL each), and ultra-pure qPCR-grade d.H_2O (5.2 µL) were added together for each template DNA amplification. The solution was mixed thoroughly and used immediately.

Table 2.4 Primer sets for semi-quantitative real-time PCR

Target gene	Forward Primer (3' to 5')	Reverse Primer (5' to 3')
Asc	TGCCTTGGGAGTCAGACCTATG	GGAGATGGAGCAACTGGAGGAA
β2M	TCCAGAAAACCCCTCAAATTCA	AGTATGTTCGGCTTCCCATTCTC
Caspase-1	TGCCTGCCCAGAGCACAAG	TGGTCCCACATATTCCCTCCTG
eIF-2	AGCCACATCCAGGAAGTGACAAG	ACAGGAGTAGGAGCCGCATCA
GAPDH	CATGGCCTTCCGTGTTCCTA	CCTGCTTCACCACCTTCTTGA
GCLC	ACTGGCAGACAATGAGGTTTAAGC	ACCACGAATACCACATAGGCAGAG
GCLM	ACTGCTCTCTGAGGCAAGTTTCC	CCACAGCGGCACCCAATCC
IL-1β	TGAGCACCTTCTTTTCCTTCA	GGAGCCTGTAGTGCAGTTGTC
Myd88	CCGCATGGTGGTGGTTGTTTC	AGGAATCAGTCGCTTCTGTTGGA
Nalp3	CAGGTTCAGTGTGTTTTCCCAGAC	TTGAGAAGAGACCACGGCAGAAG
Nrf1	GATGGCACCGTGTCGCTCAT	TGTGGTTGGCAGTTCTGAAGCA
Nrf2	ACATGGAGCAAGTTTGGCAGGA	TGTGGCTTCTGGGCTGGGA
Puma	TGCGTGTGGAGGAGGAGGAG	AGGGTGAGGGTCGGTGTCG
RAGE	ACCCTAGCCACGGACCTCAG	CAGACTCACCCACAGAGCCTTC
Sma	GGCTCTGGGCTCTGTAAGG	CTCTTGCTCTGGGCTTCATC
Sod2	GTT ACA ACT CAG GTC GCT CTT CAG	AGC AAC TCT CCT TTG GGT TCT CC
Sod3	CTT GTT CTA CGG CTT GCT ACT G	ATG CTG GTC GCC TAT CTT CT
StAR	CTCACTTGGCTGCTCAGTATTGAC	CAGGTGGTTGGCGAACTCTATCT
TLR2	CACTGGTGTCTGGAGTCTGCTG	CACGCCCACATCATTCTCAGGTA
TLR3	TCTGGGCTGAAGTGGACAAATCTC	AAGGAACCGTTGCCGACATCA
TLR4	CTGGGGAGGCACATCTTCTGG	CTCTGCTGTTTGCTCAGGATTCG
TLR5	AGACTGCGATGAAGAGGAAGCC	GACTACAAGGGTGATGACGAGGAA
TLR6	GGCTGTCACTGGGGCTTTCC	CCTGTGCCTGGTCTGTGTCC
TLR7	GTGATGCTGTGTGGTTTGTCTGG	TTTGACCTTTGTGTGCTCCTGGA
TLR8	GTGCTTTTGTCTGCTGTCCTCTG	GGGAGTTGTGCCTTATCTCGTCA
TLR9	GCACCCTCCTCCAGAAACTCG	GAGAATGTTGTGGCTGAGGTTGAC

Abbreviations for Table 2.4: Asc, apoptosis-associated-speck-like protein containing a caspase recruitment domain; β2M, β2-microglobulin; eIF-2, eukaryotic initiation factor 2α; GAPDH, glyceraldehyde 3-phosphate dehydrogenase; GCLC, glutamate-cysteine ligase, catalytic subunit; GCLM, glutamate-cysteine ligase, regulatory subunit; IL, interleukin; MyD88, myeloid differentiation primary response gene 88; Nalp3, NLR family, pyrin domain containing 3; NRF1, nuclear respiratory factor 1; NRF2, nuclear factor, erythroid derived-2, like-2; PUMA, Bcl-2 binding component 3/p53 upregulated modulator of apoptosis; RAGE, MAPK/MAK/MRK overlapping kinase; Sma, smooth muscle actin; Sod2, superoxide dismutase-2, mitochondrial; Sod3, superoxide dismutase-3, extracellular; StAR, sterol regulatory element binding protein-1; TLR, toll-like receptor

2.9.3.2 Procedure

Master-mix solution (16 µL) containing the forward and reverse primers (Table 2.4) was pipetted into Bio-Rad 96-well PCR plates. cDNA samples, standards, and non-template controls (PCR-grade d.H_2O) were added (4 µL/well), after which plates were sealed (Bio-Rad clear Microseal® adhesive seals), vortexed then centrifuged to remove droplets from seal cover. qPCR reactions were carried out in a Bio-Rad IQ5 Themocycler (Hercules, CA) under the following conditions: polymerase activation at 95°C (3min), followed by 45 cycles consisting of 95°C (10 sec), 65°C (20 sec), and 72°C (20 sec). SYBR green I fluorescence emission was reported after

each successive cycle, and iQ5 Optical Systems software (Bio-Rad, Hercules, CA) was used to established sample quantity. Gene expression was expressed as relative gene expression, typically normalised to levels in control group (primary hepatocytes untreated with LDL). Melt curves were run after each PCR reaction to assess amplicon product quality and to check for primer-dimer production.

2.10 Protein isolation for hepatocytes and subcellular fractions

Different methods were used to isolate the following protein fractions: primary hepatocyte lysates, nuclear, cytoplasmic, and mitochondrial fractions. As described in Chapter 4, these compartments were used to establish the expression of each protein of interest. The methods used to isolate each protein fraction are described below:

2.10.1 Total hepatocellular protein

2.10.1.1 Reagents

Protease and phosphatase inhibitors were purchased commercially and required no additional preparation prior to use.

Cell lysis buffer (50 mM HEPES, 150 mM NaCl, 1.5 mM $MgCl_2$, 1 mM EGTA, 10% glycerol, 0.1% triton X-100). HEPES (5.96 g), NaCl (4.84 g), $MgCl_2$ (71.5 mg), EGTA (190 mg), glycerol (50 mL), and triton X-100 (500 µL) were mixed together and made up to 500 mL with d.H_2O. Solutions was aliquot (5 mL) and stored at –20°C. Protease and phosphatase inhibitors (10 µL/mL) were added to cell lysis buffer before use.

2.10.1.2 Procedure

Following primary hepatocyte culture (Section 2.5.1), cells were scraped into cell lysis buffer (120 µL). Homogenates were gently mixed (1 h, 4^{o}C, dark) before centrifugation (12,000 x g, 4°C, 15 min). Supernatants containing extracted cellular protein were aliquoted (7 µL for protein determination, the rest for western blot), and stored at −80°C until further use.

2.10.2 Hepatic nuclear and cytoplasmic protein fractionation

Nuclear and cytoplasmic proteins were extracted from primary hepatocytes using NE-PER nuclear/cytoplasmic extraction kit (Thermo, Rockford, IL), as per the Manufacturer's instructions. Protease and phosphatase inhibitors (Sigma-Aldrich) were added to buffers to prevent protein degradation. Isolated protein fractions were aliquoted (7 µL for protein determination, the rest for western blot) and frozen at –80°C until ready for use. The cytoplasmic fractions isolated via this method contain organelles, in particular mitochondria and will not be used in the analysis of mitochondrial-mediated cell death pathways, described in later chapters.

2.10.3 Mitochondrial and cytoplasmic (mitochondria-free) protein isolation

In order to isolate cytoplasmic fractions free of mitochondrial contamination, methods described by Chen and colleague (Chen *et al.* 2007) were employed. Details of reagents and methods are described below:

2.10.3.1 Reagents

Buffer B (10 mM HEPES, 150 mM NaCl, 1.5 mM $MgCl_2$, 1 mM EGTA, pH 7.4). HEPES (119 mg), NaCl (438 mg), $MgCl_2$ (15.24 mg), EGTA (19.01 mg) were combined, dissolved and made up 50 mL of d.H_2O, pH adjusted to 7.4.

Digitonin 0.05% [m/v]. Digitonin (Sigma-Aldrich) (25 mg) was dissolved in 50 mL of buffer B.

2.10.3.2 Procedures

Following the termination of primary hepatocyte experiments, cell pellets were collected (Section 2.5.1) and treated with 0.05% digitonin in buffer B (10 mM HEPES, 150 mM NaCl, 1.5 mM $MgCl_2$, 1 mM EGTA, pH 7.4), followed by centrifugation (10,000 x g, 4°C, 10 min). The supernatant, containing mitochondria-free cytosolic fraction was analysed (Section 2.13.2) for presence of COX-IV by WB to confirm purity. Pellets from the above procedures contained the mitochondrial fraction, and were resuspended in buffer B containing 3-([3-cholamidopropyl]-diethylammoniol)-1-propanesultofonate (CHAPS), or treated with cell lysis buffer (Section 2.10.1.1) containing protease and phosphatase inhibitors (Sigma Aldrich).

2.11 Protein determination

Total protein content of the above preparations was determined with a commercial kit (DC™ Protein Assay, Bio-Rad, Hercules, CA), as per the Manufacturer's instructions. Briefly, the methodology is outlined below:

2.11.1 Reagents

1.45 mg/mL of bovine serum albumin stock.

Reagent A' (35 µL/well). This is made fresh by addition of 20 µL of reagent *S* to 1 mL of reagent A, both provided by the Manufacturer of DC™ Protein Assay.

Reagent B (275 µL/well). This is provided by the Manufacturer of the DC™ Protein Assay, and required no additional preparation.

2.11.2 Methods

Protein samples were diluted in d.H_2O (dilution factors for homogenate of whole liver, primary hepatocellular protein, protein fractions and EVs are shown in Table 2.5). Diluted samples, along with standards, were pipetted onto clear 96 well plates (7 µL). Freshly prepared reagent A' (35 µL/well) and reagent B (275 µL/well) were added to samples, before incubation (15 min, RT, orbital shaker) and quantification of absorbance (750 nm, FLUOstar OPTIMA plate reader). Standard curve absorbance values were used to calculate corresponding protein concentrations.

Table 2.5 Dilution factors for protein determination

Protein origin	Dilution factor
Liver homogenate from whole liver	1:30
Primary hepatocellular protein	1:7
Hepatocyte culture media	1:9
Mitochondria fraction	1:10
Cytoplasmic fraction (mitochondria-free)	Neat
Cytoplasmic fraction (isolated using NE-PER nuclear/cytoplasmic extraction kit)	1:9
Nuclear fraction	1:7
Microparticles	1:5

2.12 Sodium dodecyl sulfate polyacrylamide gel electrophoresis (SDS-PAGE)

Protein samples were separated by size using sodium dodecyl sulfate polyacrylamide gel electrophoresis (SDS-PAGE). The Bio-Rad Mini-PROTEAN® electrophoresis system (0.75 mm thick) was used according to the Manufacturer's instructions. The method is briefly outlined below.

2.12.1 Reagents

Tetramethylethylenediamine (TEMED), 30% acrylamide, and molecular weight markers (Bio-Rad Precision Plus Protein Prestained Standards) were all purchased commercially and require no additional preparation.

1 M Tris-HCl, pH 6.8. Tris (121.14 g) was dissolved in d.H_2O (0.8 L), pH adjusted to 6.8 with HCl, and final volume made up to 1 L with addition of d.H_2O.

3 M Tris-HCl, pH 8.8. Tris (363.42 g) was dissolved in d.H_2O (0.8 L), pH adjusted to 8.8 with HCl, and final volume made up to 1 L with d.H_2O.

10% APS stock. APS (1 g) was dissolved in d.H_2O (10 mL), aliquoted, and stored at −20°C.

10% SDS stock. SDS (50 g) was dissolved in d.H_2O (450 mL), pH adjusted to 7.2 with HCl, and final volume made up to 1 L with d.H_2O.

10 M DTT in d.H_2O. DTT (1.54 g) was dissolved in d.H_2O (1 mL), aliquoted and stored at −20°C.

5X reducing treatment buffer (300 mM Tris-HCl, pH 6.8, 10% [m/v] SDS, 50% [v/v] glycerol, 0.04% [m/v] bromophenol blue, 0.5 M DTT). Tris (1.81 g) was dissolved in d.H_2O (15 mL), pH adjusted to 6.8 SDS (5 g), glycerol (25 mL), bromophenol blue (20 mg) added, pH rechecked and final volume made up to 47.5 mL with d.H_2O. Buffer was aliquoted (0.95 mL) and stored at −20°C. Just before use, 10 M DTT was added.

Running buffer (100 mM Tris, 76 mM glycine, 0.1% SDS, pH 8.3).

2.12.2 Procedure

The Bio-Rad Mini-PROTEAN® electrophoresis gel casing apparatus was assembled as per Manufacturer's specifications. Gels were prepared as described in Table 2.6, with resolving and loading gels poured and set sequentially before being transferred into Bio-Rad Mini-PROTEAN® electrophoresis modules containing running buffer. Protein samples were standardised to concentration of either 6.25 mg/mL (for total hepatocellular and culture media protein) or 5.0 mg/mL (for isolated nuclear, cytoplasmic, mitochondria fractions and EV). Samples were standardised by diluting protein in d.H_2O. Standardised protein samples were subsequently reduced in 5X reducing treatment buffer, heated (100°C, 5 min) and loaded (62.5 µg/well for total hepatocellular and 50 µg/well for nuclear, cytoplasmic and mitochondria protein), along with commercial BioRad protein molecular weight markers (10 µL/well) prior to electrophoresis (120 V, 2 h, RT) in running buffer.

Table 2.6 Volume of SDS-PAGE reagent used for preparation of four Bio-Rad mini-PROTEAN® 0.75 mm thickness gels of varying running gel pore size

Solution	Running gel (2.7% C)				Stacking gel
	15% T	12.5% T	10% T	7.5% T	(4% T, 2.7% C)
30% [m/v] Acrylamide	7.00 mL	5.30 mL	4.40 mL	3.30 mL	1.04 mL
3M Tris-HCl, pH 8.8	3.30 mL	3.30 mL	3.30 mL	3.30 mL	–
1M Tris-HCl, pH 7.8	–	–	–	–	2.00 mL
10% [w/v] SDS	250 µL	250 µL	250 µL	250 µL	160 µL
d.H_2O	2.72 mL	4.42 mL	5.32 mL	6.42 mL	4.88 mL
10% [w/v] APS	100 µL	100 µL	100 µL	100 µL	50 µL
TEMED	10 µL	10 µL	10 µL	10 µL	10 µL
Final volume	13.38 mL	13.38 mL	13.38 mL	13.38 mL	8.14 mL

Abbreviations: % C, cross-linker percentage concentration; % T, total percent concentration; APS, ammonium persulfate; SDS, sodium dodecyl sulphate; TEMED, tetramethylethyllenediamine

2.13 Western blotting

Western blotting was employed to quantify specific proteins through the use of protein-antibody interactions (Renart *et al.* 1979). The methodology incorporates two major steps. The first involves immobilisation of SDS-PAGE separated proteins onto PVDF membrane by electrophoresis. The second is a "probing" step, using specific (commercially purchased) antibodies (Towbin *et al.* 1979). The SDS-PAGE protocol is described in Section 2.12.2, and subsequent steps for protein immobilisation and probing are outlined below.

2.13.1 Reagents

Transfer buffer (25 mM Tris-HCl, 192 mM glycine, 20% methanol, 0.01% SDS, pH 8.3). Tris (9 g) and glycine (43.2 g) were dissolved in d.H_2O (2.4 L). SDS (2 mL of 10% stock solution, Section 2.12.1), methanol (600 mL) was added, and buffer was stored at 4°C without pH adjustment.

Tris-buffered saline, containing Tween-20 (TBST) (20 mM Tris-HCl, 200 mM NaCl, pH 7.4, 0.05% Tween-20). Tris (2.42 g) and NaCl (11.7 g) were dissolved in d.H_2O (950 mL). The pH was adjusted to 7.4 with HCl. Tween-20 (2 mL of 25% stock) was added and final volume made up to 1 L.

Blocking solution (5% skim milk power in TBST, pH 7.4). Skim milk powder (5 g) was dissolved in TBST (100 mL). The solution was prepared just prior to use.

Antibody diluent (either BSA or skim milk) was dissolved in TBST and prepared just prior to use.

2.13.2 Procedure

The western blot procedure outlined in this section is identical to methods described by Furuyama and Fujisawa (Furuyama and Fujisawa 2000). Following SDS-PAGE electrophoresis (Section 2.12.2), gels, along with blotting paper (4 sheets/gel), 90 x 60 mm pieces of PVDF membrane (0.45 µm pore) were activated in 100% methanol (30 sec, RT), then equilibrated in ice-cold transfer buffer. Protein transfer sandwiches were assembled using Trans-Blot® Semi-Dry Transfer Cell electrophoresis cassettes according to the Manufacturer's instructions. Briefly, two sheets of blotting paper (pre-soaked in ice cold transfer buffer) were placed at the bottom of transfer tray, followed by PVDF membrane, followed by resolved SDS-PAGE gels (Section 2.12.2) on top of this, and finally two more sheets of blotting paper (pre-soaked in ice cold transfer buffer) to complete the protein transfer sandwich. Care was taken to ensure no air bubbles were trapped between each layer (Towbin *et al.* 1979). The gels were transferred (20 min, 25 V, 5.5 mA/cm^2), after which PVDF membranes were stained using Ponceau S to determine transfer efficiency. Ponceau S stain was removed with d.H_2O, and drop-wise addition of 10

M NaOH solution. PVDF membranes were stored in TBST buffer until ready for probing.

PVDF membranes were blocked against non-specific protein-protein interactions with 5% skim milk powder diluted in Tris-buffered saline with 0.05% Tween-20 (1 h, RT, orbital shaker). Membranes were subsequently incubated with primary antibodies (see Table 2.1) diluted in BSA- or skim milk-TBST antibody diluent (16 h, 4°C, orbital shaker), and washed (TBST, 3 x 5 min). Immunoreactivity was subsequently detected by incubating membranes with HRP-conjugated secondary antibodies diluted in BSA- or Skim-TBST (see Table 2.2). A final wash step was carried out (TBST, 3 x 5 min), after which membranes were immersed in SuperSignal West (Femto/Pico) or Western Lightning Plus ECL and proteins detected using a digital-enhanced chemiluminescence image capture system (LAS-4000, FujiFilm, Tokyo, Japan). Analysis of densitometry was performed (MultiGauge V3.0, FujiFilm, Tokyo, Japan) and values were normalised to house-keeping gene expression (β-actin, HSP-90, HSP-60, and TATA box-binding protein [TBP]). Protein expression data were subsequently normalised to the control group (see later Chapters). Western blots were run in triplicate or quadruplicate, with experiments repeated at least twice.

2.14 Localisation of free cholesterol

Methodologies for lipid staining and subcellular organelle co-localisation are identical to those described by Mari *et al*. (2006) and are briefly described below.

2.14.1 Reagents

Filipin III complex (5 µg/mL filipin in DMSO). Filipin (1 mg, Sigma-Aldrich) was dissolved in PBS (20 mL). This solution was shielded from light.

3.7% paraformaldehyde working solution buffered in PBS, pH 7.4. Paraformaldehyde stock solution (10 mL of 8% stock solution) was diluted in PBS (11.6 mL). This solution was prepared immediately before use.

Permeabilisation/block solution (0.1% saponin, 1% BSA in PBS). Saponin (0.025 g) and BSA (0.25 g) were dissolved in PBS (25 mL). This solution was prepared immediately before use.

Saponin wash solution (0.0025% saponin in PBS). Saponin (13 mg) was dissolved in PBS (500 mL).

Antibody diluent (0.5% BSA in PBS). BSA (0.25 g) was dissolved in PBS (50 mL).

2.14.2 Procedure

Primary hepatocytes were grown on 4 chamber plastic slides (Nunc, Roskilde, Denmark). Following 24 h of experiment, culture media was removed, then cell debris washed away once with PBS, before fixing in 3.7% (m/v) paraformaldehyde (15 min, RT). Following fixation, slides with fixed hepatocytes were washed in PBS, incubated with filipin working solution (16 h, 4°C, moisture chamber, in dark). Filipin staining solution was removed and slides were washed, and permeabilised with blocking/permeabilisation solution (5 min, RT, dark). Slides were rinsed (3 x 10 sec) (3 x 10 sec, PBS, dark) and incubated with primary antibodies (Table 2.1) diluted in antibody diluent (Section 2.14.1) (≥5 h, RT, dark). Slides were subsequently washed (3 x 10 sec, PBS, dark) and incubated with fluorescent secondary antibodies (Table 2.2) (90 min, RT, dark), and washed (3 x 10 sec, PBS, dark and 2 x 10 sec, saponin, dark). Finally, nuclei were stained (see Table 2.7 below for conditions), and slides were desalted (1 x 10 sec, d.H_2O, dark, followed by 3 x 10 sec, PBS, subjected to a final rinse 1 x 10 sec, d.H_2O, dark), and air-dried in the dark. Slides were mounted using ProLong® Gold antifade reagent, and sealed using clear nail varnish.

For esterified lipid localisation, primary hepatocytes were fixed in 3.7% (m/v) paraformaldehyde (15 min, RT), washed (3 x 10 sec, PBS), and incubated with Nile red working solution (30 min, RT, in dark). Slides were washed (3 x 10 sec, PBS, dark), then nuclei were stained as described above and mounted using ProLong® Gold antifade, and sealed using nail varnish. Fluorescent images were captured using Zeiss Axioplan2 microscope with Apotome (Zeiss, GmbH, Germany). Images were analysed with AxioVision V4.8 (Zeiss, GmbH, Germany).

Table 2.7 Invitrogen™ nuclear labelling kit fluorophobe options and preparation details

Stain	Spectral colour	Wavelength (nm)		Dilution of stock	Incubation time
		Excitation	Emission		
DAPI	Blue	358	461	1:300 in PBS	2 min
SYTOX	Green	504	523	1:300 in water	15 min
7-AAD	Red	546	647	1:50 in water	45 min
TO-PRO-3	Far Red	642	661	1:300 in PBS	15 min

Abbreviation: 7-AAD, 7-aminoactinomycin D; DAPI, 4',6-diamidino-2-phenylindole; SYTOX, green nucleic acid stain; TO-PRO-3, thiazole orange derivative fluorophore

2.15 Cell injury and cell death analysis

2.15.1 Lactate dehydrogenase (LDH) leakage in culture media

Culture media lactate dehydrogenase (LDH) leakage were used to assess hepatocellular injury, using a commercially available kit, Cytotox 96© non-radioactive cytotoxicity assay (Promega, Madison, WI). Methods were as the per Manufacturer's instructions, and are briefly outlined below.

2.15.2 Methods

Primary hepatocytes were grown on clear 96-well plates (200 µL culture media/well). Following 24 h experiments, 50 µL of supernatant was transferred to separate 96 well plates and set aside (for pre-lysis LDH analysis). A further 50 µL was removed, leaving 100 µL in the 96-well culture plates. 10X lysis buffer (10 µL) was added to this volume and the plates re-incubated (45 min, 37°C, 5% CO_2). Subsequently, the 96-well plates were centrifuged (250 x g, 4 min, RT) to sediment floating cell debris following cell lysis. Supernatant (50 µL) was then transferred to a clean 96-well plate (post-lysis LDH analysis). Finally, 50 µL/well of substrate mix was added to both pre- and post-lysis LDH sample plates, incubated (30 min, RT, dark), before reactions terminated using stop solution (50 µL). Plates were read at 495 nm (FLUOstar OPTIMA plate reader) and LDH leakage from injured hepatocytes was calculated as follows:

$$\text{LDH leakage (\%)} = \frac{\text{Pre-lysis LDH}}{\text{Pre- + post-lysis LDH}} \text{ x } 100$$

2.15.3 Cell death analysis

Hepatocellular apoptosis was quantified by nuclear morphology, using Höechst 33342 (Sigma-Aldrich) and propidium iodide (BD Bioscience), as described by Mari *et al*

(2006). Cells with condensed or fragmented nuclei on Höechst 33342 staining were considered apoptotic, while necrotic cells were detected by positive nuclei propidium iodide staining.

2.15.3.1 Reagents

Propidium iodide stock (74.8 µM). This was purchased commercially and stored at 4°C.

Propidium iodide working solution (10 µM). This was diluted from PI stock solution in PBS and prepared just before use and shielded from light.

Höechst 33342 stock (35 mM). Höechst 33342 (50 mg/mL) was dissolved in d.H_2O (10 mL) to yield stock solution of 35 mM, before aliquoting (500 µL), shielded from light and stored at –20°C.

Höechst 33342 working solution (10 µM). This was diluted from Höechst 33342 stock solution in d.H_2O and prepared just before use and shielded from light.

2.14.2.2 Methods

Primary hepatocytes were isolated and cultured, as described in Section 2.5.1, and grown on four chamber plastic slides. At experimental endpoints, cells were gently washed (ice-cold PBS), followed by fixation (ice-cold 100% methanol, 30 min, 4°C). After fixation, methanol was aspirated and primary hepatocytes were incubated (5 min, RT, in dark) with PI working solution (10 µM), followed by washing (1X PBS, RT). Finally Höechst 33342 working solution (10 µM) was added and allowed to incubate (15 min, RT, in dark), before washing (3X PBS, RT, in dark). Slides mounted with glass coverslips prior to viewing. A minimum of six high-powered field images were obtained using an Olympus IX70 microscope fitted with a high-resolution CCD camera (Olympus, Wendenstrasse, Hamburg, Germany). Apoptotic cells were quantified as a percentage of cells with abnormal Höechst 33342 nuclear morphology, while necrotic cells by PI-positive staining.

2.16 Statistical analyses

All data presented within this thesis are presented as mean ± standard error of the mean (SEM), with the number (*n*) of independent replicates clearly stated for each

experiment. In regards to the general approach to statistical analysis, data were generally non-parametric and were subject to analysis of variance (ANOVA) with subsequent post-hoc testing using Tukey's procedure (SPSS V17.0, Chicago, IL, USA). Statistical significance is defined as $P<0.05$.

CHAPTER 3

In vitro hepatocellular free cholesterol loading: a model for testing cholesterol lipotoxicity

3.1 Introduction

NAFLD is currently the commonest form of chronic liver disease affecting both adults and children worldwide (Gan *et al.*, 2011). NAFLD embraces a pathological spectrum of liver disease, ranging from benign simple steatosis (SS) or "non-NASH" (without hepatocellular injury or inflammation), through steatohepatitis (NASH), to liver cirrhosis (Farrell *et al.*, 2012).

Excess retention of lipids in hepatocytes is the prerequisite for NAFLD development (Alkhouri *et al.*, 2009). The mechanisms of steatosis development, and more importantly the potential links between steatosis and liver damage resulting in disease progression to NASH and cirrhosis remain elusive. However, the details of this disease process are highly relevant, as their identification may help to find novel therapeutic targets to prevent or treat NASH, and so prevent cirrhosis.

As discussed in Chapter 1, steatosis reflects an increase in hepatic TG content, but it is increasingly recognised that TG is likely the safe storage form for excess lipid. As such, TG accumulation may not be harmful to hepatocytes; instead, its formation may represent a protective mechanism from lipotoxicity caused by FFA or DAG (Listenberger *et al.*, 2003). *In vivo* experiments have provided support for such a protective effect of TG. Investigators used leptin receptor-mutated *db/db* mice placed on a MCD diet to produce hepatic steatosis, liver injury and apoptosis, with increased generation of ROS and fibrosis but a decline in hepatic TG content over time. Blocking TG synthesis by suppression of DGAT2 expression (using *DGAT2* antisense oligonucleotides) in these animals significantly increased hepatocyte FFA content, and concomitantly worsened oxidative stress, hepatocellular apoptosis, liver inflammation and fibrosis (Yamaguchi *et al.*, 2007).

Since TG appears to be a safe storage lipid, identification of the toxic lipid species, which trigger transition from benign SS to inflammatory NASH, is now a major focus for NAFLD research. To date, saturated FFA (sFFA) and its metabolites (ceramide, DAG, lysophosphatidylcholine [LPC]) have been the most studied 'toxic lipid species' in relation to production of liver injury (Neuschwander-Tetri, 2010). However, there is now emerging evidence to support the role of FC as a toxic lipid species that can mediate the transition from SS to NASH (discussed below).

Lipidomic evidence shows that hepatic FFA levels are increased in all forms of NAFLD and do not differ between NASH and "non-NASH" (or SS) phenotypes, either in humans (Puri *et al.*, 2007) or in mice (Van Rooyen *et al.*, 2011). Instead, levels of biologically reactive, non-esterified FC are high in NASH but unaltered (compared with lean livers) in SS (Puri *et al.*, 2007, Caballero *et al.*, 2009). A correlation between dietary cholesterol content and resultant hepatocyte FC levels with NASH severity (Van Rooyen *et al.*, 2011), and the beneficial effects of cholesterol lowering drugs on liver pathology provides indirect evidence that FC accumulation in NASH leads to hepatocyte cell death, inflammatory recruitment and fibrosis (Kiyici *et al.*, 2003, Rallidis *et al.*, 2004, Min *et al.*, 2012, Van Rooyen *et al.*, 2013).

The landmark study by Mari *et al* showed that FC accumulation sensitises murine hepatocytes to TNF-α and FasL-mediated apoptosis: the authors proposed that this could lead to progression from steatosis to NASH (Ginsberg, 2006, Marí *et al.*, 2006). In this study, rats were fed choline-deficient or 2% cholesterol plus sodium cholate diets to increase hepatic TG or cholesterol levels, respectively. Examination of these livers revealed that TNF-α treatment caused apoptosis, increased ROS and liver injury only in cholesterol-loaded hepatocytes (Marí *et al.*, 2006). The mechanism by which cholesterol loading sensitised hepatocytes to TNF-α, was at least partly attributable to a selective depletion of mitochondria glutathione content, possibly due to increased mitochondria FC level although this was not measured directly in this study.

In another study in human NASH, the authors found a 15-fold increase in hepatic levels of transcript for StAR, a protein responsible for transport of FC into mitochondria (Caballero *et al.*, 2009). This observation also supports a possible role for mitochondrial FC loading in NAFLD progression to NASH. Although specific analyses of the

mitochondrial cholesterol content do not appear to have been explored in any studies, presumably due to tissue limitations, the finding of increased StAR expression in NASH liver by Caballero *et al.* (2009) suggest that the subcellular site of hepatic FC depositions in NASH may be within the mitochondria. Details pertaining to the possible role of mitochondrial dysfunction in FC lipotoxicity will be addressed in Chapter 4.

Whether FC in mitochondria, or alternatively deposited in ER and/or plasma membrane could explain hepatocellular injury and disease progression in NAFLD has not been explored, partly due to lack of an adequate *in vitro* system to study the cellular mechanisms of FC-mediated hepatocyte lipotoxicity directly. Here, we describe the development of a primary murine hepatocyte cell culture model for FC loading, in order to explore the mechanisms responsible for FC lipotoxicity (later Chapters).

3.2 Purpose of study: hypotheses and aims

We hypothesised that mitochondria are a major site of FC deposition in cholesterol-loaded hepatocytes.

The specific aims addressed/explored in this Chapter were to:

1. Determine the subcellular localisation of FC in HF/HC-fed *foz/foz* mice with NASH.
2. Test the efficacy of FC-loading in primary murine hepatocytes using unmodified human LDL.
3. Assess whether the pattern of intracellular FC distribution in FC-loaded hepatocytes replicates with the patterns observed in HF/HC-fed *foz/foz* mice with NASH
4. Test whether FC-loading induces hepatocellular apoptosis and necrosis in cultured primary hepatocytes.

3.3 Methods

3.3.1 Mice and diets

Frozen liver sections were obtained from female *foz/foz* NOD.B10 mice fed HF/HC-diet (containing 0, 0.2, or 2.0% [w/w] cholesterol) 24 weeks. Details pertaining to experimental conditions and dietary composition are outlined in previous experiments conducted in the host laboratory (Van Rooyen *et al.*, 2011). Mice were maintained as described in Section 2.5.

For cell culture, female WT C57B/6J and *foz/foz* NOB.B10 mice were maintained as described in Section 2.5, until 6-8 weeks of age. *Foz/foz* NOD.B10 mice were also used to isolate primary hepatocytes in preliminary experiments. Mice were fed either chow or HF diet containing 0-1% dietary cholesterol (as indicated in Results, Table 3.1). All diets were purchased from Specialty Feeds (Glen Forrest, WA, Australia).

Primary hepatocytes were isolated as described in Section 2.5.

3.3.2 Fluorescent staining of frozen and cultured primary hepatocytes

Fluorescent staining for FC subcellular localisation of frozen liver sections was conducted as described in Section 2.14 (primary and secondary antibodies are listed in Tables 2.1 and 2.2, respectively). Images were captured using a Zeiss Axioplan2 microscope (Zeiss, GmbH, Germany). Captured images were analysed using AxioVision V4.8 software (Zeiss, GmbH, Germany).

Following established isolation and culture of primary hepatocytes, cells were loaded with FC using unmodified human LDL, as per Section 2.4. Thereafter, hepatocytes were fixed and stained for FC and subcellular markers, as described in Section 2.14.

3.3.3 Hepatocellular protein isolation and FC quantification

In separate experiments, cultured hepatocytes were washed with ice-cold PBS and lysed with RIPA buffer (a commonly used tissue culture cell lysis buffer containing 25 mM Tris-HCl, 150 mM NaCl, 1% [v/v] sodium deoxycholate, 1% SDS [m/v], pH 7.6) to lyse the cells. Lysed cellular material was scrapped off culture plates and centrifuged (16,000 x g, 15 min, 4°C). FC content within supernatant fractions was then determined biochemically using a commercially available kit (Wako, Osaka, Japan). FC levels were normalised to mg of protein, as described in Section 2.11.

Separately, nuclear and cytoplasmic fractions from cultured hepatocytes were isolated using a commercial (NE-PER) nuclear/cytoplasmic extraction kit (Thermo, Rockford, IL). These fractions were subsequently quantified and standardised, as described in Section 2.12, prior to western blotting (Section 2.13). Antibodies and conditions are detailed in Table 2.1 and 2.2.

3.3.4 Supernatant ALT quantification

In addition to LDH release, hepatocellular injury was measured by hepatocellular ALT release in some experiments. Supernatant samples from cultured hepatocytes were collected and centrifuged (16,000 x g, 15 min, 4°C) to pellet cellular debris. ALT level was measured in supernatant fractions by automated testing (Department of Clinical Chemistry, The Canberra Hospital).

3.3.5 Assessment of hepatocellular injury and cell death

Hepatocellular injury was assessed using lactate dehydrogenase (LDH) leakage (into supernatant). LDH levels were determined using Cytotox 96© non-radioactive cytotoxicity assay (Promega, Madison, WI). Further details pertaining to the calculation of LDH release are specified in Section 2.15.1.

Apoptosis of hepatocytes was quantified by nuclear morphology using Höechst 33342, while necrosis was estimated by propidium iodide staining, the combined assay being conducted in identical manner to that described Mari *et al* (2006). Specifically, cells with condensed or fragmented nuclei on Höechst 33342 staining were considered apoptotic, while nuclei with positive propidium iodide staining were considered necrotic.

3.3.6 Scanning (SEM) and transmission (TEM) electron microscopy

In this study, SEM was used for morphological assessment of FC-loaded (40 µM LDL) hepatocytes. Separately, TEM was employed for ultrastructural evaluation of hepatocellular organelle architecture and plasma membrane integrity following FC-loading. The methodologies used for SEM and TEM techniques have been published and reviewed (McCuskey 1986, McCuskey and McCuskey 1990).

3.3.6.1 Reagents

200 mM Cacodylate buffer, pH 7.2. Sodium cacodylate acid (42.8 g) was dissolved in ultra-pure d.H_2O (180 mL), pH adjusted to 7.2 and final volume made up to 200 mL. Buffer was diluted to 100 mM working concentration prior to use.

1% (v/v) Osmium tetroxide in cacodylate buffer, pH 7.2. Stock (4% [v/v]) OsO_4 was purchased from Electron Microscopy Science (Hatfield, PA). Prior to use it was diluted to 1% (v/v) in 100 mM cacodylate buffer, pH 7.2.

2% (m/v) Gluteraldehyde in 100 mM cacodylate buffer, pH 7.2. Gluteraldehyde (10 mL of 8% [m/v] stock) (Electron Microscopy Science, Hatfield, PA) was diluted in 100 mM cacodylate buffer (30 mL).

70-90% (v/v) Ethanol gradients. Absolute pure ethanol (Astral Scientific, Caringbah, NSW) was diluted in ultra-pure, hospital grade d.H_2O to yield 10% increments ranging from 70% to 90% (v/v).

3.3.6.2 Procedure

For SEM:

Primary hepatocytes were isolated and cultured on Thermanox™ coverslips (Thermo Scientific, Waltham, MA), as described in Section 2.5.1.1. At experimental endpoints, cells were washed with ice-cold HBSS and fixed with 2% gluteraldehyde buffered in 100 mM cacodylic acid buffer, pH 7.2 (30 min, RT, fume cabinet). Following fixation, cells were washed with 100 mM cacodylic acid buffer (3 x 5 min), fixed in 1% (v/v) osmium tetroxide (30 min, RT, fume cabinet), again washed in 100 mM cacodylic acid and dehydrated using graduated 70-100% (v/v) ethanol gradient washes. Once coverslips reached 100% (v/v) ethanol solution, cells were further dried with the application HMDS solution (Sigma Aldrich, St. Louis, MO) (100 µL, 3 min, RT, fume cabinet). Coverslips were subsequently removed from culture plates, attached to aluminum SEM mounting stubs (ProSciTech, Kirwan, QLD) using conductive double-sided carbon tape (ProSciTech, Kirwan, QLD) before platinum sputter coated (10 nm, 20 mA, 3 mins) (EmiTech, GmbH, Germany). Specimens were viewed on a Zeiss UltraPlus analytical field emission SEM microscope (FESEM) (Oberkochen, Germany) (3-10 kV setting).

For TEM:

Again, primary hepatocytes were isolated and cultured on Thermanox™ coverslips (Thermo Scientific, Waltham, MA) (see Section 2.5.1.1). At experimental endpoints, cells were washed and fixed with 2% gluteraldehyde and osmium tetroxide fixative, as

described above for SEM analysis. Following osmium tetroxide fixation, cells were washed several times with ultra-pure d.H_2O, before electron staining with 2% (m/v) aqueous uranyl acetate (Electron Microscopy Science, Hatfield, PA) (2 h, 4^{o}C, dark) before dehydrating and embedding in Procure/Araldite epoxy resin (ProSciTech, Kirwan, QLD), as per Manufacturer's instructions. The epoxy resin was applied directly to coverslips and adherent hepatocytes and allowed to set completely (8–12 h at ~65°C). Thereafter, coverslips were fractured off the resin by submersion in liquid nitrogen. The remaining resin blocks were cut into ultra-thin sections at the hepatocyte surface, using a diamond-bladed ultramicrotome (Leica EM UC7, Wetzlar, Germany). Ultra-thin sections were transferred to formvar-coated copper grids (Electron Microscopy Science, Hatfield, PA) prior to viewing on a JEOL 2100F (Peabody, MA) TEM microscope.

3.3.7 Statistics

Statistical analyses were carried out as described in Section 2.16.

3.4 Results

3.4.1 Hepatic FC localisation in *foz/foz* mice with NASH

To establish the subcellular sites of hepatic FC deposition in livers of *foz/foz* mice with NASH, we first explored livers obtained from earlier published experiments (conducted by Dr Derrick Van Rooyen, see Acknowledgments and Statement of Originality) in which *foz/foz* mice were fed HF diet containing increasing amounts of cholesterol (0, 0.2, 2.0% [w/w]). These mice developed NASH pathology, the severity of which correlated with hepatic cholesterol content determined by lipidomic analysis (HPLC and MS analysis) (Van Rooyen *et al.*, 2011). Here, using fluorescent subcellular markers and filipin (blue fluorescence) staining, it was shown that FC localised predominantly to the plasma membrane, with additional localisation to the mitochondrial, and ER compartments (Figure 3.1A, B, C). Interestingly, the hepatic expression of GRP78 (a marker of ER stress) was reduced in cholesterol-loaded livers (Figure 3.1B). Likewise, the intensity of COXIV (mitochondria marker) immunofluorescence in FC-loaded NASH livers was decreased, compared with SS livers (Figure 3.1C), but immunofluorescence is a qualitative method of ER and mitochondrial protein analysis. In Chapter 4 (Section 4.4.2), we describe the contribution of FC to mitochondrial dysfunction in FC-loaded hepatocytes.

An important finding salient to a lipotoxic pathogenesis of NASH was that F4/80 staining for macrophages (these include KCs and/or recruited macrophages) showed accumulation around fat-laden hepatocytes, which contained FC-rich vacuoles (Figure 3.1D). As previously described by the host laboratory, the livers of these mice display significant increases in numbers of inflammatory cells (both macrophage and neutrophils), as well as hepatocyte apoptosis and fibrosis (Van Rooyen *et al.*, 2011) which are all hallmarks of NASH.

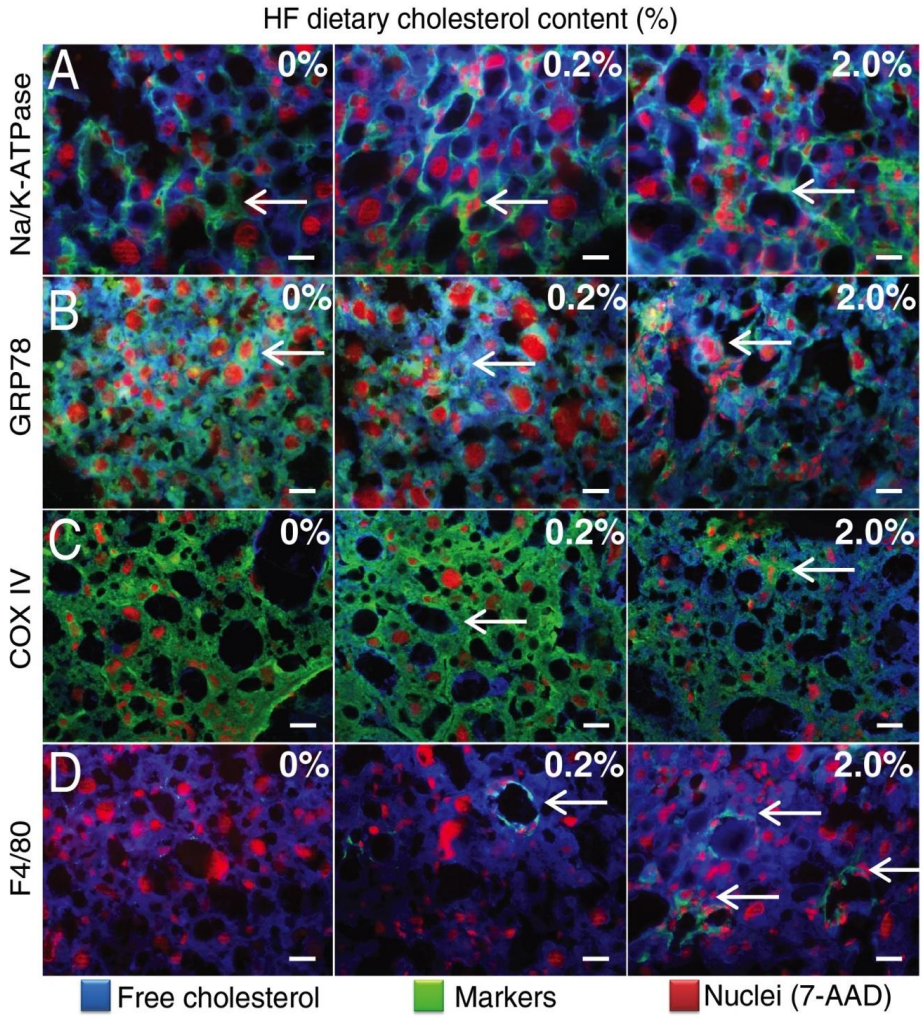

Figure 3.1 In livers of diabetic mice with NASH, free cholesterol deposits in hepatocyte plasma membrane, mitochondria and ER, and is associated with F4/80-positive macrophage recruitment.

Frozen sections were obtained from obese, diabetic *foz/foz* mice fed HF diet, containing 0, 0.2, or 2.0% [w/w] dietary cholesterol, over 24 weeks. Livers from these mice with NASH (Van Rooyen *et al.*, 2011) were stained for FC (Filipin, blue), which co-localised (arrows) to: (**A**) plasma membrane (Na/K-ATPase, green), (**B**) ER (GRP78, green) and (**C**). mitochondria (COXIV, green). (**D**) F4/80-positive macrophages (green) accumulate around FC-rich macrosteatotic hepatocytes. Histopathological NAFLD activity scoring (NAS) of these livers has been published by Van Rooyen *et al.* in the host laboratory (2011). Scale bars represent 20 µm.

3.4.2 Incubating primary hepatocytes with LDL increases FC with identical subcellular distribution as in NASH livers obtained from HF/HC-fed *foz/foz* mice

To date, no suitable *in vitro* systems have been described for the study of cellular mechanisms of FC-mediated hepatocyte lipotoxicity. We first attempted to isolate fat-laden hepatocytes from *foz/foz* mice (Arsov, 2005). These mice develop hyperphagic obesity complicated by insulin resistance with resultant diabetes, metabolic syndrome and dyslipidemia (Arsov *et al.*, 2006, Larter *et al.*, 2009). In order to prepare suitably loaded hepatocytes for *in vitro* studies, female *foz/foz* mice were fed, from weaning, with different diets (normal chow [NC], high fat diet [HFD] containing 0.2% cholesterol, and NC with 1% cholesterol diet, and HFD without cholesterol). The aim was to achieve steatotic liver, with hepatocytes loaded with, either FFA, FC or both. Unfortunately, despite multiple attempts, the viability of hepatocytes isolated from these mice was inadequate (<60%) for culturing, irrespective of mouse age or duration of dietary feeding (Table 3.1). Further, the hepatocyte cultures that were attempted (despite low cell viability) were unsuccessful due to failure of hepatocyte attachment; indeed, the fat laden hepatocytes exhibited buoyancy in aqueous media, which was likely attributable to steatosis.

Tabas *et al.* previously reported use of unmodified LDL to successfully load cultured macrophages in their studies of foam cell role in atherosclerotic plaques (Tabas *et al.*, 1985). Here, we adapted a similar strategy to achieve FC-loading in primary murine hepatocytes. To establish our system to directly study FC lipotoxicity in hepatocytes, primary murine hepatocytes were incubated in William's E (WEM) culture media supplemented with 20–40 μM unmodified human LDL (Sigma Aldrich). Such incubation resulted in dose-dependent FC accumulation, as shown by increasing intensity of filipin (blue) fluorescence (Figure 3.2A) and significantly raised intracellular FC content ($P<0.05$, Figure 3.2D). Similarly, immunofluorescent and protein determination of LDLR, a protein responsible for uptake of unmodified LDL by endocytosis (Goldstein and Brown, 1984), revealed significant increases in hepatocellular LDLR staining and immunoblotting ($P<0.05$, Figure 3.2B,C).

Table 3.1 Viabilities of primary hepatocytes isolated from *foz/foz* mice of varying ages and fed varying experimental diets.

Diet	Age (weeks) (n=4–6/gp)	Av. body weight (g)	Hepatocellular viability (%)
Chow	9	48.2	~63
	12	57.8	<40
Chow + 1% chol	6	42.8	~35
	12	56.5	<33
HF + 0.2% chol	6	44.9	~69
	10	47.4	<30
	12	54.2	<20
HF, no chol	7	55.2	<50%
	12	56.6	<40%

Foz/foz mice were fed chow or HF diet containing 0, 0.2, or 1.0% (w/w) cholesterol for 6-12 weeks. Primary hepatocytes were then isolated as described in Section 2.5. Following isolation, hepatocyte viabilities were calculated using trypan blue exclusion (Strober, 2001).

Abbreviations: Chol, Cholesterol; HF, high fat; Av, average

We used methodology described in Section 3.4.1 to characterise the subcellular localisation of FC in hepatocytes. The results recapitulated those observed in livers of HF/HC-fed *foz/foz* mice with NASH (Figure 3.1). Specifically, FC deposited predominantly within hepatocyte plasma membranes (Figure 3.3A), with some co-localisation observed between FC and mitochondria, and perceptible but less so with the ER compartment (Figure 3.3 C,D). These findings from the *in vitro* system mirror results obtained for FC-loaded *foz/foz* livers with NASH (Figure 3.1 B,C). It is important to stress that in NASH livers of *foz/foz* mice fed HF containing 2% [w/w] cholesterol and primary hepatocytes loaded with FC by highest concentration of LDL (40 μM), GRP78 fluorescent staining (indicating ER localisation) appeared to be substantially reduced (Figure 3.1B and Figure 3.3C respectively), when compared to SS livers of *foz/foz* mice fed HF containing 0.2% [w/w] cholesterol and primary hepatocytes in the control (0 μM LDL) group that were not exposed to cholesterol.

Given the strong localisation of FC within plasma membrane compartments, the effect of FC-loading on membrane fluidity was investigated. FC-loading of hepatocytes caused a significant reduction in plasma membrane fluidity, as determined by the ratio between excitatory and unexcited forms of pyrenedecanoic acid (P<0.05, Figure 3.3E).

3.4.3 FC loading injures primary hepatocytes and induces apoptosis and necrosis

To test our hypothesis that FC-loading contributes to hepatocellular lipotoxicity, we then assessed markers of hepatocellular injury and cell death.

As determined by cellular LDH and ALT release into the culture media, hepatocyte injury increased significantly in primary hepatocyte cultures following FC-loading ($P<0.05$, Figure 3.4A,B). The most notable changes followed hepatocyte incubation with 30 and 40 μM LDL ($P<0.05$, Figure 3.4A,B), which corresponded to a hepatocellular FC content of ~27.5 μg/mg hepatocyte protein (Figure 3.2D), versus ~10 μg/mg protein in control hepatocytes. Hepatocytes exposed to 40 μM LDL also exhibited a significant increase in apoptosis, as determined by changes in nuclear morphology viewed by Höechst 33342 staining ($P<0.05$, Figure 3.4C,E). More impressively, the proportion of necrotic hepatocytes was increased to greater extent ($P<0.05$), and even the lower dose (20 μM) of LDL exposure produced some necrosis (Figure 3.4D,E). Furthermore, levels of hepatocellular necrosis continued to increase in a dose-dependent manner, with ~30% of hepatocytes found to be necrotic following 40 μM LDL exposure ($P<0.05$, Figure 3.4D,E). The more detailed studies of mechanisms of cellular injury described in later Chapters were therefore conducted using 40 μM LDL.

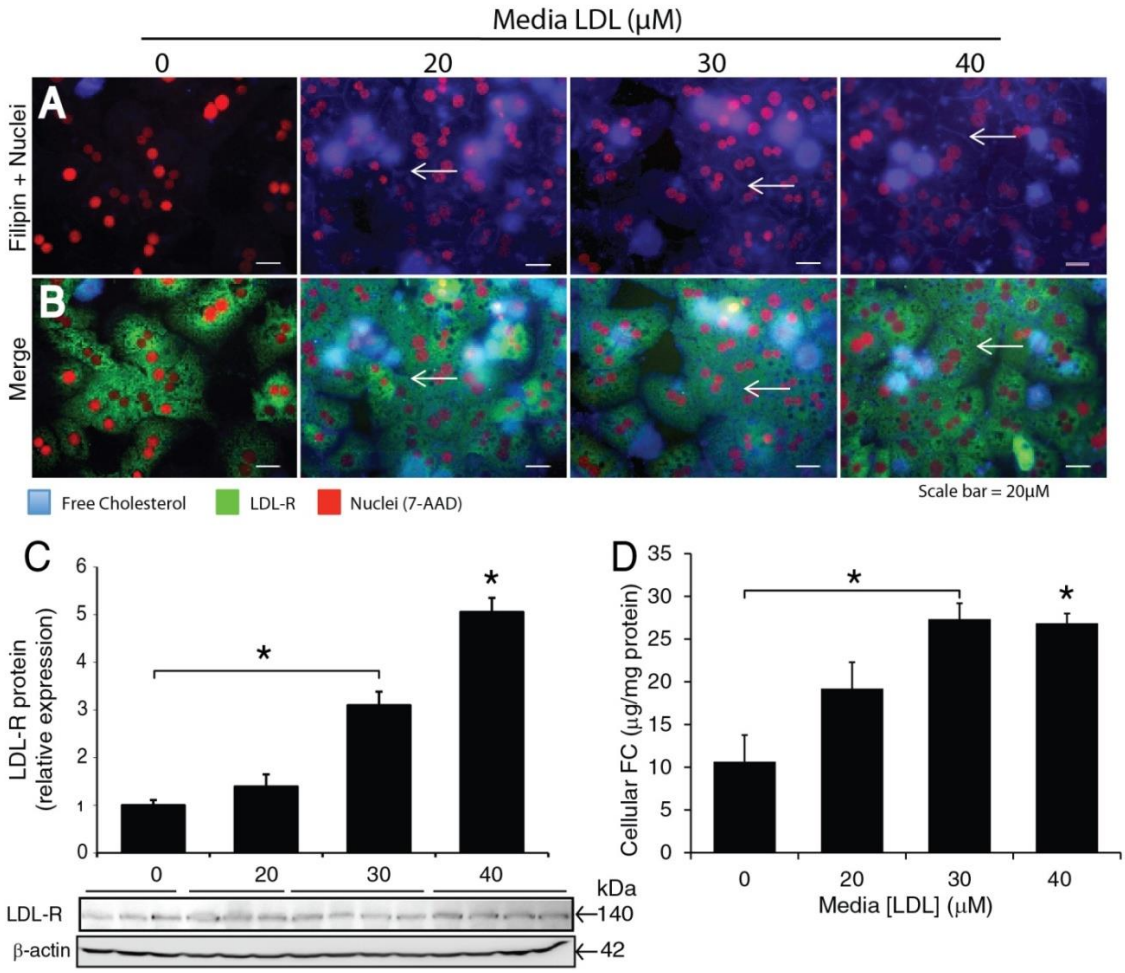

Figure 3.2 LDL supplementation of culture media increases LDLR expression and FC-loading in primary murine hepatocytes.

(**A**) Primary murine hepatocytes exposed to 0-40 μM LDL over 24 h show dose-dependent increases in filipin (blue) staining, which is associated with increased LDLR expression, as determined by (**B**) fluorescence (green) and (**C**) protein expression. (**D**) Cellular FC content (as determined by Wako kit; see Section 3.3.3), increased significantly in hepatocytes exposed to increasing concentrations of LDL. **P*<0.05, vs control. Arrows indicate areas of filipin staining which associates with LDLR expression. Scale bars represent 20 μm.

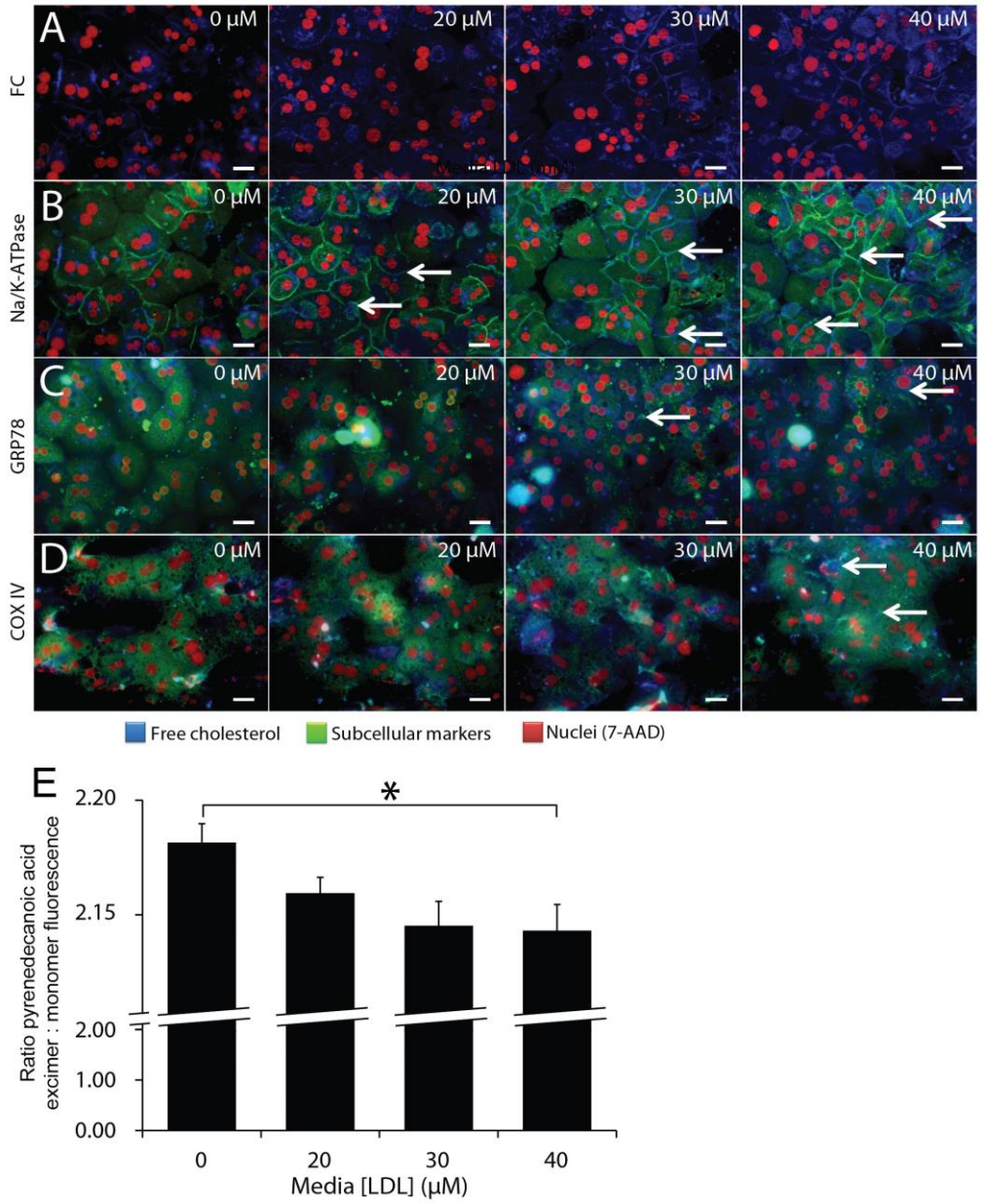

Figure 3.3 FC localises to plasma membrane, ER and mitochondria in primary murine hepatocytes loaded with LDL and reduces membrane fluidity.

WT C57B6/J hepatocytes were exposed to 20-40 µM LDL over 24 h. Cells demonstrated (**A**) dose-dependent increases in FC filipin (blue) fluorescence, which co-localises (arrows) with (**B**) plasma membrane (Na/K-ATPase, green), (**C**) endoplasmic reticulum (GRP78, green), and (**D**) mitochondrial (COXIV, green) markers. Cellular nuclei were counter-stained with 7-AAD (red fluorescence). Arrows indicate representative regions of co-localised staining between filipin and subcellular compartments. Scale bars represent 20 µm. (**E**) Primary WT hepatocytes were exposed to 0-40 µM LDL, washed and stained with pyrenedecanoic acid. Pyrenedecanoic acid excitation (dimer formation; a surrogate marker of membrane fluidity) was decreased in hepatocytes after cholesterol loading, consistent with localisation of FC in the plasma membrane (Figure 3.1A).

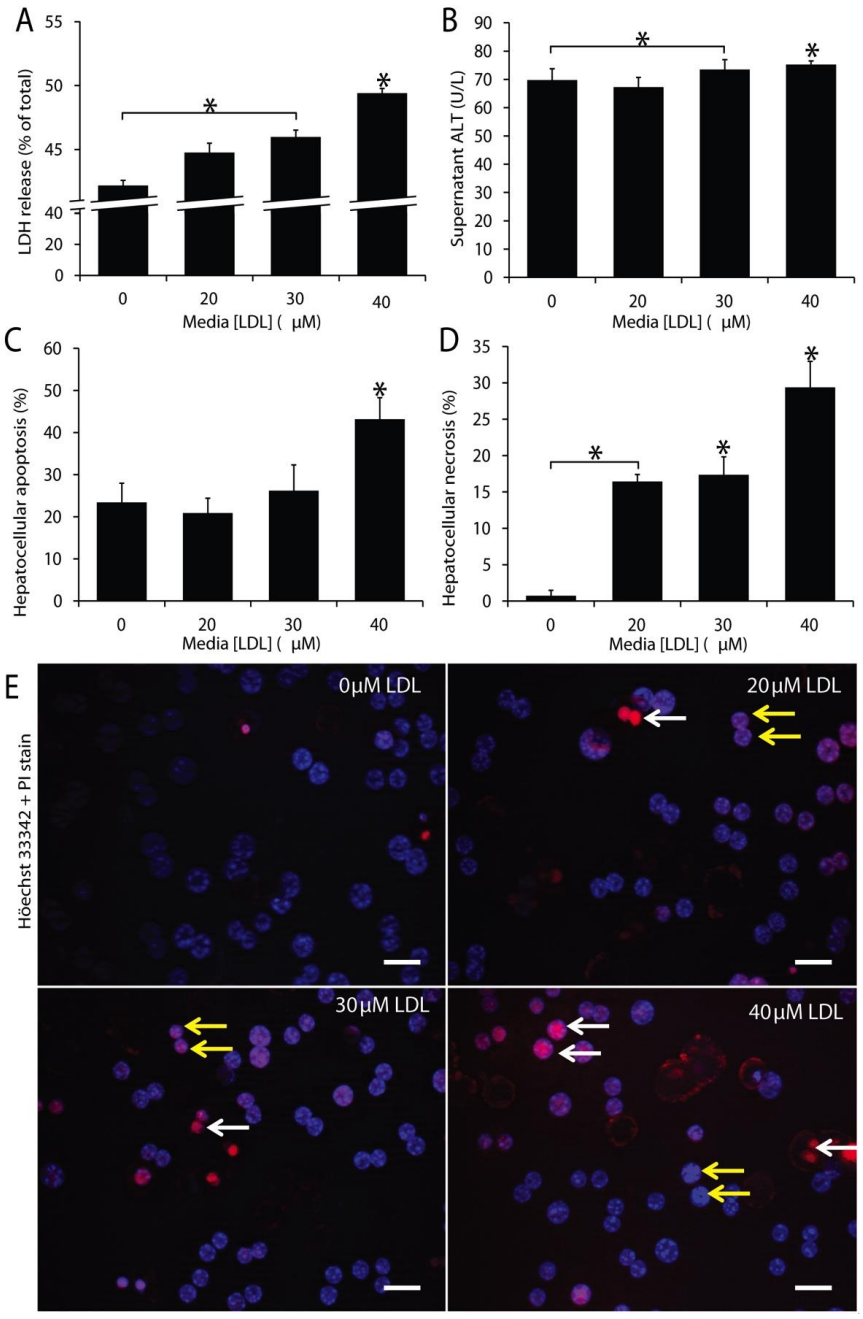

Figure 3.4 FC loading causes liver injury, apoptosis and necrosis in primary murine hepatocytes.

(A) Incubation of WT C57B6/J primary hepatocytes with unmodified human LDL (20-40 µM) for 24 h increases LDH leakage and (**B**) supernatant ALT levels in a dose-dependent manner. Cholesterol loading also incites significant increases in (**C**) apoptosis and (**D**) necrosis, as determined using morphological assessment of Höechst 33342 (blue staining) and PI (red staining) fluorescence. (**E**) Representative images of Höechst 33342 and PI staining in LDL-loaded *vs* control hepatocytes. **P*<0.05, *vs* time-matched control. Mean ± SEM from 4–6 animals. All experiments were repeated 2-4 times, *n*=8-24/gp (see Section 2.15.3 for methodological details). Yellow arrows show the pyknotic nuclei of cells undergoing apoptosis, white arrows are PI-positive cells. Scale bars: 20 µm.

3.4.4 FC loading cause ultrastructural changes within hepatocytes

The effect of FC-loading of primary hepatocytes on cellular ultrastructure was then assessed using SEM and TEM microscopy (Figure 3.5). Loading hepatocytes with 40 μM LDL resulted in a dramatic shift in the morphology of hepatocytes: internal cellular disorganisation, upregulation of autophagic vacuoles and plasma membrane derangement were observed. Hepatocytes damaged by FC-loading were also seen to undergo widespread plasma membrane blebbing, mitochondrial swelling and nuclear autophagy, the latter is shown by chromatin condensation and nuclear membrane fragmentation (Figure 3.5A,B). Interestingly, the membrane fragments produced by PM blebbing matched the reported size range of EVs (100 nm to 1.0 μm) (Figure 3.5A,B arrows).

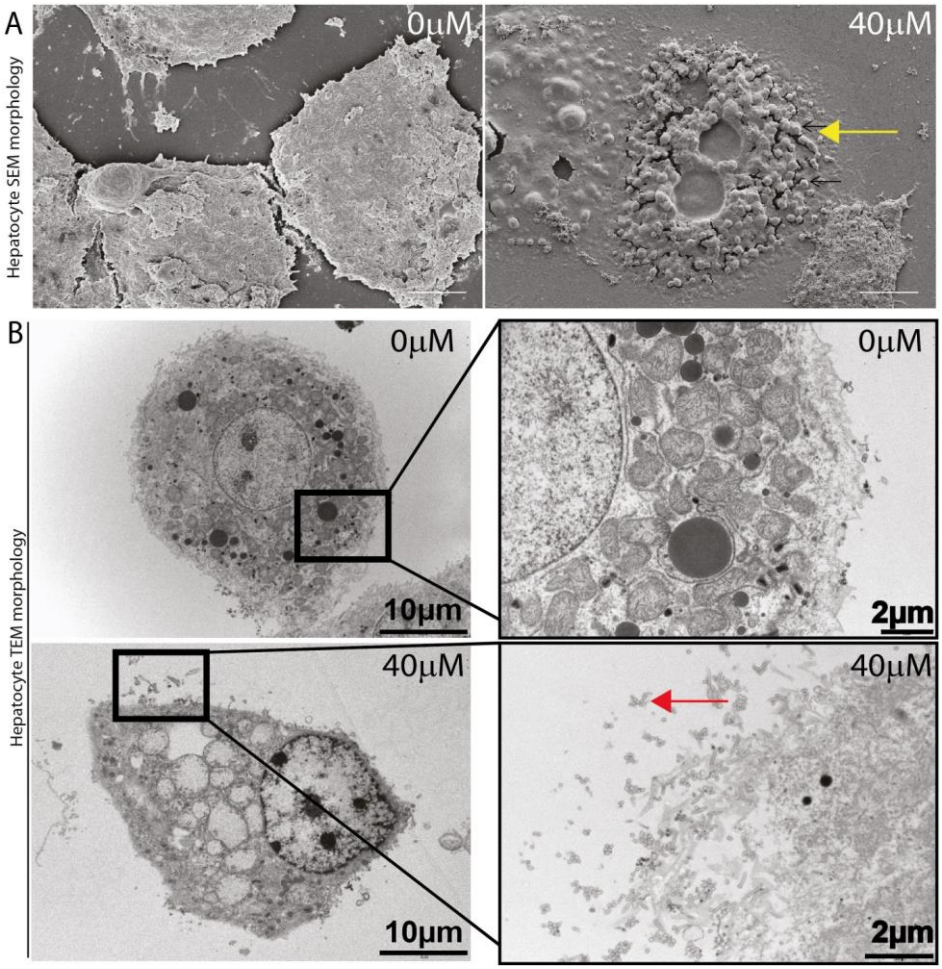

Figure 3.5 FC-loaded primary hepatocytes undergo plasma membrane blebbing and EV formation, as demonstrated by SEM and TEM

(**A**) SEM of primary C57Bl/6 WT hepatocytes exposed to 0-40 μM LDL was performed as described in Section 2.5.1. After 24 h, cells were fixed, processed and platinum sputter coated (20 nm, 20 mA, 3 mins) (EmiTech, GmbH, Germany) prior to viewing on Zeiss UltraPlus analytical FESEM (Oberkochen, Germany) (3-10 kV setting). WT hepatocytes not exposed to LDL (panels labeled 0 μM) had uniform monolayer morphology and were largely confluent with mosaic pattern architecture. Conversely, hepatocytes loaded with FC (40 μM LDL) exhibited significant alteration in hepatocyte morphology. They were less confluent and many cells showed features of apoptosis, as well as plasma membrane blebbing and extracellular vesicle (EV) release (yellow arrow). (**B**) TEM was performed as per Section 3.3.6, prior to viewing on a JEOL 2100F (Peabody, MA) TEM microscope. Hepatocytes not exposed to LDL have ordered internal ultrastructure, numerous perinuclear mitochondria and an intact plasma membrane. However, following 40 μM LDL exposure to produce FC-loading, mitochondrial disarray and reduction in total number of mitochondria, plasma membrane blebbing with EV release were observed. Panel A scale bars represent 20 μm, panel B scale bars indicated in the lower right panel quadrant.

3.5 Discussion

Two decades ago, Unger and colleagues coined the term lipotoxicity to describe the deleterious effects of excessive FFA on murine pancreatic β cell function in the pathogenesis of T2D (Lee *et al.*, 1994). This term embraces cellular injury and death, often with resultant inflammation, caused by sFFA and their metabolites, including DAG and possibly TG in excess (Neuschwander-Tetri, 2010). The tissue responses to this form of injury include inflammation and a wound-healing response with matrix deposition leading to scar formation (fibrosis) and hepatocellular regeneration. The pathogenesis of NASH is now generally regarded a consequence of hepatic lipotoxicity, whereby one or more toxic lipid species accumulate within the steatotic liver and induce hepatocellular damage, inflammatory cell recruitment and over time, fibrosis and eventually cirrhosis (Alkhouri *et al.*, 2009, Farrell *et al.*, 2012). TG, traditionally thought to be important "first hit" in the progression to NASH (Day and James, 1998), is now widely considered the safe form of lipid storage, as reviewed in Section 1.3. Whilst sFFA and their metabolites have been the most studied "toxic lipid species" in relation to production of liver injury, the role of cholesterol (and specifically FC) in NASH progression has recently gained credibility among reviewers in the field of NAFLD (Alkhouri *et al.*, 2009, Neuschwander-Tetri, 2010, Arteel, 2012, Musso *et al.*, 2013). The evidence supporting this concept was reviewed in Chapter 1, Section 1.3 of the Thesis.

Research from the host laboratory using *foz/foz* mice model of metabolic obesity demonstrated a clear correlation between increased hepatic FC content and NASH severity (Van Rooyen *et al.*, 2011). Furthermore, pharmacological modulation of cholesterol synthesis and/or uptake using atorvastatin and ezetemibe, respectively, reversed the NASH pathology (including liver fibrosis) in this model (Van Rooyen *et al.*, 2013). Elsewhere, researchers have shown similar improvement of liver histology with atorvastatin treatment in biopsy-proven human NASH (Min *et al.*, 2012). Puri *et al.* (2008) and Caballero *et al.* (2009) reported significant increases in hepatic FC in human NASH patients compared to those with SS, in addition to over-expression of SREBP-2 (a transcription factor important in regulation of cholesterol uptake via LDLR and synthesis). While these findings collectively suggest that cholesterol may play a fundamental role in NASH progression, the studies have been largely correlative and cannot fully exclude the contribution of other potential candidate lipid species

including sFFA. We sought to address whether FC can cause hepatic lipotoxicity directly, developing a reductionist model system to investigate the role of cholesterol loading within primary hepatocytes. This Chapter describes the development of this system, in which unmodified human LDL was successfully used to load hepatocytes with FC.

In order to ascertain whether the FC loading observed in this model distributed to the same organelles as FC deposition observed in livers of HF-fed *foz/foz* mice with NASH (and is therefore a representative model), we first revisited a previous *in vivo* study (Van Rooyen *et al.*, 2011). Using frozen liver sections from HF (containing cholesterol in 0, 0.2 or 2.0% w/w)-fed *foz/foz* mice to study the subcellular localisation of FC-deposits, we identified a predominant pattern of FC deposition within the PM compartment (Figure 3.2A). In addition, FC also co-localised to ER and mitochondria, albeit to an apparently lesser extent.

ER is potentially important as a subcellular site of FC deposition in NASH. However, evidence to date for the operation of ER stress in NASH pathogenesis has been inconsistent and conflicting (Puri *et al.*, 2008, Gregor *et al.*, 2009, Leclercq *et al.*, 2011, Legry et al. 2014). ER stress results from an inadequate response to the accumulation of unfolded proteins (UFP) within the ER (the UFP response, UFPR). It is usually accompanied by up-regulation of physiological unfolded protein chaperones, such as GRP78. This is perceived by one or more of 3 signalling cassettes, some of which can signal JNK to activate NF-κB (Wang *et al.*, 2009). If UFP accumulation is not reversed, cells are programmed to undergo apoptosis via migration of CHOP protein (the ER stress apoptosis execution pathway) to the nucleus. In the pathogenesis of diabetes, ER stress contributes to pancreatic β cell loss and insulin resistance (Eizirik *et al.*, 2008). Since NAFLD is closely related to metabolic syndrome, we considered whether ER stress could play a role in FC lipotoxicity. However, there was no increase in the expression of GRP78 or nuclear expression of CHOP in *foz/foz* mice with NASH (Van Rooyen *et al* [unpublished], PhD ANU, 2011), in spite of ER cholesterol localisation. The contribution of ER stress in FC-induced lipotoxicity will be addressed further in Chapter 4.

Importantly, FC co-localised with mitochondria in *foz/foz* mice with NASH (Figure

3.1C), as previously described by Mari *et al* (2006) in their *in vivo* loading model system. The deposition of FC in mitochondria is an important finding, as this has been inferred by observation in human NASH, shown by upregulation of StAR transcription factor, StAR transports cholesterol into mitochondria (Caballero *et al.*, 2009). Mitochondria FC deposition has relevant implications in understanding the mechanisms for NASH progression, as there are strong evidence to suggest mitochondrial injury occurs in human NASH (Cortez-Pinto *et al.*, 1999, Perez-Carreras *et al.*, 2003, Caldwell *et al.*, 2009); mitochondrial FC loading may explain this process. Details of the impact of mitochondrial injury and activation of mitochondrial cell death pathway by FC will be discussed further in Chapter 4.

In livers of HF/HC-fed *foz/foz* mice with NASH, we also observed accumulation of resident and/or recruited macrophages adjacent to FC-loaded (filipin intense) hepatocytes (Figure 3.1D). Recently, Ioannou *et al.* (2013) used polarised light to demonstrate that these areas of intense filipin staining show abundant birefringent crystals within a large portion of hepatocellular lipid droplets. Since these crystals stain prominently with filipin, they likely represent FC crystallisation. In the same study, similar birefringent cholesterol crystals were also discovered in human NASH livers. Notably, cholesterol crystals were absent in livers of both human and mice with SS. Furthermore, Ioannou *et al* also found similar aggregates of CD68-positive KCs, which formed "crown-like" structures only around hepatocytes which contained birefringent lipid droplets. Most of these KCs also stained positive for CD11b and TNF-α suggesting that they are of the activated (M1) phenotype (Ioannou *et al.*, 2013). These observations are consistent with the idea that KCs are recruited to FC-loaded areas (containing cholesterol crystals) in NASH livers, and become activated upon engulfment of cholesterol crystals; such activation initiates inflammatory and fibrotic pathways that cause NASH progression. Interestingly, in a recent experiment on pathogenesis of atherosclerosis, exposure of macrophages to cholesterol crystals (which is a hallmark of atherosclerotic plaques) was shown to activate inflammatory processes via stimulation of the NLRP3 inflammasome complex (Duewell *et al.*, 2010). Activation of the NLRP3 inflammasome by cholesterol crystals could be amplified by priming macrophages with other pro-inflammatory substances, like cell wall components of Gram-positive bacteria, or minimally modified LDL (Duewell *et al.*, 2010). Future studies directed at modulating cholesterol crystallisation, macrophage aggregation or inflammasome

activation are required to test whether this proposed sequence of events is relevant to NASH (see Future Directions in Chapter 7, Section 7.2).

Having characterised sites of FC deposition *in vivo*, we then achieved loading of primary murine hepatocytes with FC by incubating cells with unmodified human LDL. The efficacy of this approach was assessed with two techniques. Firstly, quantitative biochemical analyses of intracellular FC content (Figure 3.2D), and secondly fluorescent (qualitative) evaluation of FC localisation using filipin staining (Figure 3.2A). By supplementing the culture media with 30 or 40 μM LDL, we were able to significantly load WT C57B6/J hepatocytes with FC (Figure 3.2D). FC "loaded" hepatocytes contained 2-3 fold more FC than control cells (27 *vs* 10 μg/mg protein). Further, the distribution of FC within these loaded hepatocytes correlated strongly with the pattern of FC localisation observed in our *foz/foz* mice with NASH (comparison between Figures 3.1 and 3.3). As yet there are no published studies documenting the hepatic subcellular localisation of FC in human NASH; this constitutes a potential future direction of research (see Future Directions in Chapter 7, Section 7.2.1.1).

One of the interesting findings of the present study is the dose-dependent increase in LDLR expression following FC loading (Figure 3.2B,C). Under physiological conditions, SREBP-2 favours cholesterol synthesis (Horton *et al.*, 2002). In situations of cholesterol excess, such as those found in livers of both mice and humans with NASH (Puri *et al.*, 2007, Caballero *et al.*, 2009, Van Rooyen *et al.*, 2011), cholesterol excess should down-regulate the processing of SREBP-2, which in turn should result in downregulation of HMG-CoA reductase (HMGR) to prevent further cholesterol synthesis, and LDLR to reduce cholesterol uptake via LDL receptor-mediated endocytosis respectively (Brown and Goldstein, 2008). However, in human NASH (Caballero *et al.*, 2009, Min *et al.*, 2012), and *foz/foz* mice with metabolic obesity and NASH (Van Rooyen *et al.*, 2011), SREBP-2 is *inappropriately* increased, likely as a consequence of hyperinsulinemia (Van Rooyen *et al.*, 2011) or in response to inflammatory stress triggering IL-1β secretion (Zhang *et al.*, 2004, Zhao *et al.*, 2011). The contribution of inflammasome activation, in particular IL-1β generation in mechanisms of FC-mediated hepatocellular injury and KC activation will be further explored in Chapter 5. Interestingly, in human NASH, Min *et al* (2012) found increased HMGR protein and decreased expression of LDLR, which is the opposite to what was

described by Van Rooyen *et al* (2011) in the host laboratory in *foz/foz* mice with NASH. This difference could be species-specific but it could also be methodological. Van Rooyen *et al* measured HMGR enzyme activity radiometrically, whereas Min *et al* relied on estimation of HMGR protein (and its phosphorylated [inactive] form), and determination of circulating metabolites, which may not accurately reflect liver tissue HMGR activity. The mechanisms underlying disrupted cholesterol metabolism in NASH is not the focus of this Thesis, and will not be discussed further. Regardless of whether this apparent difference is real or not, what is clear is that there is overall dysregulation of hepatic cholesterol homeostasis in NASH. In particular, pathways responsible for cholesterol utilisation and transport (biotransformation [Cyps 7a1, 7b1, 27a1], canalicular export of cholesterol [ABCG5/8] and bile acid [BSEP, MRP2]), in addition to increase cholesterol uptake (via LDLR and/or CD36) or synthesis, lead to an overall increase FC in NASH livers (Van Rooyen *et al.*, 2011, Farrell and Van Rooyen, 2012, Min *et al.,* 2012, Van Rooyen *et al.*, 2013).

The observed increase in LDLR expression with FC loading of primary hepatocytes (Figure 3.2B,C) recapitulates the changes seen in livers of *foz/foz* mice with NASH (Van Rooyen *et al.,* 2011). Specifically, in WT control and *foz/foz* mice with SS, LDLR expression is restricted to sinusoidal endothelial cells, especially within centrilobular regions of the liver, whereas *foz/foz* mice fed HF-diet containing 2% cholesterol [w/w] with NASH, display LDLR expression on hepatocytes throughout the liver (Van Rooyen *et al.*, 2011).

In our quest to develop an ideal cell culture system to study mechanism of FC-induced lipotoxicity, several attempts were made to isolate and culture primary hepatocytes from *foz/foz* mice fed chow, as well as mice fed various fat and cholesterol-containing diets administered for varying durations post-weaning (6, 8, 10, and 12 weeks). Unfortunately, the viability of hepatocytes obtained from these isolations was uniformly low, despite diverse protocol modifications, including reduced perfusion flow rate and lowered collagenase concentrations (Table 3.1). We attributed this reduced viability to the early steatosis observed in *foz/foz* livers. Fat-laden hepatocytes are swollen (have larger volume and surface area) and can cause distortion of sinusoidal space (Farrell *et al.,* 2008). This may impair of microvascular perfusion during isolation of hepatocytes, thereby compromising their viability. In addition, steatotic hepatocytes are relatively

"fragile" and tend to rupture during processing, while those that survive isolation tend to float due to the buoyancy effect of their high lipid content and surface area. Inverted culture techniques exist for culturing adipocytes, however, this method requires substantially more culture media (and consequently more reagent) and is notoriously fastidious (Sugihara *et al.*, 1986, Asada *et al.*, 2011, Kuroda *et al.*, 2011). Accordingly, this method was not employed and we decided to pursue our described method of *in vitro* LDL-loading.

Another limitation to this study is the method of organelle co-localisation for subcellular FC deposits. Ideally, to appreciate the exact co-localisation of FC deposits within hepatocytes, confocal microscopy is used. This allows stereodological analysis of three-dimensional structures through precise optical section of the *Z*-axis plane (Howell *et al.*, 2002). However, the filipin staining used in this study requires UV laser (364 nm) excitation (Boutte *et al.*, 2011), which is unfortunately not available at the Australian National University (ANU) microscopy facilities. Consequently, an epi-fluorescence mercury lamp (Zeiss Axioplan2 microscope; Zeiss, GmbH, Germany) was used to acquire "pseudo-confocal" cross-sectional fluorescence images of filipin intense areas of FC-loaded hepatocytes, and this technique coupled to fluorescent markers for PM (Na/K-ATPase), endoplasmic reticulum (GRP78) and mitochondria (COXIV) was used to identify FC and organelle co-localisation. This compromises the resolution of structures and reduces validity of "semiquantitative" assessments of organelle FC content and localisation.

As discussed earlier, we confirmed FC impregnation of our primary hepatocyte culture system using two methods – biochemically using a commercially available Wako kit, which is a quantitative method and qualitatively, by intensity of blue filipin fluorescence. This is based on the premise that LDL is being taken up into hepatocytes via LDLR-specific endocytosis, where cholesteryl ester hydrolase (CEH) catalyses the hydrolysis of cholesterol ester (CE) inside the LDL complex to release FC (Hui, 1996). Ideally assessment of all the lipid species within primary hepatocytes, namely neutral lipids (CE, TG, FC, DG), FFA, total FFA and phospholipids (PL) should be confirmed using high-performance lipid chromatography (HPLC). Additionally, whilst we confirmed FC deposition in plasma membrane, mitochondria and ER by co-localisation between filipin FC staining and relevant subcellular compartment markers, a more

accurate way of determining FC deposition (in particular to mitochondria) would be performed by separately isolating these subcellular compartments and quantifying the FC content of each fraction by an analytical technique. Due to reagent limitation (expense of LDL), analysis of lipid status within hepatocytes incubated with LDL using HPLC and quantification of FC inside subcellular compartments were not possible in the present "small scale" experiments. We also cannot exclude substantial localisation of FC (or cholesterol crystals) in lysosomes (as suggested by Ioaunou *et al.* 2013) or lipid bodies.

3.6 Summary of findings

This Chapter describes the successful development of a method for loading primary murine hepatocytes with FC, by incubating them with unmodified human LDL. The major findings are:

1. In HF/HC-fed *foz/foz* mice with NASH, FC localises predominantly to plasma membrane, and to lesser extent to mitochondria and the ER.
2. Incubation of WT C57B6/J hepatocytes with unmodified human LDL produces dose-dependent FC loading, which recapitulates the subcellular localisation observed in *foz/foz* mice with NASH.
3. Effects of FC loading in PM include reduced membrane fluidity, PM blebbing and formation of EVs.
4. FC loading causes dose-dependent increase in hepatocellular injury, and cell death via apoptosis and necrosis.
5. Ultrastructural studies indicate mitochondria and PM are particularly altered by FC deposition in cultured hepatocytes.

These findings provide a suitable test system to investigate how FC injures hepatocytes to cause apoptosis and necrosis. In the next Chapter, the candidate will address the relationships between FC loading and JNK1 activation with oxidative stress and mitochondrial dysfunction. The contribution of ER stress as a lipotoxic mechanism will also be explored.

CHAPTER 4

c-Jun *N*-terminal kinase-1 activation is essential for free cholesterol-mediated hepatocyte lipotoxicity

4.1 Introduction

Chapter 3 described the development of a robust and effective *in vitro* system to load primary murine hepatocytes with FC by incubating them with unmodified human LDL at 20–40 μM concentrations. It was also shown how FC causes hepatocyte injury, manifesting as leakage of LDH and ALT into culture media (Figures 3.4A,B), alongside increases in cell death by apoptosis (Figure 3.4C), and, more strikingly, by necrosis (Figure 3.4D). We were also able to show that FC co-localises predominantly to plasma membrane, with additional deposition in ER and mitochondria in FC-loaded primary hepatocytes (Figure 3.3B,C,D), identical to the FC localisation observed in livers of *foz/foz* mice with NASH (Figure 3.1A,B,C).

In the host laboratory, Van Rooyen *et al* (2011) demonstrated that in *foz/foz* mice with NASH, the increase liver FC content is associated with liver injury (increased serum ALT), fibrosis (demonstrated by Sirius red stain), apoptosis (M30 IHC), and accumulation of F4/80 stained KCs around fat-laden hepatocytes that contained FC-rich vacuoles (Van Rooyen *et al.* 2011). Pharmacological lowering of hepatic cholesterol in these mice ameliorated development of hepatocellular apoptosis and liver fibrosis (Van Rooyen *et al.* 2013). Others have also shown that pharmacological cholesterol lowering caused similar improvements in liver enzymes and/or histology in both human and animal models with NASH (Kiyici *et al.* 2003, Rallidis *et al.* 2004, Zheng *et al.* 2008, Abel *et al.* 2009, Nozaki *et al.* 2009, Min *et al.* 2012). Together, the correlations between diet-related hepatocyte FC and NASH severity, and the beneficial effects of cholesterol-lowering drugs on liver pathology provide indirect evidence that FC accumulation in NASH could cause hepatocyte apoptosis and necrosis, inflammatory recruitment and fibrosis.

One potential mechanism linking FC to inflammatory recruitment in the liver, as well as to insulin resistance, is JNK1/2 activation. This could be caused either by direct effects of the lipotoxic lipid (FC), or indirectly by oxidative stress, ER stress or growth factor/cytokine receptor or TLR signalling.

4.1.1 Oxidative stress in the pathogenesis of NASH

Oxidative stress can be defined as a severe disturbance in the prooxidant-antioxidant balance in favour of the former. The prooxidant excess subsequently overwhelms the capacity of endogenous cellular antioxidant defense systems, leading to damage to cells and organs (da Silva *et al.* 2010). Enhanced generation of reactive oxidant species (ROS) resulting in oxidative stress has been implicated in many liver diseases, including hepatic ischemia reperfusion injury (Jaeschke 2003, Jaeschke 2003, Jaeschke *et al.* 2003), acetaminophen (APAP)-induced liver failure (Jaeschke 2003, Jaeschke 2003, Jaeschke *et al.* 2003), alcohol-induced liver injury (Adachi and Ishii 2002, Arteel *et al.* 2003, Arteel 2003), hepatic fibrosis (Okazaki *et al.* 2000, Poli 2000, Friedman 2004) and hepatocellular carcinoma (Petersen 2005).

Oxidative stress also appears to be evident in NASH, where it has been attributed to a variety of mechanisms. These include the upregulation of cytochrome P450 2E1 (Weltman *et al.* 1998, Robertson *et al.* 2001), and changes in mitochondrial function, such as increased β-oxidation or uncoupling of oxidative phosphorylation with leakage of electrons (Sanyal *et al.* 2001, Nakamura *et al.* 2009). Recruited inflammatory cells also generate prooxidants, particularly via NADPH oxidase (Neuschwander-Tetri and Caldwell 2003, Lambertucci *et al.* 2008). Oxidative stress has also been linked to pathogenesis of atherosclerosis, hypertension (Halliwell 1989, Stampfer *et al.* 1993, Griendling *et al.* 1994, Griendling *et al.* 1994, Uppal *et al.* 2014) and diabetes mellitus (Baynes 1991, De Mattia *et al.* 1998, De Mattia *et al.* 1998, Gerrits *et al.* 2014). All of these conditions are part of or have strong associations with metabolic syndrome, which seems inextricably entwined with NASH pathogenesis (Farrell and Larter 2006, Larter *et al.* 2010, Gan *et al.* 2011).

As discussed in Chapter 3, Mari *et al* (2006) showed that cholesterol-laden livers are highly susceptible to TNF-α and Fas-mediated apoptosis by a mechanism that involves FC accumulation in mitochondria and oxidative stress (Mari *et al.* 2006). Mitochondria

are normally devoid of cholesterol, but in NASH, livers show 15-fold increased levels of transcripts for StAR, the protein responsible for cholesterol transport to mitochondria to cause mitochondria FC accumulation (Caballero *et al.* 2009). Such mitochondrial FC deposition is a potential player for progression of steatosis to NASH via selective depletion of mitochondrial GSH (Mari *et al.* 2006, Mari *et al.* 2008). Together with mitochondrial injury (possibly from FC deposition into mitochondria), this results in uncoupling of mitochondrial respiratory chain, electron leakage and 'unchecked' generation of mitochondria ROS (Dawson *et al.* 1993).

Generation of ROS is important as it can lead to prolonged activation of JNK1/2 (Nieminen *et al.* 1997, Czaja *et al.* 2003, Hong *et al.* 2009). Additionally, ROS have been suggested to be involved in TLR4-mediated inflammation in murine models of steatohepatitis (Hritz *et al.* 2008, Ye *et al.* 2012). Given the strong evidence that FC is elevated in NASH livers but not with simple steatosis (Puri *et al.* 2007, Caballero *et al.* 2009, Van Rooyen *et al.* 2011, Min *et al.* 2012), and that mitochondrial FC deposition (Mari *et al.* 2006, Caballero *et al.* 2009) and mitochondrial ultrastructural changes are a reproducible feature in NASH pathogenesis (Caldwell *et al.* 2009) (Caldwell *et al.* 1999, Sanyal *et al.* 2001), we sought to establish whether there existed links between FC and oxidative stress, in particular mitochondrial-generated ROS in our FC-loaded primary hepatocyte culture system.

4.1.2 Roles of JNKs in the pathogenesis of NASH

One of the features that distinguish NASH from non-NASH NAFLD is activation of pro-inflammatory pathways. These may include ionic calcium, ROS, protein kinases, transcription factors, and most consistently NF-κB and JNK (Farrell *et al.* 2012). For the purpose of this Chapter, focus will be directed at JNK activation, though NF-κB and JNK are usually activated simultaneously, especially during oxidative stress (Farrell *et al.* 2012).

JNK can be activated by multiple stimuli, including cytokines (TNF-α, IL-1β, transforming growth factor [TGF]-β, platelet-derived growth factor [PDGF], epidermal growth factor [EGF]), intracellular and extracellular pathogens (lipopolysaccharide [LPS], peptidoglycan, and bacterial unmethylated CpG DNA all of which activate various TLRs), ROS, pathologic and environmental stress (ischemia, UV, ionising

radiation), toxins, drugs, ER stress, and metabolic changes including obesity and hyperlipidemia (Farrell *et al.* 2012, Seki and Schnabl 2012). Strong activation of JNK has been observed in the liver, fat and muscle tissues in mice placed on HFD, as well as in genetically (*ob/ob*) obese mice (Hirosumi *et al.* 2002, Solinas *et al.* 2006). In the host laboratory, JNK1/2 activation has been confirmed in livers of metabolically obese *foz/foz* mice with NASH (Figure 4.1A), and shown to be linked to FC accumulation (Van Rooyen *et al.* 2011, Van Rooyen *et al.* 2013). Further, pharmacological lowering of cholesterol in these NASH livers resulted in amelioration of inflammatory recruitment and fibrosis (discussed earlier) in concert with abrogation of JNK1/2 activation (Figure 4.1) (Van Rooyen *et al.* 2013). These links support the proposal that FC-mediated JNK activation could be critical for activation of injury and inflammatory pathways in NASH related to metabolic syndrome.

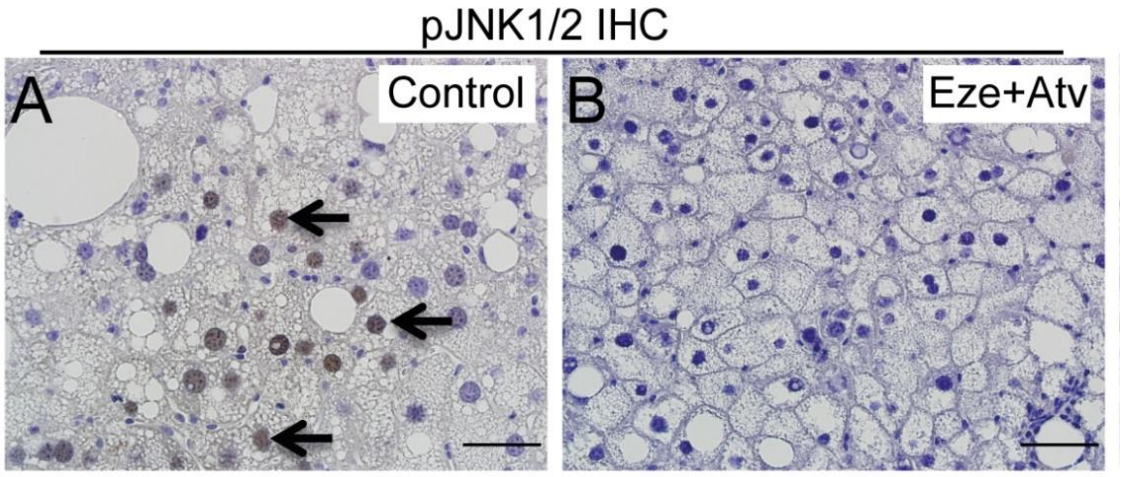

Figure 4.1 Hepatic injury in *foz/foz* mice with NASH is associated with hepatocellular activation of JNK1/2, and is reversed by ezetimibe and atorvastatin treatment.

(**A**) After 24 weeks of HF (0.2% cholesterol) feeding, livers from obese, diabetic *foz/foz* mice with NASH showed pJNK1/2 activation in hepatocyte nuclei (arrows). This activation correlated with both hepatic FC content and NASH severity (Van Rooyen *et al.* 2013), (**B**) both of which were reversed following ezetimibe (Eze) and atorvastatin (Atv) treatment for 8 weeks. Improvement in NASH severity was accompanied by significant reductions in hepatic FC content (Van Rooyen *et al.* 2013). Bars represent 20 µm. A and B are representative liver sections from a group of animals (*n*=8-9/grp, as published [Van Rooyen *et al.* 2013]).

4.1.2.1 JNK isoforms

In the last decade, researchers have become aware of the diverging roles of JNK1 and JNK2 isoforms in pathogenesis of metabolic disease and NASH. Both JNK1 and JNK2 can cause insulin resistance by phosphorylation of insulin receptor substrate (IRS)-1 and

IRS2, respectively at Ser-307 (see Figure 4.20) and Thr-348. This results in inhibition of insulin receptor signalling (Solinas *et al.* 2006, Kodama *et al.* 2009). On the other hand, JNK1 causes steatosis (Kodama *et al.* 2009). Thus, in whole animal experiments, *Jnk1*$^{-/-}$ but not *Jnk2*$^{-/-}$ animals on MCD diet were protected from liver injury (Schattenberg *et al.* 2006). Similarly, when put on HFD, *Jnk1*$^{-/-}$mice were protected from liver injury, obesity and insulin resistance (IR) (Hirosumi *et al.* 2002, Singh *et al.* 2009). On the other hand, *Jnk2*$^{-/-}$ mice, like WT mice, exhibited obesity, insulin resistance and hepatocyte injury on HFD (Singh *et al.* 2009).

Interestingly, livers from *Jnk2*$^{-/-}$ mice have greater overall JNK activity, indicating the possibility that JNK1 overcompensation could contribute to insulin resistance and liver injury (Singh *et al.* 2009). Such an effect of JNK1 overcompensation was confirmed in *Jnk2*$^{-/-}$ mice with JNK1 haploinsufficiency (*Jnk2*$^{-/-}$*Jnk1*$^{+/-}$, produced by crossing *Jnk1*$^{-/-}$ with *Jnk2*$^{-/-}$ mice); these animals were less obese, and had reduced hepatic steatosis and increased insulin sensitivity after 16 weeks of HFD (Tuncman *et al.* 2006). It is of considerable interest that other studies have demonstrated that JNK1 can phosphorylate *c*-Jun, thereby activating its transcriptional activity, whereas JNK2 does not phosphorylate *c*-Jun, and may even oppose the action of JNK1 in this respect (Sabapathy *et al.* 2004, Sabapathy and Wagner 2004, Singh *et al.* 2009).

4.2 Purpose of study: hypotheses and aims

As described in Chapter 3 (Section 3.5), lipotoxicity of hepatocytes is a form of cellular injury and cell death caused by toxic lipid species or their metabolites. This is now a widely accepted concept for NASH pathogenesis (Larter *et al.* 2010, Neuschwander-Tetri 2010, Cusi 2012). SatFFA can cause apoptosis in hepatocytes through the activation of JNK1 and the p53 mediator of apoptosis (PUMA) and Bax (Cazanave *et al.* 2009, Cazanave *et al.* 2010, Sharma *et al.* 2012). However, lipodomic analyses from both human and mice NAFLD livers showed that FC, and not satFFA, is the distinguishing differentiation in lipid species between livers showing NASH and those with simple steatosis (Puri *et al.* 2007, Caballero *et al.* 2009, Van Rooyen *et al.* 2011).

In the previous Chapter, it was demonstrated that FC is lipotoxic to primary hepatocytes, as evident by increased supernatant ALT and LDH leakage, and hepatocellular apoptosis and necrosis. Since such lipotoxicity appeared to be related to

JNK1/2 activation in our *in vivo* mouse model of metabolic obesity (discussed above), we sought to determine how FC may activate JNK and the implications of this for cell survival, in particular focusing on mitochondrial and ER stress pathways.

We hypothesised that JNK1 activation is necessary for FC-mediated liver injury, and that mitochondrial injury and ensuing activation of cell death pathways play a crucial role in this process. The specific aims of this Chapter are detailed below.

4.2 Aims of this Chapter:

1. Elucidate pathways responsible for FC-induced hepatocyte injury, in particular the role (if any) of JNK1 and -2.
2. Determine whether silencing of JNK1 or -2 gene expression, using gene-deleted mice, confers protection to hepatocytes exposed to increasing levels of cholesterol.
3. Determine whether JNK inhibition with potent, specific agents confers hepato-protection from FC-induced liver injury and death.
4. Establish the effect that FC accumulation may have on mitochondrial integrity.
5. Test whether oxidative stress and ER stress play discernible roles in FC-induced injury to hepatocytes.

4.3 Methods

4.3.1 Mice and diets

Female *foz/foz* NOD.B10 mice were fed HF/HC-diet (containing 0, 0.2 or 2.0% [w/w] cholesterol) for 24 weeks. Details pertaining to experimental conditions and dietary composition have been outlined in previous experiments conducted in the host laboratory (Van Rooyen *et al.* 2011). The studies of liver tissues were from experiments reported by the host laboratory (Van Rooyen and Farrell 2011, Van Rooyen *et al.* 2013). Mice were maintained as described in Section 2.4. At termination of experiments, livers were harvested and stored at –80°C until ready for use. JNK1 activation was assessed by WB (using JNK1-specific antibody), and IHC for phospho-JNK1/2 (the antibody used detects both isoforms), as described by Van Rooyen (2011). See Table 2.1 for antibody conditions.

To determine which JNK isoform mediates cell injury and death in FC-loaded hepatocytes, we used primary hepatocytes derived from lean female WT, *Jnk1*$^{-/-}$ and *Jnk2*$^{-/-}$ mice, all on C57Bl/6J background. WT C57Bl/6J mice were from ANU Phenomics Research Facility, while *Jnk1*$^{-/-}$ and *Jnk2*$^{-/-}$ mice (on C57Bl/6J background) were kindly provided by Dr David Nikolic-Paterson (Monash Medical Centre, Clayton, Victoria). Experimental animals were generated by crossing homozygous *Jnk1*$^{-/-}$ and *Jnk2*$^{-/-}$ with WT to produce *Jnk1*$^{+/-}$ and *Jnk2*$^{+/-}$ mice, then crossing the generated heterozygotes to produce both homozygous knockouts and WT littermates.

4.3.1.1 Reagents

Materials for primary hepatocyte isolation were as detailed in Section 2.5.1. Reagents used specifically in this Chapter are detailed below.

30 mM JNK inhibitor stock solutions (Chapter 2, Section 2.2). CC-401 (30.86 mg), CC-930 (30.55 mg) and CC-003 (30.23 mg) were dissolved in 2.65 mL, 2.27 mL and 2.77 mL respectively of 100% DMSO to achieve stock concentration of 30 mM. This was aliquoted into light protected Eppendorf containers and stored at –20°C until ready for use. In cell-based assays, IC_{50} values for phospho-*c*-Jun inhibition of CC-401 and CC-930 are at 1–5 µM and 1 µM respectively (Ma *et al.* 2007, Lim *et al.* 2011). CC-401, CC-930 and CC-003 have increasing potency and specificity for JNK1 blockade (Brydon Bennett, Celgene Inc, Personal communication, September 2014). However,

since no studies have been done using this class of JNK inhibitors in primary murine hepatocytes, we sought to establish optimal cytoprotective concentrations for each compound in FC-loaded primary hepatocytes (See section 4.4.1 for results). We used 1, 2, 5 and 10 µM inhibitor concentrations and determined cell death by apoptosis and necrosis (Figure 4.8).

4.3.1.2 Procedures

Primary hepatocytes were isolated as described in Section 2.5. They were then seeded onto rat-tail collagen-coated culture plates at ~6.5 X 10^4 viable cells/cm^2 and incubated at 37°C in 5% CO_2 and ~70% relative humidity. At 4 h, dead cells and debris were removed by washing with warm HBSS before adding JNK inhibitors. Initially different concentrations (1, 2, 5 and 10 µM) were used to determine whether compounds displayed cytotoxicity. Later experiments used only 1 and 2 µM inhibitor concentrations. At 8 h post seeding, 40 µM LDL was added to load hepatocytes with FC. Control groups received no LDL supplementation. Similarly, cyclosporin A (CyA) (10 µM), pancaspase inhibitor (50 µM), caspase 3/7 inhibitor (1 µM), and 4-phenylbutyric acid (4-PBA) (500 µM) were added to culture media after washing, then 40 µM LDL was supplemented to the media at 8 h. Supernatants were sampled for ALT and LDH immediately prior to terminating experiments at 24h post seeding.

Cells were harvested and RNA (Section 2.9.1), as well as total, nuclear, mitochondria and cytoplasmic (mitochondria-free) protein fractions were isolated (Sections 2.10.1, 2.10.2, 2.10.3, respectively). These samples were used for cDNA synthesis, real-time PCR and western blotting, as described in Sections 2.9.2, 2.9.3, and 2.13, respectively).

For immunofluorescence studies, cells were grown on 4 chamber Thermanox® plastic slides (Nunc, Roskilde, Denmark) then washed with ice-cold PBS, before fixation with 3.7% PFA (v/v). Slides were then stored at 4°C in PBS, prior to immunofluorescence studies (Section 2.15).

Primary and secondary antibodies and primers used in this study are detailed in Tables 2.1, 2.2 and 2.4, respectively.

LDH was quantified in culture supernatant as described in Section 2.15, using a

commercially available kit, Cytotox 96© non-radioactive cytotoxicity assay (Promega, Madison, WI). Culture supernatant ALT was analysed by automated techniques (Clinical Chemistry Department, The Canberra Hospital).

4.3.2 Evaluation of cellular oxidative stress

As discussed earlier (Section 4.1.1), oxidative stress occurs when endogenous cellular antioxidant defence capacity is overwhelmed by pro-oxidant factors, resulting in tissue and cellular damage (da Silva *et al.* 2010). Since oxidative stress has been implicated strongly in NASH pathogenesis, and FC has been identified as an important lipid species that accumulates in NASH livers, we utilised our *in vitro* system to test if FC led to cell death and JNK activation through oxidative stress pathways. One method to evaluate oxidative is using dihydrodichlorofluorescein diacetate (H_2DCF-DA).

4.3.1.3 2',7'-dichlorofluorescein (DCF) as measure of oxidative stress generated from release of mitochondrial cytochrome c into cytosol

Following passage through the plasma membrane, the lipophilic H_2DCF-DA is de-esterified to a hydrophilic alcohol, dihydrodichlorofluorescein (H_2DCF). H_2DCF can cross the outer mitochondrial membrane where it distributes between cytosol and the mitochondrial intermembranous space, creating a weak cytosolic and somewhat stronger mitochondrial fluorescence that indicates oxidation to 2',7'-DCF. This weak fluorescence, often interpreted as background/negative DCF test, is the result of normal mitochondrial H_2O_2 production, the presence of cytochrome c in the mitochondrial intermembranous space and minute amounts of labile iron being transported through the cytosol (Karlsson *et al.* 2010). Therefore, ROS generated in normal functioning mitochondria alone are not adequate to give rise to strong cytosolic 2',7'-DCF fluorescence. Instead, this process also requires the simultaneous presence of the following elements in the cytosol:

1) Hydroxyl radicals formed during a Fenton-type reaction, H_2O_2 and H_2DCF, or
2) Cytochrome c and H_2DCF (Karlsson *et al.* 2010).

The presence of cytochrome c in the cytosol is required to catalyse the enzymatic conversion of H_2DCF to 2',7'-DCF. We therefore used DCF fluorescence as an indirect measurement of ROS generated due to release of cytochrome *c* from mitochondria to cytosol, using the method described below.

4.3.2.1.1 Reagents

5mM H_2DCF-DA stock solution. H_2DCF-DA (20 mg) was dissolved in 100% ethanol (20.6 mL). Solution was aliquoted and stored at –20°C (light protected) until ready for use.

4.3.2.1.2 Methods

Methods for detecting 2',7'-DCF fluorescence have been described by others (LeBel *et al.* 1992, Nieminen *et al.* 1997, Karlsson *et al.* 2010). Briefly, primary hepatocytes were seeded onto rat-tail collagen coated 96 well plates (Iwaki Sterilin, Staffordshire, UK) and 4 chamber plastic slides (Nunc, Roskilde, Denmark). After a 24-hour experiment, cultured hepatocytes were loaded (10 µM H_2DCF-DA made from stock in warm William's E media, and incubated at 37°C for 30-50 min in the dark). Following this, the 96 well plates were washed with warm PBS, then fluorescence quantified by fluorometric analysis (excitation wavelength 492 nm, emission wavelength 530 nm) using a FLUOstar OPTIMA plate reader. Hepatocytes grown on 4 chamber slides were similarly treated, then images captured using an Olympus IX70 microscope fitted with a colour camera (Olympus, Wendenstrasse, Hamburg, Germany) that contained a 520 nm band filter.

4.3.2.2 Reduced glutathione (GSH) and glutathione disulfide (GSSG)

Glutathione (Figure 4.2) is present in all mammalian cells, typically at millimolar concentrations (physiological range: 0.5-10 mM) (Baker *et al.* 1990, Will *et al.* 1999). In the liver, concentrations are 4-8 mM, with nearly all the glutathione in its reduced form, and <5% as glutathione disulfide (GSSG) (Will *et al.* 1999). GSH is an important redox regulator, playing a prominent role in free radical scavenging, reducing disulphide bonds, protecting cysteines from irreversible oxidation, and in detoxification of various electrophilic metabolites of xenobiotics (Lauterburg *et al.* 1984, Lauterburg *et al.* 1984, Baker *et al.* 1990, Will *et al.* 1999, Kojer *et al.* 2012). During these processes, GSH is oxidised to GSSG, while its targets are kept in the reduced state (Will *et al.* 1999, Kojer *et al.* 2012).

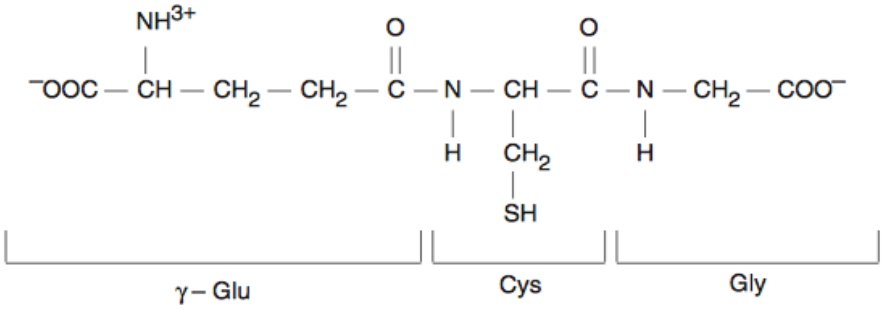

Figure 4.2 Structure of reduced glutathione, GSH

Adapted from Will *et al.* (Will *et al.* 1999).

Although most GSSG generated intracellularly is reduced by glutathione reductase to GSH in an NADPH-dependent process (Figure 4.3) (Droge 2002), during oxidative stress a substantial quantity of GSSG is secreted into bile and blood, thus creating a net loss of glutathione from the liver (Adams *et al.* 1983, Lauterburg *et al.* 1984, Lauterburg *et al.* 1984). As alluded to earlier, oxidative stress occurs due to an imbalance between production and detoxification of free radicals and other pro-oxidant molecules, which can be either exogenous or endogenous in origin. Exogenous stresses can be caused by pollutants, pesticides, drugs, and ionising radiation. Conversely, endogenous oxidative stress results primarily from mitochondrial electron transport failure (e.g. in mitochondrial injury), ischemia-reperfusion or induction of pro-oxidant enzymes (Will *et al.* 1999).

With this in mind, we assayed at GSH and GSSG levels in FC-loaded primary hepatocytes to establish the presence of oxidative stress. We used a commercially available kit (Cayman, Anne Arbor, MI), which employs an enzymatic recycling method whereby glutathione reductase is used to quantify GSH. The sulfhydryl group of GSH (Figure 4.2) reacts with 5,5'-dithio-*bis*-2-nitrobenzoic acid or Ellman's reagent (Eyer and Podhradsky 1986) (DTNB) to produce a yellow coloured (5-thio-2-nitrobenzoic acid [TNB]) product. The mixed disulfide that is produced (GSTNB) is then reduced by glutathione reductase back to GSH, which produces more TNB in the process. The rate of TNB production is directly proportional to this recycling reaction, which is in turn proportional to the concentration of GSH in the sample. GSSG measurements can be obtained using the kit, since GSSG is produced at an identical rate during the DTNB reduction as GSH. Therefore, GSSG can be measured after all GSH has been removed from solution (Baker *et al.* 1990).

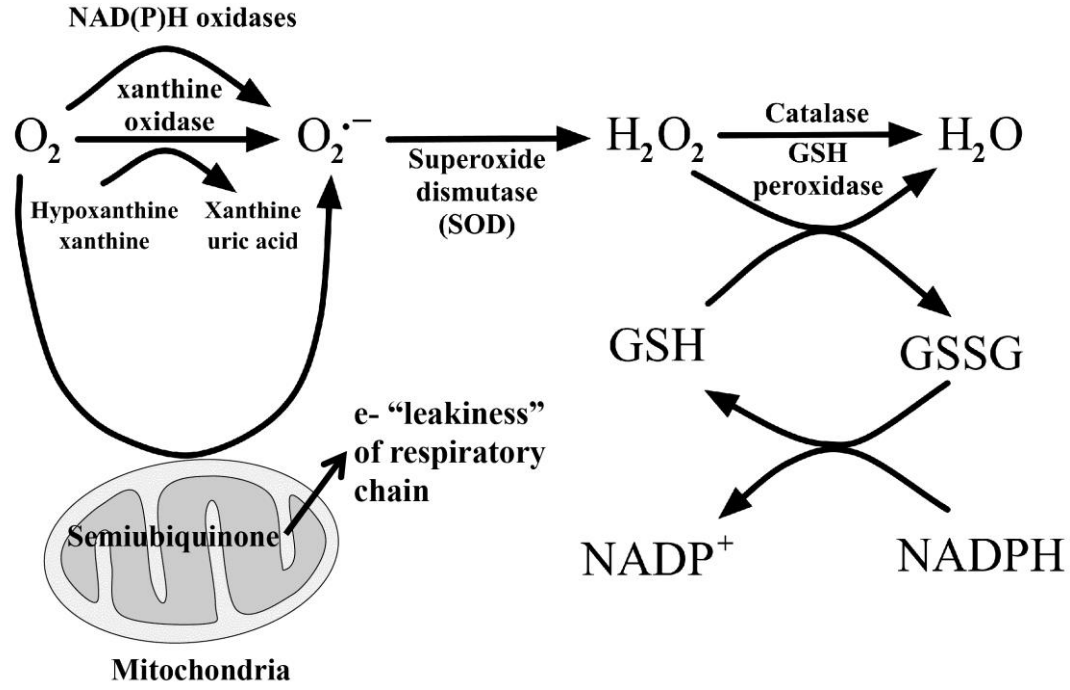

Figure 4.3 Pathways of ROS production and clearance.

Superoxide anion ($O_2^{\cdot -}$) is formed by univalent reduction of triplet-state molecular oxygen ($^3O_2$). This process is mediated enzymatically by NADPH oxidases and xanthine oxidase, or non-enzymatically by redox-reactive compound like semiubiquinone, a component of the mitochondrial electron transport chain. SODs then convert superoxide enzymatically to H_2O_2 and singlet oxygen ($^1O_2$). In the presence of reduced divalent transition metals (ferrous or copper ions), H_2O_2 can be converted to: 1) highly reactive hydroxyl radical ($^{\cdot}OH$), or 2) water by catalase activity or GSH peroxidase reactions. In the latter process, GSH is oxidised to GSSG and subsequently converted back to GSH immediately through the consumption of NADPH. Image adapted from Dröge (2002).

Abbreviations: GSH, glutathione; GSSG, glutathione disulphide; H2O2, hydrogen peroxide; H2O, water; O2, oxygen; O2.-, superoxide; NADP, nicotinamide adenine dinucleotide phosphate; NADPH, reduced NADP.

4.3.2.2.1 Reagents

Cayman's GSH assay kit was purchased commercially. It required further purchase of other reagents for GSSG and GSH determinations. All ingredients were prepared fresh prior to use.

Reagents provided with the kit:

GSH MES Buffer 2X (0.4 M 2-[*N*-morpholino]ethanesulphonic acid, 0.1 M phosphate, 2 mM EDTA, pH 6.0). This buffer was reconstituted with distilled water (60 mL) prior to use.

GSSG Standard (25 µM GSSG in MES buffer). This reagent was supplied with the kit and requires no further modification.

GSH co-factor mixture (powder $NADP^+$, glucose-6-phosphate). This reagent was reconstituted in distilled water (500 µL).

GSH enzyme mixture (glutathione reductase, glucose-6-phosphate dehydrogenase). Diluted MES buffer (2 mL) was added to the vial.

GSH DTNB (Ellman's reagent). Vial was reconstituted with distilled water (500 µL).

1.25 M of Metaphosphoric acid (MPA). MPA (5g) was dissolved in distilled water (50 mL). This reagent, when combined with TEAM, deproteinates samples to prevent contamination from sulfhydryl groups.

4 M Triethanolamine (TEAM) reagent. TEAM (531 µL) was dissolved with distilled water (469 µL). The TEAM reagent deproteinates samples by increasing pH, and can be used to assay total glutathione (i.e. reduced and oxidised glutathione).

1 M 2-vinylpyridine. 2-vinylpyridine (108 µL) was diluted in 100% ethanol (892 µL). 2-vinylpyridine was used to conjugate GSH (therefore removing it from samples) before residual GSSG was assayed with the glutathione cycling assay kit (Baker *et al.* 1990).

4.3.2.2.2 Methods

GSH and GSSG in cell culture samples were determined as reported elsewhere (Baker *et al.* 1990, Blackburn *et al.* 1999). Briefly, primary hepatocytes were isolated as described (Section 2.5) and seeded onto 55 cm^2 culture dishes at density of ~6.5 x 10^4 viable cells/cm^2. After 24 hours, experiments ware terminated. Cells were washed with ice-cold PBS, then gently scraped off and resuspended in cold PBS (10 mL) before centrifugation (5 min, 2,000 x g, 4°C). The isolated pellet was then resuspended immediately in cold MES buffer (500 µL) and sonicated (60 sec). Following sonication, samples were further centrifuged (15 min, 10,000 x g, 4°C) and supernatant transferred immediately to ice. The supernatant from the samples was then deproteinated by

addition of MPA. Solutions were vortexed and allowed to stand (5 min, RT) before centrifugation (2 min, 5,000 x g, RT). Supernatants were carefully collected before addition of TEAM reagent (50 µL). For GSSG assay, 2-vinylpyridine (10 µL) was added to sample (1 mL), prior to vortexing and incubation (60 min, RT). The glutathione assays was then performed, using provided GSSG standard for both total glutathione and GSSG determination. The absorbance was measured at 405 nm using FLUOstar OPTIMA plate reader (5 min intervals over 30 mins). GSH and GSSG concentrations were normalised to mg protein content, as determined using a commercial kit (DC™ Protein Assay, Bio-Rad, Hercules, CA) (Section 2.11.2).

4.3.3 Assessment of mitochondrial permeability pore (MPT) and cellular ATP

We previously discussed (Chapter 1 Section 1.4) that the principal function of the mitochondria in generation of cellular energy, with more than 90% of ATP being produced by mitochondria in heart, brain, liver and kidney (Nieminen 2003). ATP generation involves interplay between three dynamic energy types: redox, electrical/osmotic and chemical energy.

In the mitochondrial matrix (Figure 4.4), the citric acid/TCA cycle breaks down acetyl CoA (derived from glycolysis of pyruvate, malate and succinate; amino acid breakdown; and β-oxidation of FFA) to generate CO_2. In the process, this reduces NAD^+ and FAD^{2+} to NADH and $FADH_2$, respectively. NADH and $FADH_2$ then donate electrons to the respiratory chain. This consists of multiple coupled enzyme complexes, designated Complex I (NADH dehydrogenase), Complex II (succinate dehydrogenase), Complex III (ubiquinol cytochrome c reductase), and Complex IV (cytochrome c oxidase) (Pessayre and Fromenty 2005). The transfer of electrons down the respiratory chain, ultimately to oxygen, gives rise to protons, which, when transferred across the inner mitochondrial membrane, create a proton gradient known as the mitochondrial membrane potential ($\Delta\Psi m$). $\Delta\Psi_m$ is estimated to be ~150-180 mV more negative than cytosol (Bernardi 1999, Bernardi *et al.* 1999, Nieminen 2003, Duchen 2004, Duchen 2004, Pessayre and Fromenty 2005). This negative force underpins the production of ATP, which is driven by movement of protons down this gradient, driving the turbines of the F_1-F_0-ATP synthase to phosphorylate ADP and thereby generate ATP. ATP is then exported into cytosol by adenosine nucleotide translocase (ANT) for use by the cell.

As well as driving ATP production, $\Delta\Psi m$ also drives calcium accumulation into the mitochondrial matrix. The calcium influx pathway involves an electrogenic uniporter, which carries calcium into mitochondrial matrix down an electrochemical potential gradient whenever the concentration of extra-mitochondrial calcium rises. The accumulated (excess) calcium inside the mitochondrial matrix is then removed through the action of a Na^+/Ca^{2+} exchanger. Mitochondrial calcium uptake (and release) may impact on cellular ionic calcium signalling by affecting a fixed spatial buffering system, removing local calcium, hence regulating calcium-dependent processes (Duchen 2004, Duchen 2004).

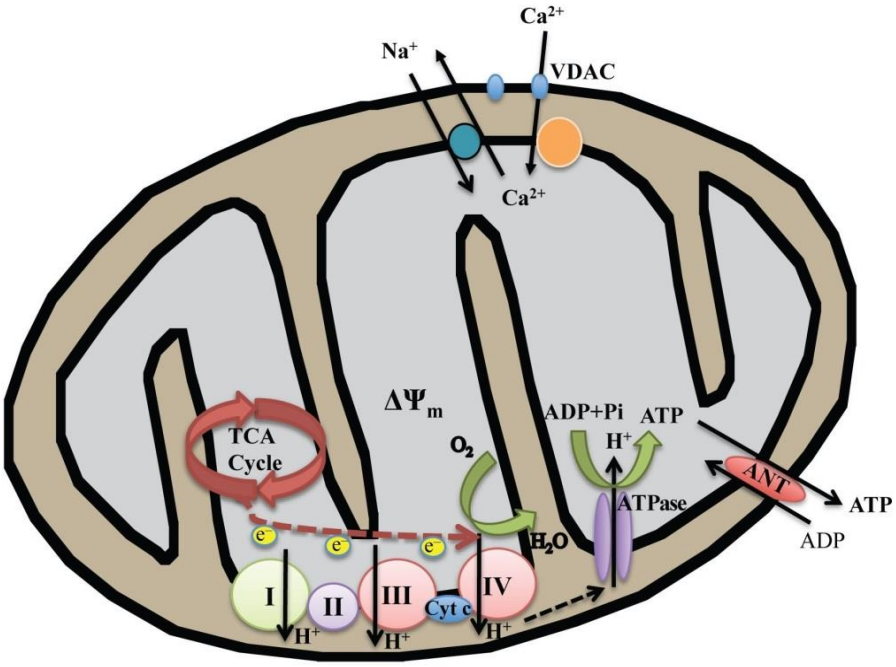

Figure 4.4. Mitochondria oxidative metabolism and energy production.

In the mitochondrial matrix, the TCA cycle catabolises acetyl CoA derivatives from pyruvate, malonate, succinate, long chain FFA (following β-oxidation), and amino acids to generate NADH and FADH2. These intermediates transfer electrons to the mitochondrial respiratory chain. The flow of electrons down the mitochondrial respiratory chain complexes (I, II, III and IV) results in extrusion of protons from the mitochondrial matrix, effectively creating an electrochemical proton gradient. This can be expressed as the mitochondrial transmembrane potential (ΔΨm), which is ~150 mV–180 mV negative to cytoplasm. In turn, by providing a negative gradient, which allows protons (through F1-F0 ATPase channel) and calcium influx into mitochondrial matrix, ΔΨm is important for ATP synthesis and calcium accumulation (Nieminen 2003, Duchen 2004, Pessayre and Fromenty 2005).

Abbreviations: ΔΨm, mitochondrial transmembrane potential; ANT, adenine nucleoside translocase; Cyt c, cytochrome c; TCA, tricarbocylic acid cycle; VDAC, voltage-dependent anion channel.

Mitochondrial permeability transition (MPT) is a large conductance pathway/pore in the inner mitochondrial membrane, probably generated in response to alterations in conformation of membrane proteins that normally perform other functions. These could include the ANT (ATP export into cytosol) and possibly voltage-dependent anion channels (Ca^{2+} influx into mitochondrial matrix) that is located in the outer membrane. MPT seems to be found at contact sites between the inner and outer mitochondrial membranes, where the voltage-dependent anion channel and the ANT are concentrated (Nieminen 2003, Duchen 2004). Cyclophilin D (the binding site for cyclosporine A [Cya]), is associated with the MPT pore complex; blocking MPT opening with CyA inhibits cell killing (shown later in Results).

A major consequence of MPT is mitochondrial uncoupling with collapse of all electrical and chemical gradients and $\Delta\Psi m$ depolarisation. This allows large amplitude mitochondrial swelling. It has been suggested that MPT plays an important role in some forms of apoptotic cell death – pore opening causes mitochondrial swelling, unfolding of mitochondrial respiratory chain proteins with release of cytochrome c into intermembranous space; subsequent rupture of outer membranes releases cytochrome c into cytosol. If the pore opens irreversibly, cells will die because the mitochondria cannot maintain transmembrane potential, so failing to generate ATP, or they start to actively consume ATP by reversal of the F_1-F_0-ATP synthase; such loss of ATP leads to necrotic cell death (Nieminen 2003, Duchen 2004).

4.3.3.1 Tetramethylrhodamine methyl ester labelling of mitochondria

In order to monitor loss of $\Delta\Psi m$, which occurs as a consequence of MPT, we used a cationic, mitochondrial-selective dye, tetramethylrhodamine methyl ester (TMRM). Polarised mitochondria (where the interior is more anionic) accumulate more of the positively charged TMRM dye. Since $\Delta\Psi m$ is lost following MPT, releasing cytochrome c into the cytosol, we used such loss of TMRM fluorescence to indicate the loss of $\Delta\Psi m$ that follows MPT and cytochrome c release. It is important to note that MPT opening is always followed by $\Delta\Psi m$ depolarisation, but $\Delta\Psi m$ depolarisation does not always lead to MPT (Bernardi 1999, Nieminen 2003). Therefore, measuring $\Delta\Psi m$ alone may not be the best way to assess MPT. It is desirable to also determine directly mitochondrial loss of cytochrome *c* into cytosol. This will be discussed later.

4.3.3.1.1 Reagent

2.11 mM TMRM stock. TMRM (10.6 mg) is dissolved in DMSO (10 mL). Solution was aliquoted and stored at –20°C (light protected) until ready for use.

4.3.3.1.2 Methods

The methods for TMRM mitochondrial loading is as described (Chazotte 2011, Chazotte 2011).

Briefly, following aspiration of culture media and washing of cells once with warm PBS, hepatocytes were loaded with TMRM by incubating (20 min, 37°C, dark) with warm William's E culture media containing 600 nM TMRM made from stock. Following this, the TMRM labelling media was removed and cells immersed in 150 nM TMRM to maintain equilibrium of distribution of fluorophobe. TMRM-emitted fluorescence was then quantified (excitation wavelength 543 nm, emission wavelength 565-615 nm) using a FLUOstar OPTIMA plate reader; images were captured using an Olympus IX70 microscope fitted with 590/50 nm band filter. Unfortunately, overlays of DCF/TMRM pictures could not be produced because TMRM is a metachromatic fluorophobe that provides both red and green fluorescence when activated by laser, and green fluorescence is much stronger than that of DCF in control cells (Karlsson *et al.* 2010).

4.3.3.2 Measurement of cellular ATP

Reduced hepatic levels of ATP homeostasis have been reported in human NASH livers (Cortez-Pinto *et al.* 1999, Cortez-Pinto *et al.* 1999). We therefore sought to determine if cellular ATP production is impaired in FC-loaded primary hepatocytes. To do this, intracellular ATP was measured using a commercially available kit that quantifies ATP using firefly luciferase and its substrate, *D*-luciferin (Molecular Probes™, Eugene, OR). This assay is based on the requirement of luciferase for ATP to produce light emission (emission maximum ~560 nm at pH 7.8) from the reaction:

$$\text{Luciferin} + \text{ATP} + O_2 \xrightarrow[\text{Luciferase}]{Mg^{2+}} \text{Oxyluciferin} + \text{AMP} + \text{pyrophosphate} + CO_2 + \text{light}$$

4.3.3.2.1 Reagents

Reagents provided with the kit and made up as per manufacturer's instructions:
D-luciferin, luciferase solution (40 µL of 5 mg/mL luciferase in 25 mM Tris-acetate, pH 7.8, 0.2 M ammonium sulfate, 15% [v/v] glycerol, 30% [v/v] ethylene glycerol), 100 mM DTT, ATP (400 µL of 5 mM solution in TE buffer), 20X reaction buffer (500 mM Tricine buffer, pH 7.8, 100 mM $MgSO_4$, 2 mM EDTA and 2 mM sodium azide).

Cell lysis buffer (150 mM NaCl, 50 mM Tris pH 7.5, 1% [v/v] Triton 100X, 1% [m/v] SDS, 1% [m/v] sodium deoxycholate). The following were dissolved in distilled water (250 mL), NaCl (2.19 g), Tris (1.52 g), Triton 100X (2.5 mL), SDS (0.25 g) and sodium deoxycholate (2.5 g).

0.1 mM Tris acetate. In distilled water (500 mL), Tris (6.1 mg) and sodium acetate (4.1 mg) were dissolved and mixed well.

4.3.3.2.2 Methods

Methods for determining cellular ATP in cultured cells were adapted from those previously described for ATP measurement in whole liver lysate (Evans *et al.* 2008).

Briefly, hepatocytes were obtained from WT C57Bl/6J mice as previously described in Section 2.5. In order to obtain adequate samples, cells were seeded onto 55 cm^2 culture plates in triplicate (per intervention group) (40 *vs* 0 µM LDL). To determine the point at which ATP depletion occurs, cells were harvested at 6 hourly intervals, as follows. Cells were washed with ice-cold PBS, then centrifuged (2 min, 1,000 x g, 4°C) before pellets were snap-frozen in liquid nitrogen and stored at –80°C until ATP analysis. To analyse ATP, an ATP standard curve was generated by reading the luminance from a series of ATP concentrations (each diluted from ATP kit stock). Thawed samples were then added to ice-cold cell-lysis buffer before pellets were subjected to ultrasound sonication (60 sec). Homogenates were transferred into fresh Eppendorf tubes before adding 1.5% tricholoroacetic acid (ATPase inhibitor). These solutions were then boiled (3 min, 100°C) before centrifugation (5 min, 16,000 xg, 4°C). Supernatants were collected and diluted 1:50, 1:30 and 1:20 in 0.1 mM Tris acetate. Luciferin-luciferase solution was then added to each sample to start the reaction. ATP concentrations were

immediately measured using FLUOstar OPTIMA plate reader (emission wavelength ~560 nm). For normalisation between samples, total cellular protein from each sample was determined using commercial kit (DC™ Protein Assay, Bio-Rad, Hercules, CA) as previously described in Section 2.11.2.

4.3.4 Assessment of mitochondrial ultrastructure using transmission electron microscopy

In 1977, Petersen reported findings of swollen mitochondria in diabetic, obese patients with fatty liver disease (Petersen 1977, Petersen 1977). Subsequently, other researchers confirmed these changes, and found that, compared to control and NAFLD patients without NASH, NASH livers have swollen, round (mega-) mitochondria, with stacks of linear intra-mitochondrial crystalline inclusion bodies and some loss of cristae (Caldwell *et al.* 1999, Sanyal *et al.* 2001, Caldwell *et al.* 2009). We used TEM to ascertain if similar mitochondrial changes are present in FC-loaded primary hepatocytes.

4.3.4.1 Reagents

All TEM reagents were prepared, as described in Section 3.3.6.

4.3.4.2 Methods

TEM methodology is detailed in Section 3.3.6.

4.3.5 Statistics

Statistical analyses were carried out as described in Section 2.16.

4.4 Results

4.4.1 JNK1 is essential for FC lipotoxicity to hepatocytes

In Chapter 3, the earlier finding that hepatic FC level is elevated in *foz/foz* mice with NASH but not SS was discussed (Van Rooyen *et al.* 2011). More recently, it was shown that in these obese mice with NASH, JNK1/2 activation correlated with such FC deposition (Figure 4.1) (Van Rooyen *et al.* 2013), while pharmacological lowering of hepatic FC (with combination ezetimibe [5 mg/kg] and atorvastatin [20 mg/kg]) abolished such JNK activation (Figure 4.1), in association with improved serum ALT, liver inflammation and less apoptosis (Van Rooyen *et al.* 2013). In Chapter 3 we

demonstrated that FC could be loaded successfully into WT primary murine hepatocytes (on C57B6/J background) by incubating them with increasing concentrations of LDL (20–40 μM) (Figure 3.2D). Such FC loading caused hepatocellular lipotoxicity manifest as cell injury (LDH and ALT leakage) and death by both apoptosis and necrosis. The latter findings were especially pronounced at 40 μM LDL concentration (Figure 3.4). Earlier *in vitro* studies by Gregory Gores *et al.* showed that hepatocyte lipotoxicity from satFFA (palmitate) involves a JNK1-dependent process (Cazanave *et al.* 2009), likely through generation of lipid metabolites such as one of the lipid species (besides FC) shown to be elevated in human NASH (but not SS) livers, lysophosphatidylcholine (LPC) (Caballero *et al.* 2009, Kakisaka *et al.* 2012, Kakisaka *et al.* 2012).

We first revisited FC-loaded livers from *foz/foz* mice with NASH (Van Rooyen *et al.* 2011, Van Rooyen *et al.* 2013), and confirmed that the observed activation of JNK1/2 (Figure 4.1A) was associated with downstream phosphorylation of nuclear *c*-Jun (Figure 4.5A). As for the earlier observations of increased JNK1/2 phosphorylation, this increase in *c*-Jun correlated closely with hepatic FC content (Figure 4.5B).

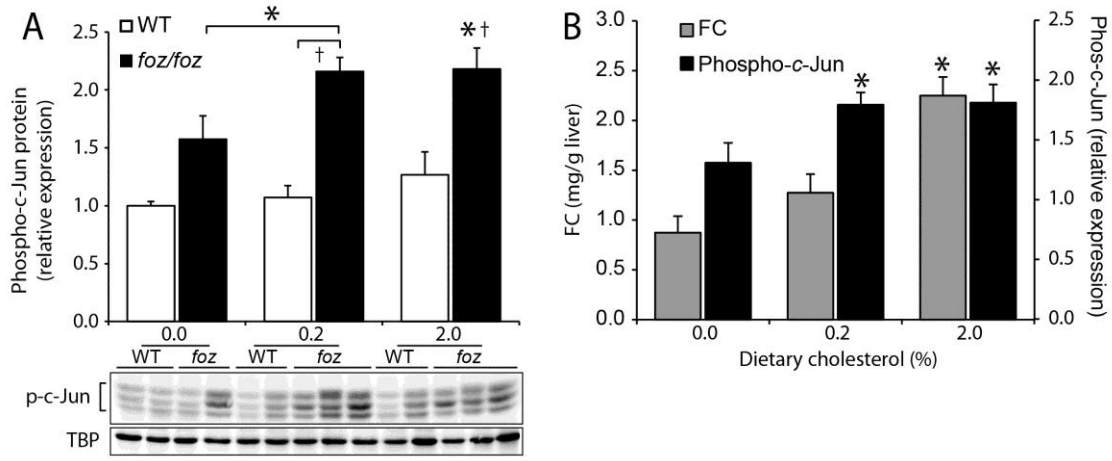

Figure 4.5 Livers from *foz/foz* mice with NASH show increase nuclear expression of phospho-*c*-Jun that is proportional to hepatic FC content.

After 24 weeks of HF/HC diet, *foz/foz* mice with NASH (Van Rooyen *et al.* 2011) but not similarly treated WT controls with SS, show (**A**) increased activation of *c*-Jun (shown by nuclear p-*c*-Jun) *vs* WT. (**B**) In *foz/foz* mice with NASH, this increased *c*-Jun activation is associated with increased liver FC content. Mice **P*<0.05, *vs* genotype-matched, 0% dietary cholesterol group. †*P*<0.05, *vs* dietary-matched, *WT* control. Data represent mean ± SEM. Data from panels A and B represent ~9 animals/group.

Subsequent experiments involved incubation of primary hepatocytes with 40 μM LDL for 24 hours. This intervention caused significant (P<0.05) phosphorylation of the 46 kDa JNK1/2 protein (Figure 4.6A,B) and a substantial increase in phosphorylation of JNK1 (Figure 4.6C). Such JNK1 phosphorylation was associated increased JNK1 activity, as evident by phosphorylation of hepatocellular phospho-*c*-Jun (Figure 4.6D). Specifically, increased nuclear phospho-*c*-Jun was identified both by WB and immunofluorescence (Figure 4.6E,F), reflecting upstream JNK1 activation. These data indicate that the *in vitro* system of loading primary hepatocytes with FC recapitulates the findings for JNK activation, and specifically JNK1 activation, as observed in mice with NASH.

Interestingly, after only 2 hours of exposure to 40 μM LDL, WT primary hepatocytes exhibit significantly (P<0.05) increased cell death by apoptosis (Figure 4.7A), before LDH leakage was apparent, or cell death by necrosis (Figure 4.7A). This apparent FC-induced apoptotic cell death was associated with an increase in the 54 kDa (but not the 46 kDa) JNK1/2 isoform phosphorylation (Figure 4.7B), and downstream phosphorylation of *c*-Jun, reflecting JNK activation (Figure 4.7B). This suggests that, at this early time point, the increase in phospho-JNK1/2 is attributable to higher molecular weight 54 kDa isoform (but not specifically JNK1), whereas later, the 46 kDa JNK1/2 becomes activated to cause downstream *c*-Jun phosphorylation. The implication of this early increase in *c*-Jun phosphorylation with FC loading will be discussed later (Section 4.6).

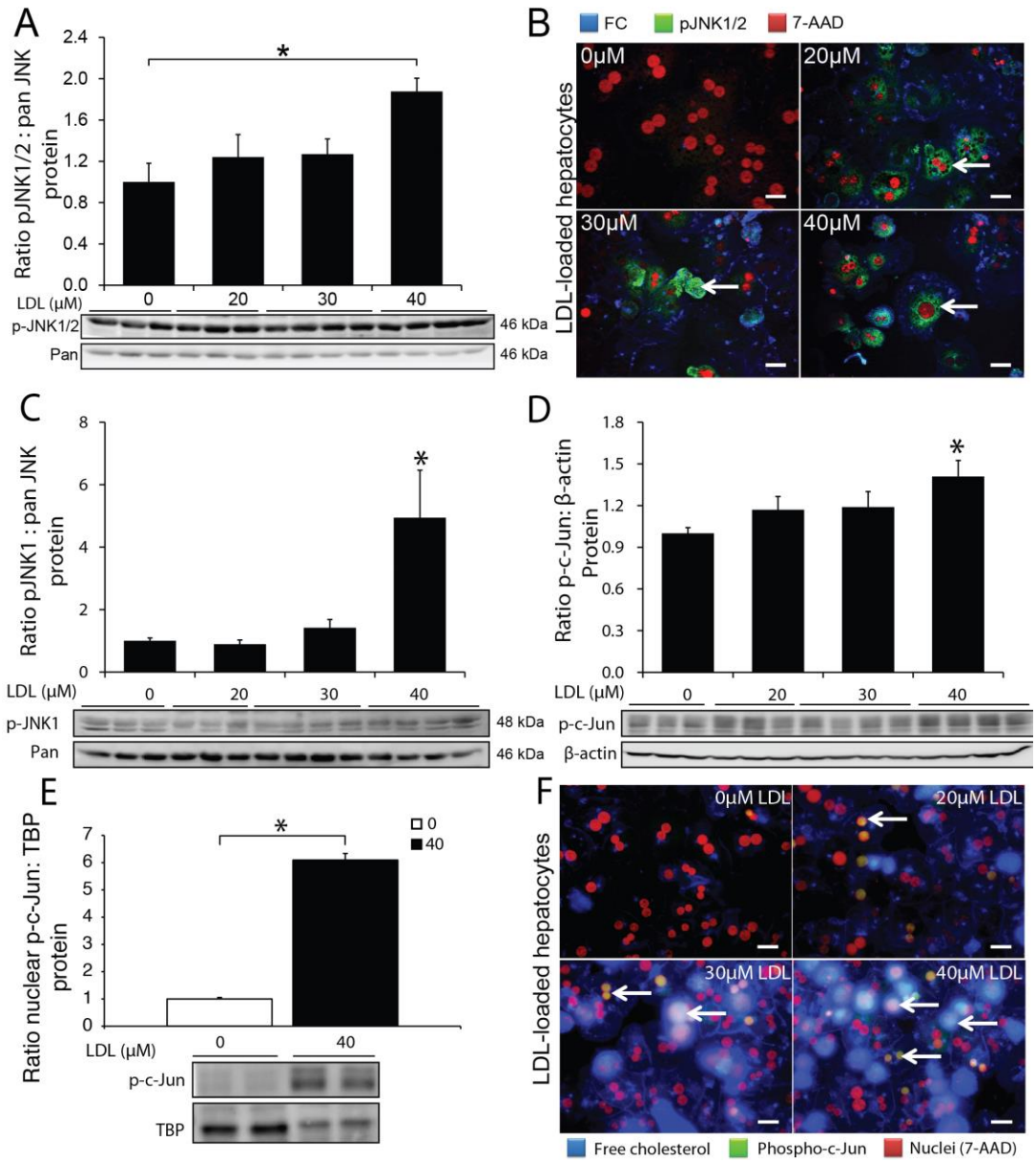

Figure 4.6 FC-loading of primary hepatocytes increases JNK1/2 activation, specifically JNK1 with downstream activation of p-*c*-Jun.

(**A**) Cellular phospho-JNK1/2 protein in *WT* hepatocytes incubated with 0–40 μM LDL. (**B**) Immunofluorescence showing increasing 46 kDa phospho-JNK1/2 (green) fluorescence proportional to filipin (blue) fluorescence, indicating FC loading. (**C**) Use of JNK1-specific antibody indicates specificity of JNK1 activation in FC-loaded hepatocytes. Total 46 kDa panJNK (panel A and C) was used as loading control. (**D**) Hepatocellular *c*-Jun activation is evident with 40 μM LDL loading, (**E**) specifically, nuclear phospho-*c*-Jun, and (**F**) immunofluorescence (phospho-*c*-Jun [green] co-localises with nucleus [red]), shown by arrows. β-actin (panel A) and TATA box-binding protein, TBP (panel E) were used as loading controls for hepatocellular and nuclear phospho-*c*-Jun, respectively. **P*<0.05, *vs* time-matched control receiving no LDL. Data represent mean ± SEM from *n*=4–6 pooled animals, with 4-6 replicates/group. Bars represent 20 μm.

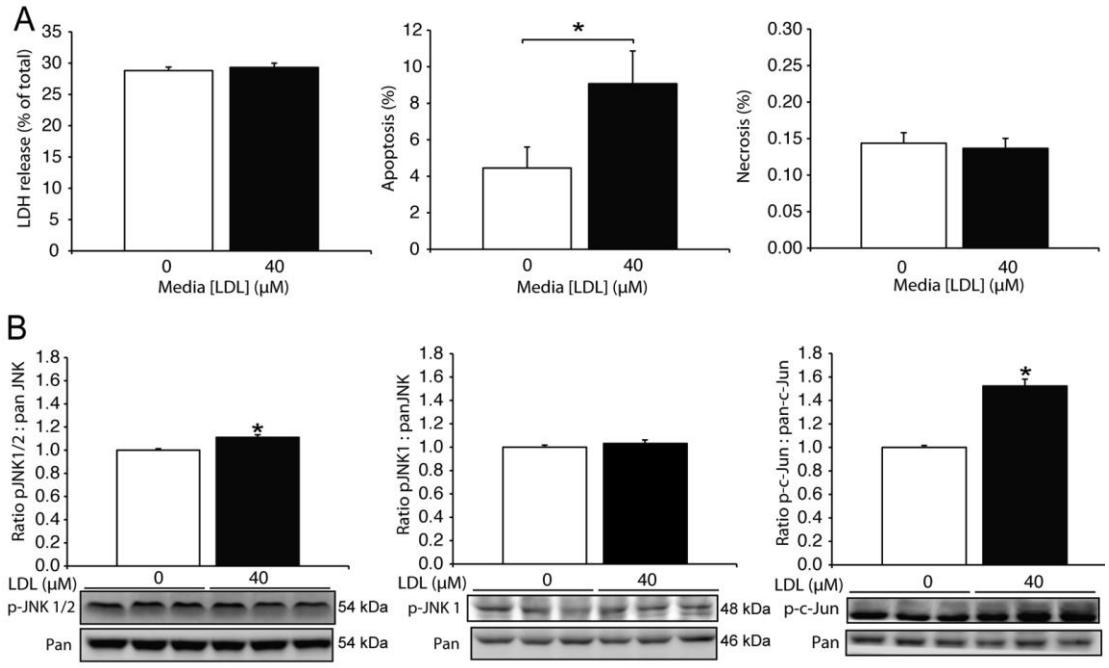

Figure 4.7 Two hours of incubation with 40 μM LDL causes hepatocellular apoptosis in association with phospho-*c*-Jun activation.

(**A**) In WT hepatocytes, incubation with 40 μM LDL for 2 h caused cellular apoptosis, but was insuffient to cause LDH release or necrotic cell injury (see Figure 3.4, data for 24 hours). (**B**) Western blotting analysis revealed significant activation of 54 kDa phospho-JNK1/2 and phospho-*c*-Jun. JNK1 phosphorylation was not significantly increased following FC-loading. Total 54 kDa panJNK and pan-c-Jun were used as loading controls for 54 kDa phospho-JNK1/2 and phospho-*c*-Jun western blot, respectively. Total 46 kDa panJNK was used as loading control for phospho-JNK1. **P*<0.05, vs time-matched control receiving no LDL. Data are presented as mean ± SEM from *n*=4 pooled animals, with 10–32 replicates per treatment group for panel A, and 8 replicates per treatment group for panel B.

As discussed earlier (Section 4.1.2), JNK activation has been implicated as a potential mechanism in the development of NASH. For example, HF diet causes obesity, insulin resistance and steatohepatitis in WT and *Jnk2*$^{-/-}$, but not *Jnk1*$^{-/-}$ mice (Hirosumi *et al.* 2002, Singh *et al.* 2009). In biopsy-proven obese patients with NASH, there is increased phospho-JNK1/2 and increased JNK1-dependent PUMA phosphorylation, which is downstream of JNK1. This is not observed in obese patients with normal livers or those showing only SS (Cazanave *et al.* 2009). Further, *c*-Jun/AP-1 activation has been recently shown to be responsible for the development and progression in mice and human NASH (Dorn *et al.* 2014). To test whether JNK, specifically JNK1 activation is essential for FC-injury, two approaches were adopted in the present experiments, which were conducted for 24 h:

1. WT cells were pretreated with potent JNK inhibitors (CC-401, CC-930 and CC-003 [Celgene, San Diego, CA]) prior to FC loading, and the effects on cell injury, apoptosis and necrosis were measured.
2. *Jnk1*$^{-/-}$ and *Jnk2*$^{-/-}$ primary hepatocytes were loaded with FC, and markers of cell injury and cell death compared to similarly loaded WT and *Jnk2*$^{-/-}$ hepatocytes.

The potent and specific inhibitors used to block JNK1 were CC-401, CC-930 and CC-003 have been developed by Celgene (San Diego, CA) and are currently undergoing preclinical and early development. These compounds all competitively inhibit the ATP-binding site of the active, phosphorylated, form of JNK, thereby preventing downstream phosphorylation of JNK target molecules, such as the amino terminus of *c*-Jun (Ma *et al.* 2007, Ma *et al.* 2009, Ma *et al.* 2009, Reich *et al.* 2012). CC-003 has been de-identified as it is the first highly JNK1-specific inhibitor molecule to be developed by Celgene, and has yet to be approved for scientific publication.

To establish optimal cytoprotective dose of the JNK inhibitors in FC loaded primary hepatocytes, concentrations of 1, 2, 5 and 10 μM of each inhibitor were assessed for protection against hepatocyte apoptosis and necrosis following 40 μM LDL exposure. In preliminary analyses, 1 μM CC-930 and CC-003 were both found to protect hepatocytes from FC-induced apoptosis (Figure 4.8A) and necrosis (Figure 4.8B) (see arrows). At 2 μM, CC-401 achieved similar protection (Figure 4.8A,B as indicated by arrows). Subsequent JNK inhibitor experiments were therefore performed using 1 and 2 μM concentrations of CC-401, CC-930 and CC-003 added prior to cholesterol loading.

We found that 1 and 2 μM concentrations of CC-401 and CC-930 decreased both hepatocellular apoptosis (Figure 4.9A) and necrosis (Figure 4.9B), despite evidence of FC loading as demonstrated by filipin blue fluorescence (Figure 4.9C). We also confirmed that 1 μM CC-930 effectively blocked phosphorylation of JNK1/2, as demonstrated by immunofluorescence (Figure 4.9C) and WB (Figure 4.9D). This activation specifically involved phospho-JNK1 activation as reflected by changes in phospho-*c*-Jun (Figure 4.9D).

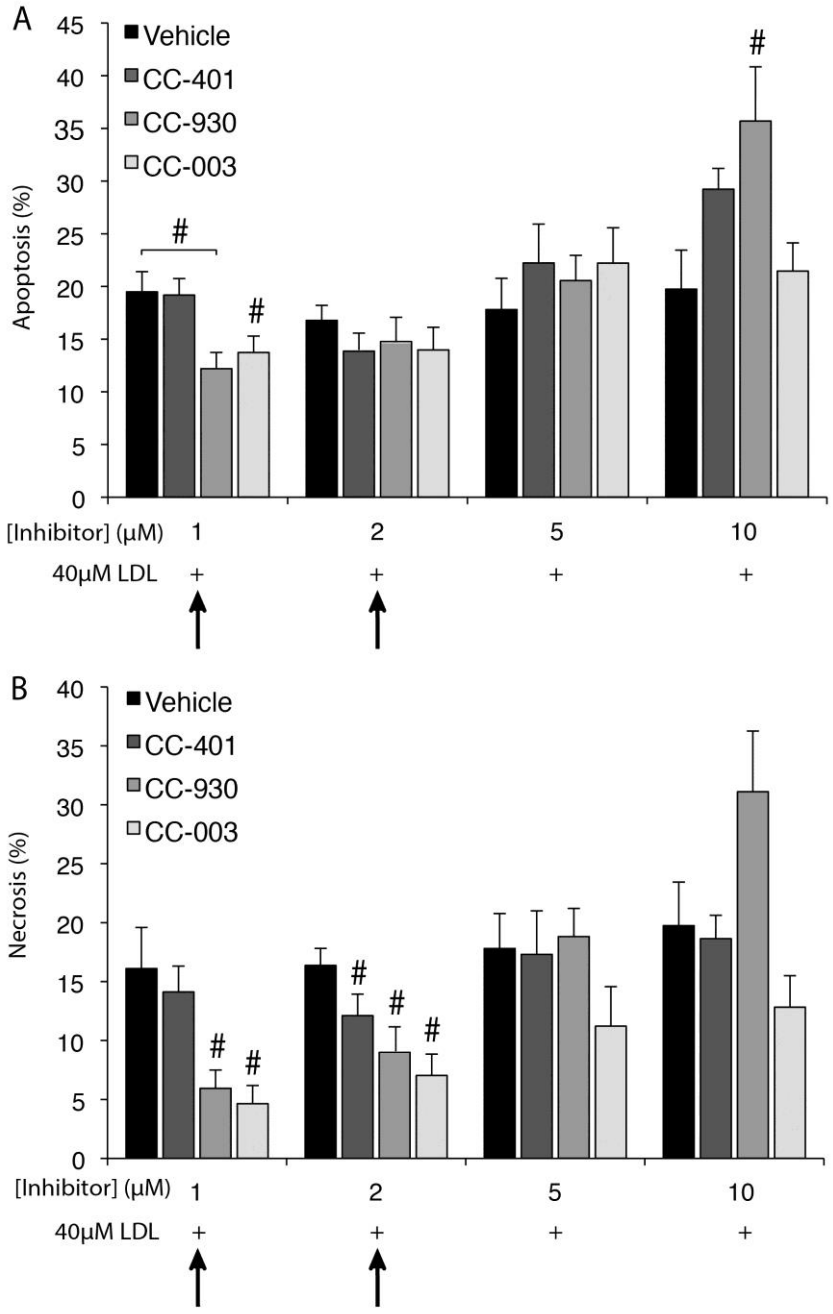

Figure 4.8 Dose-dependents effects of JNK inhibitors CC-401, CC-930 and CC-003 on apoptosis and necrosis in FC-loaded hepatocytes.

(**A**) Apoptosis, and (**B**) necrosis in WT primary hepatocytes pretreated with 1, 2, 5 and 10 μM of CC-401, CC-930 and CC-003 prior to loading with 40 μM LDL. Equivalent volumes of DMSO (vehicle) were used to dilute the JNK inhibitors. 1–2 μM of CC-401 and CC-930 conferred most cytoprotection from 40 μM LDL loading, whereas 5 μM gave minimal protection or caused cytotoxicity (increased cell death). $^{\#}P<0.05$, *vs* dose-matched control receiving 40 μM LDL. Data are represented as mean ± SEM. Experiments are results from 3 pooled animals, repeated twice, with 6 replicates per treatment group, n=12/gp.

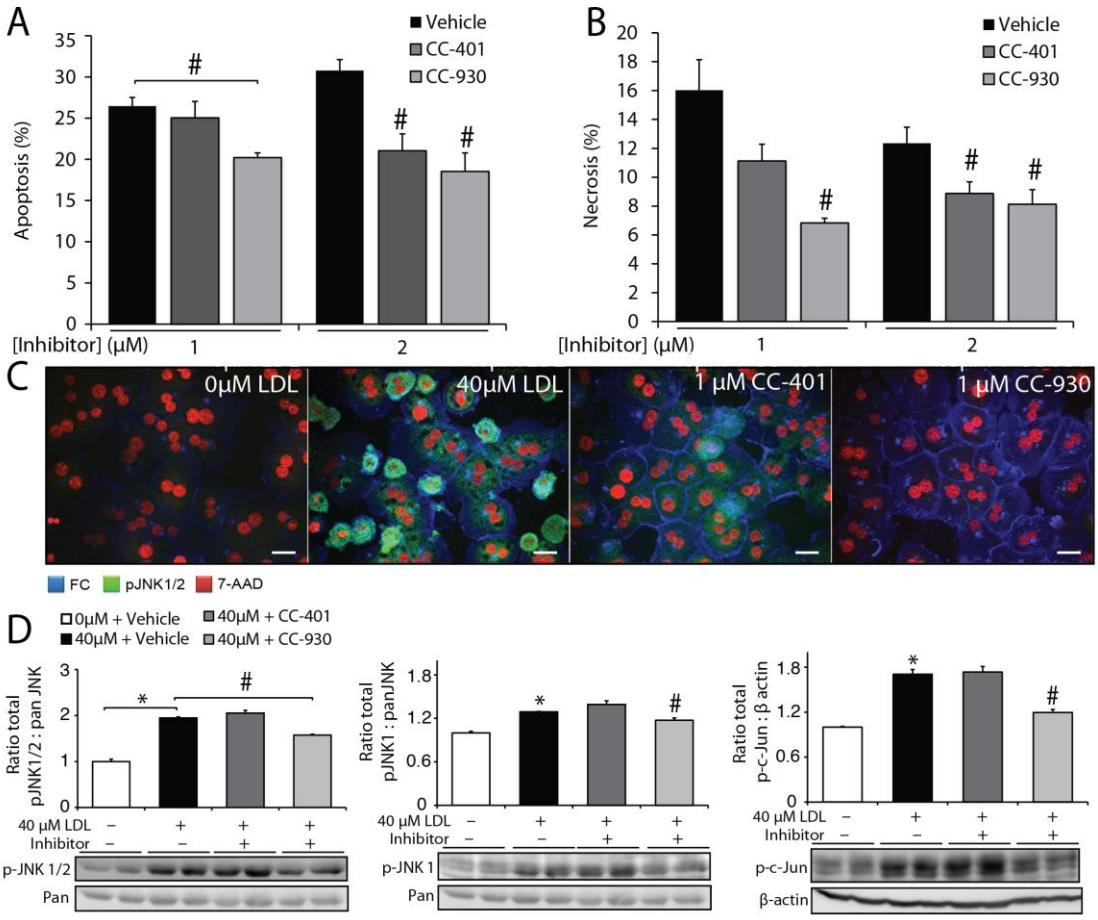

Figure 4.9 Specific JNK inhibitors abrogate FC-induced hepatocyte cell death.

Potent JNK inhibitors (1–2 μM CC-401 or CC-930) lessen: (**A**) apoptosis, and (**B**) necrosis in FC-loaded hepatocytes, (**C**) despite similar FC loading shown by filipin fluorescence (blue). 1 μM CC-401 and CC-930 blocked phospho-JNK1/2 phosphorylation as demonstrated by immunofluorescence (green), and (for CC-930 only) (**D**) levels of phospho-JNK1/2, more specifically phospho-JNK1 and phospho-c-Jun. Total 46 kDa panJNK (panel D) was used as loading controls for 46 kDa phospho-JNK1/2 and 48 kDa phospho-JNK1, and β-actin for phospho-c-Jun. *P<0.05, *vs* time-matched control receiving no LDL, #P<0.05, *vs* time- and dose-matched control receiving 40 μM LDL. Data in panels A, B and D are means ± SEM from 4 pooled animals, with three replicates per treatment group and experiment repeated thrice, *n*=9/gp. Bars represent 20μm.

Subsequently, *Jnk1*$^{-/-}$, *Jnk2*$^{-/-}$ and *Wt* hepatocytes were exposed to 40 μM LDL (Figure 4.10). As determined by LDH leakage into culture media, *Jnk1*$^{-/-}$ cells were completely refractory to FC-induced injury (Figure 4.11A). Further, *Jnk1*$^{-/-}$ hepatocytes show no phosphorylation of JNK1 with increasing concentrations of LDL (Figure 4.11C) and no JNK1 activation, as reflected by *c*-Jun phosphorylation (Figure 4.11D). Conversely, *Jnk2*$^{-/-}$ hepatocytes were just as susceptible to FC-induced apoptosis (Figure 4.11E) and

necrosis (Figure 4.11F) as *Wt* cells. At 40 µM LDL, *Jnk2*$^{-/-}$ cells resembled *Wt* by also showing increased phosphorylation of JNK1/2, JNK1 and *c*-Jun (Figure 4.11G-I).

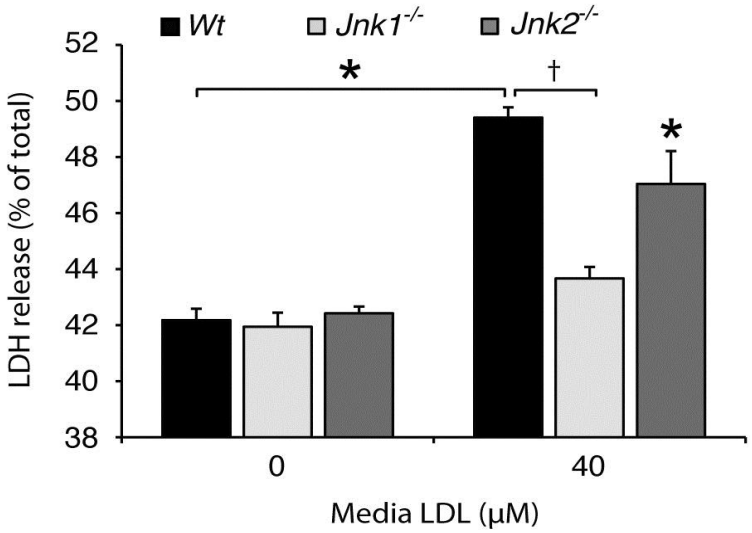

Figure 4.10 *Jnk1*$^{-/-}$ but not *Jnk2*$^{-/-}$ hepatocytes are protected from FC-induced hepatocellular injury.

Jnk1$^{-/-}$ hepatocytes are protected from FC-induced injury, but LDH leakage was similar in *Jnk2*$^{-/-}$ and *Wt* hepatocytes exposed to 40 µM LDL. *P<0.05, *vs* genotype-matched control receiving no LDL exposure, †*P*<0.05, *vs Wt* (C57Bl/6) hepatocytes exposed to 40 µM LDL. Data are mean ± SEM of 4 pooled animals/gp with 8 replicates/treatment group, *n*=8/gp.

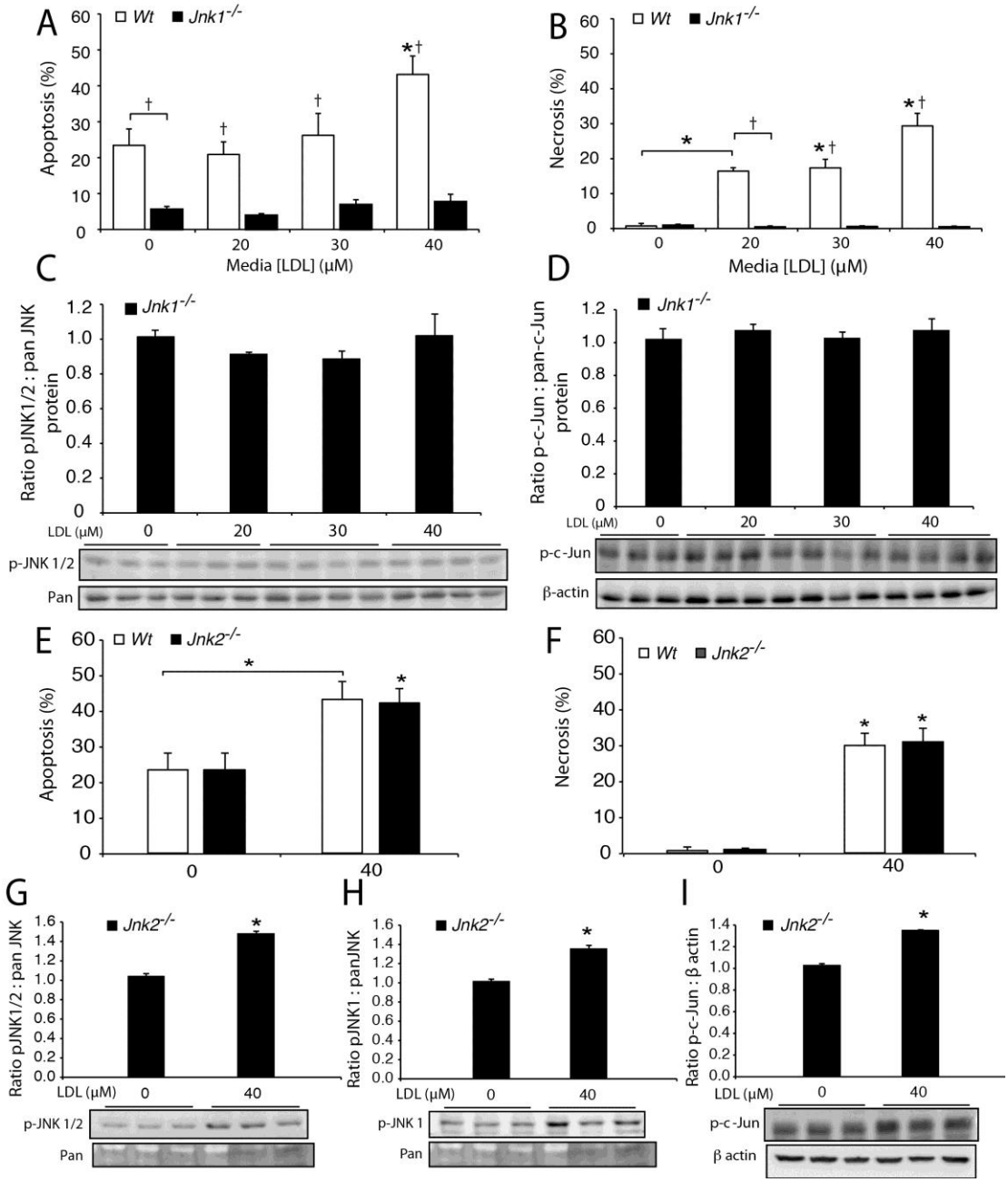

Figure 4.11 *Jnk1*$^{-/-}$ but not *Jnk2*$^{-/-}$ primary hepatocytes are protected from FC-induced cell death.

Jnk1$^{-/-}$ hepatocytes were protected from FC-induced: (**A**) apoptosis and (**B**) necrosis compared with *Wt* cells. As expected, *Jnk1*$^{-/-}$ hepatocytes showed no change in expression of (**C**) 46 kDa phospho-JNK1/2 or (**D**) phospho-*c*-Jun. Total panJNK (panel C) and β-actin (panel D) were used as loading controls for phospho-JNK1/2 and hepatocellular phospho-*c*-Jun, respectively. Conversely, FC loading of *Jnk2*$^{-/-}$ hepatocytes, as observed in *Wt* primary hepatocytes, induced hepatocellular (**E**) apoptosis, (**F**) necrosis and increased (**G**) 46 kDa phospho-JNK1/2, (**H**) phospho-JNK1 with downstream increase of (**I**) nuclear phospho-*c*-Jun protein. **P*<0.05, vs control receiving no LDL, †*P*<0.05, *vs* treatment-matched, Wt control. Data represent mean ± SEM from 4–6 animals pooled together with a total of 4 replicates per group (*n*=4/gp).

4.4.2 FC-induced JNK activation leads to oxidative stress, mitochondrial injury and ATP depletion.

Oxidative stress is one pathway by which FC can activate JNK (Hong *et al.* 2009). In this work, there was a direct correlation between hepatocellular FC content and ROS accumulation, as demonstrated by increased intensity of oxidised 2',7'-DCF green fluorescence (LeBel *et al.* 1992, Karlsson *et al.* 2010) (Figure 4.12A, fluorescence images shown in Figure 4.12B). Oxidative stress was also evident by accumulation of oxidised glutathione (GSSG) with a reciprocal depletion of GSH (Figure 4.12C). When expressed as a ratio of GSSG:GSH, accumulation of oxidised glutathione was directly proportional to hepatocellular FC content (Figure 3.2D and 4.12D).

In response to the generation of ROS, FC-loaded *Wt* hepatocytes showed increased expression of both Nrf1 and Nrf2 mRNA (Figure 4.13A,B,C). These genes are members of the "cap n collar" basic leucine zipper (CNC-bZIP) family responsible for activating antioxidant response elements (ARE) (Leung *et al.* 2003, Xu *et al.* 2005). The enzymes regulated by AREs include superoxide dismutases (SODs), catalase, glutathione peroxidase and glutathione *S*-transferases (Madamanchi *et al.* 2005, Madamanchi *et al.* 2005, Nakano *et al.* 2006, Nakano *et al.* 2006). In the present work, there appeared to be a trend for an increased expression of SOD2, although the apparent change was not significant (Figure 4.13D). SOD2 has been shown to play a role in oxidant scavenging in protection against oxidative injury and atherogenesis (Madamanchi *et al.* 2005) and is one of the mitochondrial first line defense against generated ROS (Mari *et al.* 2013).

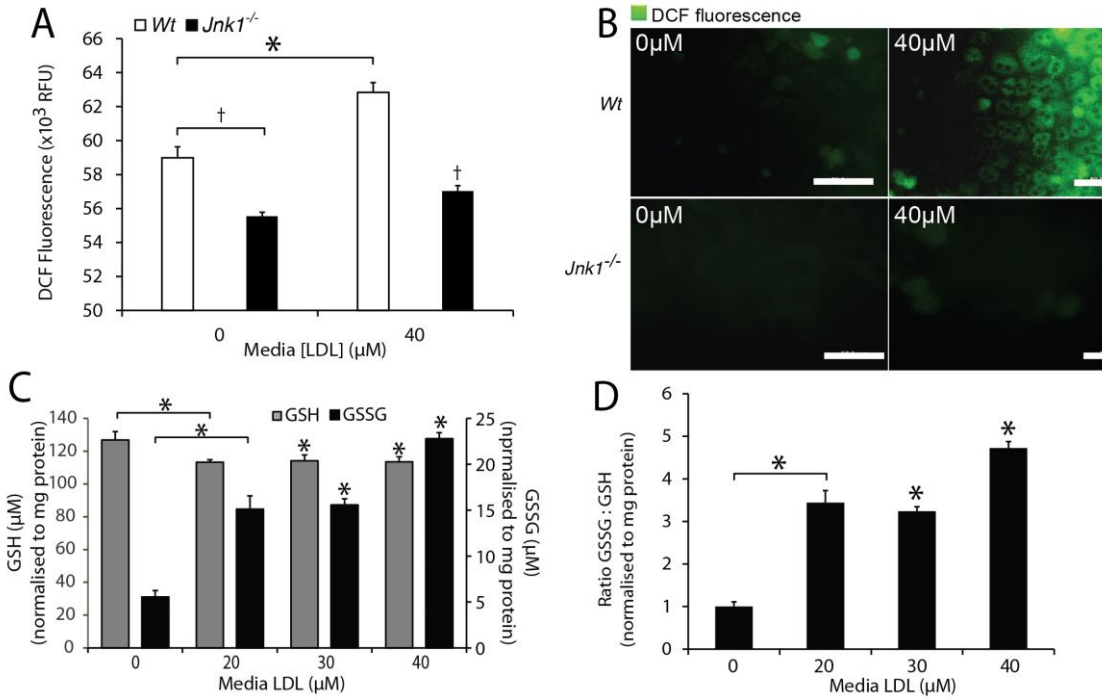

Figure 4.12 Effects of hepatocyte FC loading on ROS generation and oxidative stress.

When exposed to 40 μM LDL, *Wt* but not *Jnk1*$^{-/-}$ hepatocytes show cellular oxidative stress by 2'-7'-DCF fluorescence intensity (A) by spectrofluorometric analysis, and (B) green immunofluorescence. (C) With increasing LDL concentrations, *Wt* hepatocytes show lowering of cellular anti-oxidant GSH levels (grey bars), with a reciprocal increase in oxidised glutathione, GSSG (black bars) (note different scales indicated on the two y-axes). (D) This resulted in a dose-dependent increase in oxidised:reduced glutathione (GSSG:GSH). **P*<0.05, *vs* control receiving no LDL, †*P*<0.05, *vs* treatment-matched, *Wt* control. Data are mean ± SEM from 4–6 animals pooled together, 4 replicates/gp, *n*=4-6/gp. Scale bars represent 50 μm.

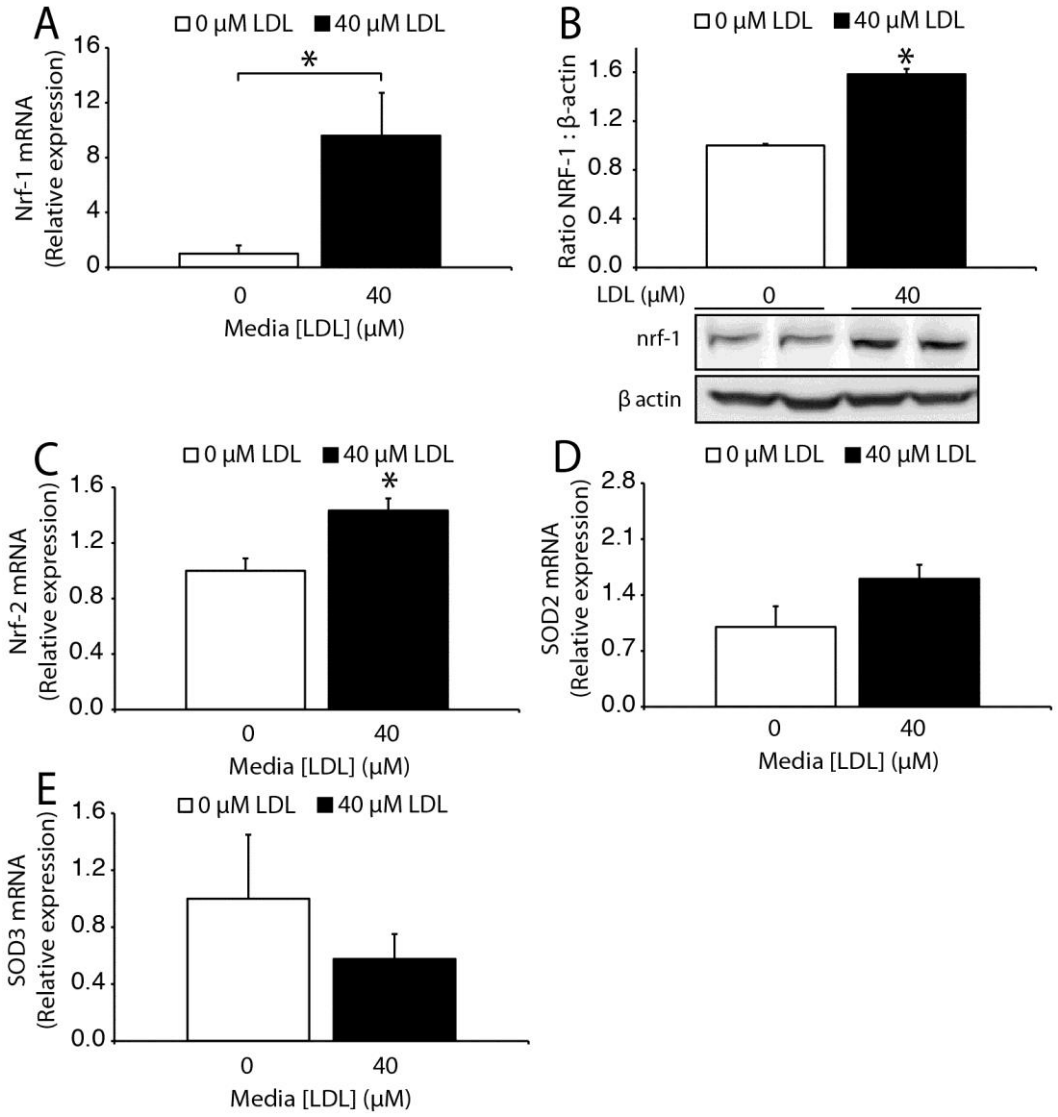

Figure 4.13 Nrf-1 and Nrf-2 are activated in FC-loaded hepatocytes

Wt hepatocytes showed increases in (**A**) Nrf-1 mRNA and (**B**) protein, as well as (**C**) increase in Nrf-2 mRNA. Among *Nrf* target genes, (**D**) mitochondrial-located SOD2 mRNA showed an increase trend (not significant), but there was no change to (**E**) extracellularly excreted SOD3 mRNA. Western blot quantification of NRF-1 was normalised to β-actin expression. Data are mean ± SEM. **P*<0.05, *vs* time-matched control receiving no LDL. NS, non-significant. Data are from 4–6 pooled animals with ≥3 replicates/gp, *n*=4-6/gp.

Oxidative stress and JNK activation are both triggers for mitochondrial permeability transition (MPT), which causes opening of high conductance permeability transition pores across the *inner* mitochondrial membrane so as to allow free distribution of ions, solutes and small molecular weight molecules (<1500 Da) across the membrane (Nieminen *et al.* 1997, Isenberg and Klaunig 2000, Czaja *et al.* 2003, Nieminen 2003, Shen and Liu 2006). Induction of MRT causes a significant fall in $\Delta\Psi m$, which can be monitored by using TMRM fluorescence (Section 4.3.3).

In these experiments, we first showed quenching of TMRM fluorescence in hepatocytes from *Wt* mice (white bars) that were incubated with 40 μM LDL (Figure 4.14B, fluorescence images in Figure 4.14C), indicating a fall in Ψm and MPT complex opening. The collapse of $\Delta\Psi m$ with MPT opening has been shown by others to result in mitochondrial swelling (Isenberg and Klaunig 2000, Nieminen 2003). As evident by TEM, mitochondria within hepatocytes exposed to 40 μM LDL were larger (average mitochondrial diameter ~1.5 μm *vs* ~1.0 μm) than control hepatocytes (0 μm LDL) (Figure 4.15A,B). Further, subcellular mitochondrial structure revealed disarray of cristae (Figure 4.15A,B). These mitochondrial changes (ultrastructural and MPT induction) could be the result of FC impregnation of mitochondria, as indicated by the earlier observation (Chapter 3) that FC localises within mitochondria (colocalisation of filipin with mitochondrial marker, COX-IV) in mouse livers with NASH (Figure 3.1C), and FC-loaded primary hepatocytes (Figure 3.3D). Further support for this proposal was provided by measurement of mRNA for StAR, the pathway for mitochondrial uptake of FC (Caballero *et al.* 2009), which was significantly increased in hepatocytes exposed to 40 μM LDL ($P<0.05$, Figure 4.14A).

Loss of $\Delta\Psi m$ and MPT leads to mitochondrial swelling and uncoupling of the electron transport chain, thereby arresting ATP production. Here, depletion of cellular ATP was observed as early as 6 hours after incubation with 40 μM LDL (Figure 4.14D). This was accompanied by an increase in hepatocyte injury, as manifest by raised ALT levels (Figure 4.14E). The profound ATP depletion observed in these experiments likely explains the striking increase in necrotic cell death (Figure 3.4D) observed as early as 2 hours after incubation of cells with 40 μM LDL (Figure 4.7), although ATP was not measured in the 2 h experiment.

To establish whether ROS drives JNK1 activation, or whether, instead, activation of JNK1 causes ROS accumulation, mitochondrial studies were conducted in *Jnk1*$^{-/-}$ and *Wt* hepatocytes loaded with FC (Figure 4.14). TMRM fluorescence was used as a marker of $\Delta\Psi$m and MPT preservation. In *Wt* cells, FC-loading attenuated TMRM fluorescence (Figure 4.14B, fluorescence images in Figure 4.14C). In contrast, *Jnk1*$^{-/-}$ cells maintained baseline TMRM fluorescence after FC-loading (Figure 4.14B, fluorescence images in Figure 4.14C), suggesting preserved $\Delta\Psi$m and MPT. These data support the role of JNK1 as a direct mediator of FC-induced lipotoxicity via a mitochondrial pathway. Further, JNK1 activation induces oxidative stress, which itself triggers JNK. In this manner, FC-induced JNK1 activation is self-propagating, creating more ROS to accentuate mitochondrial dysfunction and ultrastructural changes.

4.4.3 Mitochondria injury and not ER stress plays an important role in FC lipotoxicity.

Cytochrome c is normally bound to the inner mitochondrial membrane by its association with cardiolipin. Onset of MPT disrupts this interaction, allowing cytochrome c to be solubilised. In this form it can be extruded into the extra-mitochondrial milieu once the outer mitochondrial membrane is breached. There are two distinct mechanisms by which the outer mitochondria membrane can be breached: Ca^{2+}*-dependent* or Ca^{2+}*-independent.* In the first instance, mitochondrial Ca^{2+} overloading promotes opening of the permeability transition pore, allowing increased permeability of the inner mitochondrial membrane; this leads to matrix swelling, rupture of the outer membrane, and subsequent release of cytochrome *c*. In the Ca^{2+} independent process, cytochrome *c* release appears to be governed by members of the Bcl-2 family of proteins, in particular Bax permeabilisation of the outer mitochondrial membrane. This allows release of cytochrome c once it has been liberated from the inner mitochondria membrane, possibly after disruption of the inner membrane by oxidation of cardiolipin and other mitochondrial lipids (Ott *et al.* 2002). Once released into the extra-mitochondrial environment, cytochrome *c* signals the onset of caspase 3-mediated cell death pathways (Nieminen 2003, Crow *et al.* 2004).

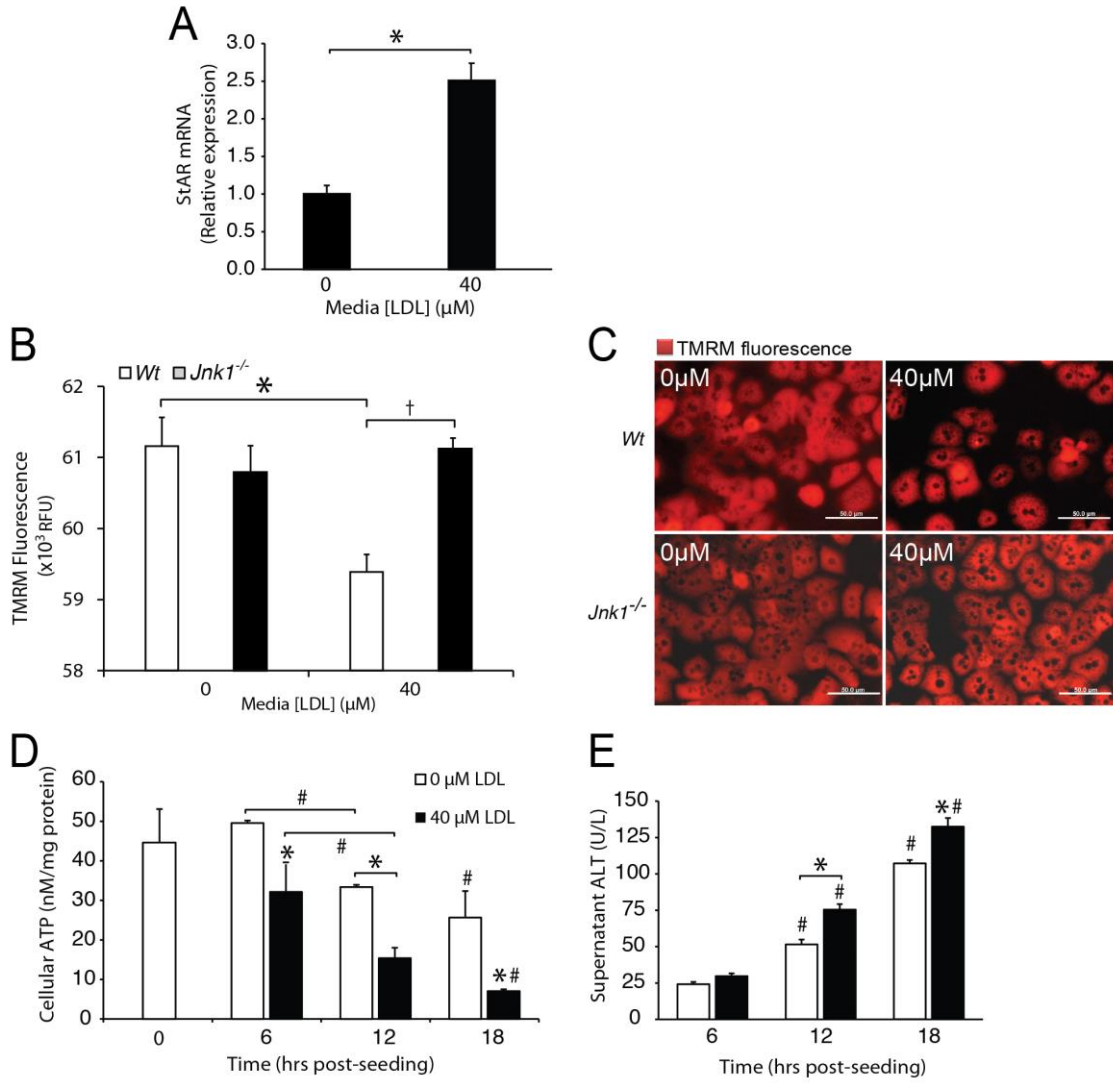

Figure 4.14 Hepatocyte FC loading is associated with up-regulation of StAR, MPT and fall in cellular ATP content, and these changes accompany onset of cellular injury.

(**A**) Incubation of primary hepatocytes with 40 μM LDL is associated with upregulation of StAR mRNA. (**B**) *Wt* but not *Jnk1*$^{-/-}$ hepatocytes exposed to FC show quenching of TMRM fluorescence, measured by spectophotometric analysis, and (**C**) on immunofluorescence intensity (red), indicating MPT. (**D**) *Wt* hepatocytes exhibit ATP depletion as early as 6 hours following FC loading (40 μM LDL), *vs* control (no LDL), which corresponds to (E) an increase in liver injury, manifest as increased ALT release into supernatant (compared with control hepatocytes). Data represent mean ± SEM, 4–6 pooled animals with ≥3 replicates and experiment repeated thrice, n=9 per experiment. *P<0.05, *vs* genotype-matched control receiving no LDL, $^{\#}P$< 0.05, *vs* treatment-matched control receiving at 6 hours post seeding, †P<0.05, *vs* treatment-matched WT control. Bars represent 50 μm.

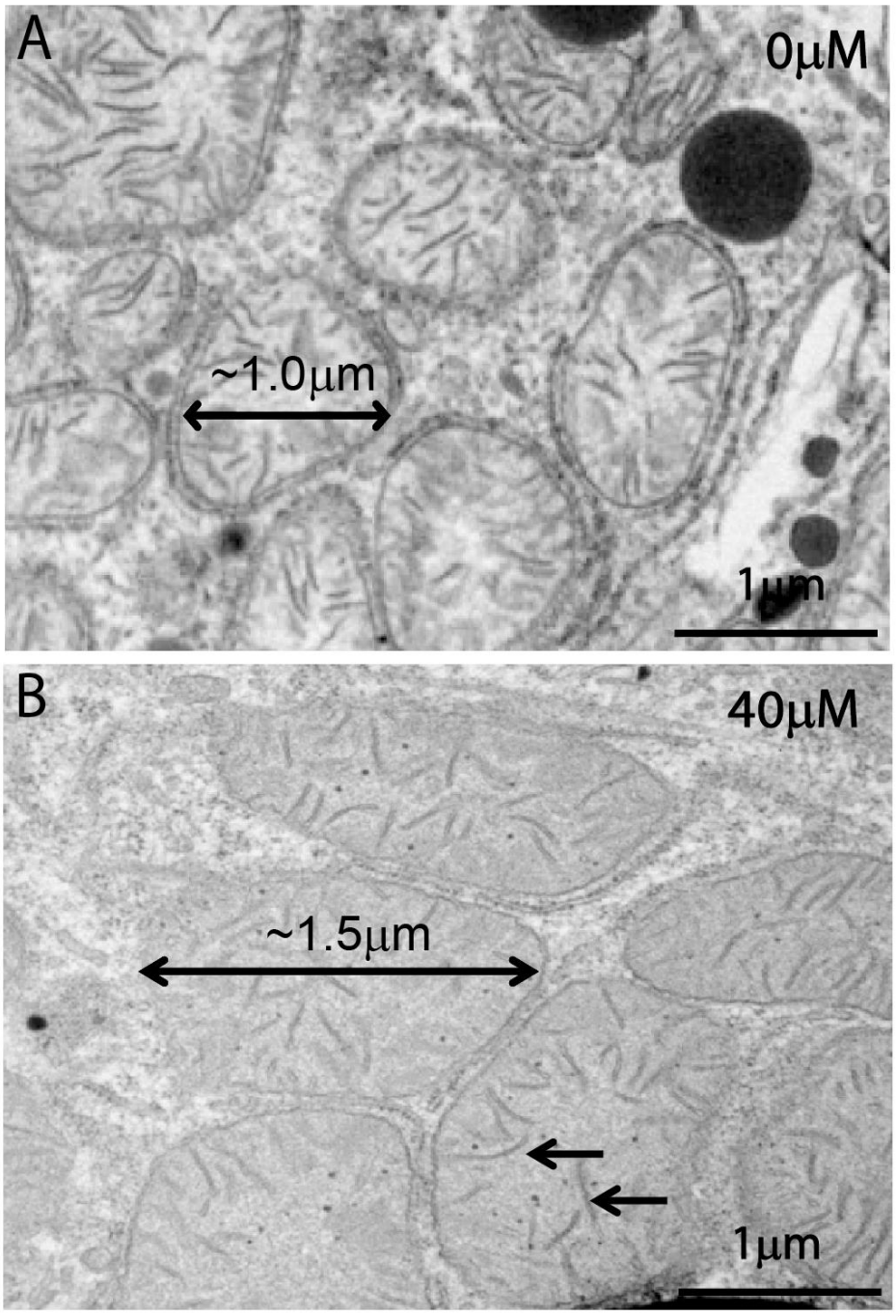

Figure 4.15 Changes to mitochondrial ultrastructure with FC loading.

(**A**) Mitochondria of control hepatocytes (not exposed to LDL) have normal cristae and average ~1.0 μm in organelle diameter. (**B**) In contrast, mitochondria from hepatocytes loaded with FC (40 μM LDL exposure) show increase in diameter to 1.5 μm and disarray of cristae (arrows). Bars represent 1 μm.

In these experiments, we demonstrated cytochrome c translocation from mitochondria to cytosol (Figure 4.16B), and also showed that FC-loaded hepatocytes exhibit down-regulation of anti-apoptotic Bcl-xl. In addition, there appeared to be a slight increase (but not significant) of pro-apoptotic Bax in the mitochondrial fractions of cells

incubated with 40 μM LDL (Figure 4.16A). If JNK1-mediated mitochondrial MPT and translocation of cytochrome c plays a role in FC-mediated apoptosis, blocking MPT with CyA or inhibiting resultant caspase 3 activation (Figure 4.16C, D) should offer the same cellular protection as the JNK inhibitors. To test this, we showed that CyA, caspase inhibitor II (a pan-caspase inhibitor), and caspase-3 inhibitor II (a targeted caspase 3 inhibitor) all abrogated apoptosis and necrosis (Figure 4.16C) induced by hepatocyte incubation with 40 μM LDL.

ER stress is another pathway to activation of JNK and NF-κB (Wang *et al.* 2009), and is thought to be an important mechanism in the pathogenesis of T2D (Eizirik *et al.* 2008). In Chapter 3, we showed that FC localises (Figure 3.1B) to ER in livers of mice with NASH, and in FC-loaded hepatocytes (Figure 3.3C). Despite such FC localisation, we found no increase of GRP78 (Figure 4.17A) or its downstream pro-apoptosis protein, CHOP (Figure 4.17B,C). Even more importantly, 4-phenylbutyric acid (4-PBA), an UFP chaperone that improves ER folding capacity, failed to protect against apoptosis and necrosis cell death in cells loaded with FC (Figure 4.16C, D).

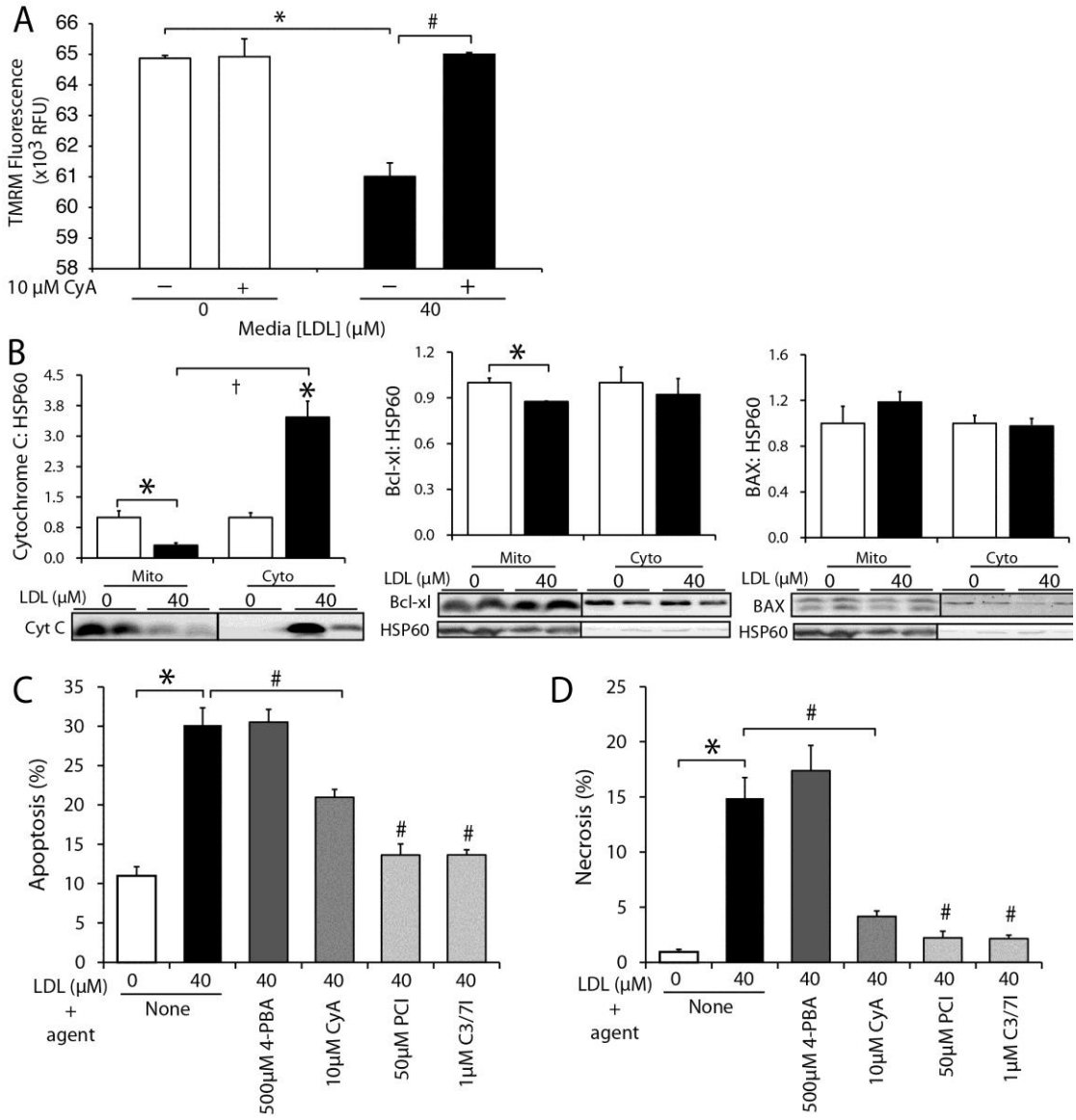

Figure 4.16 Mechanisms of free cholesterol lipotoxicity involve mitochondrial but not ER stress pathways to cell death (apoptosis and necrosis).

(**A**) By preventing mitochondria MPT, 10 µM CyA leads to preservation of TMRM fluorescence in cells loaded with 40 µM LDL. (**B**) Relative expression of cytochrome *c*, Bcl-xL, BAX in mitochondria and cytoplasmic fractions. HSP60 was used as loading control. (**C**) Apoptosis and (**D**) necrosis (PI positive cells) in FC-loaded hepatocytes is reduced by CyA, pancaspase inhibitor (PCI) and caspase 3/7 inhibitor (C3/7I), but not by 4-phenylbutyric acid (4-PBA). Data are represented as means ± SEM with experiments conducted in duplicate or triplicate, *n*=6-8 per experiment. **P*<0.05, *vs* time-matched control receiving no LDL, $^{\#}$*P*<0.05, *vs* dose-matched control receiving 40 µM LDL, †*P*<0.05, 40 µM LDL *vs* control.

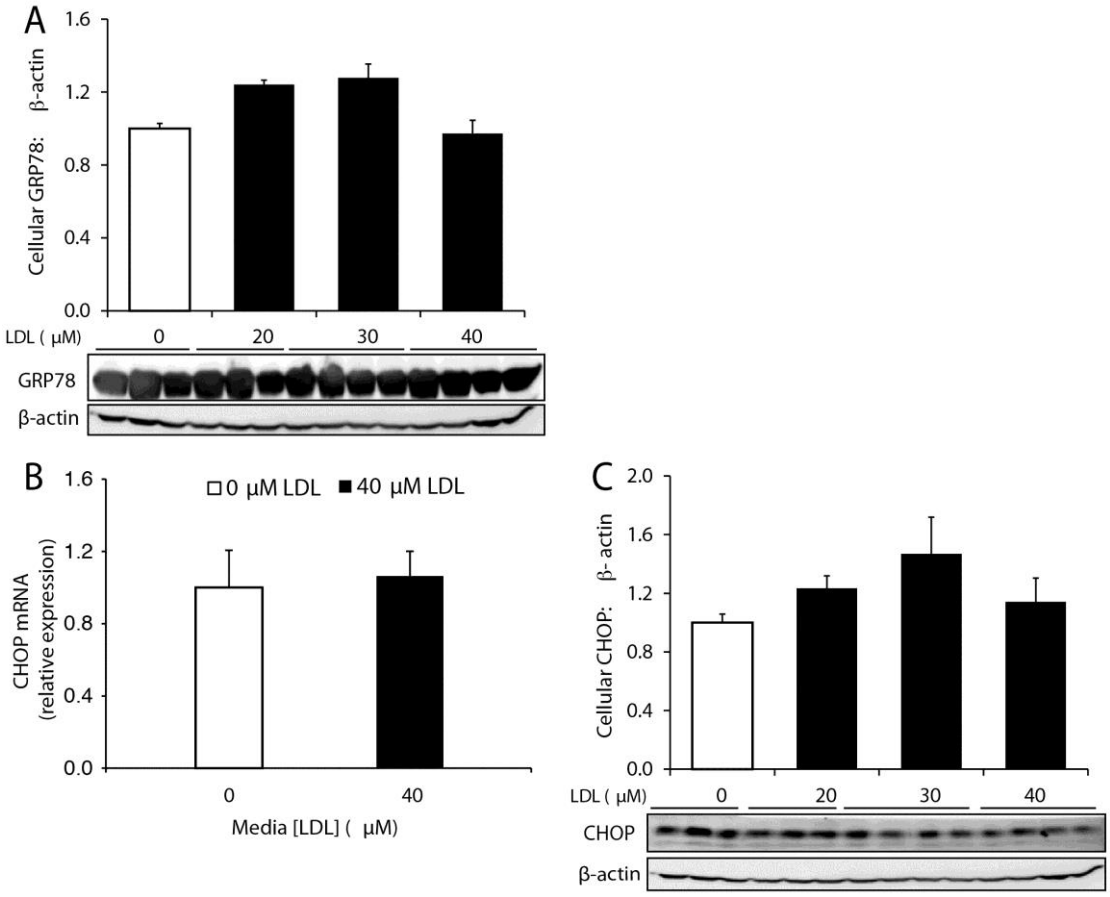

Figure 4.17 ER stress is not induced during FC-induced hepatolipotoxicity.

FC loading of *Wt* Hepatocytes does not alter (**A**) GRP78 protein, (**B**) CHOP mRNA or (**C**) CHOP expression. β-actin was used as loading control. Data are presented as means ± SEM from 4 pooled animals, with experiments repeated more than twice in triplicate ($n \geq 6$).

4.5 Discussion

In mice placed on HF diet and in genetically (*ob/ob*) mice, JNK activation occurs in liver, fat, and muscle tissues (Hirosumi *et al.* 2002, Solinas *et al.* 2006, Seki and Schnabl 2012) and may be implicated in development of insulin resistance. In addition, JNK1 activation also appears to be crucial in several experimental models of steatohepatitis (Schattenberg *et al.* 2006, Kodama and Brenner 2009, Singh *et al.* 2009). Further, HF diet causes obesity in WT, but not *Jnk1*$^{-/-}$ mice (Hirosumi *et al.* 2002, Solinas *et al.* 2006, Singh *et al.* 2009). Further, compared with *Wt*, *Jnk1*$^{-/-}$ mice on HF diet have decreased phosphorylation of the IRS-1 at Ser 307 (an inhibitory site) and increased insulin-induced tyrosine phosphorylation at IRS-1, which is the physiological phosphorylation pathway of insulin receptor signalling (Hirosumi *et al.* 2002).

Researchers have observed that lipoapoptosis caused by satFFA is JNK1-dependent

(Malhi *et al.* 2006, Cazanave *et al.* 2009, Kakisaka *et al.* 2012, Sharma *et al.* 2012) (Figure 4.20). However, hepatocyte satFFA levels, while high do not differentiate NASH from "not NASH NAFLD" in humans or in experimental murine models related to obesity and metabolic syndrome (Puri *et al.* 2007, Caballero *et al.* 2009, Van Rooyen and Farrell 2011, Arteel 2012, Min *et al.* 2012). Instead, FC is high in NASH but not in "non-NASH NAFLD". To date no studies have directly linked hepatic FC content to JNK activation in NASH. Whether FC activates JNK1/2 in hepatocytes, and how this may be related to hepatocellular injury and inflammatory recruitment therefore remains unclear.

In the previous Chapter, loading primary hepatocytes with FC caused lipotoxicity manifest as liver injury and cell death, which are known hallmarks of NASH. Further, it was demonstrated that such FC distributes to the plasma membrane, mitochondria and ER, recapitulating the subcellular deposition sites of FC in *foz/foz* mice with NASH (Van Rooyen *et al.* 2011). The functional significance of FC deposition in plasma membrane of FC-laden hepatocytes will be discussed in the Chapter 5 in the context of inflammatory recruitment in NASH. Mari *et al* (2006) showed that *in vivo* mitochondrial FC loading causes oxidant stress and sensitises hepatocytes to TNF-α and Fas-mediated cytolysis (Mari *et al.* 2006). Our present *in vitro* studies extend these findings – linking FC lipotoxicity to mitochondrial cell death pathways by a JNK1-dependent process. We also explored how such pathways could be utilised for therapeutic intervention.

The first major observation of this Chapter was that FC-loading of primary hepatocytes activates JNK1 in association with lipotoxicity. Administration of potent JNK inhibitors, in particular CC-930, inhibited JNK1 activation and this afforded near-complete protection against FC-induced cell death. Further, *Jnk1*$^{-/-}$, but not *Jnk2*$^{-/-}$ hepatocytes, were refractory to FC-induced lipotoxicity. To date, links between hepatic FC and JNK1 activation have been indirect. For example, research in the host laboratory found activation of JNK1/2 in livers of *foz/foz* mice with NASH correlated closely with hepatic FC content, while lowering FC levels with pharmacological agents abrogated the JNK1/2 activation in association with amelioration of liver injury, inflammation and fibrosis (Van Rooyen and Farrell 2011, Van Rooyen *et al.* 2013). The current *in vitro* studies provide, for the first time, strong evidence for a direct (likely causal)

relationship between FC and JNK activation.

The present data also demonstrate that JNK1 is the relevant JNK isomer in FC-induced lipotoxicity pathway. However, it is important to note that Sabio *et al* (2008 and 2009) found that hepatocyte JNK1 deletion resulted in glucose intolerance, IR and hepatic steatosis in HF diet-fed mice (Sabio *et al.* 2008), while JNK1 deletion in adipose tissue conferred protection against HF diet-induced IR and steatosis (Sabio *et al.* 2008). These findings differ from those of others; *Jnk1*$^{-/-}$ mice given MCD HF diet were protected from liver injury, hepatic steatosis and IR (Singh *et al.* 2009), while mice subjected to MCD were protected from liver injury and inflammation if they were JNK1 deleted (Schattenberg *et al.* 2006). Similarly, JNK1 inhibitor (SP 600125) administered intraperitoneally protected against IR and glucose intolerance in HF diet-fed mice (Kaneto *et al.* 2004). These findings suggest that compensatory mechanisms to JNK inhibitors may exist in other tissues (e.g. adipocytes and potentially pancreatic β cell), resulting in upregulation of JNK1 in these tissues, resulting in IR and steatosis. In the present *in vitro* system, we removed the possibility of such a compensatory mechanism by conducting studies in primary hepatocytes.

Given the effective hepatocellular protection offered by specific JNK inhibitors in this *in vitro* model, oral administration of these novel agents is worth testing as a possible therapeutic option for experimental NASH, and this is underway in the host laboratory in *foz/foz* mice. If successful, it could lead to a phase I trial in human NASH. In this regard, Celgene has recently developed a novel highly specific JNK1 inhibitor compound (CC-003), which would be better suited to this application (development of CC-930 is on hold for undisclosed reasons). Unfortunately at this time the compound has not been approved for experimentation or publication.

The second finding of this Chapter is that JNK1 activation is *essential* for FC-lipotoxicity, by a mechanism that involves mitochondrial injury and its downstream redox consequence. Whilst oxidative stress features prominently in NASH (Weltman *et al.* 1998, Robertson *et al.* 2001, Sanyal *et al.* 2001, Neuschwander-Tetri and Caldwell 2003, Lambertucci *et al.* 2008, Nakamura *et al.* 2009), its role in cell injury and cell death has not been fully established (Lee *et al.* 2007, Syn *et al.* 2009, Syn *et al.* 2009, Neuschwander-Tetri 2010, Farrell *et al.* 2012). The present *in vitro* studies

demonstrated that TMRM fluorescence (preserved $\Delta\Psi m$) was not altered in FC-loaded *Jnk1*$^{-/-}$ hepatocytes, whereas it was profoundly reduced in both *Wt* and *Jnk2*$^{-/-}$ hepatocytes. Further, there was minimal, if any, oxidative stress (by either 2',7'-DCF fluorescence or GSSG accumulation) with JNK1 deletion. These findings indicate that JNK1 involvement is crucial in the pathways by which FC loading leads to the collapse of $\Delta\Psi m$, MPT and generation of mitochondrial ROS in FC-loaded hepatocytes.

Following onset of MPT and fall of $\Delta\Psi m$, the following series of events occurs:

1. cytochrome *c* detaches from complexes III and IV of the respiratory chain (Figure 4.4), into the intermembranous space.

2. The mitochondrial respiratory chain uncouples, with collapse of all electrical and chemical gradients.

3. This results in large-amplitude swelling driven by the difference of colloid osmotic pressure between the matrix and extramitochondrial space (Nieminen 2003). Compared to control cells (no FC), such mitochondrial swelling was clearly demonstrated on TEM in FC-loaded hepatocytes (Figure 4.15). This change is similar to the mitochondrial ultrastructural abnormalities observed in livers of human NASH (Caldwell *et al.* 1999, Sanyal *et al.* 2001, Caldwell *et al.* 2009).

4. With progressive mitochondrial swelling (the result of MPT), the inner mitochondrial membrane starts to unfold to accommodate this volume; this may account for the cristae disarray observed in mitochondria of FC-loaded hepatocytes (Figure 4.15B).

5. The outer membrane does not have such unfolding capacity, and its inevitable rupture releases cytochrome *c* into the cytosol. Once in the cytosol, cytochrome *c* interacts with cytosolic proteins, apoptotic protease activating factor-1 (Apaf-1) (Zou *et al.* 1997) and the inactive form of the proteolytic enzyme, caspase-9, to form an "apoptosome" (Li *et al.* 1997). In the presence of ATP, procaspase-9 becomes activated to in turn activate the executor caspases, procaspase-3 and -7. Following caspase-3/7 activation, an apoptotic cascade is initiated, culminating in internucleosomal DNA degradation and changes in nuclear morphology (condensation and margination of chromatin material) typical of apoptosis (Nieminen 2003).

It is possible that all or most of the changes observed in mitochondrial function and ultrastructure found with hepatocyte FC-loading in the present studies may be explained by JNK1 activation and mitochondrial FC deposition. The observed increase in StAR

transcript following LDL incubation provides one explanation for FC trafficking into the mitochondria. This finding is similar to that observed by Cabellero *et al.* (2009), who noted a 15-fold increase in StAR transcript in human NAFLD livers with NASH, but not in SS. StAR is a hormonally (gonadotropin) regulated 37 kDa protein which is trafficked to the mitochondria via an N-terminal targeting sequence. In the 37 kDa form, StAR resides in the outer mitochondrial membrane, while a smaller 30 kDa form is present in the inner mitochondrial membrane. In these positions, StAR facilitates rapid FC trafficking between mitochondrial compartments (Jefcoate *et al.* 2000).

In the present experiments, blockade of MPT with CyA or caspase 3 or pan-caspase inhibition reduced apoptosis and necrosis, almost to that of control hepatocytes (no cholesterol loading). If replicated in whole animals with NASH, this finding could have therapeutic implications in 'arresting' the mitochondria cell death pathway in NASH, thereby preventing progression to cirrhosis. A potential future direction for this work would be to quantify cellular ATP and mitochondrial FC and glutathione content when pathways of JNK-mitochondrial cell death axis are blocked, such as by JNK inhibitors, CyA or caspase-3 inhibitor). If the proposal that JNK1 activation is pivotal in FC lipotoxicity, it would be expected that ATP levels would be preserved with these protectants.

In addition to apoptosis, necrosis is a prominent feature of FC- induced lipotoxic injury to hepatocytes. Depletion of ATP is likely to contribute to this cell death pathway (Nieminen 2003). In human NASH, liver ATP homeostasis is impaired, such that ATP recovery is blunted after fructose infusion to deplete ATP (Cortez-Pinto *et al.* 1999, Cortez-Pinto *et al.* 1999). In primary hepatocytes incubated with 40 μM LDL, ATP depletion had occurred by 6 hours (earlier time points were not studied, although apoptosis starts as early as 2 hours [see Figure 4.7]). This was associated with significant liver injury, evident by ALT leakage into culture media (Figure 4.14D,E). A possible explanation for this sequence is that early JNK1 activation drives the initial collapse of $\Delta\Psi$m, uncouples the electron transport chain from ATP production, leading to generation of ROS. Initially, there may be compensatory changes in mitochondria to combat this ROS, a concept supported by increased (albeit non-significant) SOD2 mRNA expression (Figure 4.13), and likely the mitochondrial glutathione redox cycle (Mari *et al.* 2013). With continuing MPT and a fall in $\Delta\Psi$m due to mitochondrial-

generated ROS, Ca^{2+} and GSH leak out into the cytosol. Since GSH is synthesised exclusively in cytosol and its transport into mitochondria requires ATP and a functional $\Delta\Psi m$, mitochondrial glutathione becomes rapidly depleted (Mari *et al.* 2013). Eventually, ROS generation overwhelms the redox stress defence mechanisms, resulting in prolonged JNK activation with further MPT; the latter may function as a self-amplifying 'switch', that, once activated (e.g. by JNK, ROS), leads to irreversible cell death (Nieminen *et al.* 1997, Isenberg and Klaunig 2000) (Figure 4.18). In addition, it is possible that necrosis is activated as part of programmed cell death, a process that involves RIP-1 and RIP-3. This pathway was not studied in the present work, partly due to the paucity of cell protein for more detailed analyses.

In Chapter 3 it was shown that a subpopulation of FC is localised to the ER compartment, and ER stress is another factor that is known to activate JNK (Wang *et al.* 2009, Wang *et al.* 2009). Overall, the evidence that ER stress is a critical pathway in lipotoxicity and NASH pathogenesis is inconsistent and not convincing (Puri *et al.* 2008, Gregor *et al.* 2009, Leclercq *et al.* 2011). ER stress has been shown to contribute to pancreatic β cell loss and insulin resistance in the pathogenesis of T2D (Eizirik *et al.* 2008). Others reported evidence that ER stress could be relevant to satFFA lipotoxicity (Cazanave *et al.* 2009). However, genetic silencing of *Chop* expression reduces hepatocyte toxicity *in vitro* only at overly high doses of FFA (500 μM palmitate) (Pfaffenbach *et al.* 2010). Further, in nutritional models of NAFLD Chop gene deletion failed to reduce disease severity through ER stress resistance (Pfaffenbach *et al.* 2010).

To clarify a possible role for ER stress in NASH pathogenesis expression, we assessed expression of ER stress markers. There was no upregulation of the chaperone protein GRP78 which is required for an unfolded protein response, nor was there increased cellular expression of CHOP. Importantly, pre-treatment of cells with 4-PBA, a UFP chaperone, had no effect on the fate of FC-loaded hepatocytes. These data are consistent with earlier observations in *foz/foz* mice with NASH that GRP78 and nuclear CHOP expression fail to increase in relation to NASH severity (Van Rooyen *et al* [unpublished], PhD ANU, 2012). More recently, Legry *et al* (2014) from Isabelle Leclercq's laboratory (in collaboration with the host laboratory) demonstrated that ER stress does not contribute to steatohepatitis in obese, insulin resistant HF-fed *foz/foz* mice. These investigators explored ER stress markers in the liver of *foz/foz* mice in

response to HFD at several time points. Additional studies addressed the metabolic and hepatic features of mice administered tunicamycin to induce ER stress, or tauro-ursodeoxycholic acid (TUDCA) to block it. Using these complementary approaches, the authors found no expression of ER stress nor contribution to the pathogenesis of either IR or steatohepatitis in this murine model (ER stress was present in *ob/ob* mice, and may be a model-specific phenomenon; it is not present in human NASH [Puri *et al.* 2008]). Development of NASH was not associated with activation of upstream unfolded protein response (phospho-eIL2α, IRE1α activity, or spliced Xbp1). Further, induction of chronic ER stress by tunicamycin failed to worsen obesity, glucose intolerance and NASH pathology. Although the ER protectant TUDCA reduced steatosis, combating ER stress failed to improve glucose intolerance, hepatic inflammation and apoptosis in HFD-fed *foz/foz* mice. The authors concluded that while ER stress could play a role in development of simple steatosis, evident by activation of JNK and up-regulation of *Atf4* and *CHOP* transcripts, it plays no role in cell death and inflammatory recruitment involved in transition to NASH (Legry *et al.*).

It is also noteworthy that ursodeoxycholic acid at 15–18 mg/kg/d (UCDA) (ER stress protectant), failed to reverse NASH pathology in clinical studies (Laurin *et al.* 1996, Lindor *et al.* 2004). Higher dosages of UCDA had been reported as useful in other diseases. For this reason, two trials have used higher dosage UCDA in NASH. The first enrolled 126 patients with biopsy-proven NASH, and randomised care to UCDA at 28–35 mg/kg/d for a year, or placebo (Ratziu *et al.* 2011). There was significant improvement of ALT and GGT, associated with improvement of serum glucose and HOMA-IR scores with high dose UCDA compared to the placebo group. The weakness of this study was lack of histological proof of fibrosis improvement attributed to UCDA treatment and the high frequency of unpleasant side effects associated with ultra high dose UCDA. The second study randomised 185 patients to receive 23–28 mg/kg/d of UCDA or placebo for 18 months. A second liver biopsy after treatment failed to show histological improvement, even though GGT levels improved compared to the placebo group (Leuschner *et al.* 2010). It therefore seems unlikely that attempts to combat ER stress in NASH will improve histological and clinical outcomes of this disorder.

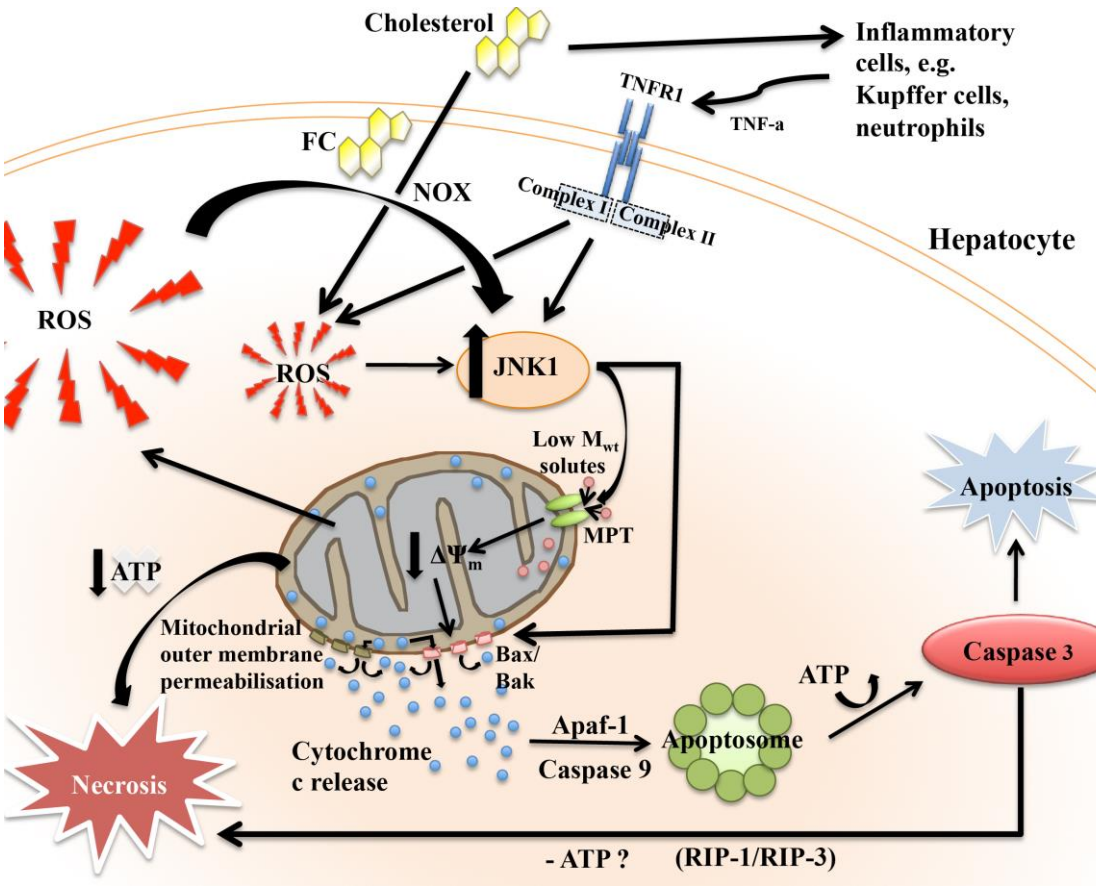

Figure 4.18 FC-mediates hepatocyte lipotoxicity via a JNK1-dependent mitochondrial cell death pathway

JNK1 can be activated by FC (possibly by ROS generated via NOX activation), which causes mitochondrial MPT, and fall in $\Delta\Psi_m$. This releases cytochrome c into the intermembranous space. MPT allows passage of low molecular weight (Mwt) solutes from the cytosol into the mitochondrial matrix, leading to mitochondrial swelling. Together with JNK driven Bax/Bak permeabilisation and rupture of the outer mitochondrial membrane due to mitochondrial swelling, cytochrome *c* is released into the cytoplasm, where ATP-dependent activation of caspase 3 causes cell death by apoptosis. Collapse of $\Delta\Psi_m$, possibly coupled with FC deposition in mitochondria, results in generation of mitochondrial ROS. ROS overwhelms compensatory mechanisms when mitochondrial glutathione is depleted, and in turn provides a continuing stimulus for JNK1 activation. ATP production is crippled as mitochondria are unable to maintain the proton gradient necessary for ATPase-dependent generation of ATP. Collectively, these events culminate in cellular necrosis.

Abbreviations: ATP, adenosine triphosphate; Apaf-1, apoptotic protease activating factor-1; Bak and Bax; BH_3-only protein members; JNK, *c*-Jun-N terminal kinase; FC, free cholesterol; MPT, mitochondrial permeability transition; M_{wt}, molecular weight; NOX, NADPH oxidases; ROS, reactive oxygen species; $\Delta\Psi_m$ mitochondrial membrane potential

In summary, the results described in this chapter provide the first direct demonstration that accumulated FC activates JNK1 to kill hepatocytes by apoptosis and necrosis. ER

stress has no role in FC lipotoxicity. Rather, the cellular mechanism of injury involves JNK1-dependent mitochondrial MPT with cytochrome *c* release into cytoplasm, oxidative stress and ATP depletion, leading to apoptosis and necrotic cell death (Figure 4.18). Importantly, novel and potent JNK inhibitors (including a JNK1-specific inhibitor) blocked FC-induced cell death, as did blocking the mitochondrial cell death pathway using inhibitors, cyclosporine A, and a caspase-3/7 inhibitor.

4.6 Summary of findings in Chapter 4

This chapter describes how loading primary hepatocytes with FC activates JNK1-mitochondrial pathways of FC-mediated lipotoxicity. The major findings are:

1. FC activates JNK1.
2. JNK1 activation is essential for FC-mediated liver injury and cell death.
3. A mitochondrial cell death pathway operates in FC lipotoxicity and results in both apoptosis and necrosis. Necrosis is likely a consequence of the observed ATP depletion, due to evident mitochondrial injury.
4. FC loading is also associated with a JNK1-dependent increase in oxidative stress; this is not found in *Jnk1*$^{-/-}$ hepatocytes.
5. Ultrastructural changes (swelling, cristae number) in mitochondria of FC-loaded hepatocytes are similar to those observed in livers of human NASH.
6. Potent JNK inhibitors (CC401 and CC-930), block FC-mediated lipotoxicity, as did inhibitors of the mitochondrial cell death pathway (CyA, pancaspase, caspase 3/7 inhibitors).
7. ER stress does not appear to be a conspicuous pathway in FC lipotoxicity.

These findings provide insights into how the FC activates the JNK1-mitochondrial cell death pathway. The inhibitor studies have identified potential new therapeutic options in the treatment of NASH. However, NASH is an inflammatory disorder; to be relevant to NASH pathogenesis, lipotoxicity to hepatocytes must in some way engage innate immunity to provoke and attract this inflammatory response and its resultant fibrogenesis. In the next Chapter, the candidate will explore the mechanisms by which FC-loaded hepatocytes could orchestrate inflammatory recruitment in NASH.

CHAPTER 5

HMGB1-containing extracellular vesicles arising from free cholesterol-induced hepatocellular lipotoxicity activate Kupffer cells via TLR4

5.1 Introduction

Thus far, the role of cholesterol as a lipotoxic mediator of hepatocellular injury has been explored using an *in vitro* approach to load primary murine hepatocytes. In Chapter 4, the relationship between hepatocellular FC content and hepatocellular injury with activation of cell death pathways (both apoptosis and necrosis) was defined. The findings suggested direct links between intracellular FC and JNK1 activation (seen as *c*-Jun phosphorylation), and subsequent generation of mitochondrial permeability pore transition (MPT). This results in cytochrome *c* release and mitochondrial injury, which is evident ultra-structurally as mitochondrial swelling and deranged cristae array, and functionally as impaired ATP production. These events also generated oxidant stress, with further activation of JNK1 activation in a proposed feed-forward fashion. In the present Chapter, experiments are described which examine the mechanisms by which FC-injured hepatocytes may be responsible for inflammatory recruitment in NASH, specifically the role of high-mobility group box 1 protein (HMGB1) and toll-like receptor (TLR)-4 for KC activation. This introduction will provide a brief background for why HMGB1 and TLR4 were studied in this research.

5.1.1 HMGB1

As previously mentioned in Chapter 1, HMGB1 is a 30 kDa protein originally isolated in 1973 and characterised in 1976 by Walker, Goodwin and Johns (Goodwin and Johns 1973, Goodwin *et al.* 1973, Walker *et al.* 1976). These investigators described HMGB1 as a loosely-bound nucleosomal protein ubiquitously expressed by all eukaryotic cells. Physiologically, HMGB1 is responsible for DNA bending, facilitating transcription and stabilisation of the DNA-histone complex within the nucleus (Figure 5.1) (Singh and Dixon 1990, Yamanaka *et al.* 2002). Following its release from blood monocytes, HMGB1 was noted to produce pyrogenic responses (Dinarello *et al.* 1977). Since then,

the roles of HMGB1 have expanded. It is now known that HMGB1 is integral to multiple autocrine and paracrine inflammatory processes (see Figure 5.1), as well as contributing to the pathogenesis of fibrotic diseases including systemic sclerosis, cystic fibrosis, hepatic, renal, pulmonary and myocardial fibrosis. The role of HMGB1 in these various disease processes has been reviewed extensively by Li *et al.* (2014) and Kang *et al.* (2014).

Briefly, HMGB1 functions as a damage-associated molecular pattern (DAMP) cytokine, but like the IL-1 family, it lacks a secretory peptide domain required for the ER-Golgi vesicle trafficking that typifies secreted proteins. Instead, HMGB1 is secreted in a non-classical "leaderless" fashion (Nickel 2003). A rise in intracellular ionic calcium (Ca^{2+}) concentration triggers HMGB1 translocation from the nucleus to the cytoplasm (Zhang *et al.* 2008). This precedes active secretion from macrophages, dendritic (DC) and natural killer (NK) cells in response to endotoxaemia and bacterial infection (Wang *et al.* 2004). Cellular damage also results in presentation of HMGB1 to the plasma membrane, from where it is released along with heat-shock and S100 proteins. All these proteins promote inflammatory cell diapedesis and recruitment (Lolmede *et al.* 2009). Following its plasma membrane presentation and/or release, HMGB1 activates several pattern-recognition receptors (PRR); these include TLRs 2 and 4, and receptor for advanced glycosylation end-products (RAGE) (Yu *et al.* 2006, Luan *et al.* 2010). These receptors activate NF-κB p65 to induce sterile inflammation (Figure 5.1) (Andersson and Tracey 2011) via the pro-inflammatory pathways described below. Extensive research has shown that secreted HMGB1 may be packaged in small membrane-bound EVs (Pisetsky 2014).

5.1.2 NF-κB inflammatory pathways

The NF-κB and TLR pathways have been extensively discussed in Chapter 1. Briefly, TLR4 activates NF-κB p65 through a series of adapter proteins, including toll-interleukin 1 receptor domain-containing adapter protein (TIRAP) and myeloid differentiation primary response gene-88 (Myd88); the latter signals a downstream complex responsible for NF-κB and JNK activation (Takeuchi *et al.* 2000, Fitzgerald *et al.* 2001). NF-κB is a transcription factor comprised of 5 peptides, which form a series of hetero and homo-dimers. The p65 hetero- and homo-dimers regulate inflammatory and apoptotic responses (Aoudjit *et al.* 1997, Manna and Aggarwal 1999).

Activation of NF-κB is initiated by the IκB kinase (IKK) complex. This phosphorylates the cytoplasmic binding protein inhibitor of NF-κB, IκB, thereby allowing its ubiquintination. In turn, such ubiquitination targets the NF-κB –IκB complex to the 26S proteasome, where IκB is degraded. Liberated NF-κB hetero- and/or homo-dimers then migrate to the nucleus where they are taken up and bind to target DNA sites (Hanausek-Walaszek *et al.* 1990, Ballard *et al.* 1992, Ten *et al.* 1992). Once within the nucleus, NF-κB p65 promotes transcriptional regulation of numerous pro-inflammatory genes, several of which may be involved in the pathogenesis of NASH (Tian *et al.* 2014).

Murine NASH is associated with FC accumulation, JNK1 activation and hepatocyte cell death (see Chapter 1, Section 1.7.3). In such livers, FC accumulation is accompanied by activation of NF-κB p65, which by IHC appears to be located predominantly in non-parenchymal cells (Figure 5.1) (Van Rooyen *et al.* 2013). Other research in fractionated livers from HF-fed *foz/foz* mice demonstrated that NF-κB activation is most prominent in non-parenchymal cells, but some activation is also evident in hepatocytes (Dr Claire Larter, unpublished data, PhD thesis 2008, University of Sydney).

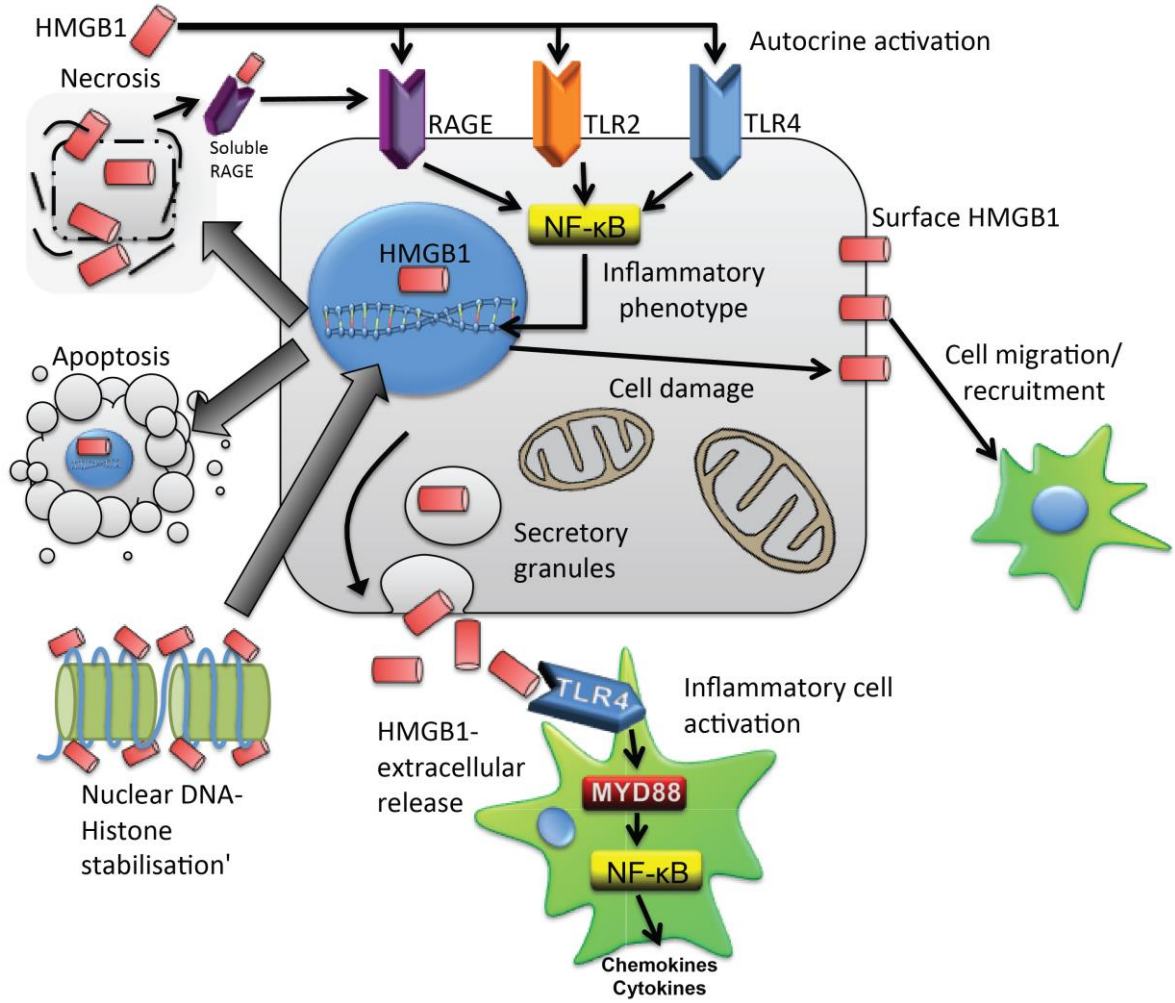

Figure 5.1 Physiological and disease-related functions of high mobility group box 1 (HMGB1).

Image adapted from Diebold *et al.* (2013). HMGB1 is responsible for normal bending and stablisation of the DNA-histone complex within the nucleus. Cellular damage precedes the pro-inflammatory roles of HMGB1. Necrosis results in substantial release of HMGB1 complexed to receptor for advanced glycosylation end products (RAGE)-HMGB1. HMGB1 is then capable of activating adjacent cells through RAGE and TLR-2 and -4 receptors. Ligating to these receptors results in activation of Myd88 and IκB kinase complex, leading to activation of nuclear factor κB (NF-κB) p65. In turn, NF-κB is responsible for up-regulation of TNF, interleukin (IL)-1 and IL-6. Apoptotic cell death causes significantly less HMGB1 release since this pathway results in nuclear sequestration of cellular HMGB1 prior to autophagic degradation. Separately, HMGB1 may be released into the extracellular fluid (ECF) compartment via secretory granules.

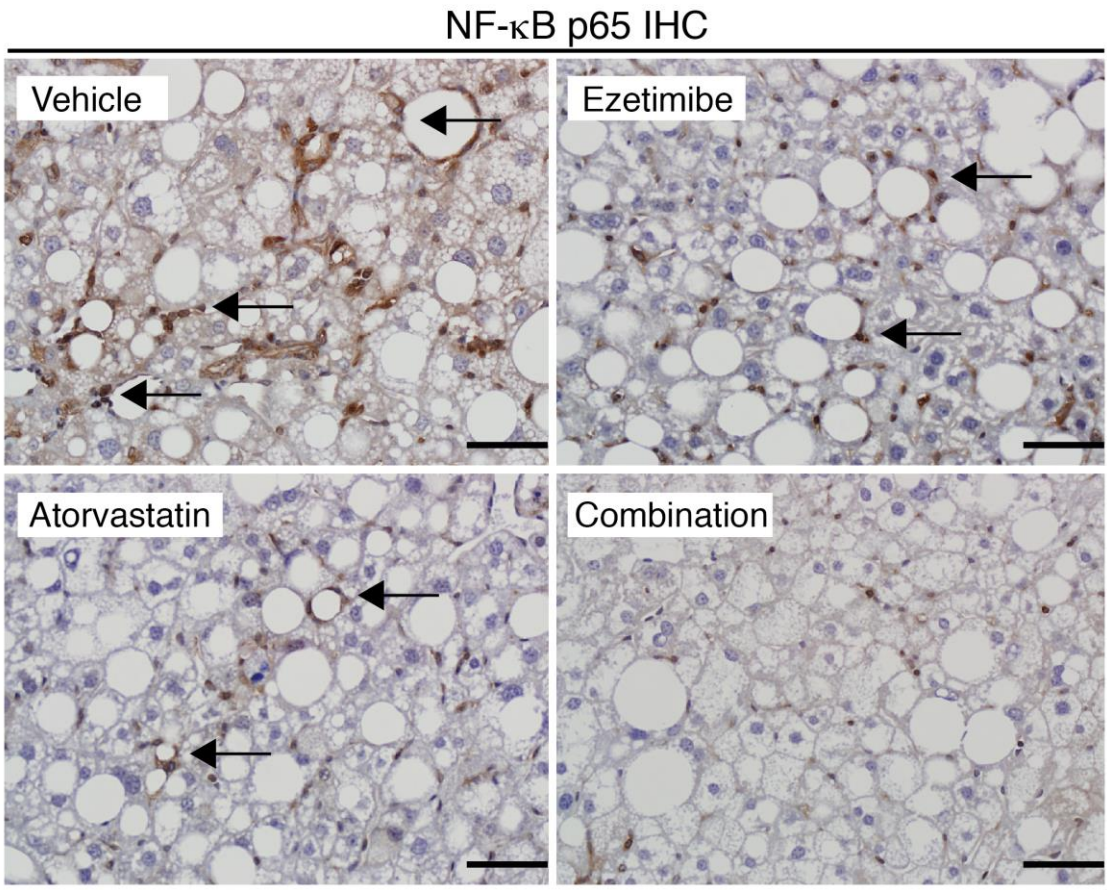

Figure 5.2 NASH in atherogenic diet-fed *foz/foz* mice is associated with NF-κB p65 activation in non-parenchymal cells.

In this work (Van Rooyen *et al.* 2013), NF-κB p65 expression correlated with hepatic cholesterol content (see (Van Rooyen *et al.* 2011) for details). Paraffin-embedded liver sections (7 μm) were obtained from atherogenic (HF) diet-fed (24 weeks) obese, diabetic *foz/foz* mice (vehicle controls). Separately, *foz/foz* mice fed an identical diet for 16 weeks before receiving HF-diet containing ezetimibe and/or atorvastatin. Drug treatment continued for 8 weeks. Liver sections from these mice (Van Rooyen *et al.* 2011) were probed for NF-κB p65 expression using immunohistochemistry, as described in Section 5.3. Scale bars represent 50 μm. Arrows indicate positive NF-κB p65 staining in non-parenchymal cells. IHC staining presented in this figure was performed by the candidate, however the original feeding studies were completed by Dr Derrick Van Rooyen (ANU thesis 2012) (see Acknowledgments).

5.2 Scope of research described in this Chapter:

The principal aims of this Chapter were to test the hypothesis that the FC-induced hepatocyte damage described in Chapters 3 and 4 can give rise to proinflammatory responses. The specific aims were to:

1. Determine if experimental NASH is associated with increased HMGB1 production, cytosolic migration (from nucleus) and release (blood levels).

2. Establish whether hepatocyte injury by lipotoxicity releases HMGB1-containing EVs and/or soluble HMGB1 that subsequent activates KCs.
3. Test whether antibody neutralisation of HMGB1 confers protection against KC activation by conditioned media from lipotoxic hepatocytes.
4. Characterise the role of TLR4 in KC activation.

5.3 Methods

5.3.1 Experimental approaches

Several experimental approaches were used to address the above-mentioned aims, including analysis of *in vivo* feeding experiments previously published in the host laboratory. These approaches are detailed below.

5.3.1.1 Mice and diets

Experimental details pertinent to the two *in vivo* experiments have been previously described in Section 3.3.1. Archived frozen tissue sections and liver samples from these studies were used by the candidate to explore the role of HMGB1 and NF-κB p65 in the *foz/foz* model of experimental NASH. The candidate performed the assays documented in this Chapter.

5.3.1.2 Primary hepatocyte cultures

For primary hepatocyte FC localisation, cells were isolated, cultured, and loaded with FC using unmodified human LDL, as outlined in Section 2.5 and Chapter 3. Thereafter, cells were fixed with 3.7% paraformaldehyde-PBS and stained with filipin for FC and subcellular markers, as described in Section 2.14.

5.3.2 Experimental procedures

5.3.2.1 Fluorescent subcellular localisation

Fluorescent staining (for FC subcellular localisation) of frozen liver sections was conducted as described in Section 2.14, using primary and secondary antibodies as listed in Tables 2.1 and 2.2. A Zeiss Axioplan2 microscope (Zeiss, GmbH, Germany) with AxioVision V4.8 software (Zeiss, GmbH, Germany) was used to capture images and perform post-acquisition analysis.

5.3.2.2 Immunohistochemistry (IHC) on paraffin-fixed liver sections

IHC was used to evaluate NF-κB p65 expression in liver sections from HF-fed *foz/foz* mice treated with atorvastatin and/or ezetimibe (Section 5.3.1, and reference Van Rooyen *et al.* [2013]), as described below.

5.3.2.2.1 Reagents

Epitope unmasking buffer (10 mM sodium-citrate, 0.05% [v/v] tween-20, pH 6.0). Sodium citrate dehydrate tribasic (2.94 g) and tween-20 (0.5 mL) were dissolved in d.H_2O (950 mL), prior to pH adjustment (6.0) and final volume adjustment to 1 L.

Additional IHC reagents including antibody diluent and IHC wash solutions were all purchased from Chemicon (Millipore, Billerica, MA). Anti-HMGB1 antibody (details are listed in Table 2.1) and biotin conjugated anti-rabbit IgG (Santa Cruz Biotechnology, Inc, Santa Cruz, CA) were diluted in commercial antibody diluent (Millipore, Billerica, MA), as per Manufacturer's instructions.

5.3.2.2.2 Procedure

Liver sections (7 μm) from formalin-fixed, paraffin-embedded samples were dewaxed and rehydrated using xylene and ethanol gradients. Antigen retrieval using epitope-unmasking buffer (123^{o}C, 5 min) was subsequently performed using a Decloaking Chamber™ (Biocare Medical, Concord, CA), before non-specific epitopes were blocked (Chemicon blocking solution, 5 min, RT). Anti-HMGB1 was then applied to liver sections and slides incubated (1:100 dilution, 60 min, RT). Bound antibody was detected using biotin conjugated anti-rabbit secondary antibody (1:250 dilution in antibody diluent buffer, 30 min, RT). Signal from bound secondary antibody was amplified using streptavidin conjugated horse-radish peroxidase (HRP) (Chemicon) (10 min, RT) and diaminobenzidine (DAB) solution (10 min, RT). Sections were counterstained for nuclei using Gill's haematoxylin formulation (45 sec). They were then mounted in plasticiser (di-*N*-butyle phthalate in xylene [DPX]) prior to viewing.

5.3.2.3 Protein isolation and western blotting

Total hepatic, cytoplasmic and nuclear proteins were isolated as described in Sections 2.10.1 and 2.10.2, respectively. Specific proteins were then qualitatively (molecular

weight) and quantatively (expression relative to controls) assessed using western blotting, as per Section 2.12.

5.3.2.4 Quantification of intracellular cholesterol and assessment of hepatocellular injury

In primary hepatocytes, intracellular FC content, LDH release and apoptosis/necrosis determination were performed as described in Sections 2.15.1 and 2.15.3, respectively.

5.3.2.5 HMGB1 antibody neutralisation assay

In order to test the potential of HMGB1 to activate KCs, an anti-HMGB1 antibody inhibition assay was performed, as follows.

5.3.2.5.1 Reagents

Anti-HMGB1 antibody was purchased from Antibodies Online (Atlanta, GA) and required no additional preparation before use.

5.3.2.5.2 Procedure

For HMGB1 blocking experiments on KC cultures, antibody was prepared (10 µg/mL) in media (RPMI 1640, see Section 2.8). This was added to culture supernatants used to test stimulation of KCs, and incubated (60 min, 37^{o}C) prior to KC exposure.

5.3.2.6 Serum IL-1β

Serum IL-1β was determined using a commercially purchased enzyme-linked immunosorbent assay (ELISA) (RnD Systems, Minneapolis, MN). All reagents were provided and the assays were performed in accordance with the Manufacturer's instructions.

5.3.2.7 Supernatant cytokine levels

Supernatants isolated from primary hepatocytes cultured in the presence of 0 or 40 µM LDL-treated hepatocytes (Section 2.5.1) were analysed for the presence of multiple cytokines using Bio-Rad Bioplex™ assays (Bio-Rad, Hercules, CA), as per Manufacturer's instructions. This analysis was performed by Eagle Chu in the lab of Professor Jun Yu (Department of Medicine and Therapeutics at The Chinese University

of Hong Kong [CUHK]), a longstanding collaboration between the supervisor and Professor Yu (see Acknowledgments).

5.3.2.8 Scanning electron microscopy

SEM was used to identify morphological features of KC activation. The reagents and procedure for this technique are detailed in Section 3.3.6.

5.3.2.9 Statistical analyses

Statistical analyses were carried out as described in Section 2.16. All data presenting in this Chapter represent mean ± SEM (with *n* value stated). Statistical significance is defined as $P<0.05$.

5.4 Results

5.4.1 FC loading activates NF-κB p65 in primary hepatocytes to cause proinflammatory cytokine secretion.

Previous research in the host laboratory had demonstrated that NF-κB p65 expression is increased in non-parenchymal cells in the livers of *foz/foz* mice with NASH (Figure 5.1) (Van Rooyen *et al.* 2013), but whether this proinflammatory pathway could also be activated by FC in hepatocytes is less clear. To establish this, hepatocytes were loaded with FC as described in Chapter 3. In turn, nuclear and cytoplasmic NF-κB p65 fractions were prepared so as to appreciate cytoplasmic to nuclear translocation of this transcription factor (Manna and Aggarwal 1999). Following incubation with 40 μM LDL to load cells with FC, the cytoplasmic level of NF-κB p65 was significantly reduced ($P<0.05$, Figure 5.3A), with a reciprocal increase in nuclear NF-κB p65 ($P<0.05$, Figure 5.3B). These findings confirm nuclear translocation of NF-κB is a consequence of FC-loading.

Next, the supernatant isolated from 40 μM LDL-treated (FC-loaded) hepatocytes was examined using a commercial multiplexed assay (Bio-Plex, Bio-Rad, Hercules, CA) to detect secreted cytokines. Several of these are under direct NF-κB transcriptional control. Importantly, FC loading significantly increased supernatant IL-6 and TNF-α ($P<0.05$, Figure 5.3C, H). IL-6 is an acute phase reactive protein, expressed by hepatocytes and here may represent a direct acute response to FC loading. Further, elevation of IL-6 and TNF-α is consistent with previously published data on the

inflammatory phenotypes observed in animal models of NASH, as well as in human NAFLD (Farrell *et al.* 2012).

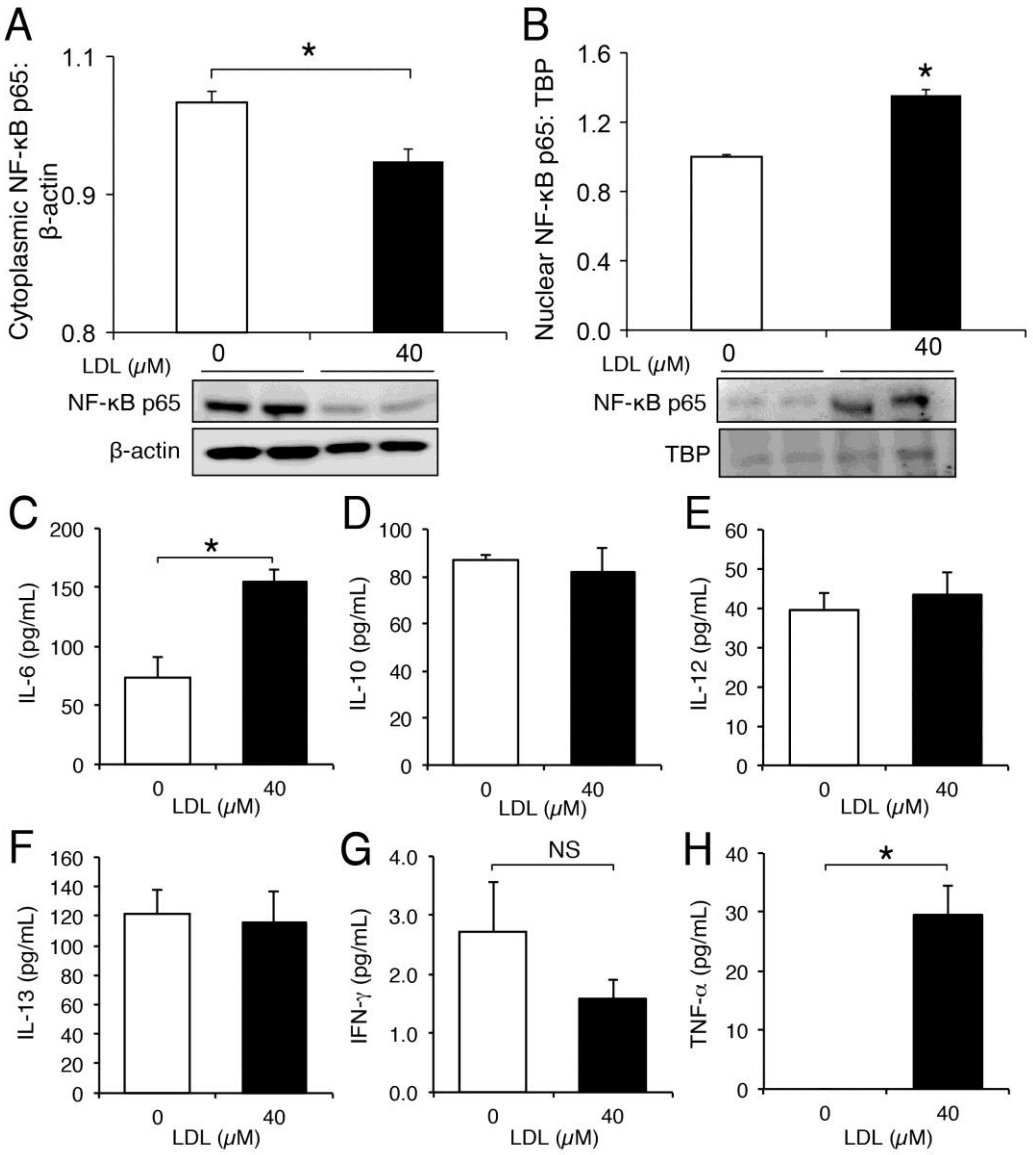

Figure 5.3 FC loading of primary murine hepatocytes increases nuclear expression of NF-κB, as well as secretion of IL-6 and TNF-α.

Hepatocytes incubated with 40 μM LDL showed translocation of NF-κB from (**A**) cytoplasm into (**B**) nucleus. β-actin and TATA box-binding protein (TBP) were used as loading control for cytoplasmic and nuclear protein, respectively. Bio-Plex Assay (Bio-Rad, Hercules, CA) was performed by Eagle Chu (CUHK) (see Acknowledgments) to quantify the secretion of multiple cytokines, including (**C**) IL-6, (**D**) IL-10, (**E**) IL-12, (**F**) IL-13, (**G**) IFN-γ, and (**H**) TNF-α. Data represent means ± SEM from n=4–6 pooled animals, with 4-6 replicates/group ($n \geq 16$). *P<0.05 *vs* time-matched control receiving no LDL.

5.4.2 HMGB1 is increased in murine NASH livers.

NF-κB and JNK (Chapter 4) are well-known proinflammatory and pro-apoptotic signalling pathways observed both *in vivo* in the *foz/foz* model of NASH, and *in vitro* in FC-induced lipotoxicity to primary hepatocytes. Innate immunity signalling has been strongly implicated in the activation of these pathways (Farrell *et al.* 2012, Ganz and Szabo 2013, Vonghia *et al.* 2013). The present experiments explored these pathways, with specific focus on the "danger pathway" which includes the DAMPs and receptors described earlier (Section 5.1.1). A particular focus here was on HMGB1 and TLR4.

Using atherogenic diet containing increasing amounts of cholesterol (0, 0.2, 2.0% [w/w]), NASH was produced in *foz/foz* mice, with stepwise increase in severity (by ALT, histology and fibrosis) according to hepatic FC content (Van Rooyen *et al.* 2011). In these livers, there was a significant increase in total hepatic HMGB1 expression proportional to hepatic cholesterol content ($P<0.05$, Figure 5.4A). This increase was further illustrated using fluorescent localisation of HMGB1 in frozen liver sections (Figure 5.4B). This approach revealed increased HMGB1 expression was accompanied by its translocation from nuclear to (peri-) plasma membrane location (Figure 5.4B arrows).

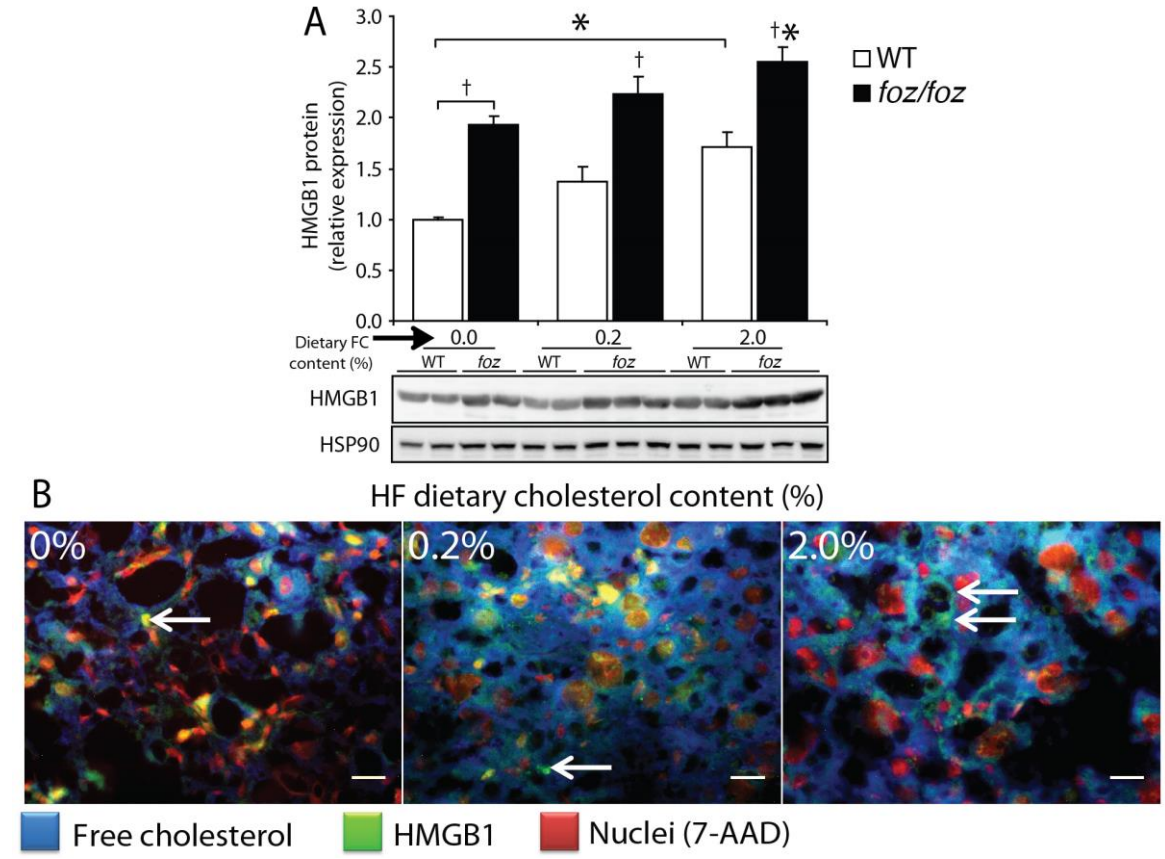

Figure 5.4 HMGB1 increases in NASH livers of *foz/foz* mice fed HFD containing 0-2% (w/w) cholesterol.

(**A**) High-mobility group box 1 (HMGB1) protein expression was increased in liver lysates from *foz/foz* mice with NASH but not in WT mice with simple steatosis after 24 weeks of feeding atherogenic diets containing 0, 0.2 or 2.0% (w/w) cholesterol. Protein expression was normalised to heat shock protein 90 (HSP) loading control and data are expressed relative to values in WT mice fed the diet with no (0%) cholesterol. (**B**) Frozen sections of the same mice fed 0, 0.2 or 2% (w/w) cholesterol-containing atherogenic diet (top left label of panels) to cause NASH (Van Rooyen *et al.* 2011) were stained for FC (Filipin, blue) and HMGB1 (FITC, green). As FC content increased in these livers, there was translocation of HMGB1 (green) from nucleus into cytosol (white arrows). **P*<0.05, *vs* genotype-matched dietary control (0% cholesterol). †*P*<0.05, *vs* WT control. Data in panel A are mean ± SEM, representing 8-10 animals/gp. Scale bars represent 20 µm.

5.4.3 HMGB1 is released from FC-loaded hepatocytes by a JNK1-dependent process that may involve oxidant stress and/or necrosis.

To verify whether FC could be directly implicated in HMGB1 release from hepatocytes, we then assessed HMGB1 expression and release from primary hepatocytes loaded with FC (see Section 2.5). After 24 h incubation with LDL (20-40 µM), there was concomitant reduction of HMGB1 colocalisation with hepatocyte nuclei, as

demonstrated by immunofluorescence (Figure 5.5C). There was also a decrease in hepatocellular HMGB1 protein ($P<0.05$, Figure 5.5A, black bars), which we attributed to release of HMGB1 into supernatant. This was demonstrated by a reciprocal, significant increase in supernatant HMGB1 ($P<0.05$, Figure 5.5B). Furthermore, on SEM HMGB1-rich "vesicles" were seen budding off the plasma membrane surface of FC-loaded hepatocytes (Figure 5.5C, arrows).

In Chapter 4, it was shown that hepatocytes from *Jnk1*$^{-/-}$ knock-out mice were protected against FC-induced apoptosis and necrosis (Figure 4.12A and B). Both oxidant stress and cellular necrosis are known to cause HMGB1 release. It was therefore anticipated that *Jnk1*$^{-/-}$-deficient hepatocytes would not release HMGB1 after FC loading. Unlike WT, FC-loading failed to decrease hepatocellular HMGB1 expression in *Jnk1*$^{-/-}$ cells ($P<0.05$, Figure 5.5A). Further, while FC-loading of WT (and *Jnk2*$^{-/-}$) hepatocytes resulted in translocation of HMGB1 into the supernatant (Figures 5.5B and 5.5E), FC-loaded *Jnk1*$^{-/-}$ hepatocytes retained HMGB1 as demonstrated by unchanged supernatant HMGB1 protein levels compared to control ($P<0.05$ *cf* WT, Figure 5.5B).

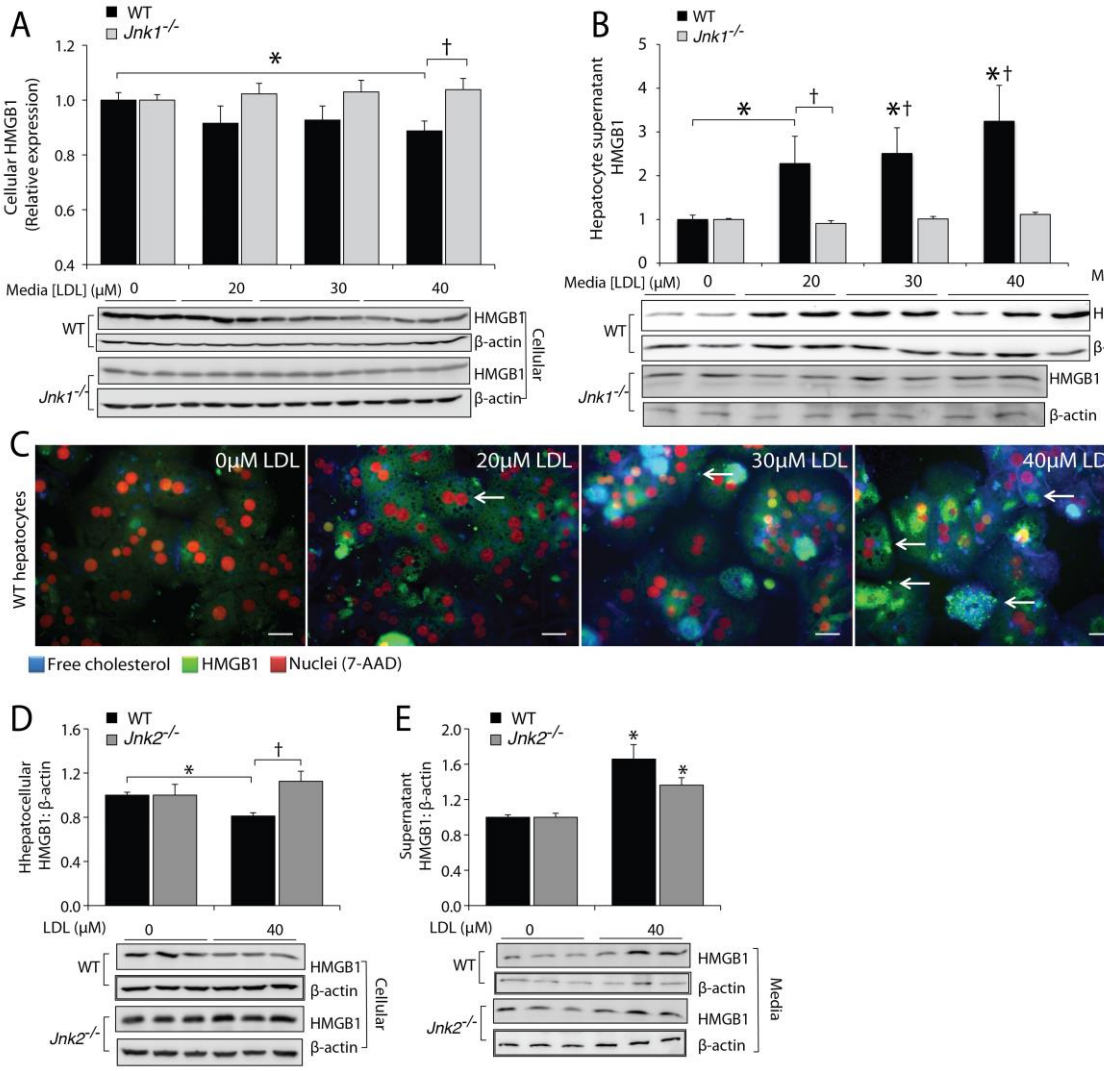

Figure 5.5 JNK1, but not JNK2, is involved in release of intracellular HMGB1 from FC-loaded hepatocytes.

With FC loading using LDL, (**A**) hepatocellular HMGB1 tended to fall (NS) in WT but increase in *Jnk1*$^{-/-}$ hepatocytes, while (**B**) supernatant HMGB1 levels increased significantly in WT but not *Jnk1*$^{-/-}$ samples. HMGB1 expression was normalised to β-actin loading control. (**C**) WT hepatocytes exposed to 20–40 μM LDL (see top right label panel) show dose-dependent increases in filipin (blue) intensity, which coincides with the translocation of HMGB1 (green) from nucleus into cytosol, and release into culture media (arrows). (**D**) *Jnk2*$^{-/-}$ hepatocytes loaded with 40 μM LDL show no significant change in cellular HMGB1, compared to the fall in FC-loaded WT. However, (**E**) both *Jnk2*$^{-/-}$ and WT loaded with 40 μM LDL release HMGB1 into culture media. **P*<0.05 *vs* time- and genotype-matched receiving no LDL. †*P*<0.05, *vs* treatment-matched WT control. Data are mean ± SEM from 4–6 pooled animals/gp with *n*=8 replicates/gp. Scale bars represent 20 μm.

5.4.4 HMGB1 released from FC-loaded hepatocytes activates TLR4 and activates downstream inflammatory pathways.

Since HMGB1 is a cognate ligand for TLR4 in the proinflammatory cascade, we explored the specific role of TLR4 receptor-signalling, using a combination of WT and *Tlr4*$^{-/-}$ cells. An interesting, and somewhat unexpected observation was that FC loading significantly increased TLR4 expression in WT hepatocytes; this occurred in a dose-responsive manner (P<0.05, Fig. 5.6). In order to clarify whether HMGB1 liberated by lipotoxic injury to hepatocytes contributes to a feed-forward autocrine/paracrine mechanism of lipotoxic cell death to hepatocytes involving the TLR4 receptor (as suggested *in vivo* by Li et al 2011), we compared apoptosis and necrosis in FC-loaded *Tlr4*$^{-/-}$ hepatocytes with WT.

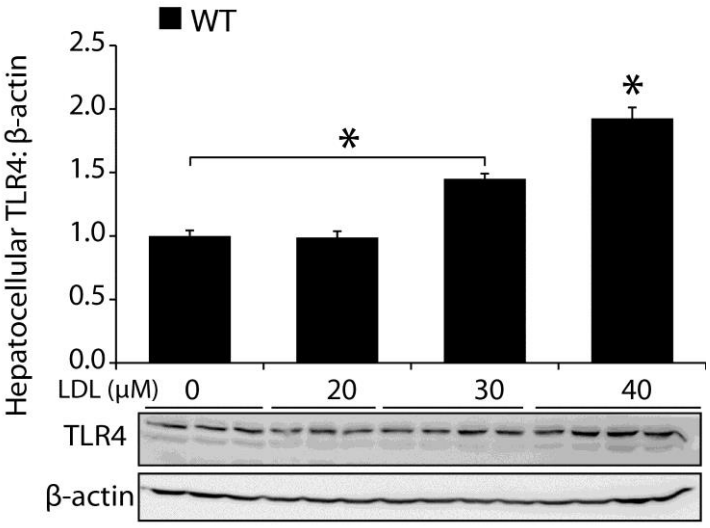

Figure 5.6 FC-loading induces dose-responsive TLR4 expression in WT hepatocytes.

FC loading induces hepatocyte expression of TLR4 protein in WT hepatocytes. β-actin was used as loading control. *P<0.05 *vs* genotype-matched receiving no LDL. Data are mean ± SEM from 4–6 pooled animals/gp with n≥8 replicates/gp, experiment performed in duplicate.

We first confirmed the efficacy of FC-loading in *Tlr4*$^{-/-}$ hepatocytes by incubating them with human LDL for 24 h (Section 3.3.1). The intracellular cholesterol content in *Tlr4*$^{-/-}$ hepatocytes exposed to 20-40 μM LDL (Figure 5.7) was similar to that of WT hepatocytes (Figure 3.2D). However, in contrast to WT hepatocytes, *Tlr4*$^{-/-}$ hepatocytes were refractory to injury (by LDH leakage) and both apoptosis and necrosis (P<0.05, Figure 5.8A, B, C). Moreover, incubation of *Tlr4*$^{-/-}$ primary hepatocytes with LDL failed to induce HMGB1 release into supernatant (P<0.05, Figure 5.8D,E), despite the

evident increase in FC and cellular HMGB1 content (Figure 5.8). Like *Jnk1*$^{-/-}$ cells described earlier (Figure 5.5B), *Tlr4*$^{-/-}$ hepatocytes also failed to release HMGB1 following FC-loading (Figure 5.8D,E).

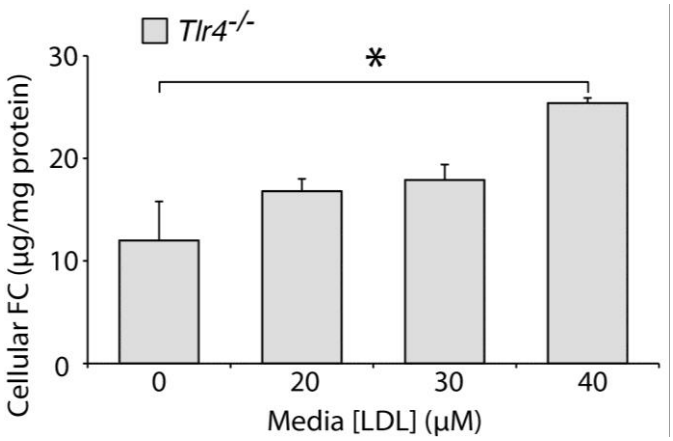

Figure 5.7 LDL exposure results in FC-loading in *Tlr4*$^{-/-}$ hepatocytes.

Incubation of *Tlr4*$^{-/-}$ hepatocytes with LDL increased cellular FC content. **P*<0.05 *vs* genotype-matched receiving no LDL. Data are mean ± SEM from 4–6 pooled animals/gp with *n*≥8 replicates/gp, experiment performed in duplicate.

An alternative explanation for TLR4 activation could be lipopolysaccharide (LPS) contamination of the LDL preparations. Although we consider this unlikely because of the pyrogen-free procedures used, we tested for any possible LPS contamination in separate experiments by adding polymyxin B to LDL preparations. Polymyxin B binds to and neutralises LPS. In the present experiments, polymyxin B failed to protect hepatocytes against cell injury and apoptosis during incubation with LDL, and only minimally decreased necrotic cell death (Figure 5.9). This indicates that LDL preparations used in these experiments are unlikely to activate KCs because of LPS contamination.

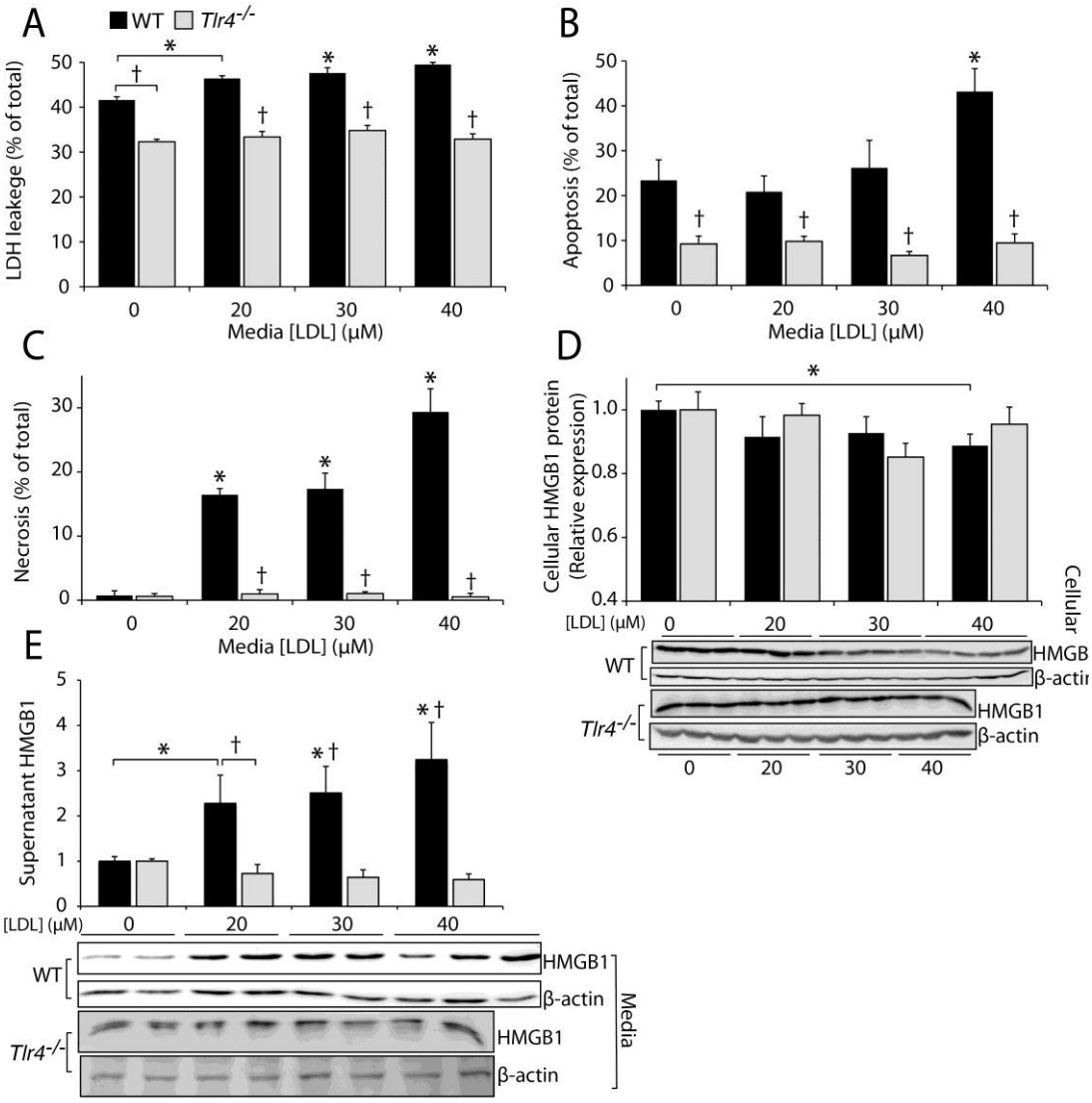

Figure 5.8 FC-loading causes hepatocyte injury and cell death resulting in release of HMGB1 via a TLR4-dependent process.

(**A**) FC-loaded *Tlr4*$^{-/-}$ hepatocytes are refractory to FC-induced injury (as determined by LDH leakage; results in WT hepatocytes, as presented earlier [Section 3.4.3], are shown again here for comparison), as well as (**B**) apoptosis and (**C**) necrosis. (**D** and **E**) FC-loaded WT but not *Tlr4*$^{-/-}$ hepatocytes release HMGB1 into culture media, as demonstrated by reduced cellular HMGB1 (panel **D**) and reciprocally increased supernatant HMGB1 (panel **E**). β-actin was used as loading control. **P*<0.05 *vs* time- and genotype-matched receiving no LDL. †*P*<0.05, *vs* treatment-matched WT control. Data are mean ± SEM from 4–6 pooled animals/gp with $n \geq 8$ replicates/gp, experiment performed in duplicate.

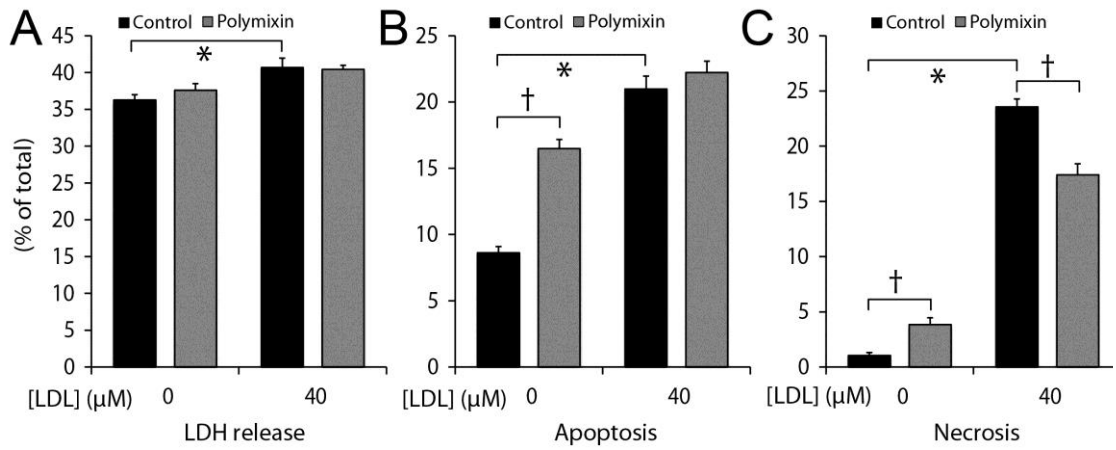

Figure 5.9 Addition of polymyxin B to LDL fails to protect FC-loaded hepatocytes from injury or cell death.

Addition of polymyxin B (10 μg/mL) to hepatocyte culture media during LDL incubation (**A**) did not dampen liver injury (left panel), as shown by LDH leakage, or (**B**) reduce cell death by apoptosis (middle panel). (**C**) It did slightly decrease necrosis (right panel) compared to hepatocytes without polymyxin B added (treatment-matched control). **P*<0.05, vs control (0 μM LDL). †*P*<0.05, vs treatment-matched vehicle control (no addition of polymyxin B). Data are mean ± SEM from 4–6 pooled animals/gp with $n \geq 8$ replicates/gp, experiment was performed in duplicate ($n \geq 16$).

5.4.5 HMGB1 neutralisation ameliorates FC-induced lipotoxicity.

Having shown that TLR4 is important in FC-induced hepatocellular lipotoxicity, the role of HMGB1 was tested mechanistically using a specific HMGB1 neutralising antibody, as previously described (Cummings *et al.* 2011). Addition of the neutralising antibody (10 μg/mL) to FC-loaded primary WT hepatocyte reduced JNK activation, as shown by hepatocellular phospho-*c*-Jun expression (*P*<0.05, Figure 5.10A), and substantially reduced apoptosis and necrosis (*P*<0.05, Figure 5.10B and C).

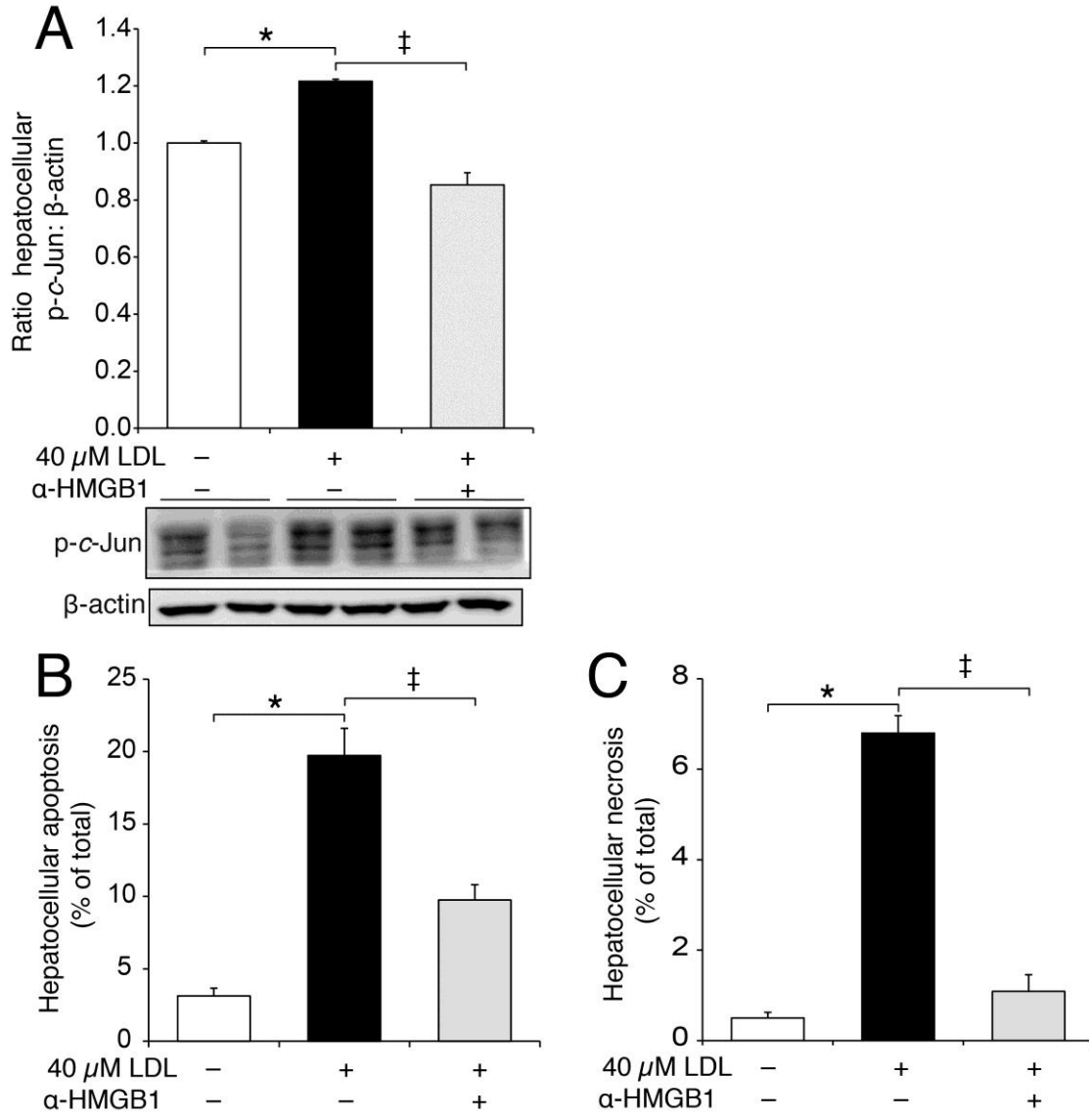

Figure 5.10 HMGB1 neutralising antibody abrogates JNK activation and cell death in primary hepatocytes.

(**A**) In FC-loaded (40 μM LDL) WT hepatocytes, addition of HMGB1 neutralising antibody (10 μg/mL) prevented JNK activation, as shown by cellular phospho-*c*-Jun levels, and abrogates (**B**) apoptosis and (**C**) necrosis. β-actin was used as loading control. **P*<0.05, *vs* 0 μM LDL. ‡*P*<0.05, *vs* FC-loaded (40 μM LDL) vehicle control. Data are mean ± SEM from 4–6 pooled animals/gp with *n*≥8 replicates/gp, experiment was performed in duplicate (*n*≥16).

5.4.6 Supernatant from FC-loaded hepatocytes activates primary Kupffer cells via HMGB1 interaction with TLR4.

HMGB1 has previously been shown to activate macrophages (Klune *et al.* 2008, Bianchi 2009, Hreggvidsdottir *et al.* 2012) and Liang Li *et al.* proposed a role for hepatocyte-derived HMGB1 in stimulation of KCs in NAFLD (Li *et al.* 2011). Having demonstrated HMGB1 release from and TLR4 activation of hepatocytes undergoing FC

lipotoxicity, and the subsequent autocrine amplification of hepatocellular TLR4 pathways (Figures 5.5, 5.8, 5.10), we then sought to establish whether the molecules (such as danger-associated-molecular patterns, DAMPs) released into supernatant could also activate resting KCs. To test this hypothesis, supernatant derived from FC-injured hepatocytes was added to resting primary KCs from WT mice. Such "enriched" of conditioned media induced KC activation, as determined by increased nuclear NF-κB p65 (Figure 5.11A top panel), alteration in KC morphology (observed using SEM, Figure 5.11B, right panel) and increased IL-1β secretion ($P<0.05$, Figure 5.11C).

To confirm that this activation was attributable to HMGB1 released from FC-injured hepatocytes, a separate experiment was conducted in which a commercial anti-HMGB1 neutralising antibody was added to hepatocyte supernatants prior to exposing the resting KCs to supernatant. Anti-HMGB1 antiserum ameliorated KC activation, as demonstrated by a significant reduction in IL-1β release (Figure 5.11D). As control for residual LDL in the hepatocyte culture media, addition of 40 μM LDL directly to KC culture media (with or without polymyxin, data not presented) failed to activate them, demonstrated by lack of IL-1β release (Figure 5.12A) and no nuclear translocation of NF-κB p65 (Figure 5.12B). These observations make it unlikely that the LDL preparations used in these studies contributed directly to KC activation.

To confirm that HMGB1 activated KCs via TLR4, separate KC activation experiments were performed, in which primary KCs from *Tlr4*$^{-/-}$ mice were exposed to enriched supernatants from 40 μM LDL-loaded WT hepatocytes. In striking contrast to WT KCs, *Tlr4*$^{-/-}$ KCs failed to respond to culture medium from lipotoxic hepatocytes. This non-responsiveness was indicated by absence of NF-κB p56 immunofluorescence (Figure 5.11A, bottom panel) and undetectable IL-1β release (Figure 5.11C). Likewise, KCs with deletion of the TLR4 downstream signalling intermediate, Myd88, also failed to release IL-1β after exposure to enriched culture supernatant from hepatocytes undergoing FC lipotoxicity (ND, Figure 5.11D). These data confirm the importance of the HMGB1/TLR4/Myd88 pathway in the activation of NF-κB p65 by products released from lipotoxic hepatocytes.

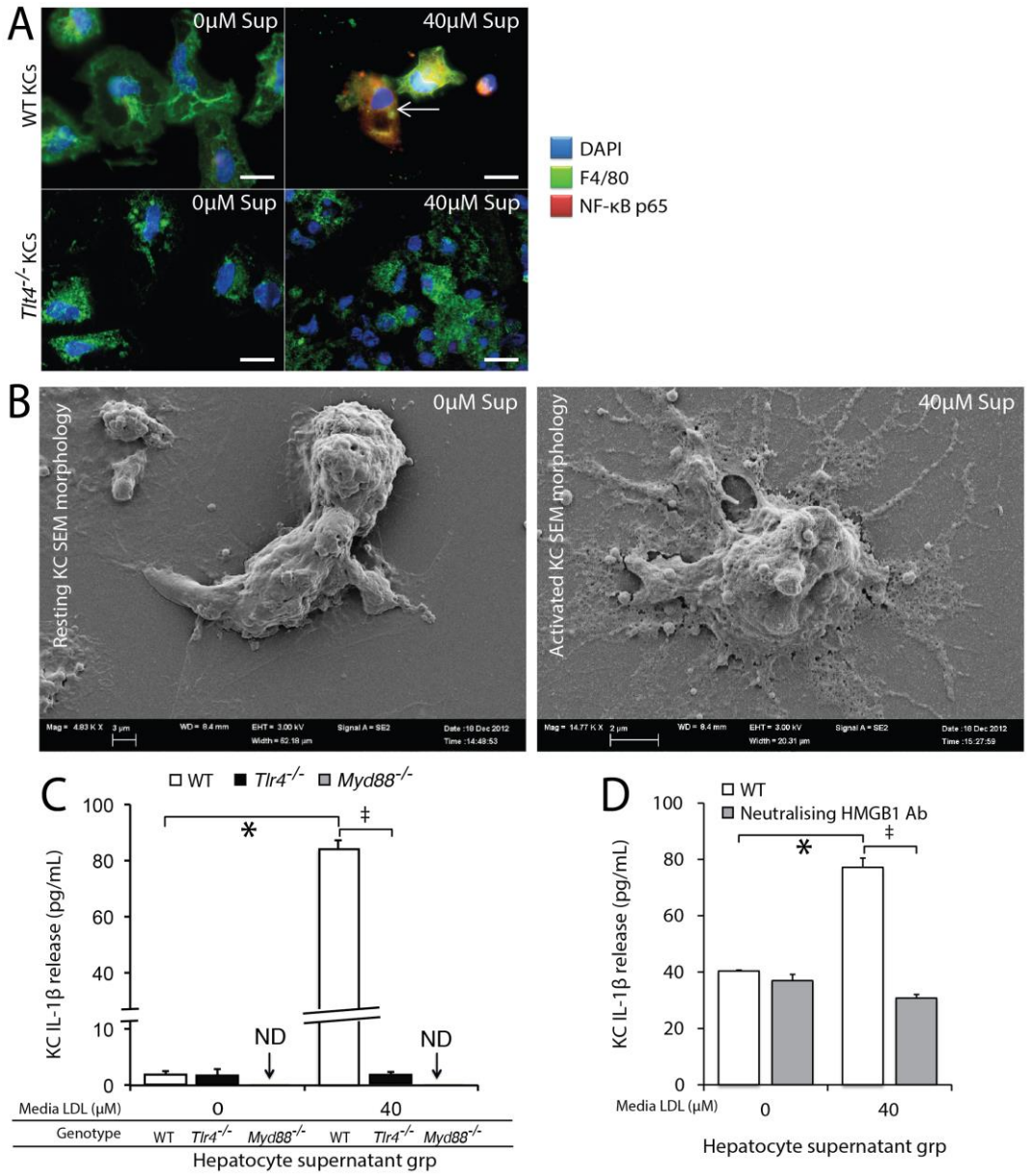

Figure 5.11 Effects of culture media supernatant from FC-loaded primary hepatocytes on WT, *Tlr4*$^{-/-}$ and *Myd88*$^{-/-}$ Kupffer cells.

(**A**) Lipotoxic hepatocyte culture media activates WT KCs (F4/80, green, top panel), but not *Tlr4*$^{-/-}$ KC (bottom panel), as shown by nuclear translocation of NF-κB (red). KC nuclei were stained with DAPI (blue). (**B**) SEM of resting KC (left panel) treated with culture media from control (0 μM LDL) hepatocytes and activated KC (right panel) treated with culture media from hepatocytes injured by FC (40 μM LDL). Methodology for SEM is described in Section 3.3.6. (**C**) WT KCs release IL-1β, whilst *Tlr4*$^{-/-}$ and *Myd88*$^{-/-}$ KCs do not when treated with the same media. ND = not detected. (**D**) Neutralising HMGB1 antibody (10 μg/mL) abrogates IL-1β release from KCs after exposure to lipotoxic hepatocyte media. **P*<0.05, *vs* control KC group treated with hepatocyte supernatant from control (0 μM LDL). $^{\#}$*P*<0.05, *vs* WT control receiving similar treatment. ‡*P*<0.05, *vs* vehicle control receiving similar treatment. Scale bars represent 20 μm unless otherwise indicated. Data are mean ± SEM from 4–6 pooled animals/gp with *n*=8 replicates/gp, experiment was performed in duplicate (*n*≥16).

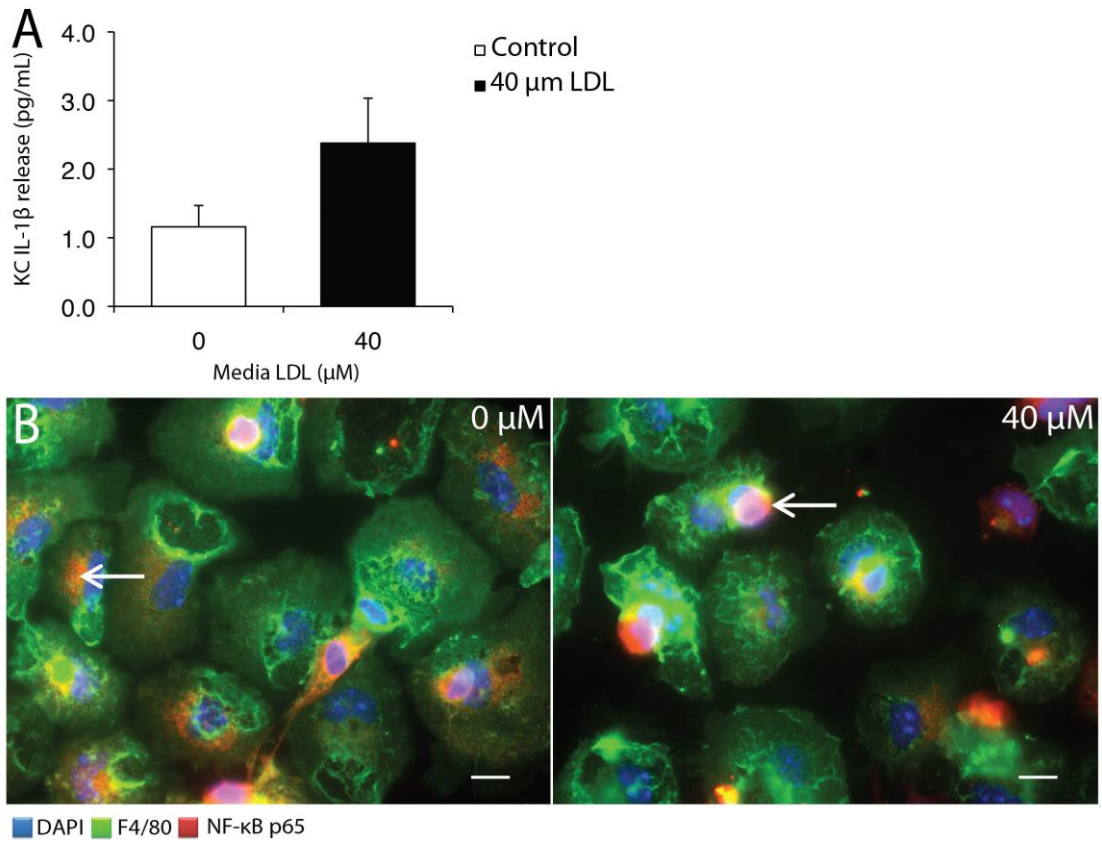

Figure 5.12 Kupffer Cells are not activated by direct incubation with 40 μM LDL.

Addition of 40 μM LDL to KCs culture media (16 h) fails to activate KCs (F4/80, green) as indicated by (**A**) failure to significantly increase IL-1β release (compared with Figure 5.10C) and (**B**) nuclear translocation of NF-κB (arrows indicate cytosolic NF-κB). Bars represent 20 μm. Data are mean ± SEM from 4–6 pooled animals/gp with *n*=8 replicates/gp, experiment was performed in duplicate ($n \geq 16$).

5.4.7 Purified EV fractions produce amplified inflammatory response in KCs.

EV fractions were isolated from supernatants of primary hepatocytes exposed to 0 μM or 40 μM LDL, using the method described in Section 2.7. These fractions were washed, quantified, standardised and assessed for HMGB1 content using western blotting. In EVs isolated from conditioned media from WT hepatocytes exposed to 40 μM LDL, HMGB1 content was significantly increased ($P<0.05$, Figure 5.13A). Added these HMGB1-rich EVs to primary murine KCs produced an "amplified" KC activation response. Impressively, KC IL-1ß release increased ~two-fold versus KCs stimulated with unmodified, undiluted supernatant from 40 μM LDL-exposed primary hepatocytes ($P<0.05$, Figure 5.13A). Similarly, NF-κB p65 fluorescent staining intensity was markedly increased compared with cells treated with unmodified supernatant (Figure 5. 13B compared with Figure 5.11A).

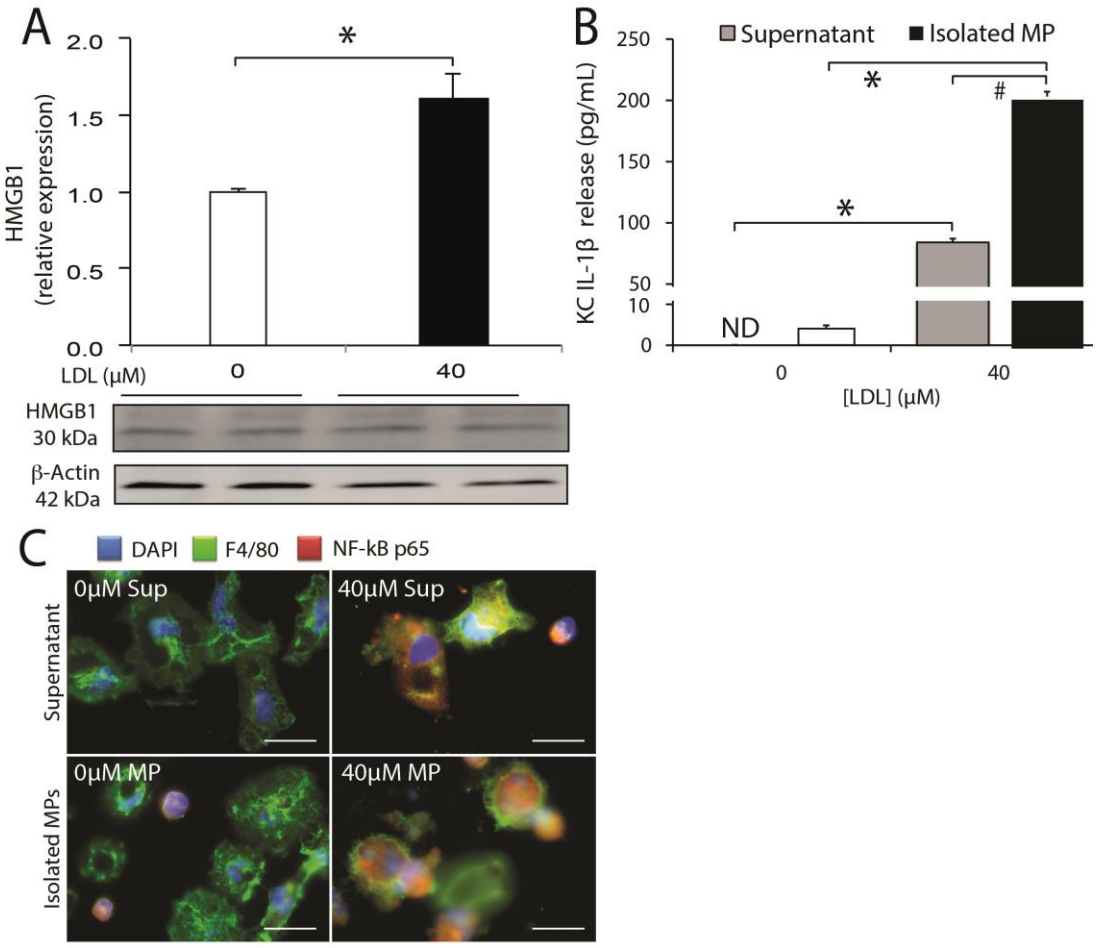

Figure 5.13 Extracellular vesicles isolated from FC-loaded hepatocytes contain HMGB1 and activate Kupffer cells.

(**A**) EVs isolated from enriched hepatocyte (40 μM LDL) supernatant contain significantly more HMGB1 *vs* those from 0 μM LDL supernatant. (**B**) Exposure of KCs to 40 μM LDL hepatocyte supernatants caused a significant release in interleukin (IL)-1β release (shown in Figure 5.10, repeated here for comparison). This release was further amplified by exposure to EVs isolated from this media. (**C**) KC NF-κB p65 expression (red fluorescence) was significantly increased by 40 μM LDL supernatant and EV exposure (green F4/80 fluorescent staining). Nuclear NF-κB p65 translocation was also observed in these KC groups (colocalisation of red NF-κB p65 staining with blue [DAPI] KC nuclei). **P*<0.05, *vs* control group hepatocyte (0 μM LDL) supernatant. $^{\#}P$<0.05, *vs* 40 μM LDL exposed, FC-loaded hepatocyte supernatant. Scale bars represent 20 μm. Data represent means ± SEM from *n*=4–6 pooled animals, with 4-6 replicates/grp, experiments were performed in duplicate (*n*≥16).

5.5 Discussion

Liver cell injury and hepatic inflammation are the pathognomonic characteristics of NASH (Brunt *et al.* 2011, Farrell *et al.* 2012). Following hepatocyte injury with resultant activation of proinflammatory pathways, recruitment of inflammatory cells occurs, and these may ultimately be responsible for hepatic stellate cell activation with

extracellular matrix deposition that causes liver fibrosis. Progressive liver fibrosis leads to replacement of normal liver parenchyma and consequential chronic liver disease that can advance to cirrhosis and liver failure. Accordingly, pathways of inflammatory cell recruitment and activation constitute a potential therapeutic target in treatment of NASH.

Previous research from the host laboratory has implicated cholesterol as a potential lipotoxic mediator of hepatocellular injury, liver inflammation and fibrosis in experimental NASH (Van Rooyen *et al.* 2011, Van Rooyen *et al.* 2013). To date, however, the relationship between hepatic cholesterol content to the key features of NASH (in addition to steatosis, hepatocellular injury, inflammation and fibrosis) have been largely associative. The exact pathways responsible for cholesterol-induced injury and its relationship to inflammation have not been fully elucidated.

In Chapters 3 and 4, we described an *in vitro* model to address the mechanism of FC lipotoxicity to hepatocytes. The findings appeared to recapitulate some of the *in vivo* findings observed in HF-fed *foz/foz* mice with NASH, such as FC accumulation within hepatocytes causing cellular injury, apoptosis and necrosis. This reductionist model provided the opportunity to examine several classical pathways involved cellular injury. Collectively, the data described in Chapters 3 and 4 led to the generation of the following working model:

Following LDL receptor-mediated uptake of cholesterol to load hepatocytes with FC, FC distributes to the plasma membrane, mitochondrial and ER. Shortly thereafter (<24 hrs in primary hepatocytes), FC-dependent JNK1/c-Jun activation initiates mitochondrial MPT formation with cytochrome c release and respiratory chain uncoupling. This leads to mitochondrial formation of ROS, decreased ATP generation, apoptosis and necrosis.
A schematic representation of this model is presented in Figure 5.14.

While this model fits much of what is known *in vivo*, until now the precise pathways responsible for FC-mediated inflammation have not been identified. Here (and in the next Chapter), we pursue the possible implications of innate immunity operating directly by release of DAMPs and indirectly (or more remotely) via proinflammatory

EVs generated from dying hepatocytes. In particular, the results of experiments in this Chapter have: (a) identified hepatocyte NF-κB activation with release of NF-κB responsive gene products, TNF-α and IL-6, (b) lipotoxic hepatocyte HMGB1 release (both soluble and in the form of EVs), and (c) HMGB1-mediated activation of TLR4.

In vivo dietary studies of *foz/foz* mice with NASH have demonstrated NF-κB p65 activation was evident in liver lysates, and particularly in the subfraction of non-parenchymal cells (Larter *et al.* 2009). The degree of such activation appeared proportional to hepatic cholesterol content (Van Rooyen *et al.* 2011), and NF-κB activation was reversed by pharmacological lowering of hepatic FC content, using atorvastatin and/or ezetimibe to block cholesterol synthesis and/or reuptake (Van Rooyen *et al.* 2013) (Figure 5.2). While these studies did not clearly demonstrate NF-κB p65 expression in hepatocytes, unpublished data from the host laboratory indicate that whilst NF-κB activation in non-parenchymal cells features prominently in NASH, NF-κB is also activated in hepatocytes. Similar data have been reported in the MCD steatohepatitis model (Dela Pena *et al.* 2005). Here, using the combination of a "re-interrogation" approach to liver sections stored from previous *in vivo* experiments and new *in vitro* experiments, NF-κB p65 activation within hepatocytes has been unequivocally demonstrated in NASH and following FC loading (Figure 5.3). Further, nuclear p65 expression *in vitro* was associated with IL-6 and TNF-α secretion cytokines by hepatocytes. Increases in these (and other) chemokines and cytokines have been previously reported in experimental and clinical NASH (Saad *et al.* 1995, Hui *et al.* 2004). An overarching theme of the present thesis is that NF-κB p65 may be activated as a consequence of the triggering of innate immunity.

IL-6 has chemokine (for polymorphs) as well as cytokine properties (Borish *et al.* 1989, Fielding *et al.* 2008). Unlike IL-6, TNF-α can augment injury and inflammation via activation of NF-κB and JNK. This is effected through a series of protein signals triggered by the TNF receptors (TNFR)-1 and TNFR2 (Schwabe *et al.* 2004). Following binding of TNF to TNFR-1/2, TNF receptor associated death domain (TRADD) adapter protein activates TNFR-associated factor 2 (TRAF2). In turn, these adaptor proteins regulate NF-κB p65 and JNK activation (Kieser *et al.* 1999, Tsao *et al.* 2000, Sethi *et al.* 2007, Chen *et al.* 2008). As previously described (Sections 1.6 and 5.1.1), DAMPs,

and most specifically HMGB1, can activate TLR4 to also give rise to NF-κB activation, which in turn transcriptionally up-regulates expression of proinflammatory IL-6 and TNF-α. Given the increased NF-κB p65 activation observed in hepatocytes treated with 40 μM LDL, we conducted further experiments to explore the HMGB1/TLR4 pathway.

The first key finding of these studies was that in WT C57Bl/6 hepatocytes damaged by FC loading, HMGB1 expression and localisation within cells change significantly. Specifically, HMGB1 translocated from the nucleus to the PM and was secreted into the supernatant (Figure 5.5). In an unexpected additional finding, FC-loading simultaneously up-regulated hepatocyte expression of TLR4. This process was shown to be reliant upon the presence of functional JNK1 because *Jnk1*$^{-/-}$ hepatocytes not only failed to secrete HMGB1, but TLR4 expression increased following FC-loading (Figure 5.5). Accordingly, these data indicate that HMGB1 and TLR4 are both involved in FC-mediated lipotoxic hepatocyte injury. This entirely novel finding for FC-mediated lipotoxicity may be pertinent to NASH pathogenesis, which is known to involve FC and to be dependent on TLR4 (Li 2011).

Since TLR4 activation has been extensively implicated in the pathogenesis of NASH (Ye *et al.* 2012, Petrasek *et al.* 2013, Roh and Seki 2013), we explored the role of HMGB1 for activating this receptor using *Tlr4*$^{-/-}$ C57Bl/6 mice. Interestingly, despite equivalent FC loading compared with WT C57Bl/6 hepatocytes, hepatocytes from *Tlr4*$^{-/-}$ mice, as with *Jnk1*$^{-/-}$hepatocytes, were protected against FC-mediated hepatocellular injury and HMGB1 release. Using a warm hepatic ischaemia model, Nace *et al.* (2013) identified oxidant stress as a factor leading to HMGB1 release and TLR4 activation. In the previous Chapter, FC-loading induced significant oxidant stress in hepatocytes, and it seems reasonable to propose that this may contribute to the increased HMGB1 release and TLR4 expression described here in FC-loaded hepatocytes. Further, the finding that FC lipotoxicity is associated with increased TLR4 expression has profound implications for NASH pathogenesis. In particular, these data are consistent wit the proposal that activation of TLR4 may constitute an early event in these cascades, and provide a pathway for the "auto-propagation" of liver injury that is a key feature of NASH pathology and disease outcomes.

It is also plausible that FC loading incites release of HMGB1, perhaps in response to decreased membrane fluidity, which can induce sheer stress and HMGB1 release (Park *et al.* 1998, DeVerse *et al.* 2012). Subsequent activation of TLR4 receptors on neighbouring (or the same) hepatocytes would result in downstream inflammatory (NF-κB p65, TNF-α, IL-6) and apoptotic (JNK-1/*c*-Jun) pathways, thereby inciting a feed-forward pathway responsible for amplified HMGB1 release and TLR4 activation. This is an attractive explanation for the significant step-wise translocation of cellular HMGB1 into the extracellular compartment/environment and simultaneous increase in TLR4 expression observed in FC-loaded hepatocytes (see Figures 5.6).

Within the liver, local HMGB1 release would have a different effect on hepatic inflammatory responses than would HMGB1 enclosed within (or on) EVs, which would most likely enter the circulation to propagate peripheral/systemic inflammatory responses. While this phenomenon has not been described in human studies, several animal models underscore the importance of HMGB1 in acute and chronic disease processes. Schierbeck *et al.* (2011) demonstrated monoclonal anti-HMGB1 antibody protection in two experimental arthritis models. Similarly, acute injury models, including ischaemic stroke (Liu *et al.* 2007) and lipopolysaccharide-induced sepsis (Yang *et al.* 2004) are abrogated through biological neutralisation of HMGB1 (anti-HMGB1 monoclonal antibody). The systemic effects of HMGB1 could also explain circulating inflammatory markers associated with increased cardiovascular risk in patients with NASH (Misra *et al.* 2009, Domanski *et al.* 2012). Both local and systemic roles have also been clarified for soluble and EV-bound CD36, a transmembrane glycoprotein that is a free fatty acid and cholesterol transporter that has been implicated in disordered lipid metabolism, diabetes, inflammation, insulin-resistance and stroke (Alkhatatbeh *et al.*).

Although beyond the scope of this study, HMGB1 has been shown to activate and induce hepatic stellate cell proliferation, thereby directly inducing hepatic fibrosis (Kao *et al.* 2008). Further Kao *et al.* (2008) demonstrated that circulating HMGB1 down-regulates membrane metalloproteinase (MMP)-2, but not MMP-9, further contributing to extracellular matrix deposition and thus fibrogenesis in NASH. Additionally, neutralisation of circulating HMGB1 ameliorates development of atherosclerosis in vascular disease-prone ApoE-deficient mice. Specifically, anti-HMGB1 antibody

treatment reduced CD11c and CD83, markers of total and mature dendritic cells, respectively (Kanellakis *et al.* 2011). Whether these functions of HMGB1 could be relevant to fibrogenesis in NASH is a tantalizing question that merits further investigation. To further pursue a potential dual HMGB1 role in inflammation with NASH, EVs isolated from FC-injured hepatocytes and from HF-fed *foz/foz* mice with NASH are characterised in the next Chapter.

In the present study, EVs were isolated from the supernatant of FC-loaded hepatocytes. These particles appear to be the vectors of at least one pro-inflammatory molecule, in terms of HMGB1 delivery to TLR4, thereby initiating NF-κB-dependent inflammatory signals (Figure 5.14). Additional proinflammatory proteins have also been identified within EVs isolated from FC-loaded hepatocytes and HF-fed *foz/foz* mice with NASH, including vascular cell adhesion molecule-1 (VCAM-1) and intercellular adhesion molecule-1 (ICAM-1) (data not shown) as has been reported for the host lab recently for ischemia reperfusion injury (Teoh *et al.* 2014). Circulating EVs can fuse with target cell plasma membranes after binding to target cell receptors (Camussi *et al.* 2010). Thus, Fabbri and colleagues (2012) have identified that small non-coding microRNAs (miRNAs) within cancer cell-derived EVs can induce pro-inflammatory responses in immune cells via TLR receptors. Whether such miRNAs could play a role in EV inflammatory responses in NASH is of interest (not addressed here) and constitutes an important future direction. Likewise, the methodology used here for isolation of EVs specifically gates for microvesicles (100 nm-1 μm). Whether smaller particles, such as exosomes (1-100 nm) which also circulate (though in lesser amounts) in experimental NAFLD, or lipid rafts play a pro-inflammatory role requires further study.

The possibility of HMGB1 antagonism as a therapeutic approach to NASH raises the issue of HMGB1's physiological role. In this respect, Huang *et al.* (2014) demonstrated some negative effects of hepatocyte-specific HMGB1 deletion. Specifically, HMGB1-deficient hepatocytes exposed to sub-lethal ischaemia reperfusion showed uncontrolled poly-(ADP-ribose) polymerase 1 expression, which resulted in profound ATP depletion. As well, mitochondrial instability, susceptibility to oxidant stress and net amplification of hepatocellular damage were observed. Accordingly, while the results described in this chapter implicate HMGB1 in FC-induced autocrine and paracrine inflammatory responses, the physiological and pathophysiological roles of HMGB1 appear to be

intrinsically intertwined. Notwithstanding this, targeted biological neutralisation of secreted HMGB1 (as shown in Figures 5.10 and 5.11) ameliorated hepatocellular apoptosis, necrosis and KC activation. This approach may therefore constitute a potential therapeutic approach for human NASH.

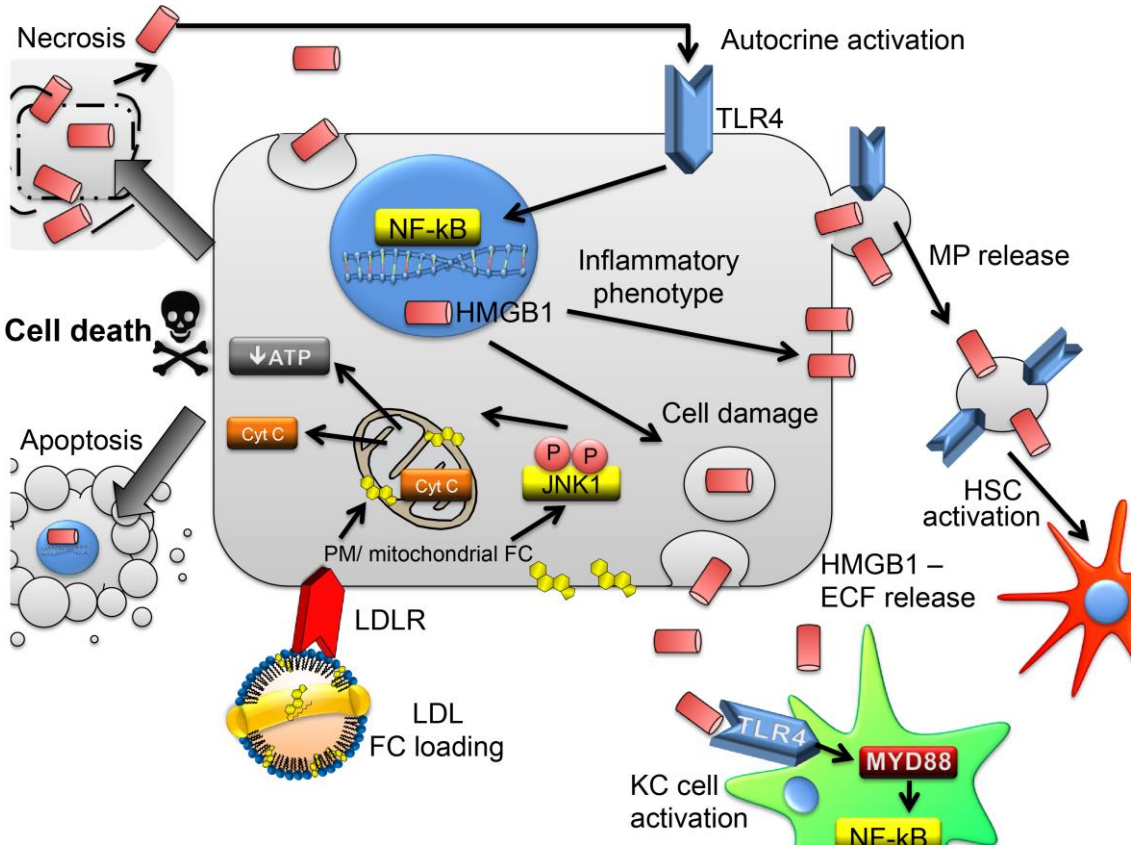

Figure 5.14 Hypothesised pathways of free cholesterol-mediated hepatocellular damage, extracellular vesicle release and inflammatory cell activation.

Cholesterol loading of hepatocytes leads to plasma membrane (PM) and mitochondrial FC accumulation. Resultant reductions in PM fluidity and mitochondrial permeability transition (MPT) pore generation leads to cytochrome c (CytC) translocation to the cytoplasm to activate apoptosome with consequent caspase 3 activation. Further, mitochondrial dysfunction leads to reduced ATP generation and a fall in cell energy levels. Extracellular vesicles (EV)s generated at this stage (facilitated by caspase 3 cleavage to submembranous cytoskeleton) are enriched with HMGB1, which is capable of activating KCs and hepatic stellate cells (HCSs) though a TLR4-dependent process, which occurs via MYD88 with resultant NF-κB p65 activation and downstream IL-1β expression and extracellular secretion.

Abbreviations: CytC, cytochrome C; FC, free cholesterol; HMGB1, high-mobility group protein 1; HSC, hepatic stellate cell; IL-1β, interleukin-1β; JNK, *c*-Jun N-terminal kinases; LDL, low-density lipoprotein; MYD88, myeloid differentiation primary response gene (88); PM, plasma membrane; TLR, toll-like receptor

There are two potentially important limitations for interpretation of the *in vitro* data presented in this Chapter:

1. Modeling the liver tissue microenvironment using two purified cell types (hepatocytes and KCs) over-simplifies the cellular interactions in the intact liver. However, the advantages of this modelled *in vitro* system is to characterise separate cellular participants (Rosso *et al.* 2014).

2. The human unmodified LDL preparation used to load murine hepatocytes with FC could be contaminated with LPS (this was suggested by a reviewer of an earlier version of the manuscript Gan *et al.* 2014). We considered this unlikely because all materials used pyrogen-free preparations. If this were the case, polymyxin B (which binds LPS) should prevent hepatocellular injury (Figure 5.8). LDL preparations do have a proclivity for LPS contamination, due in part to the lipid binding capacity of ApoB100 and the strong association between LPS-binding protein (LBP) and ApoB100 (Vreugdenhil *et al.* 2001). Therefore, the presence of LPS as a direct stimulant of TLR4 needed to be excluded in order to exclude LPS-mediated (rather than FC) TLR4 activation. To this end, polymyxin B was used to bind and inhibit any LPS residues. Polymyxin B is a complex antibiotic molecule derived from *Bacillus polymyxa,* which possesses a cyclic domain capable of binding and thereby neutralising LPS (Stansly and Schlosser 1947). Here, the failure of polymyxin to alter LDL-mediated hepatocellular injury (Figure 5.8) verifies that the hepatocellular responses to LDL exposure are in fact not attributable to LPS contamination of LDL preparations.

As with all new findings, the data reported in this Chapter raise several unanswered questions. First, the capacity of FC-loaded hepatocyte-derived EVs to activate hepatic stellate cells was not assessed. Further experiments are required to determine whether EVs can activate these cells directly or indirectly through KC activation and resultant cytokine and growth factor secretion. Given the significant HMGB1/TLR4 content within hepatocyte-derived EVs, it is plausible that EVs arising from cholesterol-enriched hepatocytes are capable of directly activating stellate cells, as described by others (Kao *et al.* 2008). This may contribute to hepatic fibrosis following hepatocyte cell death. Additionally, activated KCs may amplify such a response, in a paracrine fashion through inflammatory cytokine signalling. In the present study FC-loading led to increased IL-6 and TNF-α secretion for hepatocytes and/or KCs, the levels of which

may be sufficient to activate hepatic stellate cells, as described by Thirunavukkarasu and colleagues (2006).

5.6 Summary of findings

The research presenting in this Chapter focused on pathways responsible for KC activation following FC-mediated hepatocellular injury. The major findings are illustrated in Figure 5.14 and summarised below.

1. Loading primary hepatocytes with FC activates NF-κB p65 with release of IL-6 and TNF-α, as well as blebbing of plasma membrane and EV formation.
2. EVs isolated from FC-loaded hepatocytes are highly enriched with HMGB1 and TLR4.
3. Both HMGB1 and TLR4 are essential for mediating FC-induced hepatocellular cell death through JNK1/*c*-Jun activation.
4. EVs released from necrotic/apoptotic hepatocytes function as delivery vectors for HMGB1 and possibly TLR4/HMGB1 complexes.
5. Conditioned media from FC lipotoxicity to hepatocytes activates KCs by an HMGB1- and TLR4-dependent mechanism.

CHAPTER 6

Extracellular vesicles bearing HMGB1 and TLR4 arise from hepatocytes undergoing FC lipotoxicity, and circulate in both murine and human NASH

6.1 Introduction

In Chapter 3, plasma membrane vesicles were seen budding from FC-loaded hepatocytes undergoing liver injury (Figure 3.5). The idea that cells shed small membrane vesicles from their plasma membrane was first reported 40 years ago. At this time, the process was described as release of "cell/platelet dust" (Boulanger and Dignat-George 2011). More recently however, the concept of cellular dust formation has been replaced with the term *microvesicle* formation, which describes small (usually submicron) membrane vesicle shedding from damaged, activated or apoptotic cells (Boulanger and Dignat-George 2011). Microvesicles (MVs) (also known as ectosomes) are vesicular plasma membrane fragments formed by reverse budding and membrane fission. Depending on their size, particles can be classified as exosomes (40-100 nm), EVs (100-1000 nm; 0.1-1 μm) or final stage apoptotic body vesicles (1000-3000 nm; 1-3 μm) (Barteneva *et al.* 2013). Because the size gating used in the present study encompassed 0.1-1.45 μm, these particles are subsequently referred to as EVs.

The surface lipid composition of EVs depends on particle size, but is typically lyso-bis-phosphatidic acid together with a small amount of PS. EVs and apoptotic bodies, however, predominantly express PS (Thery *et al.* 2002). This unique feature of EVs allows them to be quantified using annexin V immunostaining; annexin V binds PS residues (Grisendi *et al.* 2015). In addition to their lipid membrane, exosomes, Evs (ectosomes) and apoptotic vesicles each contain a variety of macromolecules, including proteins, lipids, mRNAs, microRNA (miRNA) and other non-coding RNAs, and DNA (Barteneva *et al.* 2013). Due to their varying composition, EVs appear to have differential physiological and pathophysiological functions. These functions have been implicated in intercellular protein transfer, cell-cell signalling and adjacent cell communication, procoagulation, vascular dysfunction, blood brain barrier

communication, and epigenetic cellular reprogramming (Barteneva *et al.* 2013). The cell of origin of the particle and its contents largely determine these functions.

In NASH, HMGB1 has been identified as one of the EV proteins capable of activating TLR4 and inciting NF-κB p65 inflammatory responses (Nagata *et al.* 2007, Guo and Friedman 2010, Pisetsky *et al.* 2011, Yang and Seki 2012, Ye *et al.* 2012, Pisetsky 2014). In Chapter 5, EVs isolated from hepatocytes exposed to 40 μM LDL were shown to contain HMGB1 (Figure 5.13A) and, more importantly, these vesicles were capable of activating primary KCs via a TLR4-dependent pathway. In this Chapter, EVs isolated from the *in vitro* model described in Chapters 3 to 5 will be further characterised. In addition, EVs isolated from the circulation of atherogenic (ATH) diet-fed *foz/foz* mice with NASH will also be analysed. Finally, EVs were isolated from patients with NAFLD of varying severity. The composition of these EVs was studied, and results were compared between groups with apparently healthy controls.

6.2 Aims and hypotheses:

In this Chapter, EVs were isolated and characterised from:

1. Primary hepatocytes undergoing FC lipotoxicity, from the experiments described in Chapter 5.
2. ATH diet-fed *foz/foz* mice with NASH and wildtype (WT) mice with simple steatosis.
3. Human controls, patients with simple steatosis (SS), NASH without advanced fibrosis (F0-F2), and NAFLD with advanced fibrosis (F3-F4).

The over-riding hypothesis was that EVs arising from lipotoxic hepatocytes will contain HMGB1, and that similar EVs arising from hepatocytes (as well as other cell-types) circulate in NASH to a greater extent than in SS.

6.3 Methods

6.3.1 Experimental approaches

We used 3 experimental approaches to characterise EVs in both *in vitro* and *in vivo* model systems.

6.3.1.1 Primary hepatocyte cultures

For primary hepatocytes, cells were isolated, cultured, and exposed to unmodified human LDL (as outlined in Section 2.5 and Chapter 3). After 24 h, supernatant was collected and EVs isolated, as described in Section 2.7.1.1.

6.3.1.2 Mice and diets

The animal experimentation reported in this Chapter was approved by the ANU Animal Experimentation Ethics Committee (protocol F.MS2012.22). Briefly, female *foz/foz* and WT NOD.B10 mice were bred and housed (3-5/cage) at The Canberra Hospital Animal Facility, with environmental parameters standardised to 23^{o}C, 40% relative humidity and a constant 12 hour light/12 hour dark cycle. All cages, bedding, food and water were sterilised prior to use. Cages were individually ventilated (Tecniplast, Philadelphia, PA) with ~70 volume air changes per hour. At 6 weeks of age, *foz/foz* and WT mice were fed either chow (5% fat, 67% carbohydrate, 19% protein, 0% cholesterol) or atherogenic diet (23% fat, 45% carbohydrate, 20% protein, 0.2% cholesterol). Diets were purchased from Specialty Feeds (Glen Forrest, WA, Australia). Access to food and water was provided *ad-libitum*.

After 12 weeks of feeding (18 weeks of age), mice were fasted for 4 h (commencing at 7 AM), anaesthetised with 100 mg/kg ketamine hydrochloride and 20 mg/kg xylazine hydrochloride. Anthropometric data were collected before blood was drained through cardiac puncture into citrate tubes. EVs were subsequently isolated as described in Section 2.7.1.2. Samples of liver were fixed in 10% neutral-buffered formalin and processed for histopathological grading of NAFLD severity.

6.3.1.3 Human NAFLD and cirrhotic EV samples

In order to study sufficient NAFLD cases across varying severity, we combined patients who had been subjected to a diagnostic liver biopsy at three centres (Hong Kong, Perth and Canberra, Australia). These biopsies had been performed for a clinical indication, and had therefore been reported by local pathologists, each experienced in assessment of NAFLD biopsies and all using the same histological criteria (see below). In order to study a larger number of patients with cirrhosis (for whom liver biopsy is not usually needed), we included patients with 2 or more of the following clinicopathological and/or imaging criteria: clinical evidence of liver cirrhosis (hard liver edge, spider

naevi), portal hypertension manifesting as splenomegaly, ascites and presence of oesophageal varices on endoscopic examination or intraabdominal varices by imaging studies. Patients with liver biopsies had clinical data collected within a year of biopsy. Each gave informed consent to provide 20 mL of blood, which was collected in citrate-containing tubes for EV analyses. These studies were approved by the respective Institutional Review Boards (Hong Kong, Perth, and ACT Health Human Research Ethics Committee).

The combined clinical database was compiled of 211 patients, of whom 26 were excluded due to missing data, leaving 185 for analysis (119 from Hong Kong, 33 from Perth, and 33 from Canberra). Among the 185, 25 were controls and 160 NAFLD cases (156 confirmed on liver biopsies, 4 had clinical and imaging evidence of liver cirrhosis as described above). Apparently healthy volunteers (n=19) and patients undergoing bariatric surgery whose liver biopsy showed normal histology (n=6) were used as the 25 "normal controls" for this study. The healthy volunteers were selected based on normal BMI, liver-stiffness measurement (LSM) by transient elastography (TE) using FibroScan®. NAFLD was defined as having steatosis ≥5% on liver biopsy. The severity of NAFLD was stratified into 3 histological groups according to the NAFLD activity score (NAS) (Kleiner *et al.* 2005) and Brunt's fibrosis score (Brunt *et al.* 1999) as per Table 6.1. In a large dataset of prospectively obtained clinical data and results from liver biopsies blindly reviewed by a committee comprised of pathologists from 9 different centres in the United States involved in the NASH Clinical Research Network (CRN), the histological criteria for *definite steatohepatitis (SH)* was met in 75% of subjects with NAS ≥5 compared with only 25% of those with NAS≤4 (Brunt *et al.* 2011). Therefore, while not an ideal value, subjects with NAS=4 (regardless of fibrosis stage) were also excluded to prevent the overlap and ambiguity.

Table 6.1. Classification of NAFLD severity based on NAS and Brunt's fibrosis scores.

NAS	Brunt's fibrosis score	*n*	Categorisation
1-3	0	33	Simple steatosis
4	0, 1	26	Ambiguous, not studied
5-8	0-2	61	NASH
1-8	3-4	36	F4/F4

NB: The third Brunt's fibrosis score (Brunt *et al.* 1999) category (3-4) could includes any patient with NAFLD, not all of whom had NASH at the time of liver biopsy.

6.3.2 Histological analysis

Liver samples were fixed in 10% phosphate-buffered formalin (16 h, 4^{o}C) prior to ethanol-gradient dehydration and paraffin embedding. Liver sections (4 µm) were cut and stained with haematoxylin and eosin (H&E) (John Curtin School of Medical Research, ANU, Canberra), and blinded sections were scored by Associate Professor Matthew Yeh (MMY), an expert liver pathologist (Department of Pathology, University of Washington Medical Centre, Seattle, WA) (see Acknowledgments). Slides from liver biopsies of NAFLD patients in Canberra prepared by Department of Anatomical Pathology at The Canberra Hospital (TCH) were also sent to MMY for blinded scoring. The NAFLD activity scoring (NAS) system, originally described by Kleiner and colleagues (Kleiner *et al.* 2005) was used to determine NAFLD severity. This histological scoring system combines separate scores for hepatic steatosis (0-3), inflammation (0-3), and hepatocyte ballooning (0-2). In addition, a global assessment was made of "NASH", borderline NASH, simple steatosis or normal liver (Brunt *et al.* 1999, Kleiner *et al.* 2005).

6.3.3 Protein isolation and western blotting

EVs were isolated from hepatocyte supernatant samples and murine blood samples (collected in citrate tubes) as described in Sections 2.7.1.1 and 2.7.1.2, respectively. Following isolation, specific proteins were assessed qualitatively (molecular weight) and quantitatively (expression relative to controls) using western blotting, as per Section 2.13.

6.3.4 Flow cytometry

Flow cytometry is an extremely sensitive analytical technique, which utilizes a series of lasers to analyse multiple particle/cell parameters simultaneously (Olszewski 1981, Arraud *et al.* 2014). The specific fluorescent conjugated flow cytometry antibodies used to characterise mouse and human EVs in this Chapter are listed in Tables 6.2 and 6.3, respectively.

6.3.4.1 Reagents

Fluorescent-activated cell sorting (FACS) wash buffer (0.5% [v/v] fetal calf serum in PBS). FCS (500 µL) was diluted in 99.5 mL of ultrapure hospital grade d.H_2O. This buffer was prepared fresh and stored at 4^{o}C prior to use.

Annexin V binding buffer (140 mM NaCl, 4 mM KCl, 750 µM $MgCl_2$, 10 mM HEPES, pH 7.4). This solution was purchased commercially from BD Bioscience (Franklin Lakes, NJ) and prepared as per Manufacturer's instructions.

85 mM $CaCl_2$ in ultrapure hospital grade d.H_2O. Anhydrous $CaCl_2$ (0.943 g) was dissolved completely in ultrapure hospital grade d.H_2O (100 mL). Solution was filter-sterilised through a 0.22 µm filter (BD Bioscience, Franklin Lakes, NJ) and stored at room temperature.

6.3.4.2 Procedure

EVs were isolated from supernatant samples of cell culture experiments and murine or human blood, as described in Sections 2.7.1.1 and 2.7.1.2, respectively. Following the last ultracentrifugation (100,000 x g, 90 min, RT), pellets were kept in 2 mL thin-walled Ultra-Clear™ ultracentrifuge tubes (Beckman Coulter, Indianapolis, IN) and resolubilised in FACS buffer (100 µL). Primary antibodies (Table 2.3, 6.2 and 6.3) were added, at 1:200 dilutions for all antibodies. After incubation (60 min, RT, dark), unbound antibody was removed by adding FACS buffer (1 mL) to ultracentrifuge tubes. EVs were then centrifuged (100,000 x g, 90 min, RT), supernatants discarded and pellets resuspended in FACS buffer (100 µL). For annexin V staining, pellets were resolublised in annexin V binding buffer (100 µL) with annexin V-fluorophore (10 µL), and 85 mM $CaCl_2$ (1.2 µL) added approximately 20 mins prior to reading. All flow cytometry analyses were performed at the John Curtin School of Medical Research

(JCSMR) using a BD LSR Fortessa™ particle analyser (Franklin Lakes, NJ) equipped with five lasers (ultraviolet [UV; 350 nm], violet [405 nm], blue [488 nm], yellow [561 nm], and red [633 nm]). This flow cytometer is capable of detecting 18 fluorophores simultaneously. Post-capture data were analysed using BD FACS Diva™ Software (Franklin Lakes, NJ).

The candidate conducted the analyses presented in this Chapter with the assistance of Drs Brenda Chen and Sharon Pok in some experiments, and with the guidance and advice of Dr Harpreet Vohra (Flow cytometry specialist, John Curtin School of Medical Research, ANU) (see Acknowledgments).

Table 6.2 Antibodies used in flow cytometry for murine EV characterisation.

Abs	Conjugated	Wavelength (nm)		Company	Catalog #
		Excitation	Emission		
Annexin V	AX350	343	442	Life Technologies Corporation	A23202
CD4	BV605	407	602	Biolegend	100548
CD8a	V500	415	500	BD Biosceince	560778
CD36	AX647	633	670	Biolegend	102610
CD147	PE-CF594	496	612	BD Bioscience	562836
F4/80	PE/Cy5	480	670	Biolegend	123112
HMGB1	PE	565	578	Biolegend	651404
SLC10A1	FITC	495	519	Antibodies-Online	ABIN675915
TLR4	PE/Cy7	743	767	Biolegend	145408

Abbreviations: AX, Alexa; BV, brilliant violet; CD, cluster of differentiation; Cy, cyanine dye; F4/80, EGF-like module-containing mucin-like hormone receptor-like 1; FITC, fluorescein isothiocyanate; HMGB1, high-mobility group protein 1; PE, phycoerythrin; PE-CF594, tandem phycoerythrin cyanine and CF594 hydroxylamine fluorophores; PE/Cy, tandem phycoerythrin cyanine fluorophore; SLC10A1, Na^+-taurocholate cotransporting polypeptide; TLR, toll-like receptor; V, violet.

Suppliers listed in Table 6.2: Antibodies-Online (Aachen, Germany); Biolegend (San Diego, CA); BD Bioscience (Franklin Lakes, NJ); Life Technologies Corporation (Carlsbad, CA).

Table 6.3 Antibodies used in flow cytometry for human EV characterisation.

Abs	Target	Conjugate	Wavelength (nm)		Company	Catalog #
			Excitation	Emission		
Annexin V	EVs	AX350	343	442	Life Technologies Corporation	A23202
ASGPR1/2	Hepatocyte	FITC	495	519	ANOVUS Biologicals	NBP1-51109
CD4	T-cell	BV650	405	645	Biolegend	317435
CD8a	T-cell	PE/Cy7	743	767	Biolegend	344711
CD36	FFA receptor	APC/Cy7	650	785	Biolegend	336214
CD147	MMP	BV421	407	421	BD Bioscience	562583
CD14	Macrophage	PERCP/Cy5.5	482	695	Biolegend	550787
CD11b	Macrophage / neutrophil	BV605	407	602	Biolegend	101237
CD144	Sinusoidal endothelial cell	PE	565	578	Biolegend	348505
CD41	Resting platelet	FITC	495	519	Biolegend	303703
CD62P	Activated platelet	APC	594	633	Biolegend	304910
CD16	Neutrophil	BV711	405	711	BD Bioscience	563127
HMGB1	DAMP	PE	565	578	NOVUS Biological	NB-2322PE
SLC10A1	Hepatocyte	PE/Cy7	743	767	Antibodies Online	ABIN675921
TLR4	TLR receptor	BV 421	407	421	Biolegend	312811

Abbreviations: AX, Alexa; BV, brilliant violet; CD, cluster of differentiation; Cy, cyanine dye; DAMP, danger-associated molecular pattern; F4/80, EGF-like module-containing mucin-like hormone receptor-like 1; FITC, fluorescein isothiocyanate; HMGB1, high-mobility group protein 1; PE, phycoerythrin; PE-CF594, tandem phycoerythrin cyanine and CF594 hydroxylamine fluorophores; PE/Cy, tandem phycoerythrin cyanine fluorophore; SLC10A1, Na^+-taurocholate cotransporting polypeptide; TLR, toll-like receptor; V, violet.

Suppliers listed in Table 6.3: Antibodies-Online (Aachen, Germany); Biolegend (San Diego, CA); BD Bioscience (Franklin Lakes, NJ).

6.3.5 Statistical analyses

Statistical analyses were carried out as described in Section 2.16. All data presenting in this Chapter represent mean ± SEM. Statistical significance is defined as $P<0.05$.

6.4 Results

6.4.1 Primary hepatocytes undergoing FC lipotoxicity release extracellular vesicles that contain TLR-4, HMGB1 and asialoglycoproteins-1/2.

Here, several experiments were conducted with the aim of further characterising the EVs isolated from the FC-lipotoxic hepatocytes described in the previous Chapters (3, 4 and 5). First, supernatant fractions from hepatocytes exposed to 0-40 µM LDL were analysed for EV content, using a commercially available kit to quantify annexin V. The aim of this experiment was to determine whether EV release is proportional to the extent of FC-related hepatocyte injury. As previously mentioned (Section 6.1), PS detected by annexin V binding is a surrogate marker for EVs (Schneider *et al.* 2012). Not surprisingly, FC-loading of primary hepatocytes resulted in a significant dose-responsive release of EVs into culture media ($P<0.05$, Figure 6.1A). Interestingly, this pattern of EV release correlated with hepatocellular FC content (Figure 3.2D) and necrosis (Figure 3.4D), as well as with JNK1 activation demonstrated in Chapter 4 (Figure 4.6C). Due to paucity of material and the necessity to pool multiple EV samples, subsequent characterisations focused on the 0 and 40 µM LDL experiments.

In Chapter 5, it was shown that EVs shed from 40 µM LDL-exposed hepatocytes contained significantly higher amounts of HMGB1 than did those from control hepatocytes (0 µM LDL) ($P<0.05$, Figure 5.13A). Here, both TLR4 and ASGPR-1/2 were also identified in EVs from FC-loaded hepatocytes ($P<0.05$, Figure 6.1B, C). These analyses were by WB as it was not possible to conduct flow cytometric analysis on EVs derived from hepatocytes *in vitro* due to persistent background particulate interference.

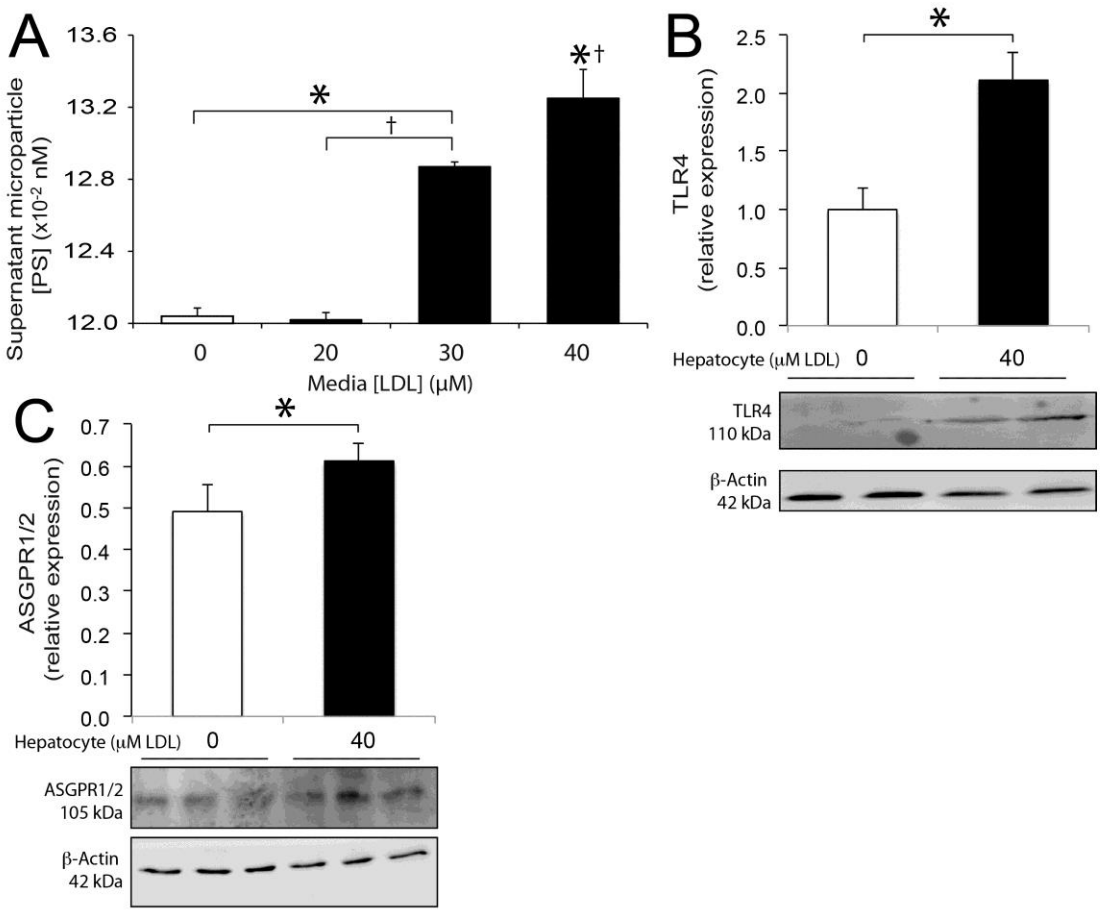

Figure 6.1 FC lipotoxicity to primary hepatocytes releases annexin V-positive extracellular vesicles, which contain TLR4 and asialoglycoprotein receptors 1/2.

(A) FC loading of hepatocytes by exposure to 20-40 μM LDL induces dose-responsive release of EVs at 30 or 40 μM LDL. EVs isolated from hepatocytes incubated with 40 μM LDL contain more (B) TLR4 and (C) ASGPR1/2 protein, as assessed by western blotting (Section 2.13) than vesicles harvested from control hepatocytes (0 μM LDL). **P*<0.05, *vs* 0 μM LDL. †*P*<0.05, *vs* 20 μM LDL. Data are mean ± SEM from 4–6 pooled animals/gp with *n*≥8 replicates/gp for data in Panel A, and *n*=3 replicates/gp for data in Panel B. Experiments were performed in duplicate (*n*≥6).

6.4.2 Serum EVs increase in HF-fed *foz/foz* mice with NASH

Having shown that FC-loaded hepatocytes release EVs, the next question was whether similar vesicles circulate in NASH, thereby reflecting the process of lipotoxicity *in vivo*. To test this, we examined EV fractions from blood of *foz/foz* mice with NASH and compared the results with atherogenic diet-fed WT and chow-fed *foz/foz* mice, which develop simple steatosis, as well as with lean controls (chow-fed WT). Female *foz/foz* and WT mice were fed chow or atherogenic diet for 12 weeks, with the sole intention of harvesting sufficient EV populations from blood in relation to liver histology.

In accord with previously published anthropomorphic and histological data (Larter *et al.* 2009), *foz/foz* mice were heavier than their WT counterparts at 12 wks, irrespective of dietary intake ($P<0.05$, Figure 6.2A). Atherogenic dietary feeding however, resulted in substantial hepatomegaly in *foz/foz* mice, with an average of 6% body weight attributed to liver mass ($P<0.05$, Figure 6.2B) versus ~2% for WT groups. At this time, significant intralobular ballooning and inflammation as well as severe steatosis were conspicuous in livers from atherogenic-fed *foz/foz* mice (Figure 6.2C), whereas livers from chow-fed *foz/foz* and atherogenic diet-fed WT mice exhibited SS without inflammatory foci (Figure 6.2C). Blinded histological scoring performed by MMY, (see Acknowledgements) confirmed marked increases in hepatic steatosis, ballooning, and lobular inflammation ($P<0.05$, Figures 6.2D-F) in atherogenic diet-fed *foz/foz* mice compared with dietary and genotype controls. Summation of these separate histological indices provides an overall NAFLD activity score (NAS), which is roughly proportional to the degree of liver injury. The NAS score was significantly higher in HF-fed *foz/foz* mice than dietary and genotype controls ($P<0.05$, Figure 6.2G), thereby confirming the development of NASH in this experimental group.

Having confirmed the development of NASH in this cohort of atherogenic diet-fed *foz/foz* mice, EVs were isolated and analysed by flow cytometry (as detailed in Sections 2.7.1 and 6.3.4) in order to characterise their protein tags, reflecting the cell types of origin (Headland *et al.* 2014).

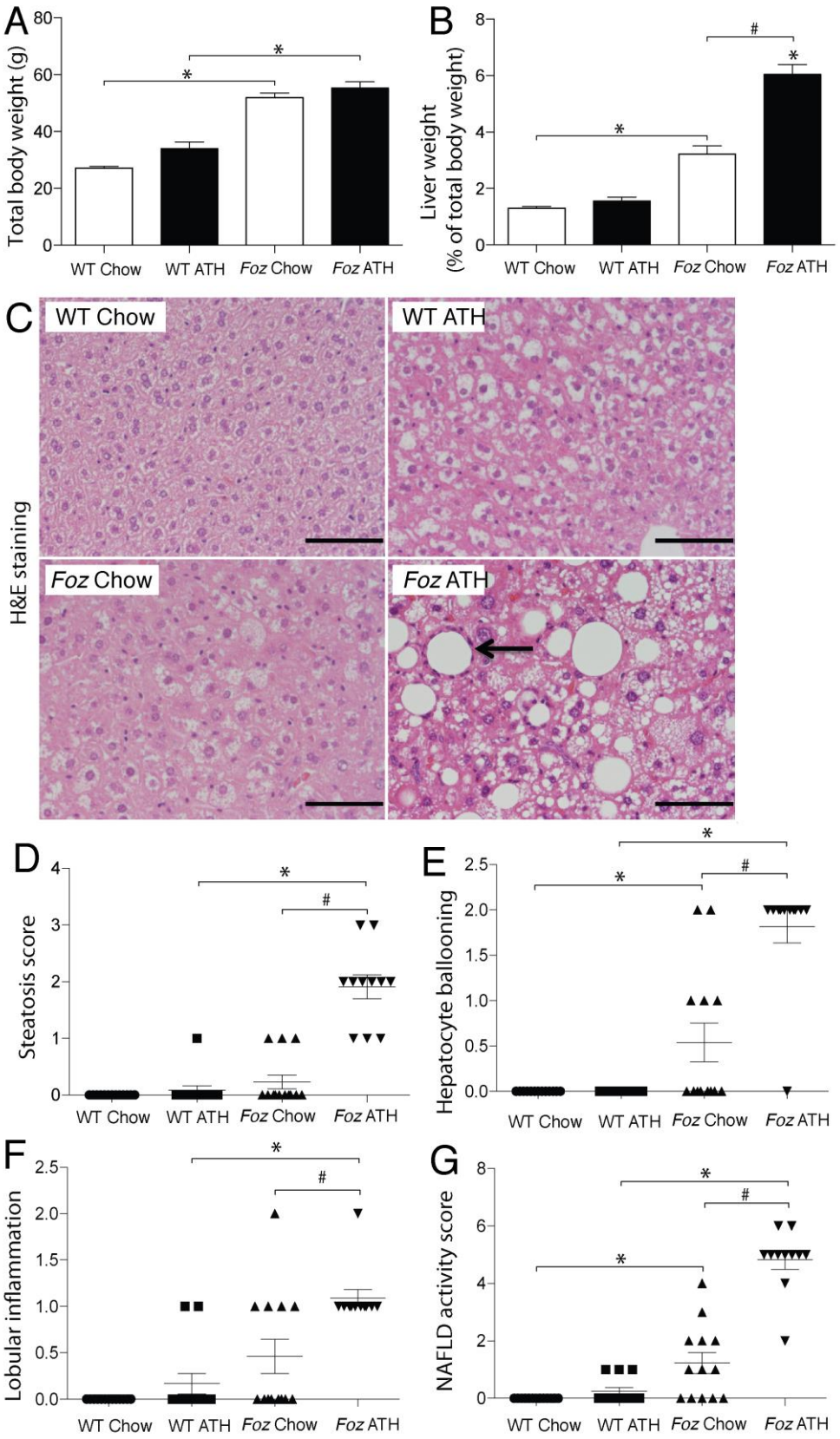

Figure 6.2 Liver phenotype in *foz/foz* and WT mice, according to dietary intake after 12 weeks of feeding.

Legend for Figure 6.2. *Foz/foz* (▲ chow; ▼ ATH) and WT (● chow; □ ATH) mice (*n*=6-8/grp) were fed either chow or atherogenic diet for 12 wks. (**A**) Atherogenic diet-fed *foz/foz* mice weighed significantly more, and (**B**) their relative liver weight was increased compared with dietary and genotype-matched mice with steatosis and lean controls. (**C**) Histology showed macrosteatosis and lobular inflammatory foci and ballooning in atherogenic diet-fed *foz/foz* mice, with (**D**) steatosis, (**E**) ballooning (arrows indicate hepatocyte ballooning), (**F**) lobular inflammation. (**G**) The overall NAS was significantly higher in atherogenic diet-fed *foz/foz* mice. Data are mean ± SEM. **P*<0.05, vs. diet-matched WT control. $^{\#}P$<0.05, vs. genotype-matched, chow group.

6.4.3 In atherogenic diet-fed *foz/foz* mice with NASH, PS-positive EVs can be isolated from the circulation. These contain HMGB1, TLR4 and hepatocyte markers.

We saw that serum from artherogenic-fed *foz/foz* mice with NASH contained higher serum PS-positive EVs (by ELISA) compared with that of control (chow-fed WT) and SS (ATH-fed WT and chow-fed *foz/foz*) groups; [PS] averaged 14 nM in NASH vs control or SS group at 6-10 nM (P<0.05, data not presented).

Here, we employed flow cytometry (Section 6.3.4) to characterise the circulating EVs after standardising particle density between groups to approximately 35 particles per reaction (Figure 6.3A). In light of the implication of HMGB1 and TLR4 in the mechanism of FC-mediated lipotoxicity to primary murine hepatocytes (see Chapters 4 and 5 and Figure 6.1), we first evaluated HMGB1 and TLR4 fluorescent staining on EVs. This demonstrated increases in both HMGB1 and TLR4 proteins on EVs isolated from atherogenic diet-fed *foz/foz* mice with NASH compared with SS and lean control mice (P<0.05, Figure 6.3B,C).

We then examined whether EVs that circulate in *foz/foz* mice with NASH contained another hepatocyte marker, SCL10A1, a solute transporter confined to hepatocytes. Interestingly, EVs isolated from *foz/foz* mice with NASH exhibited similar or lower SCL10A1 staining than those from dietary and genotype controls (Figure 6.3E). CD36 is another surface protein expressed on hepatocytes as well as other cell types. It is a scavenger receptor responsible for transporting FFAs, FC, oxidised LDL, and fibrillar and soluble amyloid-β. Here, EVs isolated from atherogenic diet-fed foz/foz mice with

NASH appeared to contain higher amounts of CD36-positive EVs ($P<0.05$, Figure 6.3D).

CD147, a regulator of membrane metalloproteinase activity, is involved in the activation of hepatic stellate cells, and thereby plays a role in liver fibrosis (Calabro *et al.* 2014). CD147 EVs was higher in *foz/foz* mice with NASH than with SS or with lean control mice, but this expression in circulatory EVs failed to reach statistical significance (NS, Figure 6.3F).

6.4.4 Circulating EVs in *foz/foz* mice with NASH contain T cell markers.

In human NAFLD, circulating EVs contain markers of CD4-positive (helper T-cells, which include Th1, Th2, Th17 and T-reg subsets) and CD8-positive (cytotoxic T-cells) lymphocytes (Kornek *et al.* 2012). To establish whether similar changes occur in our murine model, EVs isolated from circulation of chow- and atherogenic-fed WT and *foz/foz* mice were scrutinised for CD4 and CD8 expression. Chow-fed *foz/foz* mice showed increased CD4-positive expression compared to chow-fed WT. Otherwise, there were no significant differences in CD4- and CD8-positive EV expression were evident between groups (Figure 6.3G, H).

Overall, these findings are consistent with the proposal that at least a proportion of the EVs isolated from the circulation of mice with NASH are released from hepatocytes, and contain both HMGB1 and TLR4.

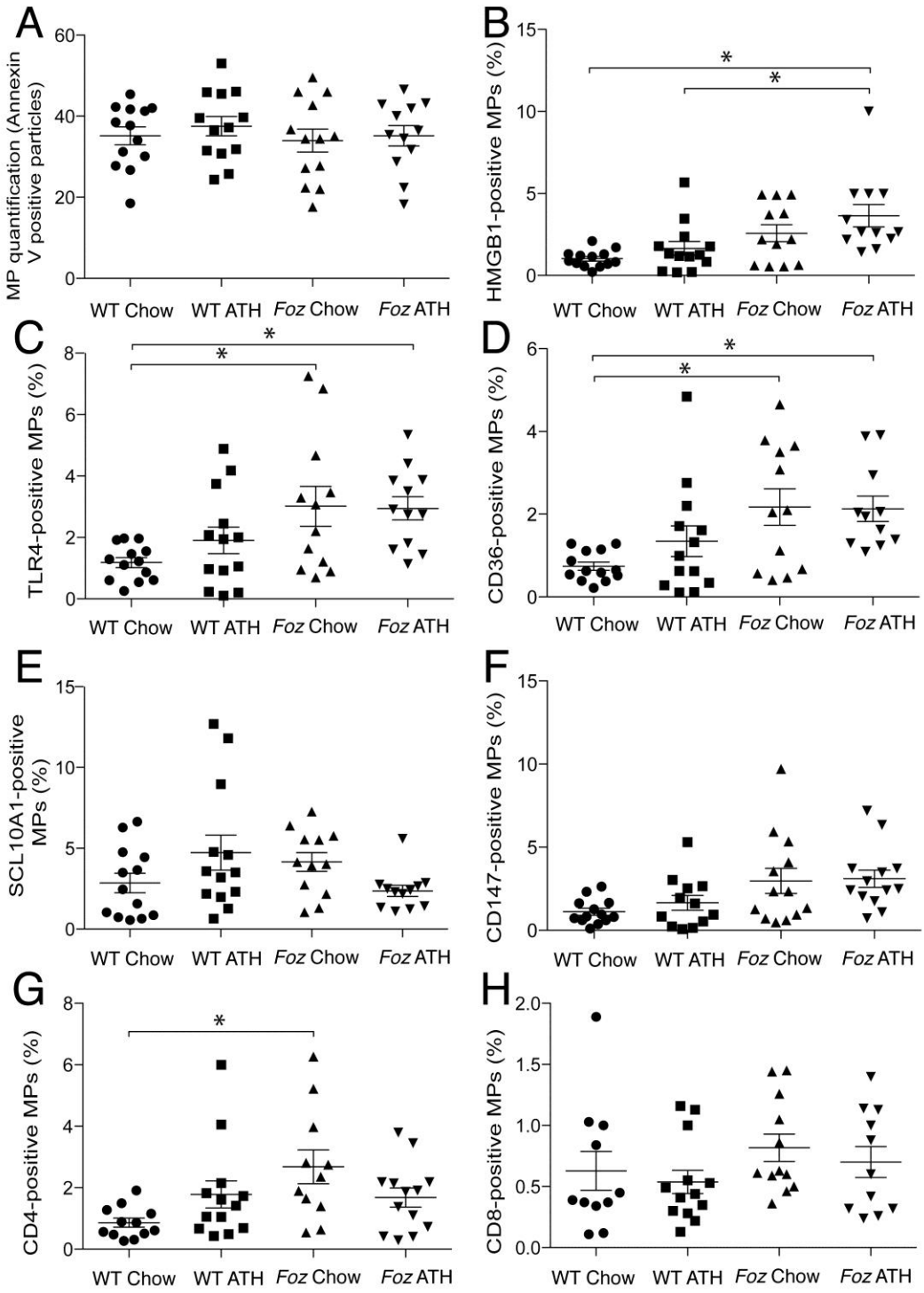

Figure 6.3 Characterisation of EVs isolated from mice with NASH (*Foz* HF).

EVs were isolated from plasma of *foz/foz* (▲ chow; ▼ ATH) and WT (● chow; □ ATH) mice as described in Section 2.6.1, labelled using antibodies against specific protein tags and annexin V conjugation of PS (as per Table 6.2). (**A**) Equivalent numbers of annexin-V-positive EVs were analysed in each group by flow cytometry and then probed for (**B**) HMGB1, (**C**) TLR4, (**D**) CD36, (**E**) SCL10A1, and (**F**) CD147, (**G**) CD4, and (**H**) CD8 proteins. Data are mean ± SEM. **P*<0.05, vs. diet-matched WT control. $^{\#}P$<0.05, vs. genotype-matched, chow group.

6.4.5 Characterisation of circulating EVs harvested from patients with NAFLD

To establish whether the findings in *foz/foz* mice are relevant to the human NASH, we analysed annexin V-positive EVs isolated from venous blood and assessed whether they bore markers of hepatocyte, inflammatory and lymphocyte markers, as described earlier (Section 6.3.4.2). We assessed circulating annexin V-positive EVs from patients with NAFLD phenotypes of increasing disease severity, as well as controls with normal livers. The focus was on hepatocyte-specific markers and cell signalling molecules involved in innate immunity. In order to compare the composition of EVs between groups by flow cytometry, an equivalent number of annexin V-positive particles was studied for each patient populations (Figure 6.4A).

Consistent with the findings from murine models, higher EV expression of both HMGB1 and TLR4 was observed in NASH and F3/F4 patients compared with SS or healthy controls ($P<0.05$, Figure 6.4B,C). Among patients with NASH with or without advanced fibrosis (F3/F4), EVs were more likely to bear ASGPR1/2 than those with SS ($P<0.05$, Figure 6.4E).

The relative proportion of CD36 and CD147-bearing EVs was also significantly higher in NASH than simple steatosis, with a further increase in F3/F4 cases ($P<0.05$, Figure 6.4D,F). While these findings in a large cohort of human NAFLD and control cases supports the operation of CD36, CD147 and molecules of innate immunity (HMGB1 and TLR4) in NASH, the data do not allow their cell-type of origin of these molecules to be identified.

The lymphocytic markers CD4 and CD8 were also then assessed. There were stepwise increases in proportion of both these markers, being highest in F3/F4, then NASH without severe fibrosis, and simple steatosis versus control. There were also significant differences between NASH and simple steatosis ($P<0.05$, Figure 6.4G,H).

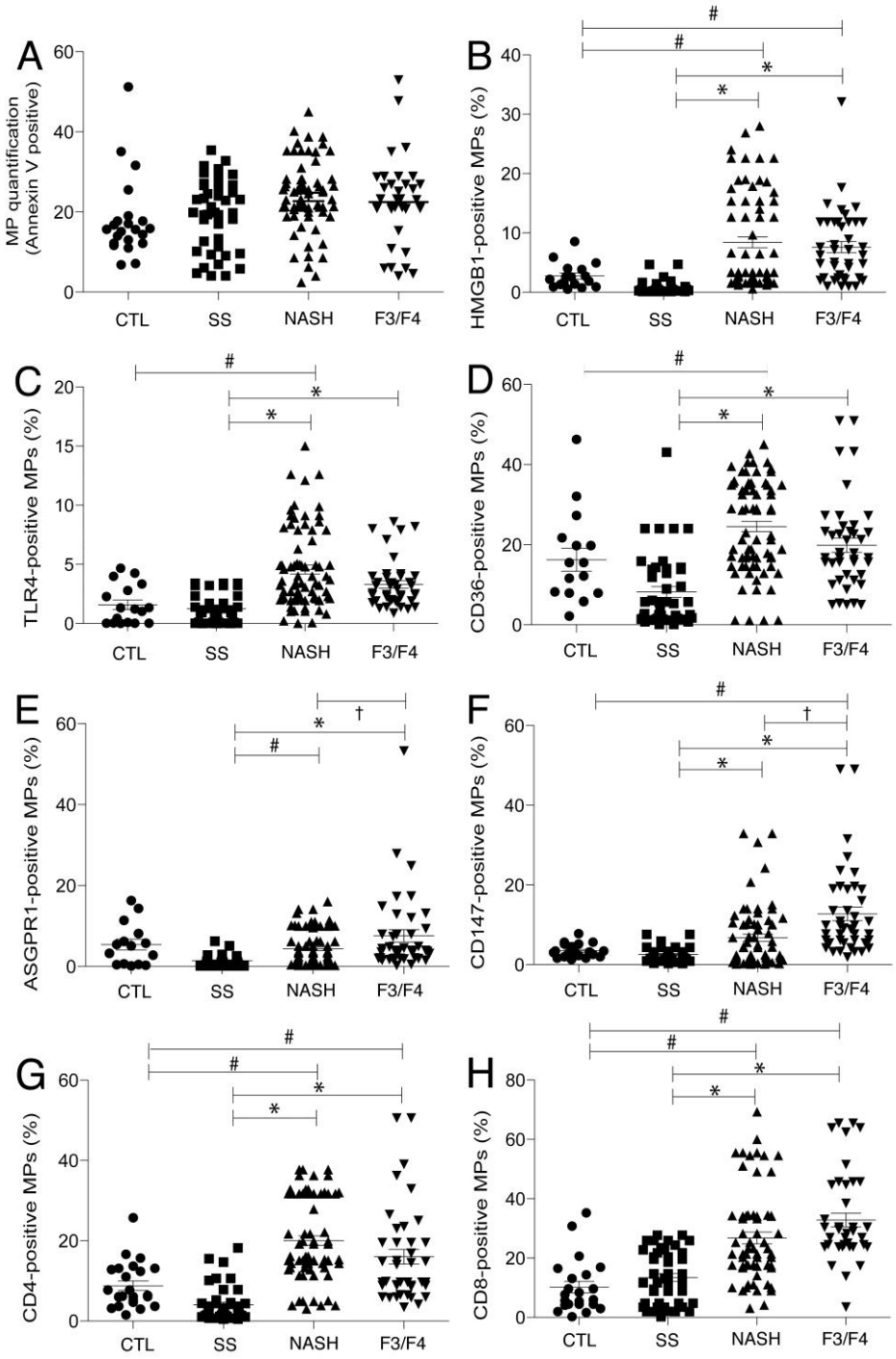

Figure 6.4 Characterisation of circulating EVs isolated from patients with NAFLD of increasing severity versus controls with normal liver histology (controls).

EVs were isolated from plasma of patients with NASH, F3/F4 cirrhosis, SS and healthy controls, as described in Section 6.3.1.3. They were labelled (Section 6.3.4) prior to quantification using annexin V conjugation. (**A**) Plasma EVs were quantified and probed for (**B**) HMGB1, (**C**) TLR4, (**D**) CD36, (**E**) ASGPR1, and (**F**) CD147, (**G**) CD4, and (**H**) CD8. EV parametric data were captured using a BD LSRFortessa™ particle analyser (Franklin Lakes, NJ) and post-capture analysis performed with BD FACS Diva™ Software (Franklin Lakes, NJ). Data are mean ± SEM. **P*<0.05, *vs.* patients with SS. $^{\#}P$<0.05, *vs.* normal liver controls. $^{\dagger}P$<0.05, *vs.* patients with NASH.

6.5 Discussion

Increasing experimental and clinical evidence supports the operation of innate immunity in NASH, thereby accounting for sterile inflammation as a central feature of this disorder. However, the links between lipotoxic liver injury and innate immunity require clarification. In the previous Chapters, it was shown that exposure of primary murine hepatocytes to LDL causes FC loading of hepatocytes with FC deposition occurs in the mitochondria and the plasma membrane (Figure 3.3B, D). The later decreases plasma membrane fluidity, while FC activates JNK1-dependent mitochondrial injury, with cytochrome *c* release, apoptosome formation and caspase 3 activation (Chapter 4). Active caspase 3 cleaves the cell cytoskeleton to cause budding at the surface of cells (Figure 3.5) while the stiff PM predisposes to rupture (exocytosis) of these buds as membrane-bound EVs. EVs also circulate in obesity, diabetes, atherosclerosis, each of which is strongly associated with NASH. They have also been reported in NAFLD and cirrhosis. However the particular emphasis of earlier studies have been on lymphocyte, macrophage and platelet-derived EVs in cirrhosis from viral hepatitis and alcoholic liver diseases, as well as NAFLD (Fusegawa *et al.* 2002, Ogasawara *et al.* 2005, Sayed *et al.* 2010).

HMGB1 and TLR4

In order to account for species difference, studies included both experimental (murine) and human samples. The first important finding of the present research is a greater release of hepatocyte-derived EVs in NASH and NAFLD with advanced fibrosis both in murine and human samples, compared to those with SS or lean controls. Further, the markers borne by these circulating EVs in NASH also reflect involvement of cell-cell signalling molecules known to be operative in innate immunity, namely HMGB1 and TLR4. The significance of both these molecules, in particular their function in recruitment of inflammatory cells like KCs, has been extensively explored in Chapter 5. It should be noted, however, that while the *in vitro* studies described here demonstrate that hepatocytes can be the source of HMGB1-bearing EVs, the cellular origins of plasma EVs population containing HMGB1 cannot be fully characterised using current techniques. In future work, this could be addressed by using fluorescent particulate sorting or co-labelling annexin V-positive EVs with HMGB1 and surface cell marker of interest (e.g. hepatocytes, KCs, infiltrating monocytes and macrophages, endothelial cells, lymphocytes, stellate cells).

If lipotoxicity is a central mechanism for NASH pathogenesis, there should be clear links between this type of hepatocellular injury and inflammatory recruitment. The present observations provide strong support for such links. Earlier, we established that there is stepwise increase expression of HMGB1 protein in the livers of both WT and *foz/foz* mice fed atherogenic diet containing 2% cholesterol (Figure 5.4). In addition to the presence of HMGB1 (discussed earlier), EVs that circulate in both murine and human NASH also bear TLR4 (Figures 6.3D and 6.4D) but no increase in TLR2 signals (data not presented). These data are consistent with a recent study in human NASH by Cengiz *et al*. (2015): serum samples from consecutive biopsy proven NASH (*n*=57) and healthy controls (*n*=57) were assayed for soluble TLR2 and TLR4 using ELISA – only serum TLR4 correlated both with NASH and liver fibrosis evaluated using Brunt's Criteria (Cengiz, Ozenirler et al. 2015). Among the TLRs, the evidence for involvement in NAFLD is strongest for TLR4 (Li *et al.* 2011, Miura *et al.* 2013, Roh and Seki 2013, Miura and Ohnishi 2014, Cengiz *et al.* 2015, Li *et al.* 2015). There is some evidence for TLR9, but this is an endosomal rather than cell surface receptor so it will not be present on EVs (Roh and Seki 2013, Csak *et al.* 2014, Miura and Ohnishi 2014). On the other hand, involvement of TLR2 has been implicated in some but not all experimental systems for NAFLD (Li *et al.* 2011, Miura *et al.* 2013, Roh and Seki 2013, Miura and Ohnishi 2014, Cengiz *et al.* 2015, Li *et al.* 2015).

Hepatic TLR4 expression increases in NASH and its deletion prevents development of steatohepatitis in response to the methionine choline deficient or a high-fat 2% cholesterol diet (Li 2012). In the latter model, activation of TLR4 was dependent on ligand HMGB1. We showed similar findings in primary hepatocytes undergoing FC lipotoxicity (Chapter 5, Sections 5.4.4 and 5.4.6) (Gan *et al.* 2014). Thus HMGB1 is released from cells undergoing oxidative stress and necrosis, and we demonstrated that it is released from primary hepatocytes in response to FC lipotoxicity (Chapter 5, Section 5.4.3). Further, such released HMGB1 was shown to interact with neighbouring hepatocytes to accentuate injury in an autocrine or paracrine "feed-forward" process mediated via TLR4 (Figures 5.6-8). The present finding that HMGB1 also circulates in EVs in NASH reiterates further the concept of how this archetypical DAMP, released during hepatocyte lipotoxicity, can interact with other hepatocytes to perpetuate injury. Whether TLR4 is expressed on EVs because it represents a site of plasma membrane budding, or whether there is increased synthesis of TLR4 in NASH requires further

study. Dr Derrick Van Rooyen (ANU thesis 2012) (see Acknowledgements) from the host laboratory found no increase in TLR4 mRNA in the livers of *foz/foz* mice with NASH, a finding that supports the first explanation. The clear implications of HMGB1 and TLR4 in experimental NASH also provides potential targets for the design of therapeutic agents to treat NASH.

As endorsement of their likely relevance, our findings that HMGB1 and TLR4 expression in EVs is increased in *foz/foz* mice with NASH, were recapitulated and extended by studies in patients with NAFLD. In fact, human data showed a more striking relationship to disease severity than did in the results of mouse models. The most likely reason for this "attenuated" difference in mice is that the models used (exposing *foz/foz* and WT mice to an atherogenic dietary regimens for 12 weeks) reflects the milder end of the NASH spectrum. The host lab has previously characterised the time course for development of NASH in this model – at 12 weeks of dietary feeding, the distinction between "established", "borderline" and "not-NASH" (or SS) was less clear cut and animals had not yet developed fibrosis; this is typically established by 24 weeks of atherogenic dietary feeding in *foz/foz* mice and 9-12 months in WT (Larter *et al.* 2009). Here, we deliberately "shaded" the model towards the milder end of the spectrum in the present studies as we were interested in pro-inflammatory and injury pathways that operate early in NASH pathogenesis. One unwanted consequence might have been failure to observe in mice, the same findings as in human NASH with advanced fibrosis.

CD36

Another important new finding in these studies is that circulating EVs in both experimental NASH (in mice) and human NASH are enriched with CD36. Involvement of CD36 has been demonstrated in T2D and in the development of atherosclerosis and Alzheimer's disease (Sheedy *et al.* 2013). In the pathogenesis of atherosclerosis, CD36 functions as an oxidised LDL receptor essential for JNK-1/2 activation in macrophages, with subsequent foam cell formation (Rahaman *et al.* 2006). Sheedy and colleagues (2013) recently demonstrated that CD36 plays a role in intracellular cholesterol crystal formation in macrophages. Further, hepatic CD36 expression is strongly increased in human NAFLD patients (Miquilena-Colina *et al.* 2011). Here, implication of CD36 accords with the increasing body of evidence that lipid uptake is involved with NASH

pathogenesis, as is already accepted in T2D and metabolic syndrome. CD36 is abundantly expressed on hepatocytes, but also on macrophages, adipocytes, and other cell types.

Earlier work from the host laboratory demonstrated up-regulation of CD36 in the *foz/foz* murine model of NASH, and correlated its expression level with dietary factors that determined the inflammatory activity of fatty liver disease (Larter *et al.* 2013). In other work, we have also shown that the LDL receptor (LDLR) is up-regulated in livers of *foz/foz* mice with NASH, and showed using primary hepatocytes, that such up-regulation is in response to insulin via SREBP2 (Van Rooyen *et al.* 2011); SREBP2 also up-regulates CD36 (Bernal-Lopez *et al.* 2010). Three groups have shown an association between SREBP2 up-regulation and hepatic FC accumulation in human NASH (*versus* simple steatosis) (Puri *et al.* 2007, Caballero *et al.* 2009, Min *et al.* 2012). In subsequent studies one of these groups did not find increased LDLR expression (Min *et al.* 2012). Instead, they attributed cholesterol accumulation (on the basis of indirect evidence) to enhanced hepatic cholesterol biosynthesis (Min *et al.* 2012); however HMG-CoA reductase activity is profoundly suppressed in *foz/foz* mice with NASH (Van Rooyen *et al.* 2011). Although species differences in cholesterol disposition remain a plausible explanation for the difference between these studies, lipid tracer studies have shown that over 80% of hepatic lipid in NASH arises from the periphery; thus, hepatic uptake of lipid molecules must be involved. CD36 was not assayed in earlier human samples (Min *et al.* 2012). The present data showing abundant CD36 expression on circulating EVs in both human and murine NASH could explain the previously discrepant conclusions. Specifically, uptake of FC, as well as free fatty acid uptake in NASH may be mediated by CD36, a plasma membrane protein known to transport both types of lipid molecule into hepatocytes. Further studies should resolve this issue by assay of CD36 in human NASH livers.

Although this is not the first study to identify circulating EVs in NAFLD (Kornek *et al.* 2012), the current work expands earlier studies by showing correlations with disease phenotype, and by characterising cells of origin of EVs and their relationship to lipotoxicity. In earlier work from the host laboratory, similar vesicles (termed microparticles) were identified in hepatic ischemia-reperfusion injury, an acute form of liver injury that, like NASH is mediated by oxidative stress and innate immunity (Teoh

et al. 2014). In that work, it was demonstrated for the first time that EVs could themselves cause hepatocyte injury by promoting oxidative stress and mitochondrial injury, in addition to the known effects on platelet activation and chemotaxis for polymorphonuclear neutrophils (Teoh *et al.* 2014).

CD4 and CD8

One of the limitations of the *in vitro* data presented in this Chapter is the over-simplification of the cellular interaction. The reductionist approach used was essential to characterise separate cellular participants but cannot address the nuances of cellular subtype interactions that occur *in vivo* in NASH (Rosso *et al.* 2014). Further, the contribution of adipose and endothelial cell dysfunction (as found in atherosclerosis) to liver injury and overall hepatic inflammation (Pasarin *et al.* 2012) have not been studied. In an attempt to address this issue, we performed flow cytometry analysis of EV particles from patients with NAFLD. Circulating EVs isolated from patients with NASH (± early fibrosis) and NAFLD with advanced fibrosis were shown to originate from $CD4^+$ and $CD8^+$ T cells (Figure 6.4E, G, H). Implications of CD4 and CD8 cells in human NASH and NAFLD with advanced fibrosis is consistent with the findings by Kornek *et. al* (2012), although in their study, disease severity was neither described nor categorised.

ASGPR1 vs SCL10A1

In earlier *in vitro* experiments, we showed a significant increase in hepatocyte-derived EV in FC-injured primary hepatocytes (determined using ASGPR1 WB, Figure 6.1C). In contrast, EVs isolated from atherogenic-fed *foz/foz* mice showed no relative increase in EV-derived from hepatocytes, determined using SCL10A1, the hepatocyte-specific sodium taurocholate cotransporting polypeptide (NTCP) (Anwer and Stieger 2014) (Figure 6.3B). There may be several explanations for the apparent disparity between murine *in vitro* and *in vivo* data. First, *foz/foz* mice may have less severe NAFLD phenotype due to relative short duration of atherogenic diet. Second, hepatocyte-derived EVs may be rapidly removed from circulation from circulation within liver by adjacent KCs, which are able to swiftly endocytose EVs in a PS-dependent manner (Willekens *et al.* 2005), especially beneath the hepatic sinusoid sieve plate, thereby preventing their re-entry into the circulation. Thirdly, these hepatocyte-derived EVs may be under-represented in plasma EV samples as a consequence of the contribution from other

organs and tissues early in metabolic disease. In this respect, adipose inflammation and adipocyte death, and atherosclerotic plaque formation may occur early, whereas hepatic damage and associated EV-release may occur later in what is a multifaceted disease process, as for example with T2D and NASH. Previous time-course experiments conducted in the host laboratory using the *foz/foz* model, have shown adipose inflammation is evident at 12 weeks, while fibrotic NASH does not occur until 16-24 weeks (Larter *et al.* 2009, Larter *et al.* 2013). Accordingly, further research to study EV compositional changes over time would be of interest.

Finally, the difference we observe in murine *in vivo* and *in vitro* experiments could be attributable to the different functions and locations of ASGPR and SCL10A1 on hepatocytes at rest and during inflammation. ASGPR, expressed mainly on sinusoidal surface of hepatocytes (Morell *et al.* 1968, Ashwell and Morell 1974, Ashwell and Harford 1982) has many roles which includes: 1) binding, internalisation and clearance of glycoproteins containing terminal galactose or *N*-acetylgalactosamine residues (asialoglycoproteins) (Pricer *et al.* 1974, Spiess 1990, Stockert 1995), 2) clearance of IgA from circulation (Baenziger and Kornfeld 1974, Stockert *et al.* 1982, Daniels *et al.* 1989, Inamoto and Brown 1991), 3) removal of apoptotic cells, LDL and chylomicron remnants (Windler *et al.* 1991), 4) disposing cellular fibronectin (Rotundo *et al.* 1999), 5) being utilised by hepatotrophic virus to gain entry into hepatocyte (namely hepatitis B virus) (Yang *et al.* 2006) and 6) eliminate activated lymphocytes from circulation (Huang *et al.* 1994, Marth and Grewal 2008, Guy *et al.* 2011). During liver inflammation (irrespective of the cause), ASGPR expression increases and its binding site changes – at rest and in normal liver, expression of ASGPR is on the sinusoidal or basolateral membrane (Spiess 1990, Burgess *et al.* 1992, Becker *et al.* 1995, Stockert 1995). During liver inflammation, ASGPR shifts towards the canalicular membrane (Burgess *et al.* 1992). Similarly, in liver cirrhosis, ASGPR is over expressed and serum level of asialoglycoprotein increases and the localisation of the receptor also shifts to canalicular surface with corresponding decrease in sinusoidal and lateral surfaces (Burgess *et al.* 1992).

In contrast to ASGPR, SCL10A1, a Na^+- dependent bile acid (BA) transporter is expressed only on basolateral membrane of hepatocytes (Esteller 2008). At resting basal state, SCL10A1 together with organic anion transporting polypeptides (OATPs), are

responsible for BA uptake from sinusoidal blood. This process, carried out against an electrochemical gradient is a saturable process (Esteller 2008). Given the different functions and localisation of ASGPR (including its participation in apoptosis and inflammation), it is not surprising perhaps, we noticed increase in hepatocyte-specific EVs released in both FC-injured murine primary hepatocytes and NAFLD patients with NASH and advanced fibrosis when ASGPR was used as the hepatocyte marker, but no change to the mice NASH model when SCL10A1 was used. In future, it would be prudent to repeat this experiment using one standardised hepatocyte marker, ASGPR1/2 to tag the released EVs. Prof A Feldstein's group (2014) found a significant difference in levels of EVs in liver and blood between 2 control groups *vs NAFLD* animals. In their work, male C57Bl/6 WT mice were placed on 7 weeks of choline deficient L-amino acid (CDAA) diet or one of two control diets (choline supplemented L-amino acid [CSAA] and normal chow [NC]) for 4,8, and 20 weeks. They also placed mice on high fat diet containing 45% kcal fat or NC diet for 12 weeks to investigate a different experimental model for NAFLD. They found: 1) EV levels were increased in both liver and blood detected by EM in NAFLD mice on CDAA diet, which correlates with more severe liver damage, determined using NAS; 2) circulating EVs isolated from PFP of NAFLD animals with established NASH were positive for annexin V, vanin-1 (a surface ectoenzyme present in EVs released from stressed hepatocytes) and ASGPR1 detected by WB; and 3) hepatocytes were important source of circulating EVs in NAFLD animals, shown by presence of abundance hepatocyte microRNA, miR-122 and miR-192 in circulating EVs from blood of mice with NASH from 20 week of CDAA diet and from mice on 12 week of HF diet (Povero *et al.* 2014).

6.6 Summary of findings

The research presented in this Chapter focused on further characterisation of the EVs released from hepatocytes *in vitro* following FC-mediated hepatocellular injury. We found that EVs released from FC-injured hepatocytes are enriched in HMGB1, ASGPR1/2 and TLR4 and sought to establish if similar EVs circulated in experimental and clinical NASH. We saw a strong correlation between presence of EVs bearing HMGB1 and TLR4 in NAFLD phenotype, with animals developing NASH having more of these EVs than those with SS or controls. We were able to replicate these data in human clinical samples. These exciting findings could provide a novel mechanistic-

based biomarker to identify patients with NASH pathology and for liver fibrosis and cirrhosis. This will be addressed in future directions.

The major findings are summarised below.

1. FC-injured hepatocytes release EVs that bear HMGB1, TLR4 and ASGPR1/2.
2. EVs circulate in both experimental and human NAFLD; compared to controls or those with SS, those with clinical NASH and advanced fibrosis have significantly more EVs enriched with HMGB1, TLR4, as well as CD4- and CD8-positive markers
3. Circulating EVs isolated from mice and human patients with NASH are enriched with hepatocyte markers, indicating their origin from damaged hepatocytes.
4. In both mice and human with NASH and advanced fibrosis, circulating EVs with CD36 and CD147 are higher when compared with SS and controls with apparently healthy livers.

CHAPTER 7

Final Discussion

7.1 Research findings

In the broader context of NAFLD, the presence of NASH is a strong risk factor for development of liver fibrosis with progressive chronic liver disease that can lead to cirrhosis (Farrell *et al.* 2012). The pathogenic mechanisms for progression from SS to NASH are thought to involve hepatocyte injury with inflammatory recruitment by an innate immune response to such injury. One or more reactive lipid species are likely central to these processes, collectively termed lipotoxicity (Alkhouri *et al.*, 2009, Farrell *et al.*, 2012). Increasing evidence has implicated cholesterol, in particular FC, as a lipotoxic mediator of hepatocellular injury in NASH (Mari *et al.* 2006, Puri *et al.* 2007, Caballero *et al.* 2009, Van Rooyen and Farrell 2011, Van Rooyen *et al.* 2011, Min *et al.* 2012, Van Rooyen 2012, Van Rooyen *et al.* 2013). However, the exact mechanisms whereby FC injures hepatocytes and how this leads to liver inflammation have not been elucidated. Accordingly, the aims of the thesis were: (1) to establish a reproducible model of loading primary hepatocytes with FC, (2) use this *in vitro* model to explore the molecular and cellular mechanisms by which FC causes cell death in hepatocytes, (3) to establish how FC-induced lipotoxicity incites an inflammatory response, with particular attention to innate immunity mediated by HMGB1/TLR4 interactions; (4) to test whether hepatocyte lipotoxicity releases pro-inflammatory EVs; and (5) to determine whether EVs circulate in human NAFLD, and whether there are differences in their titre and composition (particularly cell types of origin) for NASH versus SS. The research findings presented in this thesis have been extensively discussed in the respective results Chapters. The aim of this final Chapter is to briefly summarise the important findings, and to propose some future directions for this research.

Chapter 1 is an introduction to the clinical relevance of NAFLD as the most common liver disease, its place among metabolic complications of over nutrition and insulin resistance, and a discussion about the pathogenic phenotype of NASH and its

significance for development of cirrhosis and liver cancer. Several elements of cell biology relevant to the studies of lipotoxicity were also addressed, including physiological pathways of mitochondrial function and adaptation to oxidative stress. This Chapter also summarised current evidence for FFA, TG, and cholesterol as hepatocyte lipotoxins in NAFLD. Given the focus in this thesis and within the host laboratory on cholesterol lipotoxicity, pathways of cholesterol homeostasis and intracellular FC trafficking were reviewed.

Unfortunately, research into hepatocellular FC lipotoxicity has been hinder by a lack of suitable *in vitro* model, largely because cholesterol homeostasis is complex, involving cellular uptake, transport, biosynthesis, biotransformation, storage and export; see Chapter 1 (Sections 1.5.2 and 1.5.3). In Chapter 3, the first experimental aim was addressed. Commercially available (purified) unmodified human LDL was used to load primary murine hepatocytes with FC, thereby successfully establishing a robust experimental model for mechanistic studies. This technique allowed hepatocytes to be FC-loaded in a dose-dependent manner so that the downstream effects could be studied.

The validity of this novel *in vitro* model was tested by comparing the subcellular localisation of FC between LDL-exposed hepatocytes and an *in vivo* murine model of NASH. The intracellular distribution of FC in primary murine hepatocytes loaded in this way recapitulated the organelle localisation observed in livers of atherogenic diet-fed *foz/foz* mice with NASH (Figures 3.1 and 3.2). At higher LDL concentrations, hepatocellular FC distributed to the mitochondrial compartment and to a lesser extent to the ER, and this was associated with increasing mitochondrial dysfunction and downstream activation of apoptosis and necrosis cell death pathways. FC also localised to the PM in FC-loaded hepatocytes, with a corresponding reduction in PM fluidity. These results were consistent with the research from Mari *et al.* (2006) who identified similar FC distribution to ER, PM and mitochondria in rats fed a high-cholesterol diet. They are also consistent with clinical evidence of hepatocyte mitochondrial injury in NASH, and with the presence of plasma membrane derived EVs in the circulation, as explored later. The subcellular pathways of hepatocyte injury in FC lipotoxicity were further defined in Chapter 4.

Interestingly, electron microscopy found EVs bleb off the surface of FC-laden damaged hepatocytes. These EVs could be harvested, and were available for subsequent analyses.

In Chapter 4, the second experimental aim was addressed. Here pathways of FC-mediated hepatocyte injury were explored first by revisiting previous experiments conducted on atherogenic diet-fed *foz/foz* mice with NASH. In these livers, a strong correlation was found between the extent of hepatic FC-loading and JNK1/2 and *c*-Jun activation. These pathways were then delineated in FC-loaded hepatocytes. Our *in vitro* model recapitulated the *in vivo* data, with FC-loading responsible for both significant JNK1 and *c*-Jun phosphorylation that could be inhibited by a potent JNK1 inhibitor (CC-003). Correspondingly, hepatocytes from *Jnk1*$^{-/-}$, but not *Jnk2*$^{-/-}$ mice, were refractory to FC-mediated mitochondrial injury and cell death. Collectively, these experiments showed that *c*-Jun activation occurred as a result of JNK1 activation in FC-loaded hepatocytes, and inhibition of JNK1 or its deletion abrogated both apoptosis and necrosis (Figures 4.9 and 4.11). This finding is particularly interesting in NASH because JNK1 (but not JNK2) is pivotal for the development of insulin resistance, hepatocellular cell death pathways and HCC (Kodama and Brenner 2009).

This Chapter also explored the role of mitochondrial cell injury in FC-induced cell death in some detail. Loading hepatocytes with FC increased StAR mRNA expression and, in a JNK1-dependent fashion, caused dysregulation of mitochondrial $\Delta\Psi_m$ and MPT. In turn, this led to oxidative stress, ATP depletion and hepatocellular cell death. Blocking MPT with CyA rescued hepatocytes from short-term FC-induced cell death. Similarly, pan-caspase inhibition or inhibition of caspase 3 reduced FC-induced apoptosis and necrosis. Collectively, these findings not only reinforce other NAFLD studies, which have implicated JNK1 activation in NASH pathogenesis (Schattenberg *et al.* 2006, Kodama and Brenner 2009, Kodama *et al.* 2009, Singh *et al.* 2009), but also provide the first conclusive mechanistic link between FC loading and the hepatocellular injury that is central to the definition of NASH. Electron microscopy was also used to study the architecture of FC-loaded hepatocyte mitochondria, and swelling and deranged cristae array were observed (Figure 4.15). Others have identified mitochondrial dysfunction in NASH, noting similar ultrastructural changes as those

observed here in FC-loaded hepatocytes (Caldwell *et al.* 1999, Sobaniec-Lotowska and Lebensztejn 2003, Le *et al.* 2004).

Importantly, Chapter 4 also explored the potential role of ER stress in FC-induced hepatocyte cell injury. ER stress was found to have no role in FC lipotoxicity, which is consistent with observations in *foz/foz* mice with NASH that GRP78, *Atf4* and *CHOP* are not involved in NASH pathogenesis (Van Rooyen *et al* [unpublished], PhD ANU, 2012) (Legry *et al.*). They also accord with the weight of evidence from three clinical trials, that the anti-ER stress compound, ursodeoxycholic acid, has no therapeutic efficacy against NASH (Lindor *et al.* 2004, Adams *et al.* 2010, Xiang *et al.* 2013).

Chapter 5 explored a number of sterile proinflammatory signalling pathways that could be relevant to NASH pathogenesis, including the role of EVs isolated from FC-loaded hepatocytes as activators of KCs. NF-κB p65 activation has been reported in human NASH, and in the host laboratory *foz/foz* mouse model of NASH (Figure 5.1) (Li *et al.* 2011, Wei *et al.* 2011, Van Rooyen *et al.* 2013, Tian *et al.* 2014). This master inflammatory regulator was activated by FC-loading of hepatocytes (Figure 5.3), with downstream release of IL-6 and TNF-α. Both these cytokines circulate at higher levels in NASH patients than in controls (Poniachik *et al.* 2006, Das and Balakrishnan 2011, Braunersreuther *et al.* 2012, Farrell *et al.* 2012), and they have been implicated in experimental models of NASH (Jiang *et al.* 2015, Santos *et al.* 2015). It should be noted that IL-1β was also detected within the supernatant of these FC-loaded hepatocytes, suggesting NRLP3 involvement. Unfortunately, this observation came towards the end of the candidate's experimental work, so that the potentially exciting role of inflammasome activation, which it suggests, was not studied further.

Pathways towards NF-κB p65 activation were investigated, in particular the signalling molecule HMGB1, and the pattern recognition receptor, TLR4. A growing body of evidence implicates this pathway in NASH pathogenesis (Alisi *et al.* 2011, Li *et al.* 2011, Roh and Seki 2013, Gan *et al.* 2014). In our FC-loaded hepatocytes, marginalisation of HMGB1 from the nucleus (as seen in control cells) to the PM (Figure 5.4) compartment was evident, and the PM budded off and released EVs containing this protein into the culture supernatant. Again, JNK1 was proven to be essential for this process; there was no extracellular HMGB1 release in $Jnk1^{-/-}$ primary hepatocytes,

irrespective of the extent of FC-loading (Figure 5.5). To the author's knowledge, this is first demonstration of a dynamic relationship between JNK1 and HMGB1 release in injured hepatocytes, and it may be a pivotal process in lipotoxicity.

Another critically important experiment was described in this Chapter. Incubating FC-loaded hepatocytes with anti-HMGB1 neutralising antibody significantly mitigated the extent of hepatocellular cell death, reducing both apoptosis and necrosis. Anti-HMGB1 also inhibited KC activation by isolated EVs. These results have far-reaching implications for potential novel therapy in NASH and warrant further investigation (see future directions below). It should be noted that there is a precedent for using anti-HMGB1 neutralising antibodies therapeutically in animal models, anti-HMGB1 reversed radiation-induced pneumonitis (Wang *et al.* 2015), cystic fibrosis airway disease (Rowe *et al.* 2008), and improved survival after hemorrhagic shock (Yang *et al.* 2006).

The pathogenesis of NASH must involved connections between injured hepatocytes and activated inflammatory cells, particularly those of macrophage lineage. Towards explaining such links, the EVs isolated from lipotoxic hepatocytes were shown to function as delivery vectors for HMGB1 and possibly TLR4/HMGB1 complexes. They potently activated KCs by mechanism, which could be inhibited by anti-HMGB1 neutralising antibodies and which failed to occur in TLR4 null cells. Further, *Myd88*$^{-/-}$ primary KCs were refractory to activation by EVs, implicating Myd88, as a node in the pathway to NF-κB activation, in this process. Myd88, is an essential signalling intermediated in TLR activation. Collectively, these results demonstrate for the first time a complex paracrine relationship between hepatocyte-derived EVs and the innate immune system. The influence of these particles on other cells of the innate immune response, were not explored in this thesis and constitute an important future direction (see below). In essence, the new concept developed by these findings that EVs provide a link between FC lipotoxicity to hepatocytes and accumulation of sterile inflammatory danger signals activates inflammatory cells in NASH, has been hinted by other investigators and authors (Farrell *et al.* 2012, Ganz *et al.* 2015, Zeng *et al.* 2015). Figure 5.14 summarises the principle findings from FC lipotoxicity studies in a schematic format.

Chapter 6 examined the fifth and final research objective, namely characterisation of EVs isolated from humans with NASH, and a comparison with experimental NASH in atherogenic diet-fed *foz/foz* mice. Patients with NASH and advanced liver fibrosis had significantly higher titres of circulating EVs enriched with HMGB1 and TLR4, as well as CD4- and CD8-positive markers compared with to those with SS or apparently health controls. Further, a significant percentage of isolated EVs were enriched with hepatocyte markers, indicating their origin from damaged hepatocytes. EVs could therefore provide a potential biomarker for non-invasive diagnosis or staging of NAFLD (Ban *et al.* 2016).

Collectively, the findings presented in this thesis support the hypothesis articulated in Chapter 1 (Section 1.8), that intracellular FC accumulation causes hepatocellular injury, resulting in cell death and activation of downstream proinflammatory pathways such as KC activation in NASH.

7.2 Future directions

Several important questions have emerged from the research conducted towards this thesis, and constitute logical directions for future study. These potential avenues of research will now be discussed and sub-stratified according to areas of pathogenesis, diagnosis and treatment of NASH.

7.2.1 Future research directions for NASH pathogenesis

7.2.1.1 Characterisation of intracellular FC trafficking in human NASH

The tight regulation of intracellular FC levels is reflected by the complex pathways responsible for intra- and extra-cellular cholesterol homeostasis (Figures 1.7 and 1.8). Perturbed intracellular cholesterol trafficking is now known to play a significant role in other disease processes, such as neurodegeneration (Arenas *et al.* 2017) and development of atherosclerosis (Zhang *et al.* 2008, Yu *et al.* 2014). Pathways of intracellular cholesterol trafficking were not examined in this thesis as they were beyond the scope of the proposed studies, and would require detailed cell biological techniques. Nevertheless, the data presented in Chapters 3 and 4 highlights the importance of subcellular FC distribution and the role of FC pools in mitochondrial and PM pathways of injury and cell death. To the author's knowledge, few if any studies to date have characterised intracellular pathways of cholesterol trafficking in human

NASH, nor the role of lipid droplet regulation and biotransformation. Accordingly, further research is needed to establish which proteins are involved, such as MLN64, NPC1 and NPC2, and whether their function is physiologically appropriate or dysregulated in NASH. StAR, which is responsible for influx of FC into the mitochondrial compartment (Section 1.5.2), is significantly upregulated in human NASH livers (Caballero *et al.* 2009). The murine gene equivalent was also upregulated in FC-loaded primary murine hepatocytes (Figure 4.14). It is therefore plausible that the expression of other genes and/or subcellular localisation of encoded proteins responsible for intracellular FC trafficking are also perturbed during NASH pathogenesis. If found to play in hepatic FC lipotoxicity, manipulation of FC trafficking and subcellular distribution could provide a therapeutic approach for treating NASH and preventing its complications.

7.2.1.2 Innate immunity in NASH

The innate immune system plays an integral role in NASH pathogenesis. It involves a complex interaction between hepatic (lipotoxic hepatocytes and KCs) and extrahepatic factors, various innate cell types, as well as environmental factors, host genetics and gut microbiota (see Figure 7.1 for schematic overview). For a succinct overview of the current innate system model in NASH see the review by Arrese *et al.* (2016).

As discussed in Chapter 1 (Sections 1.6 and 1.7), and from the data presented in Chapters 4, 5 and 6, TLR receptor activation and KCs are central to inflammatory pathway activation by lipotoxic hepatocytes. It is acknowledged that this thesis only studied a small part of the innate immune system using a reductionist (mono-culture) approach, in which culture of one cell type at a time was conducted. In order to fully characterise the role of this complex system in NAFLD progression a substantial amount of research is need. Ideally it would use the combination of knockout mice and co-culture, and it would involve correlation with findings in human NASH. The focus of this research would be to further define the roles of other innate immune system pattern recognition receptors, associated signalling pathways and the various innate cellular components. These are briefly discussed below.

Pattern recognition receptors

Although this thesis focused on the HMGB1/TLR4 axis and touched on NLRP3 signalling, several other PRRs were not explored in the FC-loaded hepatocyte model. These include other TLRs, especially TLRs -2 and -9. Studies from the host laboratory, using a combination of knockout mice, bone marrow chimeras and dietary models of NASH, have implicated TLR9 in the activation of M1-macrophages, as well as neutrophil chemotaxis during NASH pathogenesis in atherogenic diet-fed *foz/foz* mice (Mridha *et al.* 2017). In regards to TLR2 involvement, Miura and colleagues (2013) found less liver inflammation, fibrosis and NLRP3 inflammasome activation in *Tlr2*$^{-/-}$ mice. These researchers also demonstrated that PA can act as a TLR2 ligand, inducing downstream KC activation via NLRP3 activation (Miura *et al.* 2013). The role of PA and other saturated Fas (as opposed to cholesterol and other crystals) in NLRP3 activation remains controversial.

Additionally, TLR2, -4, and -9 are hypothesised to link gut dysbiosis to NASH pathogenesis. Gut dysbiosis is the collective term for intestinal bacterial overgrowth and increased intestinal permeability in NAFLD first noted by Wigg et al from Adelaide in 2001 (Wigg *et al.* 2001). This leads to endotoxinaemia (absorption of bacterial DNA, LPS and peptidoglycans) (Miura *et al.* 2010, Houghton *et al.* 2016). This pathway could further amplify damage to hepatocytes already subject to liptoxic injury. It is noted that the NLRP3 inflammasomes require a PAMP priming signal prior to activation and this could link gut dysbiosis to activation of inflammatory cells in NASH. Further work is needed to test this relationship and further elucidate the role and interactions of other TLRs and NOD-like receptors.

Cellular components of innate immunity

In order to fully delineate the complex interactions between the different cellular constituents of the innate immune system occurring in NASH, co-culture experiments are needed. Here, hepatocytes could be cultured along with KCs, and/or polymorphonuclear leukocytes, dendritic cells, or natural killer (NK) cells/natural killer T-cells. Although a significant undertaking, these would be important experiments since most cells of the innate system have dual pro-inflammatory and anti-inflammatory subtypes. For example, dendritic cells can switch from an anti-inflammatory state, where they are responsible for antigen-detection and clearance of apoptotic cells, to a

pro-inflammatory state where they express CX3C chemokine receptor 1 (CX3CR1) and activate KCs and other innate immune cells. Similarly, NK T-cell populations activated by lipids can be sub-divided into: type 1, which has a proinflammatory phenotype, and type 2, with anti-inflammatory functions that limit tissue damage and protect against development of autoimmunity (Dasgupta and Kumar 2016). The M1 and M2 macrophage subpopulations, which have already been discussed (see Section 1.3.2), are another example of this "on/off" dichotomy.

7.2.2 Future research directions for NASH diagnosis

7.2.2.1 Improved non-invasive methods for detecting human NASH

As discussed in Chapter 1, NAFLD is highly prevalent worldwide. While ~75% of patients with NAFLD have steatosis without significant liver disease, identifying those with NASH and/or significant liver fibrosis remains extremely challenging and is one of the most important issues in contemporary hepatology. It therefore constitutes an important area of future research. Current approaches include clinicopathological scoring (such as the NAFLD fibrosis score), biomarkers, including procollagen III N-terminal peptide (P3NP) (Tanwar *et al.* 2013) and liver stiffness measurement (LSM) by transient elastography (or other elastographic modalities, for example shear wave; MRE). Each of these approaches has only 80-85% negative predictive values for significant liver fibrosis (F3/4), and similar or slightly higher positive predictive values. Altogether, none of these non-invasive methods approach 90-100% diagnostic accuracy. Furthermore, applicability for all NAFLD cases, across age groups and diverse ethnic populations, logistics and cost are substantive issues that limit their more widespread use.

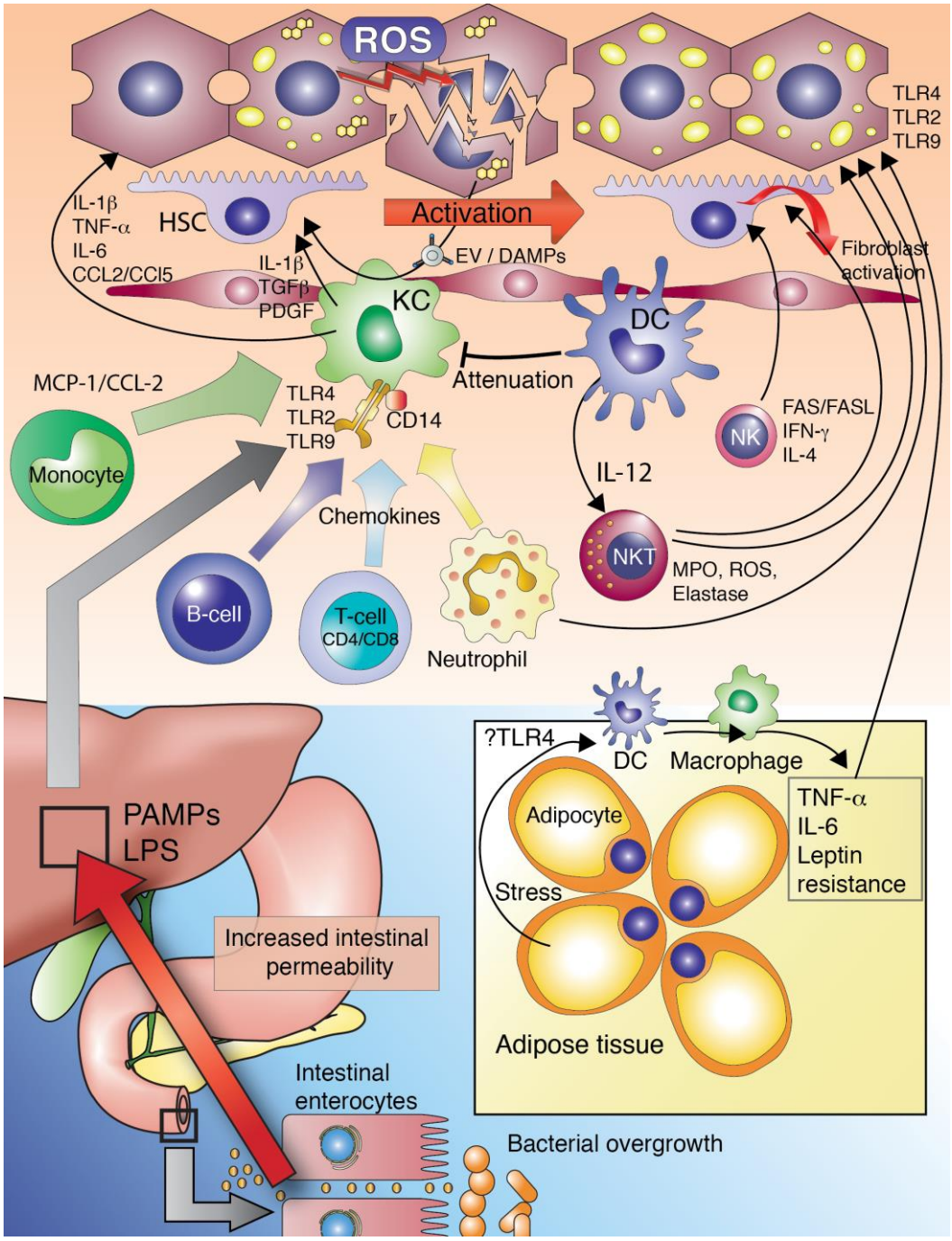

Figure 7.1 Role of innate immunity in the pathogenesis of NASH.

The innate immune system is instrumental in the development of NASH. This is likely to involve a complex interaction between multiple cell types, including B-cells, dendritic (DC), Kupffer (KC), monocytes, neutrophils, natural killer (NK), and natural killer T-cells (NKT). In addition to the liver, other organs and tissues could be involved in a whole body mechanism, such as the intestine, the gut microbiome and adipose tissue. As demonstrated in this thesis, lipotoxicity results in hepatocyte damage and cell death via reactive oxygen species (ROS), leading to release of danger activated molecular patterns (DAMP) that in turn, activate various pathways of innate immunity. Separately, increased intestinal permeability, bacterial over-growth (dysbiosis) and adipocyte inflammation are currently favoured to also contribute to innate immune system activation in NASH pathogenesis. Image adapted from Arrese *et al.* (2016).

Abbreviations for Figure 7.1: CCL-2, chemokine C-C motif ligand 2; CD, cluster of differentiation; EV, extracellular vesicle; FASL, FAS ligand; HSC, hepatic stellate cell; IFN-γ, interferon-gamma; IL, interleukin; LPS, lipopolysaccharide; MCP-1, monocyte chemoattractant protein 1; MPO, myeloperoxidase; PAMPs, pathogen-associated molecular pattern; PDGF, platelet-derived growth factor.

To provide higher diagnostic accuracy with readily available tests, the candidate explored conventional clinicopathological variables and extended their application with LSM and biomarkers. The data from these combined modalities was used to compile a clinical model that could stratify as many as possible NAFLD cases into advanced or no fibrosis, and also to identify those cases with NASH from others with simple steatosis. The preliminary data of these studies were presented at Australian Gastroenterology Week (2015), and are discussed here briefly as a direction for further research. These preliminary data should be interpreted with caution.

A clinical database of 200 biopsied NAFLD patients (defined by ≥5% hepatocytes showing steatosis), 169 with LSM data was analysed (Leon Adams). The database consisted of 135 patients from Hong Kong, 18 patients from Perth, and 16 patients from Canberra. A further 18 cases were excluded due to missing data, so that the final *n* was 151. According to NAFLD activity score (0–3=simple steatosis, 4=excluded, 5–8=NASH) and Brunt's fibrosis score (0, 1 or 2, 3 or 4), cases were grouped into 3 categories, simple steatosis, NASH with no to moderate fibrosis (F0-2) or F3/4. To allow clear separation of cases with or without NASH those with NAS=4 were excluded (*n*=3 cases) as this is an overlap/ambiguous category. The third category (F3/4) could include NASH or "not NASH" NAFLD because severe fibrosis occasionally presented without NASH pathology in NAFLD. Biomarkers included a set of anthropometric and clinical indices, serum ferritin, M30 (apoptosis marker), M65ed (overall cell death marker), hyaluronic acid (HA), P3NP, annexin V-positive microparticles (MP), and genetic predisposition (PNPLA3). Using generalised linear models in SPSS v22.0, a parsimonious decision tree was created to predict the three NAFLD categories.

The following correlated with NAFLD category: age, waist circumference (not BMI), hypertension, diabetes or fasting blood glucose, ALT, platelet count, INR, LSM, and all biomarkers except ferritin, and NAFLD fibrosis score significantly. In the multivariate analysis of the candidate indices, LSM was the dominant predictor (OR 1.22, 95% CI

1.09-1.34, *P*<0.0001). Consequently, LSM was stratified into 3 bands (<5.8; 5.8–30.3; >30.3 kPa) to maximize NAFLD category discrimination (Table 7.1). Within each LSM stratum, the candidate variables were used to further predict NAFLD categories. The significant factors entering the decision tree were P3NP (cut-off 8.7 ng/mL), ALT (cut-off of 55 U/L within the lower band, and 60 U/L within the middle LSM stratum), hypertension and LSM < or >10 kPa. Overall, 72% (109/151) agreement between predicted and histologically-observed NAFLD categories was found across the tree. The sensitivities and specificities varied by LSM band. For LSM <5.8 kPa (27 cases of SS, 22 of NASH, 1 of F3/F4), the sensitivity achieved for simple steatosis was 89% (24/27), and of NASH was 55% (12/22), with positive predictive values of 71% and 80%, respectively. In contrast, the middle LSM band (LSM 5.8–30.3 kPa, [25 cases of SS, 48 of NASH, 23 of F3/F4]) achieved 81% (39/48) sensitivity for NASH and 40% (10/25) for simple steatosis, with predictive values of 67% and 100%, respectively. The highest LSM band contained few cases; all 6 were F3/4 cases (positive predictive value of 100%).

These preliminary data show that use of transient elastography, P3NP, ALT and presence or absence of hypertension provide adequate information to discriminate NAFLD categories, particularly at the highest and lowest ends of the spectrum, thereby significantly reducing the number of cases requiring further liver investigations. This simple approach is relatively inexpensive (a P3NP assay is commercially available and currently costs ~$AUD 20, not including labor). It is independent of socio-demographic indicators, allowing it to be potentially transportable across populations. Further, it provides probabilities of diagnosis based on the number of diagnostic parameters available at the time, giving it practical value. Based on these findings, further validation of the decision model is worth pursuing and constitutes an important future direction.

Table 7.1 Preliminary data: Transient elastography (LSM) stratified into 3 bands allows significant discrimination between NAFLD categorised by NAS or Brunt fibrosis score.

<table>
<tr><th>LSM
(kPa)</th><th>N
(169)</th><th>Brunt fibrosis score ≤ 2
n (%)</th><th>Brunt's fibrosis score > 2
n (%)</th><th>P value</th></tr>
<tr><td><5.8
(Band 1)</td><td>54</td><td>53 (98%)
<table><tr><td>Actual / Predicted</td><td>SS</td><td>NASH</td><td>%</td></tr><tr><td>SS</td><td>24</td><td>10</td><td>71</td></tr><tr><td>NASH</td><td>3</td><td>12</td><td>80</td></tr><tr><td>%</td><td>89</td><td>55</td><td>74</td></tr></table></td><td>1 (2%)</td><td>< 0.0001</td></tr>
<tr><td>5.8–30
(Band 2)</td><td>109</td><td>85 (78%)
<table><tr><td>Actual / Predicted</td><td>SS</td><td>NASH</td></tr><tr><td>SS</td><td>10</td><td>0</td></tr><tr><td>NASH</td><td>14</td><td>39</td></tr><tr><td>F3/F4</td><td>1</td><td>9</td></tr><tr><td>%</td><td>40</td><td>81</td></tr></table></td><td>24 (22%)
<table><tr><td>F3/F4</td><td>%</td></tr><tr><td>0</td><td>100</td></tr><tr><td>5</td><td>67</td></tr><tr><td>18</td><td>64</td></tr><tr><td>78</td><td>70</td></tr></table></td><td></td></tr>
<tr><td>>30.3
(Band 3)</td><td>6</td><td>0 (0%)</td><td>6 (100%)</td><td></td></tr>
</table>

Numbers in sub tables do not add to grand totals due to missing data associated with predictor variables in the generalized linear models.

Abbreviations: SS, simple steatosis.

7.2.3 Future directions of NASH treatment

7.2.4 Reversing insulin resistance using pharmacological approaches – effect on FC homeostasis

Insulin resistance and lipid/cholesterol metabolism are inseparably linked to the pathogenesis of NASH. As a result, interventions which reverse insulin resistance are the subject of intense research and development, and hold potential to reverse metabolic

syndrome and its associated liver and cardiovascular diseases (Kaur 2014). It is already known that exercise has this effect (Haczeyni *et al.* 2015, Axley *et al.* 2017, de Lira *et al.* 2017, Hashida *et al.* 2017, Winn *et al.* 2018). Harnessing this potential pharmacologically constitutes an important future research direction. One possible pathway of improved using insulin resistance will now be discussed, namely farnesoid X receptor (FXR).

Farnesoid X receptor

FXR is a nuclear receptor expressed in liver, kidney, intestine and adrenal tissues. Within the liver its activation has pleiotropic effects on cholesterol homeostasis and lipid metabolism. FXR activation governs cholesterol turnover by regulating CYP7A1 and other enzymes involved in the biotransformation of FC into bile acids (BA)s, as well as cellular efflux of BAs and lipoproteins. It also regulates suppression of TG synthesis through inhibition of SREBP-1c (Figure 7.2B). An FXR agonist in current clinical trials is obeticholic acid (OCA), a 6-ethoxy-chenodeoxycholic acid, also known as 6-alpha-ethyl-chenodeoxycholic acid (6-ECDCA) (Pellicciari *et al.* 2002). OCA is a potent synthetic derivative of chenodeoxycholic acid, a major secondary BA in humans. As an FXR ligand, it is 100 times more potent than chenodeoxycholic acid (Figure 7.A) (Pellicciari *et al.* 2002). OCA is currently in phase 3 REGENERATE clinical trials (Wong *et al.* , U.S. National Library of Medicine 2018). Thus far, OCA has shown promise, with improvements in insulin sensitivity and amelioration of liver inflammation and fibrosis in NASH patients and some (but not all) experimental NASH models (Maneschi *et al.* 2013, Mudaliar *et al.* 2013, Ali *et al.* 2015, Makri *et al.* 2016, Cernea *et al.* 2017, Haczeyni *et al.* 2017, Briand *et al.* 2018). It is generally well tolerated with few adverse effects. Interestingly, however, in the FLINT study, where 110 patients received OCA *versus* 142 placebo, NAFLD activity score improvements of ≥2 points in the OCA group was accompanied by increased total and LDL cholesterol, with reciprocal decreases in HDL (Neuschwander-Tetri *et al.*). Not only do these findings raise concern for cardiovascular risk, but they also contradict the underlying hypothesis presented in this thesis, whereby increased LDL was shown to cause hepatocyte injury. It is plausible the OCA alters intracellular FC distribution and prevents mitochondrial damage despite elevations in circulating LDL levels. Nevertheless, further research is needed to fully assess the effect of OCA on

hepatocellular cholesterol metabolism as well as to establish whether the changes in circulating lipoproteins accelerate atherogenesis.

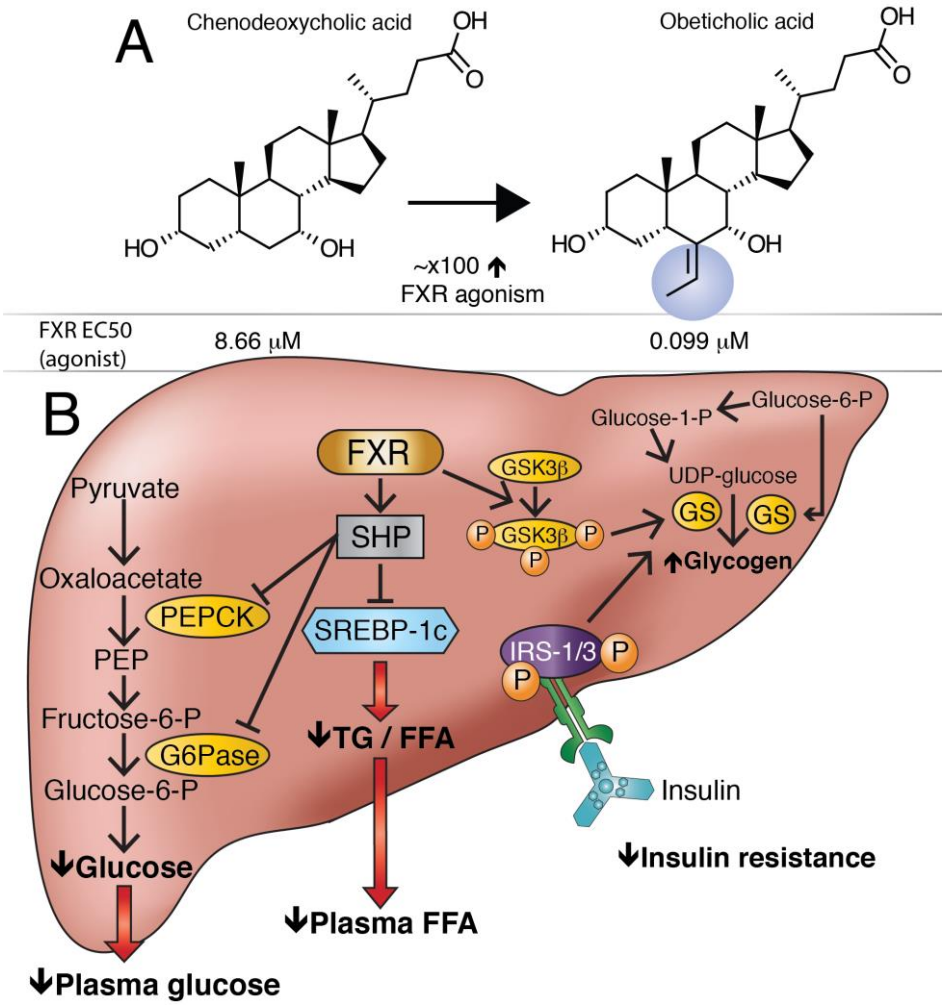

Figure 7.2 Chemical structures of FXR agonists and pathways of glucose homeostasis, lipid metabolism and insulin resistance modulated by FXR.

(**A**) Chemical structures of naturally occurring chenodeoxycholic acid and the synthetic FXR agonist obeticholic acid, which is approximately 100x more potent. The structural difference is highlighted in blue. (**B**) Once activated, FXR signals through an intermediate signalling molecule, small heterodimer partner (Shp), which in turn inhibits gluconeogenesis and lipogenesis by inhibiting enzymes responsible for biosynthesis of glucose and TG/FFAs, including, glucose-6-phosphatase (G6Pase), and phosphoenolpyruvate carboxykinase (PEPCK), and the transcriptional factor sterol regulatory element-binding protein 1c (SREBP1c). FXR induces glycogen formation by upregulating glycogen synthase (GS); this reduces circulating glucose and lipid levels, leading to improved insulin sensitivity. Panel B adapted from Zhang and Edward (Zhang and Edwards 2008).

Abbreviations: EC50, half maximal effective concentration; FFA, free fatty acid(s); IRS, insulin receptor substrate; P, phosphate; PEP, phosphoenolpyruvate; TG, triglyceride; UDP, uracil-diphosphate.

7.3 Concluding remarks

In summary, this thesis has provided the first direct evidence that hepatocellular FC accumulation is lipotoxic to hepatocytes, causing both apoptosis and necrosis. The cellular mechanism involves JNK1 activation, and lipotoxicity triggers downstream inflammatory processes involving activation of HMGB1, TLR4 and NF-κB p65 pathways. Further, hepatocellular EVs act as feed-forward autocrine/paracrine signalling vectors between hepatocytes and Kupffer cells. This research has far reaching implications for the development of therapeutic strategies to halt the progression of SS to NASH.

References

Abel, T., Feher, J., Dinya, E., Gamal Eldin, M. and Kovacs, A. (2009). *"Efficacy and safety of ezetimibe/simvastatin combination therapy in patients with type 2 diabetes and nonalcoholic fatty liver disease."* Orv Hetil **150**(21): 989-993.

Abi-Mosleh, L., Infante, R. E., Radhakrishnan, A., Goldstein, J. L. and Brown, M. S. (2009). *"Cyclodextrin overcomes deficient lysosome-to-endoplasmic reticulum transport of cholesterol in Niemann-Pick type C cells."* Proc Natl Acad Sci U S A **106**(46): 19316-19321.

Adachi, M. and Ishii, H. (2002). *"Role of mitochondria in alcoholic liver injury."* Free Radic Biol Med **32**(6): 487-491.

Adams, J. D., Jr., Lauterburg, B. H. and Mitchell, J. R. (1983). *"Plasma glutathione and glutathione disulfide in the rat: regulation and response to oxidative stress."* J Pharmacol Exp Ther **227**(3): 749-754.

Adams, L. A., Angulo, P., Petz, J., Keach, J. and Lindor, K. D. (2010). *"A pilot trial of high-dose ursodeoxycholic acid in nonalcoholic steatohepatitis."* Hepatol Int **4**(3): 628-633.

Adler, V., Schaffer, A., Kim, J., Dolan, L. and Ronai, Z. (1995). *"UV irradiation and heat shock mediate JNK activation via alternate pathways."* J Biol Chem **270**(44): 26071-26077.

Agresti, A. and Bianchi, M. E. (2003). *"HMGB proteins and gene expression."* Curr Opin Genet Dev **13**(2): 170-178.

Ajamieh, H., Farrell, G. C., McCuskey, R. S., Yu, J., Chu, E., Wong, H. J., Lam, W. and Teoh, N. C. (2015). *"Acute atorvastatin is hepatoprotective against ischaemia-reperfusion injury in mice by modulating eNOS and microparticle formation."* Liver Int **35**(9): 2174-2186.

Akira, S., Uematsu, S. and Takeuchi, O. (2006). *"Pathogen recognition and innate immunity."* Cell **124**(4): 783-801.

Alexandrov, A., Keffel, S., Goepel, M. and Michel, M. C. (1999). *"Differential regulation of 46 and 54 kDa jun N-terminal kinases and p38 mitogen-activated protein kinase by human alpha(1A)-adrenoceptors expressed in Rat-1 cells."* Biochem Biophys Res Commun **261**(2): 372-376.

Ali, A. H., Carey, E. J. and Lindor, K. D. (2015). *"Recent advances in the development of farnesoid X receptor agonists."* Ann Transl Med **3**(1): 5.

Alisi, A., Carsetti, R. and Nobili, V. (2011). *"Pathogen- or damage-associated molecular patterns during nonalcoholic fatty liver disease development."* Hepatol **54**(5): 1500-1502.

Alkhatatbeh, M. J., Mhaidat, N. M., Enjeti, A. K., Lincz, L. F. and Thorne, R. F. (2011). *"The putative diabetic plasma marker, soluble CD36, is non-cleaved, non-soluble and entirely associated with microparticles."* J Thromb Haemost **9**(4): 844-851.

Alkhouri, N., Dixon, L. J. and Feldstein, A. E. (2009). *"Lipotoxicity in nonalcoholic fatty liver disease: not all lipids are created equal."* Expert Rev Gastroenterol Hepatol **3**(4): 445-451.

Ameyar, M., Wisniewska, M. and Weitzman, J. B. (2003). *"A role for AP-1 in apoptosis: the case for and against."* Biochimie **85**(8): 747-752.

Andersson, U., Erlandsson-Harris, H., Yang, H. and Tracey, K. J. (2002). *"HMGB1 as a DNA-binding cytokine."* J Leukoc Biol **72**(6): 1084-1091.

Andersson, U. and Tracey, K. J. (2011). *"HMGB1 is a therapeutic target for sterile inflammation and infection."* Annu Rev Immunol **29**: 139-162.

Angel, A. (1970). *"Studies on the compartmentation of lipid in adipose cells. I. Subcellular distribution, composition, and transport of newly synthesized lipid: liposomes."* J Lipid Res **11**(5): 420-432.

Angel, A. and Farkas, J. (1970). *"Structural and chemical compartments in adipose cells."* Horm Metab Res **2**: Suppl 2:152-161.

Angel, A. and Sheldon, H. (1965). *"Adipose cell organelles: isolation, morphology and possible relation to intracellular lipid transport."* Ann N Y Acad Sci **131**(1): 157-176.

Angel, P. and Karin, M. (1991). *"The role of Jun, Fos and the AP-1 complex in cell-proliferation and transformation."* Biochim Biophys Acta **1072**(2-3): 129-157.

Angelovich, T. A., Hearps, A. C. and Jaworowski, A. (2015). *"Inflammation-induced foam cell formation in chronic inflammatory disease."* Immunol Cell Biol **93**(8): 683-693.

Angulo, P. (2002). *"Nonalcoholic fatty liver disease."* N Engl J Med **346**(16): 1221-1231.

Anwer, M. S. and Stieger, B. (2014). *"Sodium-dependent bile salt transporters of the SLC10A transporter family: more than solute transporters."* Pflugers Arch **466**(1): 77-89.

Aoudjit, F., Brochu, N., Belanger, B., Stratowa, C., Hiscott, J. and Audette, M. (1997). *"Regulation of intercellular adhesion molecule-1 gene by tumor necrosis factor-alpha is mediated by the nuclear factor-kappaB heterodimers p65/p65 and p65/c-Rel in the absence of p50."* Cell Growth Differ **8**(3): 335-342.

Aragones, G., Gonzalez-Garcia, S., Aguilar, C., Richart, C. and Auguet, T. (2019). *"Gut Microbiota-Derived Mediators as Potential Markers in Nonalcoholic Fatty Liver Disease."* Biomed Res Int **2019**: 8507583.

Arakane, F., Sugawara, T., Nishino, H., Liu, Z., Holt, J. A., Pain, D., Stocco, D. M., Miller, W. L. and Strauss, J. F. (1996). *"Steroidogenic acute regulatory protein (StAR) retains activity in the absence of its mitochondrial import sequence: Implications for the mechanism of StAR action."* Proc Natl Acad Sci U S A **93**(24): 13731-13736.

Arenas, F., Garcia-Ruiz, C. and Fernandez-Checa, J. C. (2017). *"Intracellular Cholesterol Trafficking and Impact in Neurodegeneration."* Front Mol Neurosci **10**: 382.

Arraud, N., Gounou, C., Linares, R. and Brisson, A. R. (2014). *"A Simple Flow Cytometry Method Improves the Detection of Phosphatidylserine-Exposing Extracellular Vesicles."* J Thromb Haemost **13**(2): 237-247.

Arrese, M., Cabrera, D., Kalergis, A. M. and Feldstein, A. E. (2016). *"Innate Immunity and Inflammation in NAFLD/NASH."* Dig Dis Sci **61**(5): 1294-1303.

Arteel, G., Marsano, L., Mendez, C., Bentley, F. and McClain, C. J. (2003). *"Advances in alcoholic liver disease."* Best Pract Res Clin Gastroenterol **17**(4): 625-647.

Arteel, G. E. (2003). *"Oxidants and antioxidants in alcohol-induced liver disease."* Gastroenterol **124**(3): 778-790.

Arteel, G. E. (2012). *"Beyond reasonable doubt: who is the culprit in lipotoxicity in NAFLD/NASH?"* Hepatol **55**(6): 2030-2032.

Ashwell, G. and Harford, J. (1982). *"Carbohydrate-specific receptors of the liver."* Annu Rev Biochem **51**: 531-554.

Ashwell, G. and Morell, A. G. (1974). *"The role of surface carbohydrates in the hepatic recognition and transport of circulating glycoproteins."* Adv Enzymol Relat Areas Mol Biol **41**(0): 99-128.

Australian Bureau of Statistics (2015). "*4125.0 - Overweight / Obesity Health Series*." Retrieved 20 November, 2015, from http://www.abs.gov.au/ausstats/abs@.nsf/Lookup/4125.0main+features3330Feb%202014.

Axley, P., Kodali, S., Kuo, Y. F., Ravi, S., Seay, T., Parikh, N. M. and Singal, A. K. (2017). *"Text messaging approach improves weight loss in patients with nonalcoholic fatty liver disease: A randomized study."* Liver Int **38**(5): 924-931.

Baenziger, J. and Kornfeld, S. (1974). *"Structure of the carbohydrate units of IgA1 immunoglobulin. I. Composition, glycopeptide isolation, and structure of the asparagine-linked oligosaccharide units."* J Biol Chem **249**(22): 7260-7269.

Bagamery, K., Kvell, K., Landau, R. and Graham, J. (2005). *"Flow cytometric analysis of CD41-labeled platelets isolated by the rapid, one-step OptiPrep method from human blood."* Cytometry A **65**(1): 84-87.

Baj-Krzyworzeka, M., Baran, J., Szatanek, R. and Siedlar, M. (2012). Application of Flow Cytometry in the Studies of Microparticles. *Flow Cytometry - Recent Perspectives*. I. Schmid. LA, USA, InTech**:** Chapter 11.

Baj-Krzyworzeka, M., Majka, M., Pratico, D., Ratajczak, J., Vilaire, G., Kijowski, J., Reca, R., Janowska-Wieczorek, A. and Ratajczak, M. Z. (2002). *"Platelet-derived microparticles stimulate proliferation, survival, adhesion, and chemotaxis of hematopoietic cells."* Exp Hematol **30**(5): 450-459.

Baker, M. A., Cerniglia, G. J. and Zaman, A. (1990). *"Microtiter plate assay for the measurement of glutathione and glutathione disulfide in large numbers of biological samples."* Anal Biochem **190**(2): 360-365.

Ballard, D. W., Dixon, E. P., Peffer, N. J., Bogerd, H., Doerre, S., Stein, B. and Greene, W. C. (1992). *"The 65-kDa subunit of human NF-kappa B functions as a potent transcriptional activator and a target for v-Rel-mediated repression."* Proc Natl Acad Sci U S A **89**(5): 1875-1879.

Ban, J. O., Hwang, I. G., Kim, T. M., Hwang, B. Y., Lee, U. S., Jeong, H. S., Yoon, Y. W., Kimz, D. J. and Hong, J. T. (2007). *"Anti-proliferate and pro-apoptotic effects of 2,3-dihydro-3,5-dihydroxy-6-methyl-4H-pyranone through inactivation of NF-kappaB in human colon cancer cells."* Arch Pharm Res **30**(11): 1455-1463.

Ban, L. A., Shackel, N. A. and McLennan, S. V. (2016). *"Extracellular Vesicles: A New Frontier in Biomarker Discovery for Non-Alcoholic Fatty Liver Disease."* Int J Mol Sci **17**(3): 376.

Bannerman, D. D., Erwert, R. D., Winn, R. K. and Harlan, J. M. (2002). *"TIRAP mediates endotoxin-induced NF-kappaB activation and apoptosis in endothelial cells."* Biochem Biophys Res Commun **295**(1): 157-162.

Baran, J., Baj-Krzyworzeka, M., Weglarczyk, K., Szatanek, R., Zembala, M., Barbasz, J., Czupryna, A., Szczepanik, A. and Zembala, M. (2010). *"Circulating tumour-derived microvesicles in plasma of gastric cancer patients."* Cancer Immunol Immunother **59**(6): 841-850.

Baranova, A. and Younossi, Z. (2007). Adipokines in Non-Alcoholic Fatty Liver Disease. *Adipose Tissue and Adipokines in Health and Disease*. G. Fantuzzi and T. Mazzone, Humana Press**:** 291-305.

Barateiro, A., Vaz, A. R., Silva, S. L., Fernandes, A. and Brites, D. (2012). *"ER stress, mitochondrial dysfunction and calpain/JNK activation are involved in*

oligodendrocyte precursor cell death by unconjugated bilirubin." Neuromolecular Med **14**(4): 285-302.

Barteneva, N. S., Fasler-Kan, E., Bernimoulin, M., Stern, J. N., Ponomarev, E. D., Duckett, L. and Vorobjev, I. A. (2013). *"Circulating microparticles: square the circle."* BMC Cell Biol **14**: 23.

Baynes, J. W. (1991). *"Role of oxidative stress in development of complications in diabetes."* Diabetes **40**(4): 405-412.

Becker, B. N., Cheng, H. F., Burns, K. D. and Harris, R. C. (1995). *"Polarized rabbit type 1 angiotensin II receptors manifest differential rates of endocytosis and recycling."* Am J Physiol **269**(4 Pt 1): C1048-1056.

Bedogni, G., Miglioli, L., Masutti, F., Castiglione, A., Crocè, L. S., Tiribelli, C. and Bellentani, S. (2007). *"Incidence and natural course of fatty liver in the general population: The Dionysos study."* Hepatol **46**(5): 1387-1391.

Beinke, S. and Ley, S. C. (2004). *"Functions of NF-kappaB1 and NF-kappaB2 in immune cell biology."* Biochem J **382**(Pt 2): 393-409.

Bell, C. W., Jiang, W., Reich, C. F., 3rd and Pisetsky, D. S. (2006). *"The extracellular release of HMGB1 during apoptotic cell death."* Am J Physiol Cell Physiol **291**(6): C1318-1325.

Berg, J. M., Tymoczko, J. L. and Stryer, L. (2002). *Biochemistry, 5th Edition*. New York, W H Freeman.

Bernal-Lopez, M. R., Llorente-Cortés, V., Gómez-Huelgas, R., Badimon, L. and Tinahones, F. (2010). *Intimate relation between genic expression of scavenger receptor CD36 and transcription factor SREBP2*.

Bernardi, P. (1999). *"Mitochondrial transport of cations: channels, exchangers, and permeability transition."* Physiol Rev **79**(4): 1127-1155.

Bernardi, P., Scorrano, L., Colonna, R., Petronilli, V. and Di Lisa, F. (1999). *"Mitochondria and cell death. Mechanistic aspects and methodological issues."* Eur J Biochem **264**(3): 687-701.

Berry, M. N., Grivell, A. R., Grivell, M. B. and Phillips, J. W. (1997). *"Isolated hepatocytes--past, present and future."* Cell Biol Toxicol **13**(4-5): 223-233.

Beutler, E. and Gelbart, T. (1986). *"Improved assay of the enzymes of glutathione synthesis: gamma-glutamylcysteine synthetase and glutathione synthetase."* Clin Chim Acta **158**(1): 115-123.

Bi, X. and Liao, G. (2010). *"Cholesterol in Niemann–Pick Type C disease."* Subcell Biochem **51**: 319-335.

Bianchi, M. E. (2009). *"HMGB1 loves company."* J Leukoc Biol **86**(3): 573-576.

Bickel, P. E., Tansey, J. T. and Welte, M. A. (2009). *"PAT proteins, an ancient family of lipid droplet proteins that regulate cellular lipid stores."* Biochim Biophys Acta **1791**(6): 419-440.

Björkegren, J., Karpe, F., Milne, R. W. and Hamsten, A. (1998). *"Differences in apolipoprotein and lipid composition between human chylomicron remnants and very low density lipoproteins isolated from fasting and postprandial plasma."* J Lipid Res **39**(7): 1412-1420.

Blackburn, R. V., Spitz, D. R., Liu, X., Galoforo, S. S., Sim, J. E., Ridnour, L. A., Chen, J. C., Davis, B. H., Corry, P. M. and Lee, Y. J. (1999). *"Metabolic oxidative stress activates signal transduction and gene expression during glucose deprivation in human tumor cells."* Free Radic Biol Med **26**(3-4): 419-430.

Blom, T. S., Linder, M. D., Snow, K., Pihko, H., Hess, M. W., Jokitalo, E., Veckman, V., Syvänen, A.-C. and Ikonen, E. (2003). *"Defective endocytic*

trafficking of NPC1 and NPC2 underlying infantile Niemann–Pick type C disease." Hum Mol Genet **12**(3): 257-272.

Borish, L., Rosenbaum, R., Albury, L. and Clark, S. (1989). *"Activation of neutrophils by recombinant interleukin 6."* Cell Immunol **121**(2): 280-289.

Botteron, C. and Dobbelaere, D. (1998). *"AP-1 and ATF-2 are constitutively activated via the JNK pathway in Theileria parva-transformed T-cells."* Biochem Biophys Res Commun **246**(2): 418-421.

Boulanger, C. M. and Dignat-George, F. (2011). *"Microparticles: An Introduction."* Arterioscler Thromb Vasc Biol **31**(1): 2-3.

Boursier, J., Mueller, O., Barret, M., Machado, M., Fizanne, L., Araujo-Perez, F., Guy, C. D., Seed, P. C., Rawls, J. F., David, L. A., Hunault, G., Oberti, F., Cales, P. and Diehl, A. M. (2016). *"The severity of nonalcoholic fatty liver disease is associated with gut dysbiosis and shift in the metabolic function of the gut microbiota."* Hepatol **63**(3): 764-775.

Boustiere, C. and Gauthier, A. (1985). *"Non-alcoholic hepatic steatosis."* Presse Med **14**(20): 1147-1150.

Bowden, K. and Ridgway, N. D. (2008). *"OSBP negatively regulates ABCA1 protein stability."* J Biol Chem **283**(26): 18210-18217.

Braunersreuther, V., Viviani, G. L., Mach, F. and Montecucco, F. (2012). *"Role of cytokines and chemokines in non-alcoholic fatty liver disease."* World J Gastroenterol **18**(8): 727-735.

Briand, F., Brousseau, E., Quinsat, M., Burcelin, R. and Sulpice, T. (2018). *"Obeticholic acid raises LDL-cholesterol and reduces HDL-cholesterol in the Diet-Induced NASH (DIN) hamster model."* Eur J Pharmacol **818**: 449-456.

Brickman, J. M., Adam, M. and Ptashne, M. (1999). *"Interactions between an HMG-1 protein and members of the Rel family."* Proc Natl Acad Sci U S A **96**(19): 10679-10683.

Browning, J. D. and Horton, J. D. (2004). *"Molecular mediators of hepatic steatosis and liver injury."* J Clin Invest **114**(2): 147-152.

Brunner, K. T., Henneberg, C. J., Wilechansky, R. M. and Long, M. T. (2019). *"Nonalcoholic Fatty Liver Disease and Obesity Treatment."* Curr Obes Rep.

Brunt, E. M. (2002). *"Alcoholic and nonalcoholic steatohepatitis."* Clin Liver Dis **6**(2): 399-420, vii.

Brunt, E. M., Janney, C. G., Di Bisceglie, A. M., Neuschwander-Tetri, B. A. and Bacon, B. R. (1999). *"Nonalcoholic steatohepatitis: a proposal for grading and staging the histological lesions."* Am J Gastroenterol **94**(9): 2467-2474.

Brunt, E. M., Kleiner, D. E., Wilson, L. A., Belt, P. and Neuschwander-Tetri, B. A. (2011). *"Nonalcoholic fatty liver disease (NAFLD) activity score and the histopathologic diagnosis in NAFLD: distinct clinicopathologic meanings."* Hepatol **53**(3): 810-820.

Brunt, E. M., Wong, V. W., Nobili, V., Day, C. P., Sookoian, S., Maher, J. J., Bugianesi, E., Sirlin, C. B., Neuschwander-Tetri, B. A. and Rinella, M. E. (2015). *"Nonalcoholic fatty liver disease."* Nat Rev Dis Primers **1**: 15080.

Burgess, J. B., Baenziger, J. U. and Brown, W. R. (1992). *"Abnormal surface distribution of the human asialoglycoprotein receptor in cirrhosis."* Hepatol **15**(4): 702-706.

Bustin, M. and Reeves, R. (1996). *"High-mobility-group chromosomal proteins: architectural components that facilitate chromatin function."* Prog Nucleic Acid Res Mol Biol **54**: 35-100.

Byrne, C. D. (2010). *"Hypoxia and non-alcoholic fatty liver disease."* Clin Sci (Lond) **118**(6): 397-400.

Caballero, F., Fernandez, A., De Lacy, A. M., Fernandez-Checa, J. C., Caballeria, J. and Garcia-Ruiz, C. (2009). *"Enhanced free cholesterol, SREBP-2 and StAR expression in human NASH."* J Hepatol **50**(4): 789-796.

Cai, L., Eckhardt, E. R., Shi, W., Zhao, Z., Nasser, M., de Villiers, W. J. and van der Westhuyzen, D. R. (2004). *"Scavenger receptor class B type I reduces cholesterol absorption in cultured enterocyte CaCo-2 cells."* J Lipid Res **45**(2): 253-262.

Calabro, S. R., Maczurek, A. E., Morgan, A. J., Tu, T., Wen, V. W., Yee, C., Mridha, A., Lee, M., d'Avigdor, W., Locarnini, S. A., McCaughan, G. W., Warner, F. J., McLennan, S. V. and Shackel, N. A. (2014). *"Hepatocyte produced matrix metalloproteinases are regulated by CD147 in liver fibrogenesis."* PLoS ONE **9**(7): e90571.

Caldwell, S. H., de Freitas, L. A., Park, S. H., Moreno, M. L., Redick, J. A., Davis, C. A., Sisson, B. J., Patrie, J. T., Cotrim, H., Argo, C. K. and Al-Osaimi, A. (2009). *"Intramitochondrial crystalline inclusions in nonalcoholic steatohepatitis."* Hepatol **49**(6): 1888-1895.

Caldwell, S. H., Swerdlow, R. H., Khan, E. M., Iezzoni, J. C., Hespenheide, E. E., Parks, J. K. and Parker, W. D., Jr. (1999). *"Mitochondrial abnormalities in non-alcoholic steatohepatitis."* J Hepatol **31**(3): 430-434.

Camussi, G., Deregibus, M. C., Bruno, S., Cantaluppi, V. and Biancone, L. (2010). *"Exosomes/microvesicles as a mechanism of cell-to-cell communication."* Kidney Int **78**(9): 838-848.

Cartwright, I. J., Plonné, D. and Higgins, J. A. (2000). *"Intracellular events in the assembly of chylomicrons in rabbit enterocytes."* J Lipid Res **41**(11): 1728-1739.

Caussy, C. and Loomba, R. (2018). *"Gut microbiome, microbial metabolites and the development of NAFLD."* Nat Rev Gastroenterol Hepatol **15**(12): 719-720.

Cazanave, S. C., Elmi, N. A., Akazawa, Y., Bronk, S. F., Mott, J. L. and Gores, G. J. (2010). *"CHOP and AP-1 cooperatively mediate PUMA expression during lipoapoptosis."* Am J Physiol Gastrointest Liver Physiol **299**(1): G236-243.

Cazanave, S. C., Mott, J. L., Elmi, N. A., Bronk, S. F., Werneburg, N. W., Akazawa, Y., Kahraman, A., Garrison, S. P., Zambetti, G. P., Charlton, M. R. and Gores, G. J. (2009). *"JNK1-dependent PUMA expression contributes to hepatocyte lipoapoptosis."* J Biol Chem **284**(39): 26591-26602.

Cengiz, M., Ozenirler, S. and Elbeg, S. (2015). *"Role of serum toll-like receptors 2 and 4 in non-alcoholic steatohepatitis and liver fibrosis."* J Gastroenterol Hepatol **30**(7): 1190-1196.

Cernea, S., Cahn, A. and Raz, I. (2017). *"Pharmacological management of nonalcoholic fatty liver disease in type 2 diabetes."* Expert Rev Clin Pharmacol **10**(5): 535-547.

Chamaillard, M., Girardin, S. E., Viala, J. and Philpott, D. J. (2003). *"Nods, Nalps and Naip: intracellular regulators of bacterial-induced inflammation."* Cell Microbiol **5**(9): 581-592.

Chan, J., Sharkey, F. E., Kushwaha, R. S., VandeBerg, J. F. and VandeBerg, J. L. (2012). *"Steatohepatitis in laboratory opossums exhibiting a high lipemic response to dietary cholesterol and fat."* Am J Physiol **303**(1): G12-G19.

Charlton-Menys, V. and Durrington, P. N. (2008). *"Human cholesterol metabolism and therapeutic molecules."* Exp Physiol **93**(1): 27-42.

Charman, M., Kennedy, B. E., Osborne, N. and Karten, B. (2010). *"MLN64 mediates egress of cholesterol from endosomes to mitochondria in the absence of functional Niemann-Pick Type C1 protein."* J Lipid Res **51**(5): 1023-1034.

Chavez-Tapia, N. C., Rosso, N. and Tiribelli, C. (2012). *"Effect of intracellular lipid accumulation in a new model of non-alcoholic fatty liver disease."* BMC Gastroenterol **12**: 20.

Chazotte, B. (2011). *"Labeling mitochondria with MitoTracker dyes."* Cold Spring Harb Protoc **2011**(8): 990-992.

Chazotte, B. (2011). *"Labeling mitochondria with TMRM or TMRE."* Cold Spring Harb Protoc **2011**(7): 895-897.

Chen, M., Wang, H., Chen, W. and Meng, G. (2011). *"Regulation of adaptive immunity by the NLRP3 inflammasome."* Int Immunopharmacol **11**(5): 549-554.

Chen, N. J., Chio, II, Lin, W. J., Duncan, G., Chau, H., Katz, D., Huang, H. L., Pike, K. A., Hao, Z., Su, Y. W., Yamamoto, K., de Pooter, R. F., Zuniga-Pflucker, J. C., Wakeham, A., Yeh, W. C. and Mak, T. W. (2008). *"Beyond tumor necrosis factor receptor: TRADD signaling in toll-like receptors."* Proc Natl Acad Sci U S A **105**(34): 12429-12434.

Chen, Z. and Lash, L. H. (1998). *"Evidence for mitochondrial uptake of glutathione by dicarboxylate and 2-oxoglutarate carriers."* J Pharmacol Exp Ther **285**(2): 608-618.

Chen, Z., Ye, Z. Q. and Shi, Q. (2007). *"Rat microsomal glutathione S-transferase 1 alters cytotoxic effects of chlorambucil on PC-3, K562, HepG2 and P388D1 cell lines."* Zhejiang Da Xue Xue Bao Yi Xue Ban **36**(3): 236-240.

Cheng, H. M., Chylack, L. T., Jr., Sang, C. N., Orzalesi, N. and Corongiu, F. P. (1983). *"GSSG-reducing activity in lenses deficient in glucose-6-phosphate dehydrogenase."* Metab Pediatr Syst Ophthalmol **7**(1): 53-57.

Cheon, H. G. and Cho, Y. S. (2014). *"Protection of palmitic acid-mediated lipotoxicity by arachidonic acid via channeling of palmitic acid into triglycerides in C2C12."* J Biomed Sci **21**(1): 13-13.

Chiasserini, D., van Weering, J. R., Piersma, S. R., Pham, T. V., Malekzadeh, A., Teunissen, C. E., de Wit, H. and Jimenez, C. R. (2014). *"Proteomic analysis of cerebrospinal fluid extracellular vesicles: a comprehensive dataset."* J Proteomics **106**: 191-204.

Chitturi, S., Abeygunasekera, S., Farrell, G. C., Holmes-Walker, J., Hui, J. M., Fung, C., Karim, R., Lin, R., Samarasinghe, D., Liddle, C., Weltman, M. and George, J. (2002). *"NASH and insulin resistance: Insulin hypersecretion and specific association with the insulin resistance syndrome."* Hepatol **35**(2): 373-379.

Choi, B. K., Chitwood, D. J. and Paik, Y. K. (2003). *"Proteomic changes during disturbance of cholesterol metabolism by azacoprostane treatment in Caenorhabditis elegans."* Mol Cell Proteomics **2**(10): 1086-1095.

Cholankeril, G., Patel, R., Khurana, S. and Satapathy, S. K. (2017). *"Hepatocellular carcinoma in non-alcoholic steatohepatitis: Current knowledge and implications for management."* World J Hepatol **9**(11): 533-543.

Cinti, S., Mitchell, G., Barbatelli, G., Murano, I., Ceresi, E., Faloia, E., Wang, S., Fortier, M., Greenberg, A. S. and Obin, M. S. (2005). *"Adipocyte death defines macrophage localization and function in adipose tissue of obese mice and humans."* J Lipid Res **46**(11): 2347-2355.

Circu, M. L. and Yee Aw, T. (2008). *"Glutathione and apoptosis."* Free Radic Res **42**(8): 689-706.

Coffey, E. T. (2014). *"Nuclear and cytosolic JNK signalling in neurons."* Nat Rev Neurosci **15**(5): 285-299.

Conforti-Andreoni, C., Ricciardi-Castagnoli, P. and Mortellaro, A. (2011). *"The inflammasomes in health and disease: from genetics to molecular mechanisms of autoinflammation and beyond."* Cell Mol Immunol **8**(2): 135-145.

Connolly, K. D., Guschina, I. A., Yeung, V., Clayton, A., Draman, M. S., Von Ruhland, C., Ludgate, M., James, P. E. and Rees, D. A. (2015). *"Characterisation of adipocyte-derived extracellular vesicles released pre- and post-adipogenesis."* J Extracell Vesicles **4**: 29159.

Cortez-Pinto, H., Camilo, M. E., Baptista, A., De Oliveira, A. G. and De Moura, M. C. (1999). *"Non-alcoholic fatty liver: another feature of the metabolic syndrome?"* Clin Nutr **18**(6): 353-358.

Cortez-Pinto, H., Chatham, J., Chacko, V. P., Arnold, C., Rashid, A. and Diehl, A. M. (1999). *"Alterations in liver ATP homeostasis in human nonalcoholic steatohepatitis: a pilot study."* JAMA **282**(17): 1659-1664.

Crow, M. T., Mani, K., Nam, Y. J. and Kitsis, R. N. (2004). *"The mitochondrial death pathway and cardiac myocyte apoptosis."* Circ Res **95**(10): 957-970.

Csak, T., Pillai, A., Ganz, M., Lippai, D., Petrasek, J., Park, J. K., Kodys, K., Dolganiuc, A., Kurt-Jones, E. A. and Szabo, G. (2014). *"Both bone marrow-derived and non-bone marrow-derived cells contribute to AIM2 and NLRP3 inflammasome activation in a MyD88-dependent manner in dietary steatohepatitis."* Liver Int **34**(9): 1402-1413.

Csak, T., Velayudham, A., Hritz, I., Petrasek, J., Levin, I., Lippai, D., Catalano, D., Mandrekar, P., Dolganiuc, A., Kurt-Jones, E. and Szabo, G. (2011). *"Deficiency in myeloid differentiation factor-2 and Toll-like receptor 4 expression attenuates non-alcoholic steatohepatitis and fibrosis in mice."* Am J Physiol Gastrointest Liver Physiol **300**(3): 433-441.

Cuenda, A. and Dorow, D. S. (1998). *"Differential activation of stress-activated protein kinase kinases SKK4/MKK7 and SKK1/MKK4 by the mixed-lineage kinase-2 and mitogen-activated protein kinase kinase (MKK) kinase-1."* Biochem J **333 (Pt 1)**: 11-15.

Cui, W., Chen, S. L. and Hu, K. Q. (2010). *"Quantification and mechanisms of oleic acid-induced steatosis in HepG2 cells."* Am J Transl Res **2**(1): 95-104.

Cummings, V., Hewitt, J., Van Rooyen, A., Currie, K., Beard, S., Thrush, S., Norkko, J., Barr, N., Heath, P., Halliday, N. J., Sedcole, R., Gomez, A., McGraw, C. and Metcalf, V. (2011). *"Ocean acidification at high latitudes: potential effects on functioning of the Antarctic bivalve Laternula elliptica."* PLoS ONE **6**(1): e16069.

Cusi, K. (2012). *"Role of obesity and lipotoxicity in the development of nonalcoholic steatohepatitis: pathophysiology and clinical implications."* Gastroenterology **142**(4): 711-725 e716.

Czaja, M. J., Liu, H. and Wang, Y. (2003). *"Oxidant-induced hepatocyte injury from menadione is regulated by ERK and AP-1 signaling."* Hepatol **37**(6): 1405-1413.

da Silva, F. C., do Carmo de Oliveira Cito, M., da Silva, M. I., Moura, B. A., de Aquino Neto, M. R., Feitosa, M. L., de Castro Chaves, R., Macedo, D. S., de Vasconcelos, S. M., de Franca Fonteles, M. M. and de Sousa, F. C. (2010). *"Behavioral alterations and pro-oxidant effect of a single ketamine administration to mice."* Brain Res Bull **83**(1-2): 9-15.

Dagenais, M., Skeldon, A. and Saleh, M. (2012). *"The inflammasome: in memory of Dr. Jurg Tschopp."* Cell Death Differ **19**(1): 5-12.

Daneker, G. W., Lund, S. A., Caughman, S. W., Swerlick, R. A., Fischer, A. H., Staley, C. A. and Ades, E. W. (1998). *"Culture and characterization of*

sinusoidal endothelial cells isolated from human liver." In Vitro Cell Dev Biol Anim **34**(5): 370-377.

Daniels, C. K., Schmucker, D. L. and Jones, A. L. (1989). *"Hepatic asialoglycoprotein receptor-mediated binding of human polymeric immunoglobulin A."* Hepatol **9**(2): 229-234.

Dara, L., Ji, C. and Kaplowitz, N. (2011). *"The contribution of ER stress to liver diseases."* Hepatol **53**(5): 1752-1763.

Das, A., Brown, M. S., Anderson, D. D., Goldstein, J. L. and Radhakrishnan, A. (2014). *"Three pools of plasma membrane cholesterol and their relation to cholesterol homeostasis."* Elife **3**.

Das, S. K. and Balakrishnan, V. (2011). *"Role of Cytokines in the Pathogenesis of Non-Alcoholic Fatty Liver Disease."* Indian J Clin Biochem **26**(2): 202-209.

Dasgupta, S. and Kumar, V. (2016). *"Type II NKT cells: a distinct CD1d-restricted immune regulatory NKT cell subset."* Immunogenetics **68**(8): 665-676.

Dawson, T. L., Gores, G. J., Nieminen, A. L., Herman, B. and Lemasters, J. J. (1993). *"Mitochondria as a source of reactive oxygen species during reductive stress in rat hepatocytes."* Am J Physiol **264**(4 Pt 1): C961-967.

Day, C. P. and James, O. F. (1998). *"Steatohepatitis: a tale of two "hits"?"* Gastroenterology **114**(4): 842-845.

de Duve, C. (1971). *"Tissue fraction-past and present."* J Cell Biol **50**(1): 20.

de Lira, C. T., Dos Santos, M. A., Gomes, P. P., Fidelix, Y. L., Dos Santos, A. C., Tenorio, T. R., Lofrano-Prado, M. C. and do Prado, W. L. (2017). *"Aerobic training performed at ventilatory threshold improves liver enzymes and lipid profile related to non-alcoholic fatty liver disease in adolescents with obesity."* Nutr Health **23**(4): 281-288.

De Maio, A. (2011). *"Extracellular heat shock proteins, cellular export vesicles, and the Stress Observation System: a form of communication during injury, infection, and cell damage. It is never known how far a controversial finding will go! Dedicated to Ferruccio Ritossa."* Cell Stress Chaperones **16**(3): 235-249.

De Mattia, G., Bravi, M. C., Laurenti, O., Cassone-Faldetta, M., Armiento, A., Ferri, C. and Balsano, F. (1998). *"Influence of reduced glutathione infusion on glucose metabolism in patients with non-insulin-dependent diabetes mellitus."* Metabolism **47**(8): 993-997.

De Mattia, G., Bravi, M. C., Laurenti, O., Cassone-Faldetta, M., Proietti, A., De Luca, O., Armiento, A. and Ferri, C. (1998). *"Reduction of oxidative stress by oral N-acetyl-L-cysteine treatment decreases plasma soluble vascular cell adhesion molecule-1 concentrations in non-obese, non-dyslipidaemic, normotensive, patients with non-insulin-dependent diabetes."* Diabetologia **41**(11): 1392-1396.

Deacon, K. and Blank, J. L. (1997). *"Characterization of the mitogen-activated protein kinase kinase 4 (MKK4)/c-Jun NH2-terminal kinase 1 and MKK3/p38 pathways regulated by MEK kinases 2 and 3. MEK kinase 3 activates MKK3 but does not cause activation of p38 kinase in vivo."* J Biol Chem **272**(22): 14489-14496.

Dela Pena, A., Leclercq, I., Field, J., George, J., Jones, B. and Farrell, G. (2005). *"NF-kappaB activation, rather than TNF, mediates hepatic inflammation in a murine dietary model of steatohepatitis."* Gastroenterology **129**(5): 1663-1674.

Deng, R., Su, Z., Lu, F., Zhang, L., Lin, J., Zhang, X., de Paiva, C. S., Pflugfelder, S. C. and Li, D. Q. (2014). *"A potential link between bacterial pathogens and allergic conjunctivitis by dendritic cells."* Exp Eye Res **120**: 118-126.

Denis, M., Haidar, B., Marcil, M., Bouvier, M., Krimbou, L. and Genest, J. (2004). *"Characterization of oligomeric human ATP binding cassette transporter A1."* J Biol Chem **279**(40): 41529-41536.

Denis, M., Haidar, B., Marcil, M., Bouvier, M., Krimbou, L. and Genest, J., Jr. (2004). *"Molecular and cellular physiology of apolipoprotein A-I lipidation by the ATP-binding cassette transporter A1 (ABCA1)."* J Biol Chem **279**(9): 7384-7394.

Descorbeth, M., Figueroa, K. F., Serrano-Illan, M. and De Leon, M. (2013). *"Protective effect of Docosahexaenoic acid (DHA) on lipotoxicity –induced cell death: implication of PI3K/AKT and MAPK pathways."* The FASEB Journal **27**(1 Supplement): 815.815.

DeVerse, J. S., Bailey, K. A., Jackson, K. N. and Passerini, A. G. (2012). *"Shear stress modulates RAGE-mediated inflammation in a model of diabetes-induced metabolic stress."* Am J Physiol Heart Circ Physiol **302**(12): H2498-2508.

Diebold, S. S. and Brencicova, E. (2013). *"Nucleic acids & endosomal pattern recognition - how to tell friend from foe?"* Front Cell Infect Microbiol **3**.

Dinarello, C. A., Renfer, L. and Wolff, S. M. (1977). *"Human leukocytic pyrogen: purification and development of a radioimmunoassay."* Proc Natl Acad Sci U S A **74**(10): 4624-4627.

Domanski, J. P., Park, S. J. and Harrison, S. A. (2012). *"Cardiovascular disease and nonalcoholic fatty liver disease: does histologic severity matter?"* J Clin Gastroenterol **46**(5): 427-430.

Dorn, C., Engelmann, J. C., Saugspier, M., Koch, A., Hartmann, A., Muller, M., Spang, R., Bosserhoff, A. and Hellerbrand, C. (2014). *"Increased expression of c-Jun in nonalcoholic fatty liver disease."* Lab Invest **94**(4): 394-408.

Dornas, W. and Lagente, V. (2019). *"Intestinally derived bacterial products stimulate development of nonalcoholic steatohepatitis."* Pharmacol Res **141**: 418-428.

Droge, W. (2002). *"Aging-related changes in the thiol/disulfide redox state: implications for the use of thiol antioxidants."* Exp Gerontol **37**(12): 1333-1345.

Du, X., Kumar, J., Ferguson, C., Schulz, T. A., Ong, Y. S., Hong, W., Prinz, W. A., Parton, R. G., Brown, A. J. and Yang, H. (2011). *"A role for oxysterol-binding protein-related protein 5 in endosomal cholesterol trafficking."* J Cell Biol **192**(1): 121-135.

Du, X. and Yang, H. (2013). *"Endosomal cholesterol trafficking: protein factors at a glance."* Acta Biochim Biophys Sin **45**(1): 11-17.

Duarte, S. M. B., Stefano, J. T. and Oliveira, C. P. (2019). *"Microbiota and nonalcoholic fatty liver disease/nonalcoholic steatohepatitis (NAFLD/NASH)."* Ann Hepatol **18**(3): 416-421.

Duchen, M. R. (2004). *"Mitochondria in health and disease: perspectives on a new mitochondrial biology."* Mol Aspects Med **25**(4): 365-451.

Duchen, M. R. (2004). *"Roles of mitochondria in health and disease."* Diabetes **53 Suppl 1**: S96-102.

Duewell, P., Kono, H., Rayner, K. J., Sirois, C. M., Vladimer, G., Bauernfeind, F. G., Abela, G. S., Franchi, L., Nunez, G., Schnurr, M., Espevik, T., Lien, E., Fitzgerald, K. A., Rock, K. L., Moore, K. J., Wright, S. D., Hornung, V. and Latz, E. (2010). *"NLRP3 inflammasomes are required for atherogenesis and activated by cholesterol crystals."* Nature **464**(7293): 1357-1361.

Edwards, P. A., Tabor, D., Kast, H. R. and Venkateswaran, A. (2000). *"Regulation of gene expression by SREBP and SCAP."* Biochim Biophys Acta **1529**(1-3): 103-113.

Eitel, J., Suttorp, N. and Opitz, B. (2010). *"Innate Immune Recognition and Inflammasome Activation in Listeria Monocytogenes Infection."* Front Microbiol **1**: 149.

Eitel, J., Suttorp, N. and Opitz, B. (2011). *"Innate immune recognition and inflammasome activation in Listeria monocytogenes infection."* Front Microbiol **1**.

Eizirik, D. L., Cardozo, A. K. and Cnop, M. (2008). *"The role for endoplasmic reticulum stress in diabetes mellitus."* Endocr Rev **29**(1): 42-61.

El-Azeem I, A. A. and Saraya, M. A. (2012). *"The effect of chronic intermittent hypoxia in the evolution of NASH."* Egypt J Chest Dis Tuberc **61**(3): 197-202.

English, G. (2010). *"Mitochondrial cholesterol trafficking: impact on inflammatory mediators."* Biosci Horiz **3**(1): 1-9.

Estabrook, R. W. and Rainey, W. E. (1996). *"Twinkle, twinkle little StAR, how we wonder what you are."* Proc Natl Acad Sci U S A **93**(24): 13552-13554.

Esteller, A. (2008). *"Physiology of bile secretion."* World J Gastroenterol **14**(37): 5641-5649.

Evans, Z. P., Ellett, J. D., Schmidt, M. G., Schnellmann, R. G. and Chavin, K. D. (2008). *"Mitochondrial uncoupling protein-2 mediates steatotic liver injury following ischemia/reperfusion."* J Biol Chem **283**(13): 8573-8579.

Eyer, P. and Podhradsky, D. (1986). *"Evaluation of the micromethod for determination of glutathione using enzymatic cycling and Ellman's reagent."* Anal Biochem **153**(1): 57-66.

Fabbri, M., Paone, A., Calore, F., Galli, R., Gaudio, E., Santhanam, R., Lovat, F., Fadda, P., Mao, C., Nuovo, G. J., Zanesi, N., Crawford, M., Ozer, G. H., Wernicke, D., Alder, H., Caligiuri, M. A., Nana-Sinkam, P., Perrotti, D. and Croce, C. M. (2012). *"MicroRNAs bind to Toll-like receptors to induce prometastatic inflammatory response."* Proc Natl Acad Sci U S A **109**(31): E2110–E2116.

Fais, S., O'Driscoll, L., Borras, F. E., Buzas, E., Camussi, G., Cappello, F., Carvalho, J., Cordeiro da Silva, A., Del Portillo, H., El Andaloussi, S., Ficko Trcek, T., Furlan, R., Hendrix, A., Gursel, I., Kralj-Iglic, V., Kaeffer, B., Kosanovic, M., Lekka, M. E., Lipps, G., Logozzi, M., Marcilla, A., Sammar, M., Llorente, A., Nazarenko, I., Oliveira, C., Pocsfalvi, G., Rajendran, L., Raposo, G., Rohde, E., Siljander, P., van Niel, G., Vasconcelos, M. H., Yanez-Mo, M., Yliperttula, M. L., Zarovni, N., Zavec, A. B. and Giebel, B. (2016). *"Evidence-Based Clinical Use of Nanoscale Extracellular Vesicles in Nanomedicine."* ACS Nano **10**(4): 3886-3899.

Farkas, J., Angel, A. and Avigan, M. I. (1973). *"Studies on the compartmentation of lipid in adipose cells. II. Cholesterol accumulation and distribution in adipose tissue components."* J Lipid Res **14**(3): 344-356.

Farrell, G. C., Chitturi, S., Lau, G. K., Sollano, J. D. and Asia-Pacific Working Party on, N. (2007). *"Guidelines for the assessment and management of non-alcoholic fatty liver disease in the Asia-Pacific region: executive summary."* J Gastroenterol Hepatol **22**(6): 775-777.

Farrell, G. C. and Larter, C. Z. (2006). *"Nonalcoholic fatty liver disease: from steatosis to cirrhosis."* Hepatol **43**(2 Suppl 1): S99-S112.

Farrell, G. C., van Rooyen, D., Gan, L. and Chitturi, S. (2012). *"NASH is an Inflammatory Disorder: Pathogenic, Prognostic and Therapeutic Implications."* Gut Liver **6**(2): 149-171.

Faustin, B. and Reed, J. C. (2013). *"Reconstituting the NLRP1 inflammasome in vitro."* Methods Mol Biol **1040**: 137-152.

Febbraio, M., Podrez, E. A., Smith, J. D., Hajjar, D. P., Hazen, S. L., Hoff, H. F., Sharma, K. and Silverstein, R. L. (2000). *"Targeted disruption of the class B scavenger receptor CD36 protects against atherosclerotic lesion development in mice."* J Clin Invest **105**(8): 1049-1056.

Feldstein, A. E., Werneburg, N. W., Canbay, A., Guicciardi, M. E., Bronk, S. F., Rydzewski, R., Burgart, L. J. and Gores, G. J. (2004). *"Free fatty acids promote hepatic lipotoxicity by stimulating TNF-alpha expression via a lysosomal pathway."* Hepatol **40**(1): 185-194.

Fernandes-Alnemri, T., Wu, J., Yu, J. W., Datta, P., Miller, B., Jankowski, W., Rosenberg, S., Zhang, J. and Alnemri, E. S. (2007). *"The pyroptosome: a supramolecular assembly of ASC dimers mediating inflammatory cell death via caspase-1 activation."* Cell Death Differ **14**(9): 1590-1604.

Fernandes-Alnemri, T., Yu, J.-W., Datta, P., Wu, J. and Alnemri, E. S. (2009). *"AIM2 activates the inflammasome and cell death in response to cytoplasmic DNA."* Nature **458**(7237): 509-513.

Fielding, C. A., McLoughlin, R. M., McLeod, L., Colmont, C. S., Najdovska, M., Grail, D., Ernst, M., Jones, S. A., Topley, N. and Jenkins, B. J. (2008). *"IL-6 Regulates Neutrophil Trafficking during Acute Inflammation via STAT3."* J Immunol **181**(3): 2189-2195.

Fitzgerald, K. A., Palsson-McDermott, E. M., Bowie, A. G., Jefferies, C. A., Mansell, A. S., Brady, G., Brint, E., Dunne, A., Gray, P., Harte, M. T., McMurray, D., Smith, D. E., Sims, J. E., Bird, T. A. and O'Neill, L. A. (2001). *"Mal (MyD88-adapter-like) is required for Toll-like receptor-4 signal transduction."* Nature **413**(6851): 78-83.

Flowers, M. T., Groen, A. K., Oler, A. T., Keller, M. P., Choi, Y., Schueler, K. L., Richards, O. C., Lan, H., Miyazaki, M., Kuipers, F., Kendziorski, C. M., Ntambi, J. M. and Attie, A. D. (2006). *"Cholestasis and hypercholesterolemia in SCD1-deficient mice fed a low-fat, high-carbohydrate diet."* J Lipid Res **47**(12): 2668-2680.

Franchi, L., Eigenbrod, T., Munoz-Planillo, R. and Nunez, G. (2009). *"The inflammasome: a caspase-1-activation platform that regulates immune responses and disease pathogenesis."* Nat Immunol **10**(3): 241-247.

Friedman, S. L. (2004). *"Mechanisms of disease: Mechanisms of hepatic fibrosis and therapeutic implications."* Nat Clin Pract Gastroenterol Hepatol **1**(2): 98-105.

Friedman, S. L., Neuschwander-Tetri, B. A., Rinella, M. and Sanyal, A. J. (2018). *"Mechanisms of NAFLD development and therapeutic strategies."* Nat Med **24**(7): 908-922.

Fritz, G. and Kaina, B. (1999). *"Activation of c-Jun N-Terminal Kinase 1 by UV Irradiation Is Inhibited by Wortmannin without Affecting c-jun Expression."* Mol Cell Biol **19**(3): 1768-1774.

Froh, M., Konno, A. and Thurman, R. G. (2003). *"Isolation of liver Kupffer cells."* Curr Protoc Toxicol **Chapter 14**: Unit14 14.

Fuhrer, C., Geffen, I., Huggel, K. and Spiess, M. (1994). *"The two subunits of the asialoglycoprotein receptor contain different sorting information."* J Biol Chem **269**(5): 3277-3282.

Furuyama, N. and Fujisawa, Y. (2000). *"Distinct roles of cathepsin K and cathepsin L in osteoclastic bone resorption."* Endocr Res **26**(2): 189-204.

Fusegawa, H., Shiraishi, K., Ogasawara, F., Shimizu, M., Haruki, Y., Miyachi, H., Matsuzaki, S. and Ando, Y. (2002). *"Platelet activation in patients with chronic hepatitis C."* Tokai J Exp Clin Med **27**(4): 101-106.

Gan, L., Chitturi, S. and Farrell, G. C. (2011). *"Mechanisms and implications of age-related changes in the liver: nonalcoholic Fatty liver disease in the elderly."* Curr Gerontol Geriatr Res **2011**: 831536.

Gan, L. T., Van Rooyen, D. M., Koina, M. E., McCuskey, R. S., Teoh, N. C. and Farrell, G. C. (2014). *"Hepatocyte free cholesterol lipotoxicity results from JNK1-mediated mitochondrial injury and is HMGB1 and TLR4-dependent."* J Hepatol **61**(6): 1376-1384.

Ganz, M., Bukong, T. N., Csak, T., Saha, B., Park, J.-K., Ambade, A., Kodys, K. and Szabo, G. (2015). *"Progression of non-alcoholic steatosis to steatohepatitis and fibrosis parallels cumulative accumulation of danger signals that promote inflammation and liver tumors in a high fat–cholesterol–sugar diet model in mice."* J Transl Med **13**: 193.

Ganz, M. and Szabo, G. (2013). *"Immune and inflammatory pathways in NASH."* Hepatol Int **7**(Suppl 2): 771-781.

Garcia-Calvo, M., Lisnock, J., Bull, H. G., Hawes, B. E., Burnett, D. A., Braun, M. P., Crona, J. H., Davis, H. R., Dean, D. C., Detmers, P. A., Graziano, M. P., Hughes, M., MacIntyre, D. E., Ogawa, A., O'Neill, K. A., Iyer, S. P. N., Shevell, D. E., Smith, M. M., Tang, Y. S., Makarewicz, A. M., Ujjainwalla, F., Altmann, S. W., Chapman, K. T. and Thornberry, N. A. (2005). *"The target of ezetimibe is Niemann-Pick C1-Like 1 (NPC1L1)."* Proc Natl Acad Sci U S A **102**(23): 8132-8137.

Garcia-Ruiz, C., Mato, J. M., Vance, D., Kaplowitz, N. and Fernández-Checa, J. C. (2015). *"Acid sphingomyelinase-ceramide system in steatohepatitis: A novel target regulating multiple pathways."* J Hepatol **62**(1): 219-233.

Garver, W. S., Jelinek, D., Francis, G. A. and Murphy, B. D. (2008). *"The Niemann-Pick C1 gene is downregulated by feedback inhibition of the SREBP pathway in human fibroblasts."* J Lipid Res **49**(5): 1090-1102.

Gerfaud-Valentin, M., Jamilloux, Y., Iwaz, J. and Seve, P. (2014). *"Adult-onset Still's disease."* Autoimmun Rev **13**(7): 708-722.

Gerrits, E. G., Alkhalaf, A., Landman, G. W., van Hateren, K. J., Groenier, K. H., Struck, J., Schulte, J., Gans, R. O., Bakker, S. J., Kleefstra, N. and Bilo, H. J. (2014). *"Serum peroxiredoxin 4: a marker of oxidative stress associated with mortality in type 2 diabetes (ZODIAC-28)."* PLoS ONE **9**(2): e89719.

Ghoshal, U. C., Baba, C. S., Ghoshal, U., Alexander, G., Misra, A., Saraswat, V. A. and Choudhuri, G. (2017). *"Low-grade small intestinal bacterial overgrowth is common in patients with non-alcoholic steatohepatitis on quantitative jejunal aspirate culture."* Indian J Gastroenterol **36**(5): 390-399.

Gicquel, T., Victoni, T., Fautrel, A., Robert, S., Gleonnec, F., Guezingar, M., Couillin, I., Catros, V., Boichot, E. and Lagente, V. (2014). *"Involvement of purinergic receptors and NOD-like receptor-family protein 3-inflammasome pathway in the adenosine triphosphate-induced cytokine release from macrophages."* Clin Exp Pharmacol Physiol **41**(4): 279-286.

Gilmore, T. D. (2006). *"Introduction to NF-kappaB: players, pathways, perspectives."* Oncogene **25**(51): 6680-6684.

Gilmore, T. D. and Gerondakis, S. (2011). *"The c-Rel Transcription Factor in Development and Disease."* Genes Cancer **2**(7): 695-711.

Gleissner, C. A., Leitinger, N. and Ley, K. (2007). *"Effects of native and modified low-density lipoproteins on monocyte recruitment in atherosclerosis."* Hypertension **50**(2): 276-283.

Goldberg, I. J., Eckel, R. H. and Abumrad, N. A. (2009). *"Regulation of fatty acid uptake into tissues: lipoprotein lipase- and CD36-mediated pathways."* J Lipid Res **50**(Suppl): S86-S90.

Goldman, J. L., Sammani, S., Kempf, C., Saadat, L., Letsiou, E., Wang, T., Moreno-Vinasco, L., Rizzo, A. N., Fortman, J. D. and Garcia, J. G. (2014). *"Pleiotropic effects of interleukin-6 in a "two-hit" murine model of acute respiratory distress syndrome."* Pulm Circ **4**(2): 280-288.

Gomez-Coronado, D., Saez, G. T., Lasuncion, M. A. and Herrera, E. (1993). *"Different hydrolytic efficiencies of adipose tissue lipoprotein lipase on very-low-density lipoprotein subfractions separated by heparin-Sepharose chromatography."* Biochim Biophys Acta **1167**(1): 70-78.

Goodwin, G. H. and Johns, E. W. (1973). *"Isolation and characterisation of two calf-thymus chromatin non-histone proteins with high contents of acidic and basic amino acids."* Eur J Biochem **40**(1): 215-219.

Goodwin, G. H., Sanders, C. and Johns, E. W. (1973). *"A new group of chromatin-associated proteins with a high content of acidic and basic amino acids."* Eur J Biochem **38**(1): 14-19.

Gorden, D. L., Ivanova, P. T., Myers, D. S., McIntyre, J. O., VanSaun, M. N., Wright, J. K., Matrisian, L. M. and Brown, H. A. (2011). *"Increased diacylglycerols characterize hepatic lipid changes in progression of human nonalcoholic fatty liver disease; comparison to a murine model."* PLoS ONE **6**(8): e22775.

Gotto, A. M., Jr. (2003). *"Treating hypercholesterolemia: looking forward."* Clin Cardiol **26**(1 Suppl 1): I21-28.

Gregor, M. F., Yang, L., Fabbrini, E., Mohammed, B. S., Eagon, J. C., Hotamisligil, G. S. and Klein, S. (2009). *"Endoplasmic reticulum stress is reduced in tissues of obese subjects after weight loss."* Diabetes **58**(3): 693-700.

Griendling, K. K., Lassegue, B., Murphy, T. J. and Alexander, R. W. (1994). *"Angiotensin II receptor pharmacology."* Adv Pharmacol **28**: 269-306.

Griendling, K. K., Minieri, C. A., Ollerenshaw, J. D. and Alexander, R. W. (1994). *"Angiotensin II stimulates NADH and NADPH oxidase activity in cultured vascular smooth muscle cells."* Circ Res **74**(6): 1141-1148.

Grisendi, G., Finetti, E., Manganaro, D., Cordova, N., Montagnani, G., Spano, C., Prapa, M., Guarneri, V., Otsuru, S., Horwitz, E. M., Mari, G. and Dominici, M. (2015). *"Detection of microparticles from human red blood cells by multiparametric flow cytometry."* Blood Transfusion **13**(2): 274-280.

Grishman, E. K., White, P. C. and Savani, R. C. (2012). *"Toll-like receptors, the NLRP3 inflammasome, and interleukin-1[beta] in the development and progression of type 1 diabetes."* Pediatr Res **71**(6): 626-632.

Guo, H., Callaway, J. B. and Ting, J. P. Y. (2015). *"Inflammasomes: mechanism of action, role in disease, and therapeutics."* Nat Med **21**(7): 677-687.

Guo, J. and Friedman, S. L. (2010). *"Toll-like receptor 4 signaling in liver injury and hepatic fibrogenesis."* Fibrogenesis Tissue Repair **3**: 21.

Gushima, H., Miya, T., Murata, K. and Kimura, A. (1983). *"Construction of glutathione-producing strains of Escherichia coli B by recombinant DNA techniques."* J Appl Biochem **5**(1-2): 43-52.

Guy, C. S., Rankin, S. L. and Michalak, T. I. (2011). *"Hepatocyte cytotoxicity is facilitated by asialoglycoprotein receptor."* Hepatol **54**(3): 1043-1050.

Haagsman, H. P. and Van Golde, L. M. G. (1984). *"Regulation of hepatic triacylglycerol synthesis and secretion."* Vet Res Commun **8**(1): 157-171.

Haczeyni, F., Barn, V., Mridha, A. R., Yeh, M. M., Estevez, E., Febbraio, M. A., Nolan, C. J., Bell-Anderson, K. S., Teoh, N. C. and Farrell, G. C. (2015). *"Exercise improves adipose function and inflammation and ameliorates fatty liver disease in obese diabetic mice."* Obesity (Silver Spring) **23**(9): 1845-1855.

Haczeyni, F., Poekes, L., Wang, H., Mridha, A. R., Barn, V., Geoffrey Haigh, W., Ioannou, G. N., Yeh, M. M., Leclercq, I. A., Teoh, N. C. and Farrell, G. C. (2017). *"Obeticholic acid improves adipose morphometry and inflammation and reduces steatosis in dietary but not metabolic obesity in mice."* Obesity **25**(1): 155-165.

Halliwell, B. (1989). *"Free radicals, reactive oxygen species and human disease: a critical evaluation with special reference to atherosclerosis."* Br J Exp Pathol **70**(6): 737-757.

Han, M. S., Park, S. Y., Shinzawa, K., Kim, S., Chung, K. W., Lee, J. H., Kwon, C. H., Lee, K. W., Lee, J. H., Park, C. K., Chung, W. J., Hwang, J. S., Yan, J. J., Song, D. K., Tsujimoto, Y. and Lee, M. S. (2008). *"Lysophosphatidylcholine as a death effector in the lipoapoptosis of hepatocytes."* J Lipid Res **49**(1): 84-97.

Hanausek-Walaszek, M., Del Rio, M. and Adams, A. K. (1990). *"Structural and immunological identity of p65 tumor-associated factors from rat and mouse hepatocarcinomas."* Prog Clin Biol Res **331**: 109-120.

Hanna, S. M., Kirk, P., Holt, O. J., Puklavec, M. J., Brown, M. H. and Barclay, A. N. (2003). *"A novel form of the membrane protein CD147 that contains an extra Ig-like domain and interacts homophilically."* BMC Biochem **4**: 17.

Hashida, R., Kawaguchi, T., Bekki, M., Omoto, M., Matsuse, H., Nago, T., Takano, Y., Ueno, T., Koga, H., George, J., Shiba, N. and Torimura, T. (2017). *"Aerobic vs. resistance exercise in non-alcoholic fatty liver disease: A systematic review."* J Hepatol **66**(1): 142-152.

Hauser, H., Dyer, J. H., Nandy, A., Vega, M. A., Werder, M., Bieliauskaite, E., Weber, F. E., Compassi, S., Gemperli, A., Boffelli, D., Wehrli, E., Schulthess, G. and Phillips, M. C. (1998). *"Identification of a receptor mediating absorption of dietary cholesterol in the intestine."* Biochemistry (Mosc) **37**(51): 17843-17850.

Havel, R. J. (1998). *"Receptor and non-receptor mediated uptake of chylomicron remnants by the liver."* Atheroscler Suppl **141**(1): S1-S7.

Hayashi, F., Means, T. K. and Luster, A. D. (2003). *"Toll-like receptors stimulate human neutrophil function."* Blood **102**(7): 2660-2669.

Hazra, S., Miyahara, T., Rippe, R. A. and Tsukamoto, H. (2004). *"PPAR Gamma and Hepatic Stellate Cells."* Comp Hepatol **3**(Suppl 1): S7-S7.

He, Y., Hara, H. and Núñez, G. *"Mechanism and Regulation of NLRP3 Inflammasome Activation."* Trends Biochem Sci **41**(12): 1012-1021.

Headland, S. E., Jones, H. R., D'Sa, A. S. V., Perretti, M. and Norling, L. V. (2014). *"Cutting-Edge Analysis of Extracellular Microparticles using ImageStreamX Imaging Flow Cytometry."* Sci Rep **4**.

Hesse, D., Jaschke, A., Chung, B. and Schürmann, A. (2013). *"Trans-Golgi proteins participate in the control of lipid droplet and chylomicron formation."* Biosci Rep **33**(1): e00001.

Hiippala, K., Jouhten, H., Ronkainen, A., Hartikainen, A., Kainulainen, V., Jalanka, J. and Satokari, R. (2018). *"The Potential of Gut Commensals in Reinforcing Intestinal Barrier Function and Alleviating Inflammation."* Nutrients **10**(8).

Hirosumi, J., Tuncman, G., Chang, L., Gorgun, C. Z., Uysal, K. T., Maeda, K., Karin, M. and Hotamisligil, G. S. (2002). *"A central role for JNK in obesity and insulin resistance."* Nature **420**(6913): 333-336.

Holmen, C., Elsheikh, E., Stenvinkel, P., Qureshi, A. R., Pettersson, E., Jalkanen, S. and Sumitran-Holgersson, S. (2005). *"Circulating inflammatory endothelial cells contribute to endothelial progenitor cell dysfunction in patients with vasculitis and kidney involvement."* J Am Soc Nephrol **16**(10): 3110-3120.

Hong, J. T., Yen, J. H., Wang, L., Lo, Y. H., Chen, Z. T. and Wu, M. J. (2009). *"Regulation of heme oxygenase-1 expression and MAPK pathways in response to kaempferol and rhamnocitrin in PC12 cells."* Toxicol Appl Pharmacol **237**(1): 59-68.

Hornung, V., Ablasser, A., Charrel-Dennis, M., Bauernfeind, F., Horvath, G., Caffrey, D. R., Latz, E. and Fitzgerald, K. A. (2009). *"AIM2 recognizes cytosolic dsDNA and forms a caspase-1-activating inflammasome with ASC."* Nature **458**(7237): 514-518.

Houghton, D., Stewart, C. J., Day, C. P. and Trenell, M. (2016). *"Gut Microbiota and Lifestyle Interventions in NAFLD."* Int J Mol Sci **17**(4): 447.

Hreggvidsdottir, H. S., Lundberg, A. M., Aveberger, A. C., Klevenvall, L., Andersson, U. and Harris, H. E. (2012). *"High mobility group box protein 1 (HMGB1)-partner molecule complexes enhance cytokine production by signaling through the partner molecule receptor."* Mol Med **18**: 224-230.

Hritz, I., Mandrekar, P., Velayudham, A., Catalano, D., Dolganiuc, A., Kodys, K., Kurt-Jones, E. and Szabo, G. (2008). *"The critical role of toll-like receptor (TLR) 4 in alcoholic liver disease is independent of the common TLR adapter MyD88."* Hepatol **48**(4): 1224-1231.

Huang, H., Nace, G. W., McDonald, K. A., Tai, S., Klune, J. R., Rosborough, B. R., Ding, Q., Loughran, P., Zhu, X., Beer-Stolz, D., Chang, E. B., Billiar, T. and Tsung, A. (2014). *"Hepatocyte-specific high-mobility group box 1 deletion worsens the injury in liver ischemia/reperfusion: a role for intracellular high-mobility group box 1 in cellular protection."* Hepatol **59**(5): 1984-1997.

Huang, L., Soldevila, G., Leeker, M., Flavell, R. and Crispe, I. N. (1994). *"The liver eliminates T cells undergoing antigen-triggered apoptosis in vivo."* Immunity **1**(9): 741-749.

Huang, P. L. (2009). *"A comprehensive definition for metabolic syndrome."* Dis Model Mech **2**(5-6): 231-237.

Hui, J. M., Hodge, A., Farrell, G. C., Kench, J. G., Kriketos, A. and George, J. (2004). *"Beyond insulin resistance in NASH: TNF-alpha or adiponectin?"* Hepatol **40**(1): 46-54.

Humar, M., Loop, T., Schmidt, R., Hoetzel, A., Roesslein, M., Andriopoulos, N., Pahl, H. L., Geiger, K. K. and Pannen, B. H. (2007). *"The mitogen-activated protein kinase p38 regulates activator protein 1 by direct phosphorylation of c-Jun."* Int J Biochem Cell Biol **39**(12): 2278-2288.

Huxford, T., Huang, D. B., Malek, S. and Ghosh, G. (1998). *"The crystal structure of the IkappaBalpha/NF-kappaB complex reveals mechanisms of NF-kappaB inactivation."* Cell **95**(6): 759-770.

Hylemon, P. B., Pandak, W. M. and Vlahcevic, Z. R. (2001). Regulation of hepatic cholesterol homeostasis. *The liver: biology and pathobiology*. I. M. Arias, J. L. Boyer and N. Fausto. Philadelphia, PA, Lippincott Williams & Wilkins**:** 231-247.

Iacono, K. T., Brown, A. L., Greene, M. I. and Saouaf, S. J. (2007). *"CD147 immunoglobulin superfamily receptor function and role in pathology."* Exp Mol Pathol **83**(3): 283-295.

Iavello, A., Frech, V. S., Gai, C., Deregibus, M. C., Quesenberry, P. J. and Camussi, G. (2016). *"Role of Alix in miRNA packaging during extracellular vesicle biogenesis."* Int J Mol Med **37**(4): 958-966.

Ikonen, E. (2006). *"Mechanisms for cellular cholesterol transport: defects and human disease."* Physiol Rev **86**(4): 1237-1261.

Ikonen, E. (2008). *"Cellular cholesterol trafficking and compartmentalization."* Nat Rev Mol Cell Biol **9**(2): 125-138.

Ilan, Y. (2012). *"Leaky gut and the liver: a role for bacterial translocation in nonalcoholic steatohepatitis."* World J Gastroenterol **18**(21): 2609-2618.

Inamoto, T. and Brown, W. R. (1991). *"IgG is associated with the asialoglycoprotein receptor in the human liver."* Hepatol **14**(6): 1070-1075.

Infante, R. E., Radhakrishnan, A., Abi-Mosleh, L., Kinch, L. N., Wang, M. L., Grishin, N. V., Goldstein, J. L. and Brown, M. S. (2008). *"Purified NPC1 Protein: II. LOCALIZATION OF STEROL BINDING TO A 240-AMINO ACID SOLUBLE LUMINAL LOOP."* J Biol Chem **283**(2): 1064-1075.

Inokuchi, S., Aoyama, T., Miura, K., Osterreicher, C. H., Kodama, Y., Miyai, K., Akira, S., Brenner, D. A. and Seki, E. (2010). *"Disruption of TAK1 in hepatocytes causes hepatic injury, inflammation, fibrosis, and carcinogenesis."* Proc Natl Acad Sci U S A **107**(2): 844-849.

Ioannou, G. N., Haigh, W. G., Thorning, D. and Savard, C. (2013). *"Hepatic cholesterol crystals and crown-like structures distinguish NASH from simple steatosis."* J Lipid Res **54**(5): 1326-1334.

Ioannou, Y. A. (2000). *"The structure and function of the Niemann-Pick C1 protein."* Mol Genet Metab **71**(1-2): 175-181.

Ise, H., Sugihara, N., Negishi, N., Nikaido, T. and Akaike, T. (2001). *"Low asialoglycoprotein receptor expression as markers for highly proliferative potential hepatocytes."* Biochem Biophys Res Commun **285**(2): 172-182.

Isenberg, J. S. and Klaunig, J. E. (2000). *"Role of the mitochondrial membrane permeability transition (MPT) in rotenone-induced apoptosis in liver cells."* Toxicol Sci **53**(2): 340-351.

Itoh, M., Kato, H., Suganami, T., Konuma, K., Marumoto, Y., Terai, S., Sakugawa, H., Kanai, S., Hamaguchi, M., Fukaishi, T., Aoe, S., Akiyoshi, K., Komohara, Y., Takeya, M., Sakaida, I. and Ogawa, Y. (2013). *"Hepatic Crown-Like Structure: A Unique Histological Feature in Non-Alcoholic Steatohepatitis in Mice and Humans."* PLoS ONE **8**(12): e82163.

Ivanov, V. N., Deng, G., Podack, E. R. and Malek, T. R. (1995). *"Pleiotropic effects of Bcl-2 on transcription factors in T cells: potential role of NF-kappa B p50-p50 for the anti-apoptotic function of Bcl-2."* Int Immunol **7**(11): 1709-1720.

Jacobs-Helber, S. M., Wickrema, A., Birrer, M. J. and Sawyer, S. T. (1998). *"AP1 regulation of proliferation and initiation of apoptosis in erythropoietin-dependent erythroid cells."* Mol Cell Biol **18**(7): 3699-3707.

Jacobs, M. D. and Harrison, S. C. (1998). *"Structure of an IkappaBalpha/NF-kappaB complex."* Cell **95**(6): 749-758.

Jaeschke, H. (2003). *"Molecular mechanisms of hepatic ischemia-reperfusion injury and preconditioning."* Am J Physiol Gastrointest Liver Physiol **284**(1): G15-26.

Jaeschke, H. (2003). *"Role of reactive oxygen species in hepatic ischemia-reperfusion injury and preconditioning."* J Invest Surg **16**(3): 127-140.

Jaeschke, H., Knight, T. R. and Bajt, M. L. (2003). *"The role of oxidant stress and reactive nitrogen species in acetaminophen hepatotoxicity."* Toxicol Lett **144**(3): 279-288.

Jander, S. and Stoll, G. (1998). *"Differential induction of interleukin-12, interleukin-18, and interleukin-1beta converting enzyme mRNA in experimental autoimmune encephalomyelitis of the Lewis rat."* J Neuroimmunol **91**(1-2): 93-99.

Janoudi, A., Shamoun, F. E., Kalavakunta, J. K. and Abela, G. S. (2016). *"Cholesterol crystal induced arterial inflammation and destabilization of atherosclerotic plaque."* Eur Heart J **37**(25): 1959-1967.

Jayakumar, S. and Loomba, R. (2019). *"Review article: emerging role of the gut microbiome in the progression of nonalcoholic fatty liver disease and potential therapeutic implications."* Aliment Pharmacol Ther.

Jefcoate, C. (2002). *"High-flux mitochondrial cholesterol trafficking, a specialized function of the adrenal cortex."* J Clin Invest **110**(7): 881-890.

Jefcoate, C. R., Artemenko, I. P. and Zhao, D. (2000). *"Relationship of StAR expression to mitochondrial cholesterol transfer and metabolism."* Endocr Res **26**(4): 663-680.

Jiang, W., Liu, J., Dai, Y., Zhou, N., Ji, C. and Li, X. (2015). *"MiR-146b attenuates high-fat diet-induced non-alcoholic steatohepatitis in mice."* J Gastroenterol Hepatol **30**(5): 933-943.

Jocelyn, P. C. (1970). *"The function of subcellular fractions in the oxidation of glutathione in rat liver homogenate."* Biochem J **117**(5): 951-956.

Jokinen, E. V., Landschulz, K. T., Wyne, K. L., Ho, Y. K., Frykman, P. K. and Hobbs, H. H. (1994). *"Regulation of the very low density lipoprotein receptor by thyroid hormone in rat skeletal muscle."* J Biol Chem **269**(42): 26411-26418.

Josephs, K. A., Van Gerpen, M. W. and Van Gerpen, J. A. (2003). *"Adult onset Niemann-Pick disease type C presenting with psychosis."* J Neurol Neurosurg Psychiatry **74**(4): 528-529.

Julich, H., Willms, A., Lukacs-Kornek, V. and Kornek, M. (2014). *"Extracellular vesicle profiling and their use as potential disease specific biomarker."* Front Immunol **5**: 413.

Jy, W., Mao, W. W., Horstman, L. L., Valant, P. A. and Ahn, Y. S. (1999). *"A flow cytometric assay of platelet activation marker P-selectin (CD62P) distinguishes heparin-induced thrombocytopenia (HIT) from HIT with thrombosis (HITT)."* Thromb Haemost **82**(4): 1255-1259.

Kadowaki, N., Ho, S., Antonenko, S., Malefyt, R. W., Kastelein, R. A., Bazan, F. and Liu, Y. J. (2001). *"Subsets of human dendritic cell precursors express different toll-like receptors and respond to different microbial antigens."* J Exp Med **194**(6): 863-869.

Kaisho, T. and Akira, S. (2006). *"Toll-like receptor function and signaling."* J Allergy Clin Immunol **117**(5): 979-987; quiz 988.

Kakisaka, K., Cazanave, S. C., Fingas, C. D., Guicciardi, M. E., Bronk, S. F., Werneburg, N. W., Mott, J. L. and Gores, G. J. (2012). *"Mechanisms of lysophosphatidylcholine-induced hepatocyte lipoapoptosis."* Am J Physiol Gastrointest Liver Physiol **302**(1): G77-84.

Kakisaka, K., Cazanave, S. C., Werneburg, N. W., Razumilava, N., Mertens, J. C., Bronk, S. F. and Gores, G. J. (2012). *"A hedgehog survival pathway in 'undead' lipotoxic hepatocytes."* J Hepatol **57**(4): 844-851.

Kanellakis, P., Agrotis, A., Kyaw, T. S., Koulis, C., Ahrens, I., Mori, S., Takahashi, H. K., Liu, K., Peter, K., Nishibori, M. and Bobik, A. (2011). *"High-mobility group box protein 1 neutralization reduces development of diet-induced*

atherosclerosis in apolipoprotein e-deficient mice." Arterioscler Thromb Vasc Biol **31**(2): 313-319.

Kaneto, H., Kawamori, D., Nakatani, Y., Gorogawa, S. and Matsuoka, T. A. (2004). *"Oxidative stress and the JNK pathway as a potential therapeutic target for diabetes."* Drug News Perspect **17**(7): 447-453.

Kang, R., Chen, R., Zhang, Q., Hou, W., Wu, S., Cao, L., Huang, J., Yu, Y., Fan, X. G., Yan, Z., Sun, X., Wang, H., Wang, Q., Tsung, A., Billiar, T. R., Zeh, H. J., 3rd, Lotze, M. T. and Tang, D. (2014). *"HMGB1 in health and disease."* Mol Aspects Med.

Kao, Y. H., Jawan, B., Goto, S., Hung, C. T., Lin, Y. C., Nakano, T., Hsu, L. W., Lai, C. Y., Tai, M. H. and Chen, C. L. (2008). *"High-mobility group box 1 protein activates hepatic stellate cells in vitro."* Transplant Proc **40**(8): 2704-2705.

Karin, M. and Ben-Neriah, Y. (2000). *"Phosphorylation meets ubiquitination: the control of NF-[kappa]B activity."* Annu Rev Immunol **18**: 621-663.

Karlsson, M., Kurz, T., Brunk, U. T., Nilsson, S. E. and Frennesson, C. I. (2010). *"What does the commonly used DCF test for oxidative stress really show?"* Biochem J **428**(2): 183-190.

Kasumov, T., Li, L., Li, M., Gulshan, K., Kirwan, J. P., Liu, X., Previs, S., Willard, B., Smith, J. D. and McCullough, A. (2015). *"Ceramide as a mediator of non-alcoholic Fatty liver disease and associated atherosclerosis."* PLoS ONE **10**(5): e0126910.

Kaur, J. (2014). *"A Comprehensive Review on Metabolic Syndrome."* Cardiol Res Pract **2014**: 943162.

Kawano, Y. and Cohen, D. E. (2013). *"Mechanisms of hepatic triglyceride accumulation in non-alcoholic fatty liver disease."* J Gastroenterol **48**(4): 434-441.

Kawasaki, T. and Kawai, T. (2014). *"Toll-like receptor signaling pathways."* Front Immunol **5**: 461.

Kellner-Weibel, G., Geng, Y. J. and Rothblat, G. H. (1999). *"Cytotoxic cholesterol is generated by the hydrolysis of cytoplasmic cholesteryl ester and transported to the plasma membrane."* Atherosclerosis **146**(2): 309-319.

Kellner-Weibel, G., Yancey, P. G., Jerome, W. G., Walser, T., Mason, R. P., Philips, M. C. and Rothblat, G. H. (1999). *"Crystallization of free cholesterol in model macrophage foam cells."* Arterioscler Thromb Vasc Biol **19**: 1891-1898.

Kieser, A., Kaiser, C. and Hammerschmidt, W. (1999). *"LMP1 signal transduction differs substantially from TNF receptor 1 signaling in the molecular functions of TRADD and TRAF2."* EMBO J **18**(9): 2511-2521.

King, S. R., Manna, P. R., Ishii, T., Syapin, P. J., Ginsberg, S. D., Wilson, K., Walsh, L. P., Parker, K. L., Stocco, D. M., Smith, R. G. and Lamb, D. J. (2002). *"An essential component in steroid synthesis, the steroidogenic acute regulatory protein, is expressed in discrete regions of the brain."* J Neurosci **22**(24): 10613-10620.

Kiyici, M., Gulten, M., Gurel, S., Nak, S. G., Dolar, E., Savci, G., Adim, S. B., Yerci, O. and Memik, F. (2003). *"Ursodeoxycholic acid and atorvastatin in the treatment of nonalcoholic steatohepatitis."* Can J Gastroenterol **17**(12): 713-718.

Klein, E. A. and Assoian, R. K. (2008). *"Transcriptional regulation of the cyclin D1 gene at a glance."* J Cell Sci **121**(23): 3853-3857.

Kleiner, D. E., Brunt, E. M., Van Natta, M., Behling, C., Contos, M. J., Cummings, O. W., Ferrell, L. D., Liu, Y. C., Torbenson, M. S., Unalp-Arida, A., Yeh,

M., McCullough, A. J., Sanyal, A. J. and Nonalcoholic Steatohepatitis Clinical Research, N. (2005). *"Design and validation of a histological scoring system for nonalcoholic fatty liver disease."* Hepatol **41**(6): 1313-1321.

Klune, J. R., Dhupar, R., Cardinal, J., Billiar, T. R. and Tsung, A. (2008). *"HMGB1: endogenous danger signaling."* Mol Med **14**(7-8): 476-484.

Kodama, Y. and Brenner, D. A. (2009). *"c-Jun N-terminal kinase signaling in the pathogenesis of nonalcoholic fatty liver disease: Multiple roles in multiple steps."* Hepatol **49**(1): 6-8.

Kodama, Y., Kisseleva, T., Iwaisako, K., Miura, K., Taura, K., De Minicis, S., Osterreicher, C. H., Schnabl, B., Seki, E. and Brenner, D. A. (2009). *"c-Jun N-terminal kinase-1 from hematopoietic cells mediates progression from hepatic steatosis to steatohepatitis and fibrosis in mice."* Gastroenterology **137**(4): 1467-1477 e1465.

Kodama, Y., Taura, K., Miura, K., Schnabl, B., Osawa, Y. and Brenner, D. A. (2009). *"Antiapoptotic effect of c-Jun N-terminal Kinase-1 through Mcl-1 stabilization in TNF-induced hepatocyte apoptosis."* Gastroenterology **136**(4): 1423-1434.

Koek, G. H., Liedorp, P. R. and Bast, A. (2011). *"The role of oxidative stress in non-alcoholic steatohepatitis."* Clin Chim Acta **412**(15-16): 1297-1305.

Kojer, K., Bien, M., Gangel, H., Morgan, B., Dick, T. P. and Riemer, J. (2012). *"Glutathione redox potential in the mitochondrial intermembrane space is linked to the cytosol and impacts the Mia40 redox state."* EMBO J **31**(14): 3169-3182.

Kojima, H., Sakurai, S., Uemura, M., Fukui, H., Morimoto, H. and Tamagawa, Y. (2007). *"Mitochondrial abnormality and oxidative stress in nonalcoholic steatohepatitis."* Alcohol Clin Exp Res **31**(1 Suppl): S61-66.

Kornek, M., Lynch, M., Mehta, S. H., Lai, M., Exley, M., Afdhal, N. H. and Schuppan, D. (2012). *"Circulating microparticles as disease-specific biomarkers of severity of inflammation in patients with hepatitis C or nonalcoholic steatohepatitis."* Gastroenterology **143**(2): 448-458.

Korytowski, W., Pilat, A., Schmitt, J. C. and Girotti, A. W. (2013). *"Deleterious Cholesterol Hydroperoxide Trafficking in Steroidogenic Acute Regulatory (StAR) Protein-expressing MA-10 Leydig Cells: implications for oxidative stress-impaired steroidognesis."* J Biol Chem **288**(16): 11509-11519.

Koumangoye, R. B., Sakwe, A. M., Goodwin, J. S., Patel, T. and Ochieng, J. (2011). *"Detachment of breast tumor cells induces rapid secretion of exosomes which subsequently mediate cellular adhesion and spreading."* PLoS ONE **6**(9): e24234.

Kunjathoor, V. V., Febbraio, M., Podrez, E. A., Moore, K. J., Andersson, L., Koehn, S., Rhee, J. S., Silverstein, R., Hoff, H. F. and Freeman, M. W. (2002). *"Scavenger receptors class A-I/II and CD36 are the principal receptors responsible for the uptake of modified low density lipoprotein leading to lipid loading in macrophages."* J Biol Chem **277**(51): 49982-49988.

Kwak, H.-B. (2013). *"Exercise and obesity-induced insulin resistance in skeletal muscle."* Integr Med Res **2**(4): 131-138.

Lacroix, R., Judicone, C., Poncelet, P., Robert, S., Arnaud, L., Sampol, J. and Dignat-George, F. (2012). *"Impact of pre-analytical parameters on the measurement of circulating microparticles: towards standardization of protocol."* J Thromb Haemost **10**(3): 437-446.

Lake, A. D., Novak, P., Hardwick, R. N., Flores-Keown, B., Zhao, F., Klimecki, W. T. and Cherrington, N. J. (2014). *"The adaptive endoplasmic reticulum stress*

response to lipotoxicity in progressive human nonalcoholic fatty liver disease." Toxicol Sci **137**(1): 26-35.

Lalor, P. F., Lai, W. K., Curbishley, S. M., Shetty, S. and Adams, D. H. (2006). *"Human hepatic sinusoidal endothelial cells can be distinguished by expression of phenotypic markers related to their specialised functions in vivo."* World J Gastroenterol **12**(34): 5429-5439.

Lam, B. and Younossi, Z. M. (2010). *"Treatment options for nonalcoholic fatty liver disease."* Therap Adv Gastroenterol **3**(2): 121-137.

Lambertucci, R. H., Hirabara, S. M., Silveira Ldos, R., Levada-Pires, A. C., Curi, R. and Pithon-Curi, T. C. (2008). *"Palmitate increases superoxide production through mitochondrial electron transport chain and NADPH oxidase activity in skeletal muscle cells."* J Cell Physiol **216**(3): 796-804.

Lange, Y. and Steck, T. L. (1997). *"Quantitation of the pool of cholesterol associated with acyl-CoA:cholesterol acyltransferase in human fibroblasts."* J Biol Chem **272**(20): 13103-13108.

Lange, Y., Swaisgood, M. H., Ramos, B. V. and Steck, T. L. (1989). *"Plasma membranes contain half the phospholipid and 90% of the cholesterol and sphingomyelin in cultured human fibroblasts."* J Biol Chem **264**(7): 3786-3793.

Larter, C. Z., Chitturi, S., Heydet, D. and Farrell, G. C. (2010). *"A fresh look at NASH pathogenesis. Part 1: the metabolic movers."* J Gastroenterol Hepatol **25**(4): 672-690.

Larter, C. Z., Yeh, M. M., Haigh, W. G., Van Rooyen, D. M., Brooling, J., Heydet, D., Nolan, C. J., Teoh, N. C. and Farrell, G. C. (2013). *"Dietary modification dampens liver inflammation and fibrosis in obesity-related fatty liver disease."* Obesity (Silver Spring) **21**(6): 1189-1199.

Larter, C. Z., Yeh, M. M., Van Rooyen, D. M., Teoh, N. C., Brooling, J., Hou, J. Y., Williams, J., Clyne, M., Nolan, C. J. and Farrell, G. C. (2009). *"Roles of adipose restriction and metabolic factors in progression of steatosis to steatohepatitis in obese, diabetic mice."* J Gastroenterol Hepatol **24**(10): 1658-1668.

Laurin, J., Lindor, K. D., Crippin, J. S., Gossard, A., Gores, G. J., Ludwig, J., Rakela, J. and McGill, D. B. (1996). *"Ursodeoxycholic acid or clofibrate in the treatment of non-alcohol-induced steatohepatitis: a pilot study."* Hepatol **23**(6): 1464-1467.

Lauterburg, B. H., Adams, J. D. and Mitchell, J. R. (1984). *"Hepatic glutathione homeostasis in the rat: efflux accounts for glutathione turnover."* Hepatol **4**(4): 586-590.

Lauterburg, B. H., Smith, C. V., Hughes, H. and Mitchell, J. R. (1984). *"Biliary excretion of glutathione and glutathione disulfide in the rat. Regulation and response to oxidative stress."* J Clin Invest **73**(1): 124-133.

Le, T. H., Caldwell, S. H., Redick, J. A., Sheppard, B. L., Davis, C. A., Arseneau, K. O., Iezzoni, J. C., Hespenheide, E. E., Al-Osaimi, A. and Peterson, T. C. (2004). *"The zonal distribution of megamitochondria with crystalline inclusions in nonalcoholic steatohepatitis."* Hepatol **39**(5): 1423-1429.

Leamy, A. K., Egnatchik, R. A. and Young, J. D. (2013). *"Molecular Mechanisms and the Role of Saturated Fatty Acids in the Progression of Non-Alcoholic Fatty Liver Disease."* Prog Lipid Res **52**(1): 10.1016/j.plipres.2012.1010.1004.

LeBel, C. P., Ischiropoulos, H. and Bondy, S. C. (1992). *"Evaluation of the probe 2',7'-dichlorofluorescin as an indicator of reactive oxygen species formation and oxidative stress."* Chem Res Toxicol **5**(2): 227-231.

Leclercq, I. A., Van Rooyen, D. M. and Farrell, G. C. (2011). *"Hepatic endoplasmic reticulum stress in obesity: deeper insights into processes, but are they relevant to nonalcoholic steatohepatitis?"* Hepatol **54**(6): 2260-2265.

Ledesma, M. D. and Dotti, C. G. (2005). *"The conflicting role of brain cholesterol in Alzheimer's disease: lessons from the brain plasminogen system."* Biochem Soc Symp(72): 129-138.

Lee, J., Xu, Y., Chen, Y., Sprung, R., Kim, S. C., Xie, S. and Zhao, Y. (2007). *"Mitochondrial phosphoproteome revealed by an improved IMAC method and MS/MS/MS."* Mol Cell Proteomics **6**(4): 669-676.

Lee, S. Y., Reichlin, A., Santana, A., Sokol, K. A., Nussenzweig, M. C. and Choi, Y. (1997). *"TRAF2 is essential for JNK but not NF-kappaB activation and regulates lymphocyte proliferation and survival."* Immunity **7**(5): 703-713.

Lee, Y., Hirose, H., Ohneda, M., Johnson, J. H., McGarry, J. D. and Unger, R. H. (1994). *"Beta-cell lipotoxicity in the pathogenesis of non-insulin-dependent diabetes mellitus of obese rats: impairment in adipocyte-beta-cell relationships."* Proc Natl Acad Sci U S A **91**(23): 10878-10882.

Legry, V., Van Rooyen, D. M., Lambert, B., Sempoux, C., Poekes, L., Espanol-Suner, R., Molendi-Coste, O., Horsmans, Y., Farrell, G. C. and Leclercq, I. A. (2014). *"Endoplasmic reticulum stress does not contribute to steatohepatitis in obese and insulin-resistant high-fat-diet-fed foz/foz mice."* Clin Sci (Lond) **127**(7): 507-518.

Lemoinne, S., Thabut, D., Housset, C., Moreau, R., Valla, D., Boulanger, C. M. and Rautou, P.-E. (2014). *"The emerging roles of microvesicles in liver diseases."* Nat Rev Gastroenterol Hepatol **11**(6): 350-361.

Leung, L., Kwong, M., Hou, S., Lee, C. and Chan, J. Y. (2003). *"Deficiency of the Nrf1 and Nrf2 transcription factors results in early embryonic lethality and severe oxidative stress."* J Biol Chem **278**(48): 48021-48029.

Leuschner, U. F., Lindenthal, B., Herrmann, G., Arnold, J. C., Rossle, M., Cordes, H. J., Zeuzem, S., Hein, J., Berg, T. and Group, N. S. (2010). *"High-dose ursodeoxycholic acid therapy for nonalcoholic steatohepatitis: a double-blind, randomized, placebo-controlled trial."* Hepatol **52**(2): 472-479.

Li, H., Yin, H., Zhang, H., Cao, X., Wang, Z. and She, M. (2002). *"Effect of NF-kappaB on the induction of PDGF-B transcription by angiotensin II in the ECV304 cell line."* Chin Med J (Engl) **115**(3): 433-438.

Li, L., Chen, L. and Hu, L. (2011). *"Nuclear Factor High-mobility Group Box1 Mediating the Activation of Toll-like Receptor 4 Signaling in Hepatocytes in the Early Stage of Non-alcoholic Fatty Liver Disease in Mice."* J Clin Exp Hepatol **1**(2): 123-124.

Li, L., Chen, L., Hu, L., Liu, Y., Sun, H. Y., Tang, J., Hou, Y. J., Chang, Y. X., Tu, Q. Q., Feng, G. S., Shen, F., Wu, M. C. and Wang, H. Y. (2011). *"Nuclear factor high-mobility group box1 mediating the activation of Toll-like receptor 4 signaling in hepatocytes in the early stage of nonalcoholic fatty liver disease in mice."* Hepatol **54**(5): 1620-1630.

Li, L. C., Gao, J. and Li, J. (2014). *"Emerging role of HMGB1 in fibrotic diseases."* J Cell Mol Med **18**(12): 2331-2339.

Li, P., Nijhawan, D., Budihardjo, I., Srinivasula, S. M., Ahmad, M., Alnemri, E. S. and Wang, X. (1997). *"Cytochrome c and dATP-dependent formation of Apaf-1/caspase-9 complex initiates an apoptotic protease cascade."* Cell **91**(4): 479-489.

Li, X., Yue, Y., Zhu, Y. and Xiong, S. (2015). *"Extracellular, but not intracellular HMGB1, facilitates self-DNA induced macrophage activation via promoting*

DNA accumulation in endosomes and contributes to the pathogenesis of lupus nephritis." Mol Immunol **65**(1): 177-188.

Li, Z. Z., Berk, M., McIntyre, T. M. and Feldstein, A. E. (2009). *"Hepatic lipid partitioning and liver damage in nonalcoholic fatty liver disease: role of stearoyl-CoA desaturase."* J Biol Chem **284**(9): 5637-5644.

Liao, W., Hui, T. Y., Young, S. G. and Davis, R. A. (2003). *"Blocking microsomal triglyceride transfer protein interferes with apoB secretion without causing retention or stress in the ER."* J Lipid Res **44**(5): 978-985.

Lieberman, M. and Marks, A. D. (2005). *Basic medical biochemistry: a clinical approach. 3rd Edition*. New York, Wolters Kluwer.

Lim, A. K., Ma, F. Y., Nikolic-Paterson, D. J., Ozols, E., Young, M. J., Bennett, B. L., Friedman, G. C. and Tesch, G. H. (2011). *"Evaluation of JNK blockade as an early intervention treatment for type 1 diabetic nephropathy in hypertensive rats."* Am J Nephrol **34**(4): 337-346.

Lindor, K. D., Kowdley, K. V., Heathcote, E. J., Harrison, M. E., Jorgensen, R., Angulo, P., Lymp, J. F., Burgart, L. and Colin, P. (2004). *"Ursodeoxycholic acid for treatment of nonalcoholic steatohepatitis: results of a randomized trial."* Hepatol **39**(3): 770-778.

Liscum, L. and Munn, N. J. (1999). *"Intracellular cholesterol transport."* Biochim Biophys Acta **1438**(1): 19-37.

Listenberger, L. L., Han, X., Lewis, S. E., Cases, S., Farese, R. V., Jr., Ory, D. S. and Schaffer, J. E. (2003). *"Triglyceride accumulation protects against fatty acid-induced lipotoxicity."* Proc Natl Acad Sci U S A **100**(6): 3077-3082.

Liu, B., Novick, D., Kim, S. H. and Rubinstein, M. (2000). *"Production of a biologically active human interleukin 18 requires its prior synthesis as PRO-IL-18."* Cytokine **12**(10): 1519-1525.

Liu, Z. G., Hsu, H., Goeddel, D. V. and Karin, M. (1996). *"Dissection of TNF receptor 1 effector functions: JNK activation is not linked to apoptosis while NF-kappaB activation prevents cell death."* Cell **87**(3): 565-576.

Llorente, A., van Deurs, B. and Sandvig, K. (2007). *"Cholesterol regulates prostasome release from secretory lysosomes in PC-3 human prostate cancer cells."* Eur J Cell Biol **86**(7): 405-415.

Lo, Y. C., Brett, L., Kenyon, C. J., Morley, S. D., Mason, J. I. and Williams, B. C. (1998). *"StAR protein is expressed in both medulla and cortex of the bovine and rat adrenal gland."* Endocr Res **24**(3-4): 559-563.

Lolmede, K., Campana, L., Vezzoli, M., Bosurgi, L., Tonlorenzi, R., Clementi, E., Bianchi, M. E., Cossu, G., Manfredi, A. A., Brunelli, S. and Rovere-Querini, P. (2009). *"Inflammatory and alternatively activated human macrophages attract vessel-associated stem cells, relying on separate HMGB1- and MMP-9-dependent pathways."* J Leukoc Biol **85**(5): 779-787.

Loomba, R., Seguritan, V., Li, W., Long, T., Klitgord, N., Bhatt, A., Dulai, P. S., Caussy, C., Bettencourt, R., Highlander, S. K., Jones, M. B., Sirlin, C. B., Schnabl, B., Brinkac, L., Schork, N., Chen, C. H., Brenner, D. A., Biggs, W., Yooseph, S., Venter, J. C. and Nelson, K. E. (2017). *"Gut Microbiome-Based Metagenomic Signature for Non-invasive Detection of Advanced Fibrosis in Human Nonalcoholic Fatty Liver Disease."* Cell Metab **25**(5): 1054-1062 e1055.

Lougheed, M., Lum, C. M., Ling, W., Suzuki, H., Kodama, T. and Steinbrecher, U. (1997). *"High affinity saturable uptake of oxidized low density lipoprotein by macrophages from mice lacking the scavenger receptor class A type I/II."* J Biol Chem **272**(20): 12938-12944.

Lougheed, M., Moore, E. D., Scriven, D. R. and Steinbrecher, U. P. (1999). *"Uptake of oxidized LDL by macrophages differs from that of acetyl LDL and leads to expansion of an acidic endolysosomal compartment."* Arterioscler Thromb Vasc Biol **19**(8): 1881-1890.

Lu, B., Nakamura, T., Inouye, K., Li, J., Tang, Y., Lundback, P., Valdes-Ferrer, S. I., Olofsson, P. S., Kalb, T., Roth, J., Zou, Y., Erlandsson-Harris, H., Yang, H., Ting, J. P., Wang, H., Andersson, U., Antoine, D. J., Chavan, S. S., Hotamisligil, G. S. and Tracey, K. J. (2012). *"Novel role of PKR in inflammasome activation and HMGB1 release."* Nature **488**(7413): 670-674.

Lu, F. Q., Kang, W., Peng, Y. and Wang, W. M. (2011). *"Characterization of blood components separated from donated whole blood after an overnight holding at room temperature with the buffy coat method."* Transfusion (Paris) **51**(10): 2199-2207.

Luan, Z. G., Zhang, H., Yang, P. T., Ma, X. C., Zhang, C. and Guo, R. X. (2010). *"HMGB1 activates nuclear factor-kappaB signaling by RAGE and increases the production of TNF-alpha in human umbilical vein endothelial cells."* Immunobiology **215**(12): 956-962.

Ludwig, J., Viggiano, T. R., McGill, D. B. and Oh, B. J. (1980). *"Nonalcoholic steatohepatitis: Mayo Clinic experiences with a hitherto unnamed disease."* Mayo Clin Proc **55**(7): 434-438.

Lusis, A. J., Fogelman, A. M. and Fonarow, G. C. (2004). *"Genetic Basis of Atherosclerosis: Part I: New Genes and Pathways."* Circulation **110**(13): 1868-1873.

Lynch, S. F. and Ludlam, C. A. (2007). *"Plasma microparticles and vascular disorders."* Br J Haematol **137**(1): 36-48.

Ma, F. Y., Flanc, R. S., Tesch, G. H., Bennett, B. L., Friedman, G. C. and Nikolic-Paterson, D. J. (2009). *"Blockade of the c-Jun amino terminal kinase prevents crescent formation and halts established anti-GBM glomerulonephritis in the rat."* Lab Invest **89**(4): 470-484.

Ma, F. Y., Liu, J. and Nikolic-Paterson, D. J. (2009). *"The role of stress-activated protein kinase signaling in renal pathophysiology."* Braz J Med Biol Res **42**(1): 29-37.

Ma, K. L., Ruan, X. Z., Powis, S. H., Chen, Y., Moorhead, J. F. and Varghese, Z. (2007). *"Sirolimus modifies cholesterol homeostasis in hepatic cells: a potential molecular mechanism for sirolimus-associated dyslipidemia."* Transplantation **84**(8): 1029-1036.

Ma, Y.-Y., Li, L., Yu, C.-H., Shen, Z., Chen, L.-H. and Li, Y.-M. (2013). *"Effects of probiotics on nonalcoholic fatty liver disease: a meta-analysis."* World J Gastroenterol **19**(40): 6911-6918.

Macaluso, F. S., Maida, M. and Petta, S. (2015). *"Genetic background in nonalcoholic fatty liver disease: A comprehensive review."* World J Gastroenterol **21**(39): 11088-11111.

Madamanchi, N. R., Hakim, Z. S. and Runge, M. S. (2005). *"Oxidative stress in atherogenesis and arterial thrombosis: the disconnect between cellular studies and clinical outcomes."* J Thromb Haemost **3**(2): 254-267.

Madamanchi, N. R., Vendrov, A. and Runge, M. S. (2005). *"Oxidative stress and vascular disease."* Arterioscler Thromb Vasc Biol **25**(1): 29-38.

Mahley, R. W. (2002). Biochemistry and physiology of lipid and lipoprotein metabolism. *Principles and practice of endocrinology and metabolism*. K. L. Becker, K. L. Bilezikian, J. P. Bremner et al., LWW**:** 1503-1527.

Makri, E., Cholongitas, E. and Tziomalos, K. (2016). *"Emerging role of obeticholic acid in the management of nonalcoholic fatty liver disease."* World J Gastroenterol **22**(41): 9039-9043.

Malaguarnera, M., Di Rosa, M., Nicoletti, F. and Malaguarnera, L. (2009). *"Molecular mechanisms involved in NAFLD progression."* J Mol Med (Berl) **87**(7): 679-695.

Malhi, H., Barreyro, F. J., Isomoto, H., Bronk, S. F. and Gores, G. J. (2007). *"Free fatty acids sensitise hepatocytes to TRAIL mediated cytotoxicity."* Gut **56**(8): 1124-1131.

Malhi, H., Bronk, S. F., Werneburg, N. W. and Gores, G. J. (2006). *"Free Fatty Acids Induce JNK-dependent Hepatocyte Lipoapoptosis."* J Biol Chem **281**(17): 12093-12101.

Malhi, H. and Kaufman, R. J. (2011). *"Endoplasmic reticulum stress in liver disease."* J Hepatol **54**(4): 795-809.

Malik, T. H., Cortini, A., Carassiti, D., Boyle, J. J., Haskard, D. O. and Botto, M. (2010). *"The alternative pathway is critical for pathogenic complement activation in endotoxin- and diet-induced atherosclerosis in low-density lipoprotein receptor-deficient mice."* Circulation **122**(19): 1948-1956.

Maneschi, E., Vignozzi, L., Morelli, A., Mello, T., Filippi, S., Cellai, I., Comeglio, P., Sarchielli, E., Calcagno, A., Mazzanti, B., Vettor, R., Vannelli, G. B., Adorini, L. and Maggi, M. (2013). *"FXR activation normalizes insulin sensitivity in visceral preadipocytes of a rabbit model of MetS."* J Endocrinol **218**(2): 215-231.

Mann, J. and Skeaff, M. (1998). Lipids. *Essentials of human nutrition.* J. Mann and A. S. Truswell. New York, Oxford University Press**:** 29-47.

Manna, S. K. and Aggarwal, B. B. (1999). *"Lipopolysaccharide inhibits TNF-induced apoptosis: role of nuclear factor-kappaB activation and reactive oxygen intermediates."* J Immunol **162**(3): 1510-1518.

Marchesini, G., Brizi, M., Bianchi, G., Tomassetti, S., Bugianesi, E., Lenzi, M., McCullough, A. J., Natale, S., Forlani, G. and Melchionda, N. (2001). *"Nonalcoholic fatty liver disease: a feature of the metabolic syndrome."* Diabetes **50**(8): 1844-1850.

Mareni, C. and Gaetani, G. F. (1976). *"NADP+ and NADPH in glucose-6-phosphate dehydrogenase-deficient erythrocytes under oxidative stimulation."* Biochim Biophys Acta **430**(3): 395-398.

Mari, M., Caballero, F., Colell, A., Morales, A., Caballeria, J., Fernandez, A., Enrich, C., Fernandez-Checa, J. C. and Garcia-Ruiz, C. (2006). *"Mitochondrial free cholesterol loading sensitizes to TNF- and Fas-mediated steatohepatitis."* Cell Metab **4**(3): 185-198.

Mari, M., Colell, A., Morales, A., Caballero, F., Moles, A., Fernandez, A., Terrones, O., Basanez, G., Antonsson, B., Garcia-Ruiz, C. and Fernandez-Checa, J. C. (2008). *"Mechanism of mitochondrial glutathione-dependent hepatocellular susceptibility to TNF despite NF-kappaB activation."* Gastroenterology **134**(5): 1507-1520.

Mari, M., Morales, A., Colell, A., Garcia-Ruiz, C., Kaplowitz, N. and Fernandez-Checa, J. C. (2013). *"Mitochondrial glutathione: features, regulation and role in disease."* Biochim Biophys Acta **1830**(5): 3317-3328.

Mariathasan, S. and Monack, D. M. (2007). *"Inflammasome adaptors and sensors: intracellular regulators of infection and inflammation."* Nat Rev Immunol **7**(1): 31-40.

Marth, J. D. and Grewal, P. K. (2008). *"Mammalian glycosylation in immunity."* Nat Rev Immunol **8**(11): 874-887.

Martin Mateos, R. and Allen, A. M. (2019). *"Characterizing specific subgroups in patients with NAFLD: overweight vs obese phenotype."* Rev Esp Enferm Dig **111**(4): 253-255.

Martínez, L., Torres, S., Baulies, A., Alarcón-Vila, C., Elena, M., Fabriàs, G., Casas, J., Caballeria, J., Fernandez-Checa, J. C. and García-Ruiz, C. (2015). *"Myristic acid potentiates palmitic acid-induced lipotoxicity and steatohepatitis associated with lipodystrophy by sustaning de novo ceramide synthesis."* Oncotarget **6**(39): 41479-41496.

Masuda, D., Hirano, K.-i., Oku, H., Sandoval, J. C., Kawase, R., Yuasa-Kawase, M., Yamashita, Y., Takada, M., Tsubakio-Yamamoto, K., Tochino, Y., Koseki, M., Matsuura, F., Nishida, M., Kawamoto, T., Ishigami, M., Hori, M., Shimomura, I. and Yamashita, S. (2009). *"Chylomicron remnants are increased in the postprandial state in CD36 deficiency."* J Lipid Res **50**(5): 999-1011.

Matsuguchi, T., Masuda, A., Sugimoto, K., Nagai, Y. and Yoshikai, Y. (2003). *"JNK-interacting protein 3 associates with Toll-like receptor 4 and is involved in LPS-mediated JNK activation."* The EMBO Journal **22**(17): 4455-4464.

Mattey, D. L. and Garrod, D. R. (1986). *"Calcium-induced desmosome formation in cultured kidney epithelial cells."* J Cell Sci **85**: 95-111.

McCoy, A. J., Koizumi, Y., Higa, N. and Suzuki, T. (2010). *"Differential regulation of caspase-1 activation via NLRP3/NLRC4 inflammasomes mediated by aerolysin and type III secretion system during Aeromonas veronii infection."* J Immunol **185**(11): 7077-7084.

McCullough, A. J. (2004). *"The clinical features, diagnosis and natural history of nonalcoholic fatty liver disease."* Clin Liver Dis **8**(3): 521-533, viii.

McCuskey, R. S. (1986). Microscopic methods for studying the microvasculature of internal organs. *Physical techniques in biology and medicine microvascual technology*. C. H. Baker and W. F. Nastuk. New York, Academic Press**:** 247-264.

McCuskey, R. S. and McCuskey, P. A. (1990). *"Fine structure and function of Kupffer cells."* J Electron Microsc Tech **14**(3): 237-246.

McIlwain, D. R., Berger, T. and Mak, T. W. (2013). *"Caspase functions in cell death and disease."* Cold Spring Harb Perspect Biol **5**(4): a008656.

Meli, R., Mattace Raso, G. and Calignano, A. (2014). *"Role of innate immune response in non-alcoholic Fatty liver disease: metabolic complications and therapeutic tools."* Front Immunol **5**: 177.

Mencacci, A., Bacci, A., Cenci, E., Montagnoli, C., Fiorucci, S., Casagrande, A., Flavell, R. A., Bistoni, F. and Romani, L. (2000). *"Interleukin 18 restores defective Th1 immunity to Candida albicans in caspase 1-deficient mice."* Infect Immun **68**(9): 5126-5131.

Meshkani, R. and Adeli, K. (2009). *"Hepatic insulin resistance, metabolic syndrome and cardiovascular disease."* Clin Biochem **42**(13-14): 1331-1346.

Meyer, R., Hatada, E. N., Hohmann, H. P., Haiker, M., Bartsch, C., Rothlisberger, U., Lahm, H. W., Schlaeger, E. J., van Loon, A. P. and Scheidereit, C. (1991). *"Cloning of the DNA-binding subunit of human nuclear factor kappa B: the level of its mRNA is strongly regulated by phorbol ester or tumor necrosis factor alpha."* Proc Natl Acad Sci U S A **88**(3): 966-970.

Miao, E. A., Mao, D. P., Yudkovsky, N., Bonneau, R., Lorang, C. G., Warren, S. E., Leaf, I. A. and Aderem, A. (2010). *"Innate immune detection of the type III*

secretion apparatus through the NLRC4 inflammasome." Proc Natl Acad Sci U S A **107**(7): 3076-3080.

Miller, W. L. and Bose, H. S. (2011). *"Early steps in steroidogenesis: intracellular cholesterol trafficking: Thematic Review Series: Genetics of Human Lipid Diseases."* J Lipid Res **52**(12): 2111-2135.

Millet, P., McCall, C. and Yoza, B. (2013). *"RelB: an outlier in leukocyte biology."* J Leukoc Biol **94**(5): 941-951.

Milosevic, I., Vujovic, A., Barac, A., Djelic, M., Korac, M., Radovanovic Spurnic, A., Gmizic, I., Stevanovic, O., Djordjevic, V., Lekic, N., Russo, E. and Amedei, A. (2019). *"Gut-Liver Axis, Gut Microbiota, and Its Modulation in the Management of Liver Diseases: A Review of the Literature."* Int J Mol Sci **20**(2).

Min, H. K., Kapoor, A., Fuchs, M., Mirshahi, F., Zhou, H., Maher, J., Kellum, J., Warnick, R., Contos, M. J. and Sanyal, A. J. (2012). *"Increased hepatic synthesis and dysregulation of cholesterol metabolism is associated with the severity of nonalcoholic fatty liver disease."* Cell Metab **15**(5): 665-674.

Mindell, J. A. (2012). *"Lysosomal acidification mechanisms."* Annu Rev Physiol **74**: 69-86.

Minkiewicz, J., de Rivero Vaccari, J. P. and Keane, R. W. (2013). *"Human astrocytes express a novel NLRP2 inflammasome."* Glia **61**(7): 1113-1121.

Miquilena-Colina, M. E., Lima-Cabello, E., Sanchez-Campos, S., Garcia-Mediavilla, M. V., Fernandez-Bermejo, M., Lozano-Rodriguez, T., Vargas-Castrillon, J., Buque, X., Ochoa, B., Aspichueta, P., Gonzalez-Gallego, J. and Garcia-Monzon, C. (2011). *"Hepatic fatty acid translocase CD36 upregulation is associated with insulin resistance, hyperinsulinaemia and increased steatosis in non-alcoholic steatohepatitis and chronic hepatitis C."* Gut **60**(10): 1394-1402.

Miserez, A. R., Muller, P. Y., Barella, L., Barella, S., Staehelin, H. B., Leitersdorf, E., Kark, J. D. and Friedlander, Y. (2002). *"Sterol-regulatory element-binding protein (SREBP)-2 contributes to polygenic hypercholesterolaemia."* Atherosclerosis **164**(1): 15-26.

Misra, V. L., Khashab, M. and Chalasani, N. (2009). *"Non-Alcoholic Fatty Liver Disease and Cardiovascular Risk."* Curr Gastroenterol Rep **11**(1): 50-55.

Mitjavila-Garcia, M. T., Cailleret, M., Godin, I., Nogueira, M. M., Cohen-Solal, K., Schiavon, V., Lecluse, Y., Le Pesteur, F., Lagrue, A. H. and Vainchenker, W. (2002). *"Expression of CD41 on hematopoietic progenitors derived from embryonic hematopoietic cells."* Development **129**(8): 2003-2013.

Miura, K. and Ohnishi, H. (2014). *"Role of gut microbiota and Toll-like receptors in nonalcoholic fatty liver disease."* World J Gastroenterol **20**(23): 7381-7391.

Miura, K., Seki, E., Ohnishi, H. and Brenner, D. A. (2010). *"Role of toll-like receptors and their downstream molecules in the development of nonalcoholic Fatty liver disease."* Gastroenterol Res Pract **2010**: 362847.

Miura, K., Yang, L., van Rooijen, N., Brenner, D. A., Ohnishi, H. and Seki, E. (2013). *"TLR2 and palmitic acid cooperatively contribute to the development of nonalcoholic steatohepatitis through inflammasome activation."* Hepatol **57**(2): 577-589.

Miura, K., Yang, L., van Rooijen, N., Brenner, D. A., Ohnishi, H. and Seki, E. (2013). *"Toll-like receptor 2 and palmitic acid cooperatively contribute to the development of nonalcoholic steatohepatitis through inflammasome activation in mice."* Hepatol **57**(2): 577-589.

Miyagi, T., Takehara, T., Tatsumi, T., Kanto, T., Suzuki, T., Jinushi, M., Sugimoto, Y., Sasaki, Y., Hori, M. and Hayashi, N. (2003). *"CD1d-mediated*

stimulation of natural killer T cells selectively activates hepatic natural killer cells to eliminate experimentally disseminated hepatoma cells in murine liver." Int J Cancer **106**(1): 81-89.

Monetti, M., Levin, M. C., Watt, M. J., Sajan, M. P., Marmor, S., Hubbard, B. K., Stevens, R. D., Bain, J. R., Newgard, C. B., Farese, R. V., Sr., Hevener, A. L. and Farese, R. V., Jr. (2007). *"Dissociation of hepatic steatosis and insulin resistance in mice overexpressing DGAT in the liver."* Cell Metab **6**(1): 69-78.

Montesi, L., Mazzotti, A., Moscatiello, S., Forlani, G. and Marchesini, G. (2013). *"Insulin resistance: mechanism and implications for carcinogenesis and hepatocellular carcinoma in NASH."* Hepatol Int **7**(2): 814-822.

Montoya, C. J., Pollard, D., Martinson, J., Kumari, K., Wasserfall, C., Mulder, C. B., Rugeles, M. T., Atkinson, M. A., Landay, A. L. and Wilson, S. B. (2007). *"Characterization of human invariant natural killer T subsets in health and disease using a novel invariant natural killer T cell-clonotypic monoclonal antibody, 6B11."* Immunology **122**(1): 1-14.

Moore, K. J., Rayner, K. J., Suárez, Y. and Fernández-Hernando, C. (2010). *"microRNAs and cholesterol metabolism."* Trends in endocrinology and metabolism: TEM **21**(12): 699-706.

Morell, A. G., Irvine, R. A., Sternlieb, I., Scheinberg, I. H. and Ashwell, G. (1968). *"Physical and Chemical Studies on Ceruloplasmin: V. METABOLIC STUDIES ON SIALIC ACID-FREE CERULOPLASMIN IN VIVO."* J Biol Chem **243**(1): 155-159.

Mridha, A. R., Haczeyni, F., Yeh, M. M., Haigh, W. G., Ioannou, G. N., Barn, V., Ajamieh, H., Adams, L., Hamdorf, J. M., Teoh, N. C. and Farrell, G. C. (2017). *"TLR9 is up-regulated in human and murine NASH: pivotal role in inflammatory recruitment and cell survival."* Clin Sci (Lond) **131**(16): 2145-2159.

Mridha, A. R., Wree, A., Robertson, A. A. B., Yeh, M. M., Johnson, C. D., Van Rooyen, D. M., Haczeyni, F., Teoh, N. C., Savard, C., Ioannou, G. N., Masters, S. L., Schroder, K., Cooper, M. A., Feldstein, A. E. and Farrell, G. C. (2017). *"NLRP3 inflammasome blockade reduces liver inflammation and fibrosis in experimental NASH in mice."* J Hepatol **66**(5): 1037-1046.

Mudaliar, S., Henry, R. R., Sanyal, A. J., Morrow, L., Marschall, H. U., Kipnes, M., Adorini, L., Sciacca, C. I., Clopton, P., Castelloe, E., Dillon, P., Pruzanski, M. and Shapiro, D. (2013). *"Efficacy and safety of the farnesoid X receptor agonist obeticholic acid in patients with type 2 diabetes and nonalcoholic fatty liver disease."* Gastroenterology **145**(3): 574-582 e571.

Mulcahy, L. A., Pink, R. C. and Carter, D. R. (2014). *"Routes and mechanisms of extracellular vesicle uptake."* J Extracell Vesicles **3**.

Murakami, T., Komiyama, Y., Masuda, M., Kido, H., Nomura, S., Fukuhara, S., Karakawa, M., Iwasaka, T. and Takahashi, H. (1996). *"Flow cytometric analysis of platelet activation markers CD62P and CD63 in patients with coronary artery disease."* Eur J Clin Invest **26**(11): 996-1003.

Murphy, D. J. (2001). *"The biogenesis and functions of lipid bodies in animals, plants and microorganisms."* Prog Lipid Res **40**(5): 325-438.

Nace, G. W., Huang, H., Klune, J. R., Eid, R. E., Rosborough, B. R., Korff, S., Li, S., Shapiro, R. A., Stolz, D. B., Sodhi, C. P., Hackam, D. J., Geller, D. A., Billiar, T. R. and Tsung, A. (2013). *"Cellular-specific role of toll-like receptor 4 in hepatic ischemia-reperfusion injury in mice."* Hepatol **58**(1): 374-387.

Nagata, K., Suzuki, H. and Sakaguchi, S. (2007). *"Common pathogenic mechanism in development progression of liver injury caused by non-alcoholic or alcoholic steatohepatitis."* J Toxicol Sci **32**(5): 453-468.

Nakajima, K., Nakano, T., Tokita, Y., Nagamine, T., Inazu, A., Kobayashi, J., Mabuchi, H., Stanhope, K. L., Havel, P. J., Okazaki, M., Ai, M. and Tanaka, A. (2011). *"Postprandial lipoprotein metabolism; VLDL vs chylomicrons."* Clin Chim Acta **412**(15-16): 1306-1318.

Nakamura, R., Ishii, K. and Hashimoto, K. (2009). *"Electronic absorption spectra and redox properties of C type cytochromes in living microbes."* Angew Chem Int Ed Engl **48**(9): 1606-1608.

Nakano, Y., Okawa, S., Prieto, R. and Sekiya, J. (2006). *"Subcellular localization and possible functions of gamma-glutamyltransferase in the radish (Raphanus sativus L.) plant."* Biosci Biotechnol Biochem **70**(7): 1790-1793.

Nakano, Y., Okawa, S., Yamauchi, T., Koizumi, Y. and Sekiya, J. (2006). *"Purification and properties of soluble and bound gamma-glutamyltransferases from radish cotyledon."* Biosci Biotechnol Biochem **70**(2): 369-376.

Nassir, F., Wilson, B., Han, X., Gross, R. W. and Abumrad, N. A. (2007). *"CD36 Is Important for Fatty Acid and Cholesterol Uptake by the Proximal but Not Distal Intestine."* J Biol Chem **282**(27): 19493-19501.

Nath, B. and Szabo, G. (2012). *"Hypoxia and Hypoxia Inducible Factors: Diverse Roles in Liver Diseases."* Hepatol **55**(2): 622-633.

Netea, M. G., Kullberg, B. J., Verschueren, I. and Van Der Meer, J. W. (2000). *"Interleukin-18 induces production of proinflammatory cytokines in mice: no intermediate role for the cytokines of the tumor necrosis factor family and interleukin-1beta."* Eur J Immunol **30**(10): 3057-3060.

Neuschwander-Tetri, B. A. (2009). *"Lifestyle modification as the primary treatment of NASH."* Clin Liver Dis **13**(4): 649-665.

Neuschwander-Tetri, B. A. (2010). *"Hepatic lipotoxicity and the pathogenesis of nonalcoholic steatohepatitis: the central role of nontriglyceride fatty acid metabolites."* Hepatol **52**(2): 774-788.

Neuschwander-Tetri, B. A. and Caldwell, S. H. (2003). *"Nonalcoholic steatohepatitis: summary of an AASLD Single Topic Conference."* Hepatol **37**(5): 1202-1219.

Neuschwander-Tetri, B. A., Loomba, R., Sanyal, A. J., Lavine, J. E., Van Natta, M. L., Abdelmalek, M. F., Chalasani, N., Dasarathy, S., Diehl, A. M., Hameed, B., Kowdley, K. V., McCullough, A., Terrault, N., Clark, J. M., Tonascia, J., Brunt, E. M., Kleiner, D. E. and Doo, E. *"Farnesoid X nuclear receptor ligand obeticholic acid for non-cirrhotic, non-alcoholic steatohepatitis (FLINT): a multicentre, randomised, placebo-controlled trial."* The Lancet **385**(9972): 956-965.

Nguyen, T. M., Sawyer, J. K., Kelley, K. L., Davis, M. A. and Rudel, L. L. (2012). *"Cholesterol esterification by ACAT2 is essential for efficient intestinal cholesterol absorption: evidence from thoracic lymph duct cannulation."* J Lipid Res **53**(1): 95-104.

Nicholson, A. C., Frieda, S., Pearce, A. and Silverstein, R. L. (1995). *"Oxidized LDL binds to CD36 on human monocyte-derived macrophages and transfected cell lines. Evidence implicating the lipid moiety of the lipoprotein as the binding site."* Arterioscler Thromb Vasc Biol **15**(2): 269-275.

Nickel, W. (2003). *"The mystery of nonclassical protein secretion. A current view on cargo proteins and potential export routes."* Eur J Biochem **270**(10): 2109-2119.

Nieminen, A. L. (2003). *"Apoptosis and necrosis in health and disease: role of mitochondria."* Int Rev Cytol **224**: 29-55.

Nieminen, A. L., Byrne, A. M., Herman, B. and Lemasters, J. J. (1997). *"Mitochondrial permeability transition in hepatocytes induced by t-BuOOH: NAD(P)H and reactive oxygen species."* Am J Physiol **272**(4 Pt 1): C1286-1294.

Nordestgaard, B. G. and Tybjærg-Hansen, A. (1992). *"IDL, VLDL, chylomicrons and atherosclerosis."* Eur J Epidemiol **8**(1): 92-98.

Nozaki, Y., Fujita, K., Yoneda, M., Wada, K., Shinohara, Y., Takahashi, H., Kirikoshi, H., Inamori, M., Kubota, K., Saito, S., Mizoue, T., Masaki, N., Nagashima, Y., Terauchi, Y. and Nakajima, A. (2009). *"Long-term combination therapy of ezetimibe and acarbose for non-alcoholic fatty liver disease."* J Hepatol **51**(3): 548-556.

O'Neill, L. A. J., Golenbock, D. and Bowie, A. G. (2013). *"The history of Toll-like receptors [mdash] redefining innate immunity."* Nat Rev Immunol **13**(6): 453-460.

Ockner, R. K., Hughes, F. B. and Isselbacher, K. J. (1969). *"Very low density lipoproteins in intestinal lymph: origin, composition, and role in lipid transport in the fasting state."* J Clin Invest **48**(11): 2079-2088.

Ogasawara, F., Fusegawa, H., Haruki, Y., Shiraishi, K., Watanabe, N. and Matsuzaki, S. (2005). *"Platelet activation in patients with alcoholic liver disease."* Tokai J Exp Clin Med **30**(1): 41-48.

Ogawa, Y., Imajo, K., Yoneda, M. and Nakajima, A. (2013). *"Pathophysiology of NAsh/NAFLD associated with high levels of serum triglycerides."* Nihon Rinsho **71**(9): 1623-1629.

Ok, D. P., Ko, K. and Bae, J. Y. (2018). *"Exercise without dietary changes alleviates nonalcoholic fatty liver disease without weight loss benefits."* Lipids Health Dis **17**(1): 207.

Oka, K., Sawamura, T., Kikuta, K., Itokawa, S., Kume, N., Kita, T. and Masaki, T. (1998). *"Lectin-like oxidized low-density lipoprotein receptor 1 mediates phagocytosis of aged/apoptotic cells in endothelial cells."* Proc Natl Acad Sci U S A **95**(16): 9535-9540.

Okamura, N., Kiuchi, S., Tamba, M., Kashima, T., Hiramoto, S., Baba, T., Dacheux, F., Dacheux, J. L., Sugita, Y. and Jin, Y. Z. (1999). *"A porcine homolog of the major secretory protein of human epididymis, HE1, specifically binds cholesterol."* Biochim Biophys Acta **1438**(3): 377-387.

Okazaki, I., Watanabe, T., Hozawa, S., Arai, M. and Maruyama, K. (2000). *"Molecular mechanism of the reversibility of hepatic fibrosis: with special reference to the role of matrix metalloproteinases."* J Gastroenterol Hepatol **15 Suppl**: D26-32.

Olkkonen, V. M. and Li, S. (2013). *"Oxysterol-binding proteins: sterol and phosphoinositide sensors coordinating transport, signaling and metabolism."* Prog Lipid Res **52**(4): 529-538.

Olszewski, W. (1981). *"Flow cytometry--advantages and disadvantages of the method."* Patol Pol **32**(2): 145-160.

Ondoa, P., Koblavi-Deme, S., Borget, M. Y., Nolan, M. L., Nkengasong, J. N. and Kestens, L. (2005). *"Assessment of CD8 T cell immune activation markers to monitor response to antiretroviral therapy among HIV-1 infected patients in Cote d'Ivoire."* Clin Exp Immunol **140**(1): 138-148.

Ong, J. P., Elariny, H., Collantes, R., Younoszai, A., Chandhoke, V., Reines, H. D., Goodman, Z. and Younossi, Z. M. (2005). *"Predictors of nonalcoholic*

steatohepatitis and advanced fibrosis in morbidly obese patients." Obes Surg **15**(3): 310-315.

Oram, J. F. (2003). *"HDL apolipoproteins and ABCA1: partners in the removal of excess cellular cholesterol."* Arterioscler Thromb Vasc Biol **23**: 720-727.

Oram, J. F. and Heinecke, J. W. (2005). *"ATP-binding cassette transporter A1: A cell cholesterol exporter that protects against cardiovascular disease."* Physiol Rev **85**: 1343-1372.

Orozco, A. F. and Lewis, D. E. (2010). *"Flow cytometric analysis of circulating microparticles in plasma."* Cytometry A **77**(6): 502-514.

Osborne, T. F. (2000). *"Sterol regulatory element-binding proteins (SREBPs): key regulators of nutritional homeostasis and insulin action."* J Biol Chem **275**(42): 32379-32382.

Ott, M., Robertson, J. D., Gogvadze, V., Zhivotovsky, B. and Orrenius, S. (2002). *"Cytochrome c release from mitochondria proceeds by a two-step process."* Proc Natl Acad Sci U S A **99**(3): 1259-1263.

Padda, M. S., Sanchez, M., Akhtar, A. J. and Boyer, J. L. (2011). *"Drug-induced cholestasis."* Hepatol **53**(4): 1377-1387.

Pagadala, M., Kasumov, T., McCullough, A. J., Zein, N. N. and Kirwan, J. P. (2012). *"Role of Ceramides in Nonalcoholic Fatty Liver Disease."* Trends in endocrinology and metabolism: TEM **23**(8): 365-371.

Panasiuk, A., Zak, J., Panasiuk, B. and Prokopowicz, D. (2007). *"Increase in expression of monocytic tissue factor (CD142) with monocytes and blood platelet activation in liver cirrhosis."* Blood Coagul Fibrinolysis **18**(8): 739-744.

Panera, N., Barbaro, B., Della Corte, C., Mosca, A., Nobili, V. and Alisi, A. (2018). *"A review of the pathogenic and therapeutic role of nutrition in pediatric nonalcoholic fatty liver disease."* Nutr Res **58**: 1-16.

Paolicelli, R. C., Bergamini, G. and Rajendran, L. (2019). *"Cell-to-cell Communication by Extracellular Vesicles: Focus on Microglia."* Neuroscience **405**: 148-157.

Park, H., Go, Y. M., St John, P. L., Maland, M. C., Lisanti, M. P., Abrahamson, D. R. and Jo, H. (1998). *"Plasma membrane cholesterol is a key molecule in shear stress-dependent activation of extracellular signal-regulated kinase."* J Biol Chem **273**(48): 32304-32311.

Pasarin, M., La Mura, V., Gracia-Sancho, J., Garcia-Caldero, H., Rodriguez-Vilarrupla, A., Garcia-Pagan, J. C., Bosch, J. and Abraldes, J. G. (2012). *"Sinusoidal endothelial dysfunction precedes inflammation and fibrosis in a model of NAFLD."* PLoS ONE **7**(4): e32785.

Peake, K. B. and Vance, J. E. (2012). *"Normalization of Cholesterol Homeostasis by 2-Hydroxypropyl-β-cyclodextrin in Neurons and Glia from Niemann-Pick C1 (NPC1)-deficient Mice."* The Journal of Biological Chemistry **287**(12): 9290-9298.

Pellicciari, R., Fiorucci, S., Camaioni, E., Clerici, C., Costantino, G., Maloney, P. R., Morelli, A., Parks, D. J. and Willson, T. M. (2002). *"6alpha-ethyl-chenodeoxycholic acid (6-ECDCA), a potent and selective FXR agonist endowed with anticholestatic activity."* J Med Chem **45**(17): 3569-3572.

Pepino, M. Y., Kuda, O., Samovski, D. and Abumrad, N. A. (2014). *"Structure-Function of CD36 and Importance of Fatty Acid Signal Transduction in Fat Metabolism."* Annu Rev Nutr **34**: 281-303.

Perez-Carreras, M., Del Hoyo, P., Martin, M. A., Rubio, J. C., Martin, A., Castellano, G., Colina, F., Arenas, J. and Solis-Herruzo, J. A. (2003).

"Defective hepatic mitochondrial respiratory chain in patients with nonalcoholic steatohepatitis." Hepatol **38**(4): 999-1007.

Perkins, N. D. (2007). *"Integrating cell-signalling pathways with NF-[kappa]B and IKK function."* Nat Rev Mol Cell Biol **8**(1): 49-62.

Persson, B., Andersson, A., Hultberg, B. and Hansson, C. (2002). *"The redox state of glutathione, cysteine and homocysteine in the extracellular fluid in the skin."* Free Radic Res **36**(2): 151-156.

Perumpail, B. J., Li, A. A., John, N., Sallam, S., Shah, N. D., Kwong, W., Cholankeril, G., Kim, D. and Ahmed, A. (2019). *"The Therapeutic Implications of the Gut Microbiome and Probiotics in Patients with NAFLD."* Diseases (Basel, Switzerland) **7**(1): 27.

Pessayre, D. and Fromenty, B. (2005). *"NASH: a mitochondrial disease."* J Hepatol **42**(6): 928-940.

Petersen, D. R. (2005). *"Alcohol, iron-associated oxidative stress, and cancer."* Alcohol **35**(3): 243-249.

Petersen, P. (1977). *"Abnormal mitochondria in hepatocytes in human fatty liver."* Acta Pathol Microbiol Scand A **85**(3): 413-420.

Petersen, P. (1977). *"Ultrastructure of periportal and centrilobular hepatocytes in human fatty liver of various aetiology."* Acta Pathol Microbiol Scand A **85**(3): 421-427.

Petrasek, J., Csak, T., Ganz, M. and Szabo, G. (2013). *"Differences in innate immune signaling between alcoholic and non-alcoholic steatohepatitis."* J Gastroenterol Hepatol **28 Suppl 1**: 93-98.

Petrilli, V., Papin, S., Dostert, C., Mayor, A., Martinon, F. and Tschopp, J. (2007). *"Activation of the NALP3 inflammasome is triggered by low intracellular potassium concentration."* Cell Death Differ **14**(9): 1583-1589.

Peverill, W., Powell, L. W. and Skoien, R. (2014). *"Evolving concepts in the pathogenesis of NASH: beyond steatosis and inflammation."* Int J Mol Sci **15**(5): 8591-8638.

Pfaffenbach, K. T., Gentile, C. L., Nivala, A. M., Wang, D., Wei, Y. and Pagliassotti, M. J. (2010). *"Linking endoplasmic reticulum stress to cell death in hepatocytes: roles of C/EBP homologous protein and chemical chaperones in palmitate-mediated cell death."* Am J Physiol Endocrinol Metab **298**(5): E1027-1035.

Pillay, J., Kamp, V. M., Pennings, M., Oudijk, E. J., Leenen, L. P., Ulfman, L. H. and Koenderman, L. (2013). *"Acute-phase concentrations of soluble fibrinogen inhibit neutrophil adhesion under flow conditions in vitro through interactions with ICAM-1 and MAC-1 (CD11b/CD18)."* J Thromb Haemost **11**(6): 1172-1182.

Pisetsky, D. S. (2014). *"The expression of HMGB1 on microparticles released during cell activation and cell death in vitro and in vivo."* Mol Med **20**: 158-163.

Pisetsky, D. S., Gauley, J. and Ullal, A. J. (2011). *"HMGB1 and Microparticles as Mediators of the Immune Response to Cell Death."* Antioxid Redox Signal **15**(8): 2209-2219.

Podrez, E. A., Poliakov, E., Shen, Z., Zhang, R., Deng, Y., Sun, M., Finton, P. J., Shan, L., Febbraio, M., Hajjar, D. P., Silverstein, R. L., Hoff, H. F., Salomon, R. G. and Hazen, S. L. (2002). *"A novel family of atherogenic oxidized phospholipids promotes macrophage foam cell formation via the scavenger receptor CD36 and is enriched in atherosclerotic lesions."* J Biol Chem **277**(41): 38517-38523.

Podrez, E. A., Poliakov, E., Shen, Z., Zhang, R., Deng, Y., Sun, M., Finton, P. J., Shan, L., Gugiu, B., Fox, P. L., Hoff, H. F., Salomon, R. G. and Hazen, S. L. (2002). *"Identification of a novel family of oxidized phospholipids that serve as ligands for the macrophage scavenger receptor CD36."* J Biol Chem **277**(41): 38503-38516.

Poli, G. (2000). *"Pathogenesis of liver fibrosis: role of oxidative stress."* Mol Aspects Med **21**(3): 49-98.

Poniachik, J., Csendes, A., Diaz, J. C., Rojas, J., Burdiles, P., Maluenda, F., Smok, G., Rodrigo, R. and Videla, L. A. (2006). *"Increased production of IL-1alpha and TNF-alpha in lipopolysaccharide-stimulated blood from obese patients with non-alcoholic fatty liver disease."* Cytokine **33**(5): 252-257.

Povero, D., Eguchi, A., Li, H., Johnson, C. D., Papouchado, B. G., Wree, A., Messer, K. and Feldstein, A. E. (2014). *"Circulating extracellular vesicles with specific proteome and liver microRNAs are potential biomarkers for liver injury in experimental fatty liver disease."* PLoS ONE **9**(12): e113651.

Povero, D., Eguchi, A., Niesman, I. R., Andronikou, N., de Mollerat du Jeu, X., Mulya, A., Berk, M., Lazic, M., Thapaliya, S., Parola, M., Patel, H. H. and Feldstein, A. E. (2013). *"Lipid-induced toxicity stimulates hepatocytes to release angiogenic microparticles that require Vanin-1 for uptake by endothelial cells."* Sci Signal **6**(296): ra88-ra88.

Pramfalk, C., Jiang, Z.-Y., Cai, Q., Hu, H., Zhang, S.-D., Han, T.-Q., Eriksson, M. and Parini, P. (2010). *"HNF1α and SREBP2 are important regulators of NPC1L1 in human liver."* J Lipid Res **51**(6): 1354-1362.

Pricer, W. E., Jr., Hudgin, R. L., Ashwell, G., Stockert, R. J. and Morell, A. G. (1974). *"A membrane receptor protein for asialoglycoproteins."* Methods Enzymol **34**: 688-691.

Puri, P., Baillie, R. A., Wiest, M. M., Mirshahi, F., Choudhury, J., Cheung, O., Sargeant, C., Contos, M. J. and Sanyal, A. J. (2007). *"A lipidomic analysis of nonalcoholic fatty liver disease."* Hepatol **46**(4): 1081-1090.

Puri, P., Mirshahi, F., Cheung, O., Natarajan, R., Maher, J. W., Kellum, J. M. and Sanyal, A. J. (2008). *"Activation and dysregulation of the unfolded protein response in nonalcoholic fatty liver disease."* Gastroenterology **134**(2): 568-576.

Qi, L., Sun, X., Li, F. E., Zhu, B. S., Braun, F. K., Liu, Z. Q., Tang, J. L., Wu, C., Xu, F., Wang, H. H., Velasquez, L. A., Zhao, K., Lei, F. R., Zhang, J. G., Shen, Y. T., Zou, J. X., Meng, H. M., An, G. L., Yang, L. and Zhang, X. D. (2015). *"HMGB1 Promotes Mitochondrial Dysfunction-Triggered Striatal Neurodegeneration via Autophagy and Apoptosis Activation."* PLoS ONE **10**(11): e0142901.

Qin, Y.-H., Dai, S.-M., Tang, G.-S., Zhang, J., Ren, D., Wang, Z.-W. and Shen, Q. (2009). *"HMGB1 Enhances the Proinflammatory Activity of Lipopolysaccharide by Promoting the Phosphorylation of MAPK p38 through Receptor for Advanced Glycation End Products."* The Journal of Immunology **183**(10): 6244-6250.

Qu, Y., Franchi, L., Nunez, G. and Dubyak, G. R. (2007). *"Nonclassical IL-1 beta secretion stimulated by P2X7 receptors is dependent on inflammasome activation and correlated with exosome release in murine macrophages."* J Immunol **179**(3): 1913-1925.

Qu, Y., Ramachandra, L., Mohr, S., Franchi, L., Harding, C. V., Nunez, G. and Dubyak, G. R. (2009). *"P2X7 receptor-stimulated secretion of MHC class II-containing exosomes requires the ASC/NLRP3 inflammasome but is independent of caspase-1."* J Immunol **182**(8): 5052-5062.

Rahaman, S. O., Lennon, D. J., Febbraio, M., Podrez, E. A., Hazen, S. L. and Silverstein, R. L. (2006). *"A CD36-dependent signaling cascade is necessary for macrophage foam cell formation."* Cell Metab **4**(3): 211-221.

Rajamaki, K., Lappalainen, J., Oorni, K., Valimaki, E., Matikainen, S., Kovanen, P. T. and Eklund, K. K. (2010). *"Cholesterol crystals activate the NLRP3 inflammasome in human macrophages: a novel link between cholesterol metabolism and inflammation."* PLoS ONE **5**(7): e11765.

Rallidis, L. S., Drakoulis, C. K. and Parasi, A. S. (2004). *"Pravastatin in patients with nonalcoholic steatohepatitis: results of a pilot study."* Atherosclerosis **174**(1): 193-196.

Ramakrishnan, P., Clark, P. M., Mason, D. E., Peters, E. C., Hsieh-Wilson, L. C. and Baltimore, D. (2013). *"Activation of the transcriptional function of the NF-kappaB protein c-Rel by O-GlcNAc glycosylation."* Sci Signal **6**(290): ra75.

Ratziu, V., de Ledinghen, V., Oberti, F., Mathurin, P., Wartelle-Bladou, C., Renou, C., Sogni, P., Maynard, M., Larrey, D., Serfaty, L., Bonnefont-Rousselot, D., Bastard, J. P., Riviere, M., Spenard, J. and Fresgun (2011). *"A randomized controlled trial of high-dose ursodesoxycholic acid for nonalcoholic steatohepatitis."* J Hepatol **54**(5): 1011-1019.

Ratziu, V., Ghabril, M., Romero-Gomez, M. and Svegliati-Baroni, G. (2019). *"Recommendations for Management and Treatment of Nonalcoholic Steatohepatitis."* Transplantation **103**(1): 28-38.

Ratziu, V., Harrison, S. A., Francque, S., Bedossa, P., Lehert, P., Serfaty, L., Romero-Gomez, M., Boursier, J., Abdelmalek, M., Caldwell, S., Drenth, J., Anstee, Q. M., Hum, D., Hanf, R., Roudot, A., Megnien, S., Staels, B., Sanyal, A., Mathurin, P., Gournay, J., Nguyen-Khac, E., De Ledinghen, V., Larrey, D., Tran, A., Bourliere, M., Maynard-Muet, M., Asselah, T., Henrion, J., Nevens, F., Cassiman, D., Geerts, A., Moreno, C., Beuers, U. H., Galle, P. R., Spengler, U., Bugianesi, E., Craxi, A., Angelico, M., Fargion, S., Voiculescu, M., Gheorghe, L., Preotescu, L., Caballeria, J., Andrade, R. J., Crespo, J., Callera, J. L., Ala, A., Aithal, G., Abouda, G., Luketic, V., Huang, M. A., Gordon, S., Pockros, P., Poordad, F., Shores, N., Moehlen, M. W., Bambha, K., Clark, V., Satapathy, S., Parekh, S., Reddy, R. K., Sheikh, M. Y., Szabo, G., Vierling, J., Foster, T., Umpierrez, G., Chang, C., Box, T. and Gallegos-Orozco, J. (2016). *"Elafibranor, an Agonist of the Peroxisome Proliferator−Activated Receptor−α and −δ, Induces Resolution of Nonalcoholic Steatohepatitis Without Fibrosis Worsening."* Gastroenterology **150**(5): 1147-1159.e1145.

Ray, T. K., Skipski, V. P., Barclay, M., Essner, E. and Archibald, F. M. (1969). *"Lipid composition of rat liver plasma membranes."* J Biol Chem **244**(20): 5528-5536.

Reich, N., Tomcik, M., Zerr, P., Lang, V., Dees, C., Avouac, J., Palumbo, K., Horn, A., Akhmetshina, A., Beyer, C., Xie, W., Bennett, B. L., Distler, O., Schett, G. and Distler, J. H. (2012). *"Jun N-terminal kinase as a potential molecular target for prevention and treatment of dermal fibrosis."* Ann Rheum Dis **71**(5): 737-745.

Renart, J., Reiser, J. and Stark, G. R. (1979). *"Transfer of proteins from gels to diazobenzyloxymethyl-paper and detection with antisera: a method for studying antibody specificity and antigen structure."* Proc Natl Acad Sci U S A **76**(7): 3116-3120.

Ribas, V., Garcia-Ruiz, C. and Fernandez-Checa, J. C. (2014). *"Glutathione and Mitochondria."* Front Pharmacol **5**.

Ribeiro, P. S., Cortez-Pinto, H., Sola, S., Castro, R. E., Ramalho, R. M., Baptista, A., Moura, M. C., Camilo, M. E. and Rodrigues, C. M. (2004). *"Hepatocyte apoptosis, expression of death receptors, and activation of NF-kappaB in the liver of nonalcoholic and alcoholic steatohepatitis patients."* Am J Gastroenterol **99**(9): 1708-1717.

Rigotti, A., Cohen, D. E. and Zanlungo, S. (2010). *"STARTing to understand MLN64 function in cholesterol transport."* J Lipid Res **51**(8): 2015-2017.

Robertson, G., Leclercq, I. and Farrell, G. C. (2001). *"Nonalcoholic steatosis and steatohepatitis. II. Cytochrome P-450 enzymes and oxidative stress."* Am J Physiol Gastrointest Liver Physiol **281**(5): G1135-1139.

Rodriguez-Pascau, L., Toma, C., Macias-Vidal, J., Cozar, M., Cormand, B., Lykopoulou, L., Coll, M. J., Grinberg, D. and Vilageliu, L. (2012). *"Characterisation of two deletions involving NPC1 and flanking genes in Niemann-Pick type C disease patients."* Mol Genet Metab **107**(4): 716-720.

Rodriguez-Rodriguez, E., Vazquez-Higuera, J. L., Sanchez-Juan, P., Mateo, I., Pozueta, A., Martinez-Garcia, A., Frank, A., Valdivieso, F., Berciano, J., Bullido, M. J. and Combarros, O. (2010). *"Epistasis between intracellular cholesterol trafficking-related genes (NPC1 and ABCA1) and Alzheimer's disease risk."* J Alzheimers Dis **21**(2): 619-625.

Roff, C. F., Goldin, E., Comly, M. E., Blanchette-Mackie, J., Cooney, A., Brady, R. O. and Pentchev, P. G. (1992). *"Niemann-Pick type-C disease: deficient intracellular transport of exogenously derived cholesterol."* Am J Med Genet **42**(4): 593-598.

Roh, Y. S. and Seki, E. (2013). *"Toll-like receptors in alcoholic liver disease, non-alcoholic steatohepatitis and carcinogenesis."* J Gastroenterol Hepatol **28 Suppl 1**: 38-42.

Rose, S., Misharin, A. and Perlman, H. (2012). *"A novel Ly6C/Ly6G-based strategy to analyze the mouse splenic myeloid compartment."* Cytometry A **81**(4): 343-350.

Rosso, N., Chavez-Tapia, N. C., Tiribelli, C. and Bellentani, S. (2014). *"Translational approaches: from fatty liver to non-alcoholic steatohepatitis."* World J Gastroenterol **20**(27): 9038-9049.

Rottiers, V. and Näär, A. M. (2012). *"MicroRNAs in metabolism and metabolic disorders."* Nat Rev Mol Cell Biol **13**(4): 239-250.

Rotundo, R. F., Vincent, P. A., McKeown-Longo, P. J., Blumenstock, F. A. and Saba, T. M. (1999). *"Hepatic fibronectin matrix turnover in rats: involvement of the asialoglycoprotein receptor."* Am J Physiol **277**(6 Pt 1): G1189-1199.

Rowe, S. M., Jackson, P. L., Liu, G., Hardison, M., Livraghi, A., Solomon, G. M., McQuaid, D. B., Noerager, B. D., Gaggar, A., Clancy, J. P., O'Neal, W., Sorscher, E. J., Abraham, E. and Blalock, J. E. (2008). *"Potential Role of High-Mobility Group Box 1 in Cystic Fibrosis Airway Disease."* Am J Respir Crit Care Med **178**(8): 822-831.

Ruan, Q., Kameswaran, V., Tone, Y., Li, L., Liou, H. C., Greene, M. I., Tone, M. and Chen, Y. H. (2009). *"Development of Foxp3(+) regulatory t cells is driven by the c-Rel enhanceosome."* Immunity **31**(6): 932-940.

Saad, B., Frei, K., Scholl, F. A., Fontana, A. and Maier, P. (1995). *"Hepatocyte-Derived Interleukin-6 and Tumor-Necrosis Factor α Mediate the Lipopolysaccharide-Induced Acute-Phase Response and Nitric Oxide Release by Cultured Rat Hepatocytes."* Eur J Biochem **229**(2): 349-355.

Sabapathy, K., Hochedlinger, K., Nam, S. Y., Bauer, A., Karin, M. and Wagner, E. F. (2004). *"Distinct roles for JNK1 and JNK2 in regulating JNK activity and c-Jun-dependent cell proliferation."* Mol Cell **15**(5): 713-725.

Sabapathy, K. and Wagner, E. F. (2004). *"JNK2: a negative regulator of cellular proliferation."* Cell Cycle **3**(12): 1520-1523.

Sabio, G., Das, M., Mora, A., Zhang, Z., Jun, J. Y., Ko, H. J., Barrett, T., Kim, J. K. and Davis, R. J. (2008). *"A stress signaling pathway in adipose tissue regulates hepatic insulin resistance."* Science **322**(5907): 1539-1543.

Sahoo, D., Trischuk, T. C., Chan, T., Drover, V. A., Ho, S., Chimini, G., Agellon, L. B., Agnihotri, R., Francis, G. A. and Lehner, R. (2004). *"ABCA1-dependent lipid efflux to apolipoprotein A-I mediates HDL particle formation and decreases VLDL secretion from murine hepatocytes."* J Lipid Res **45**(6): 1122-1131.

Sakaida, I. and Okita, K. (2005). *"The role of oxidative stress in NASH and fatty liver model."* Hepatol Res **33**(2): 128-131.

Sakamoto, A., Saotome, M., Hasan, P., Satoh, T., Ohtani, H., Urushida, T., Katoh, H., Satoh, H. and Hayashi, H. (2017). *"Eicosapentaenoic acid ameliorates palmitate-induced lipotoxicity via the AMP kinase/dynamin-related protein-1 signaling pathway in differentiated H9c2 myocytes."* Exp Cell Res **351**(1): 109-120.

Santos, J. C., de Araujo, O. R., Valentim, I. B., de Andrade, K. Q., Moura, F. A., Smaniotto, S., dos Santos, J. M., Gasparotto, J., Gelain, D. P. and Goulart, M. O. (2015). *"Choline and Cystine Deficient Diets in Animal Models with Hepatocellular Injury: Evaluation of Oxidative Stress and Expression of RAGE, TNF-alpha, and IL-1beta."* Oxid Med Cell Longev **2015**: 121925.

Sanyal, A. J., Campbell-Sargent, C., Mirshahi, F., Rizzo, W. B., Contos, M. J., Sterling, R. K., Luketic, V. A., Shiffman, M. L. and Clore, J. N. (2001). *"Nonalcoholic steatohepatitis: association of insulin resistance and mitochondrial abnormalities."* Gastroenterology **120**(5): 1183-1192.

Sattar, N., Forrest, E. and Preiss, D. (2014). *"Non-alcoholic fatty liver disease."* BMJ : British Medical Journal **349**: g4596.

Sayed, D., Amin, N. F. and Galal, G. M. (2010). *"Monocyte-platelet aggregates and platelet micro-particles in patients with post-hepatitic liver cirrhosis."* Thromb Res **125**(5): e228-233.

Schaffner, F. and Thaler, H. (1986). *"Nonalcoholic fatty liver disease."* Prog Liver Dis **8**: 283-298.

Schattenberg, J. M., Singh, R., Wang, Y., Lefkowitch, J. H., Rigoli, R. M., Scherer, P. E. and Czaja, M. J. (2006). *"JNK1 but not JNK2 promotes the development of steatohepatitis in mice."* Hepatol **43**(1): 163-172.

Schneider, J., Chromik, A. M., Uhl, W., Mugge, A. and Bulut, D. (2012). *"Apoptosis in esophagus and pancreas carcinoma cells induced by circulating microparticles is related to phosphatidyl serine and microparticle-associated caspases."* Med Oncol **29**(2): 962-969.

Schonfeld, P. and Wojtczak, L. (2016). *"Short- and medium-chain fatty acids in energy metabolism: the cellular perspective."* J Lipid Res **57**(6): 943-954.

Schopfer, F. J., Cipollina, C. and Freeman, B. A. (2011). *"Formation and Signaling Actions of Electrophilic Lipids."* Chem Rev **111**(10): 5997-6021.

Schroder, K. and Tschopp, J. (2010). *"The inflammasomes."* Cell **140**(6): 821-832.

Schulthess, G., Compassi, S., Werder, M., Han, C. H., Phillips, M. C. and Hauser, H. (2000). *"Intestinal sterol absorption mediated by scavenger receptors is*

competitively inhibited by amphipathic peptides and proteins." Biochemistry (Mosc) **39**(41): 12623-12631.

Schwabe, R. F., Uchinami, H., Qian, T., Bennett, B. L., Lemasters, J. J. and Brenner, D. A. (2004). *"Differential requirement for c-Jun NH2-terminal kinase in TNFalpha- and Fas-mediated apoptosis in hepatocytes."* FASEB J **18**(6): 720-722.

Scott, C. and Ioannou, Y. A. (2004). *"The NPC1 protein: structure implies function."* Biochim Biophys Acta **1685**(1-3): 8-13.

Seki, E. and Schnabl, B. (2012). *"Role of innate immunity and the microbiota in liver fibrosis: crosstalk between the liver and gut."* J Physiol **590**(Pt 3): 447-458.

Sethi, G., Ahn, K. S., Xia, D., Kurie, J. M. and Aggarwal, B. B. (2007). *"Targeted deletion of MKK4 gene potentiates TNF-induced apoptosis through the down-regulation of NF-kappa B activation and NF-kappa B-regulated antiapoptotic gene products."* J Immunol **179**(3): 1926-1933.

Severgnini, M., Sherman, J., Sehgal, A., Jayaprakash, N. K., Aubin, J., Wang, G., Zhang, L., Peng, C. G., Yucius, K., Butler, J. and Fitzgerald, K. (2012). *"A rapid two-step method for isolation of functional primary mouse hepatocytes: cell characterization and asialoglycoprotein receptor based assay development."* Cytotechnology **64**(2): 187-195.

Sévin, M., Lesca, G., Baumann, N., Millat, G., Lyon-Caen, O., Vanier, M. T. and Sedel, F. (2007). *"The adult form of Niemann–Pick disease type C."* Brain **130**(1): 120-133.

Sharma, L., Kaur, J. and Shukla, G. (2012). *"Role of oxidative stress and apoptosis in the placental pathology of Plasmodium berghei infected mice."* PLoS ONE **7**(3): e32694.

Shaulian, E. and Karin, M. (2002). *"AP-1 as a regulator of cell life and death."* Nat Cell Biol **4**(5): E131-E136.

Shaw, P. J., McDermott, M. F. and Kanneganti, T.-D. (2011). *"Inflammasomes and autoimmunity."* Trends Mol Med **17**(2): 57-64.

Sheedy, F. J., Grebe, A., Rayner, K. J., Kalantari, P., Ramkhelawon, B., Carpenter, S. B., Becker, C. E., Ediriweera, H. N., Mullick, A. E., Golenbock, D. T., Stuart, L. M., Latz, E., Fitzgerald, K. A. and Moore, K. J. (2013). *"CD36 coordinates NLRP3 inflammasome activation by facilitating intracellular nucleation of soluble ligands into particulate ligands in sterile inflammation."* Nat Immunol **14**(8): 812-820.

Shen, H. M. and Liu, Z. G. (2006). *"JNK signaling pathway is a key modulator in cell death mediated by reactive oxygen and nitrogen species."* Free Radic Biol Med **40**(6): 928-939.

Shet, A. S. (2008). *"Characterizing blood microparticles: technical aspects and challenges."* Vasc Health Risk Manag **4**(4): 769-774.

Shi, B., Abrams, M. and Sepp-Lorenzino, L. (2013). *"Expression of asialoglycoprotein receptor 1 in human hepatocellular carcinoma."* J Histochem Cytochem **61**(12): 901-909.

Shih, V. F., Davis-Turak, J., Macal, M., Huang, J. Q., Ponomarenko, J., Kearns, J. D., Yu, T., Fagerlund, R., Asagiri, M., Zuniga, E. I. and Hoffmann, A. (2012). *"Control of RelB during dendritic cell activation integrates canonical and noncanonical NF-kappaB pathways."* Nat Immunol **13**(12): 1162-1170.

Shugarts, S. and Benet, L. Z. (2009). *"The role of transporters in the pharmacokinetics of orally administered drugs."* Pharm Res **26**(9): 2039-2054.

Sies, H. and Summer, K. H. (1975). *"Hydroperoxide-metabolizing systems in rat liver."* Eur J Biochem **57**(2): 503-512.

Silva, M. and Melo, S. A. (2015). *"Non-coding RNAs in Exosomes: New Players in Cancer Biology."* Curr Genomics **16**(5): 295-303.

Simak, J. and Gelderman, M. P. (2006). *"Cell membrane microparticles in blood and blood products: potentially pathogenic agents and diagnostic markers."* Transfus Med Rev **20**(1): 1-26.

Simak, J., Gelderman, M. P., Yu, H., Wright, V. and Baird, A. E. (2006). *"Circulating endothelial microparticles in acute ischemic stroke: a link to severity, lesion volume and outcome."* J Thromb Haemost **4**(6): 1296-1302.

Simeonidis, S., Stauber, D., Chen, G., Hendrickson, W. A. and Thanos, D. (1999). *"Mechanisms by which IkappaB proteins control NF-kappaB activity."* Proc Natl Acad Sci U S A **96**(1): 49-54.

Singh, J. and Dixon, G. H. (1990). *"High mobility group proteins 1 and 2 function as general class II transcription factors."* Biochemistry (Mosc) **29**(26): 6295-6302.

Singh, R., Wang, Y., Xiang, Y., Tanaka, K. E., Gaarde, W. A. and Czaja, M. J. (2009). *"Differential effects of JNK1 and JNK2 inhibition on murine steatohepatitis and insulin resistance."* Hepatol **49**(1): 87-96.

Sobaniec-Lotowska, M. E. and Lebensztejn, D. M. (2003). *"Ultrastructure of hepatocyte mitochondria in nonalcoholic steatohepatitis in pediatric patients: usefulness of electron microscopy in the diagnosis of the disease."* Am J Gastroenterol **98**: 1664.

Solinas, G., Naugler, W., Galimi, F., Lee, M. S. and Karin, M. (2006). *"Saturated fatty acids inhibit induction of insulin gene transcription by JNK-mediated phosphorylation of insulin-receptor substrates."* Proc Natl Acad Sci U S A **103**(44): 16454-16459.

Sollberger, G., Strittmatter, G. E., Garstkiewicz, M., Sand, J. and Beer, H.-D. (2014). *"Caspase-1: The inflammasome and beyond."* Innate Immun **20**(2): 115-125.

Son, Y., Cheong, Y.-K., Kim, N.-H., Chung, H.-T., Kang, D. G. and Pae, H.-O. (2011). *"Mitogen-Activated Protein Kinases and Reactive Oxygen Species: How Can ROS Activate MAPK Pathways?"* Journal of Signal Transduction **2011**: 792639.

Song, G., Tian, H., Liu, J., Zhang, H., Sun, X. and Qin, S. (2011). *"H2 inhibits TNF-alpha-induced lectin-like oxidized LDL receptor-1 expression by inhibiting nuclear factor kappaB activation in endothelial cells."* Biotechnol Lett **33**(9): 1715-1722.

Souza-Mello, V. (2015). *"Peroxisome proliferator-activated receptors as targets to treat non-alcoholic fatty liver disease."* World J Hepatol **7**(8): 1012-1019.

Spiess, M. (1990). *"The asialoglycoprotein receptor: a model for endocytic transport receptors."* Biochemistry (Mosc) **29**(43): 10009-10018.

Sporea, I., Popescu, A., Dumitrascu, D., Brisc, C., Nedelcu, L., Trifan, A., Gheorghe, L. and Fierbinteanu Braticevici, C. (2018). *"Nonalcoholic Fatty Liver Disease: Status Quo."* J Gastrointestin Liver Dis **27**(4): 439-448.

Stahlberg, A., Hakansson, J., Xian, X., Semb, H. and Kubista, M. (2004). *"Properties of the reverse transcription reaction in mRNA quantification."* Clin Chem **50**(3): 509-515.

Stahlberg, A., Kubista, M. and Pfaffl, M. (2004). *"Comparison of reverse transcriptases in gene expression analysis."* Clin Chem **50**(9): 1678-1680.

Stampfer, M. J., Hennekens, C. H., Manson, J. E., Colditz, G. A., Rosner, B. and Willett, W. C. (1993). *"Vitamin E consumption and the risk of coronary disease in women."* N Engl J Med **328**(20): 1444-1449.

Stansly, P. G. and Schlosser, M. E. (1947). *"Studies on Polymyxin: Isolation and Identification of Bacillus polymyxa and Differentiation of Polymyxin from Certain Known Antibiotics."* J Bacteriol **54**(5): 549-556.

Stenstrom, M., Skold, M., Andersson, A. and Cardell, S. L. (2005). *"Natural killer T-cell populations in C57BL/6 and NK1.1 congenic BALB.NK mice-a novel thymic subset defined in BALB.NK mice."* Immunology **114**(3): 336-345.

Stockert, R. J. (1995). *"The asialoglycoprotein receptor: relationships between structure, function, and expression."* Physiol Rev **75**(3): 591-609.

Stockert, R. J., Kressner, M. S., Collins, J. C., Sternlieb, I. and Morell, A. G. (1982). *"IgA interaction with the asialoglycoprotein receptor."* Proc Natl Acad Sci U S A **79**(20): 6229-6231.

Storek, J., Dawson, M. A. and Maloney, D. G. (1998). *"Comparison of two flow cytometric methods enumerating CD4 T cells and CD8 T cells."* Cytometry **33**(1): 76-82.

Strober, W. (2001). *"Trypan blue exclusion test of cell viability."* Curr Protoc Immunol **Appendix 3**: Appendix 3B.

Subramanian, K. and Balch, W. E. (2008). *"NPC1/NPC2 function as a tag team duo to mobilize cholesterol."* Proceedings of the National Academy of Sciences **105**(40): 15223-15224.

Subramanian, S., Goodspeed, L., Wang, S., Kim, J., Zeng, L., Ioannou, G. N., Haigh, W. G., Yeh, M. M., Kowdley, K. V., O'Brien, K. D., Pennathur, S. and Chait, A. (2011). *"Dietary cholesterol exacerbates hepatic steatosis and inflammation in obese LDL receptor-deficient mice."* J Lipid Res **52**(9): 1626-1635.

Suchy, F. J. (2012). Hepatobiliary function. *Medical physiology*. W. F. Boron and E. L. Boulpaep. New York, Saunders Elsevier**:** 981-1011.

Sumida, Y., Niki, E., Naito, Y. and Yoshikawa, T. (2013). *"Involvement of free radicals and oxidative stress in NAFLD/NASH."* Free Radic Res **47**(11): 869-880.

Sutterwala, F. S., Ogura, Y., Szczepanik, M., Lara-Tejero, M., Lichtenberger, G. S., Grant, E. P., Bertin, J., Coyle, A. J., Galan, J. E., Askenase, P. W. and Flavell, R. A. (2006). *"Critical role for NALP3/CIAS1/Cryopyrin in innate and adaptive immunity through its regulation of caspase-1."* Immunity **24**(3): 317-327.

Suzuki, H., Kurihara, Y., Takeya, M., Kamada, N., Kataoka, M., Jishage, K., Ueda, O., Sakaguchi, H., Higashi, T., Suzuki, T., Takashima, Y., Kawabe, Y., Cynshi, O., Wada, Y., Honda, M., Kurihara, H., Aburatani, H., Doi, T., Matsumoto, A., Azuma, S., Noda, T., Toyoda, Y., Itakura, H., Yazaki, Y., Kodama, T. and et al. (1997). *"A role for macrophage scavenger receptors in atherosclerosis and susceptibility to infection."* Nature **386**(6622): 292-296.

Suzuki, K., Doi, T., Imanishi, T., Kodama, T. and Tanaka, T. (1997). *"The conformation of the alpha-helical coiled coil domain of macrophage scavenger receptor is pH dependent."* Biochemistry (Mosc) **36**(49): 15140-15146.

Suzuki, T., Shinjo, S., Arai, T., Kanai, M. and Goda, N. (2014). *"Hypoxia and fatty liver."* World J Gastroenterol **20**(41): 15087-15097.

Syn, W. K., Choi, S. S. and Diehl, A. M. (2009). *"Apoptosis and cytokines in non-alcoholic steatohepatitis."* Clin Liver Dis **13**(4): 565-580.

Syn, W. K., Teaberry, V., Choi, S. S. and Diehl, A. M. (2009). *"Similarities and differences in the pathogenesis of alcoholic and nonalcoholic steatohepatitis."* Semin Liver Dis **29**(2): 200-210.

Szabo, G. and Momen-Heravi, F. (2017). *"Extracellular vesicles in liver disease and potential as biomarkers and therapeutic targets."* Nat Rev Gastroenterol Hepatol **14**(8): 455-466.

Takeda, K. (2005). *"Evolution and integration of innate immune recognition systems: the Toll-like receptors."* J Endotoxin Res **11**(1): 51-55.

Takeda, K. and Akira, S. (2005). *"Toll-like receptors in innate immunity."* Int Immunol **17**(1): 1-14.

Takeuchi, O., Kaufmann, A., Grote, K., Kawai, T., Hoshino, K., Morr, M., Muhlradt, P. F. and Akira, S. (2000). *"Cutting edge: preferentially the R-stereoisomer of the mycoplasmal lipopeptide macrophage-activating lipopeptide-2 activates immune cells through a toll-like receptor 2- and MyD88-dependent signaling pathway."* J Immunol **164**(2): 554-557.

Tamura, A. and Yui, N. (2014). *"Lysosomal-specific Cholesterol Reduction by Biocleavable Polyrotaxanes for Ameliorating Niemann-Pick Type C Disease."* Sci Rep **4**: 4356.

Tang, H. W., Liao, H. M., Peng, W. H., Lin, H. R., Chen, C. H. and Chen, G. C. (2013). *"Atg9 interacts with dTRAF2/TRAF6 to regulate oxidative stress-induced JNK activation and autophagy induction."* Dev Cell **27**(5): 489-503.

Tanwar, S., Trembling, P. M., Guha, I. N., Parkes, J., Kaye, P., Burt, A. D., Ryder, S. D., Aithal, G. P., Day, C. P. and Rosenberg, W. M. (2013). *"Validation of terminal peptide of procollagen III for the detection and assessment of nonalcoholic steatohepatitis in patients with nonalcoholic fatty liver disease."* Hepatol **57**(1): 103-111.

Tatischeff, I., Bomsel, M., de Paillerets, C., Durand, H., Geny, B., Segretain, D., Turpin, E. and Alfsen, A. (1998). *"Dictyostelium discoideum cells shed vesicles with associated DNA and vital stain Hoechst 33342."* Cell Mol Life Sci **54**(5): 476-487.

Ten, R. M., Paya, C. V., Israel, N., Le Bail, O., Mattei, M. G., Virelizier, J. L., Kourilsky, P. and Israel, A. (1992). *"The characterization of the promoter of the gene encoding the p50 subunit of NF-kappa B indicates that it participates in its own regulation."* EMBO J **11**(1): 195-203.

Teoh, N. C., Ajamieh, H., Wong, H. J., Croft, K., Mori, T., Allison, A. C. and Farrell, G. C. (2014). *"Microparticles mediate hepatic ischemia-reperfusion injury and are the targets of Diannexin (ASP8597)."* PLoS ONE **9**(9): e104376.

Thery, C., Zitvogel, L. and Amigorena, S. (2002). *"Exosomes: composition, biogenesis and function."* Nat Rev Immunol **2**(8): 569-579.

Thirunavukkarasu, C., Watkins, S. C. and Gandhi, C. R. (2006). *"Mechanisms of endotoxin-induced NO, IL-6, and TNF-alpha production in activated rat hepatic stellate cells: role of p38 MAPK."* Hepatol **44**(2): 389-398.

Thobe, B. M., Frink, M., Hildebrand, F., Schwacha, M. G., Hubbard, W. J., Choudhry, M. A. and Chaudry, I. H. (2007). *"The role of MAPK in Kupffer cell toll-like receptor (TLR) 2-, TLR4-, and TLR9-mediated signaling following trauma-hemorrhage."* J Cell Physiol **210**(3): 667-675.

Tian, F., Zhang, Y. J., Li, Y. and Xie, Y. (2014). *"Celecoxib ameliorates non-alcoholic steatohepatitis in type 2 diabetic rats via suppression of the non-canonical Wnt signaling pathway expression."* PLoS One **9**(1): e83819.

Tian, F., Zhang, Y. J. and Wang, L. (2013). *"Non-canonical Wnt signaling contributes to development of non-alcoholic steatohepatitis in a rat model of type 2 diabetes mellitus."* Zhonghua Gan Zang Bing Za Zhi **21**(7): 537-542.

Tilg, H. and Moschen, A. R. (2010). *"Evolution of inflammation in nonalcoholic fatty liver disease: the multiple parallel hits hypothesis."* Hepatol **52**(5): 1836-1846.

Tohme, M. and Manoury, B. (2014). *"Intracellular Toll-like receptor recruitment and cleavage in endosomal/lysosomal organelles."* Methods Enzymol **535**: 141-147.

Tournier, C., Dong, C., Turner, T. K., Jones, S. N., Flavell, R. A. and Davis, R. J. (2001). *"MKK7 is an essential component of the JNK signal transduction pathway activated by proinflammatory cytokines."* Genes Dev **15**(11): 1419-1426.

Towbin, H., Staehelin, T. and Gordon, J. (1979). *"Electrophoretic transfer of proteins from polyacrylamide gels to nitrocellulose sheets: procedure and some applications."* Proc Natl Acad Sci U S A **76**(9): 4350-4354.

Tsao, D. H., McDonagh, T., Telliez, J. B., Hsu, S., Malakian, K., Xu, G. Y. and Lin, L. L. (2000). *"Solution structure of N-TRADD and characterization of the interaction of N-TRADD and C-TRAF2, a key step in the TNFR1 signaling pathway."* Mol Cell **5**(6): 1051-1057.

Tseng, P. H., Matsuzawa, A., Zhang, W., Mino, T., Vignali, D. A. and Karin, M. (2010). *"Different modes of ubiquitination of the adaptor TRAF3 selectively activate the expression of type I interferons and proinflammatory cytokines."* Nat Immunol **11**(1): 70-75.

Tsochatzis, E., Papatheodoridis, G. V., Hadziyannis, E., Georgiou, A., Kafiri, G., Tiniakos, D. G., Manesis, E. K. and Archimandritis, A. J. (2008). *"Serum adipokine levels in chronic liver diseases: association of resistin levels with fibrosis severity."* Scand J Gastroenterol **43**(9): 1128-1136.

Tsochatzis, E. A., Papatheodoridis, G. V. and Archimandritis, A. J. (2009). *"Adipokines in nonalcoholic steatohepatitis: from pathogenesis to implications in diagnosis and therapy."* Mediators Inflamm **2009**: 831670.

Tsung, A., Tohme, S. and Billiar, T. R. (2014). *"High-mobility group box-1 in sterile inflammation."* J Intern Med **276**(5): 425-443.

Tuncman, G., Hirosumi, J., Solinas, G., Chang, L., Karin, M. and Hotamisligil, G. S. (2006). *"Functional in vivo interactions between JNK1 and JNK2 isoforms in obesity and insulin resistance."* Proc Natl Acad Sci U S A **103**(28): 10741-10746.

U.S. National Library of Medicine (2018). "*Randomized Global Phase 3 Study to Evaluate the Impact on NASH With Fibrosis of Obeticholic Acid Treatment (REGENERATE).*" Retrieved 21 January, 2018, from https://clinicaltrials.gov/ct2/show/NCT02548351.

Unger, R. H. (1995). *"Lipotoxicity in the pathogenesis of obesity-dependent NIDDM. Genetic and clinical implications."* Diabetes **44**(8): 863-870.

Unger, R. H. and Zhou, Y. T. (2001). *"Lipotoxicity of beta-cells in obesity and in other causes of fatty acid spillover."* Diabetes **50 Suppl 1**: S118-121.

Uppal, N., Uppal, V. and Uppal, P. (2014). *"Progression of Coronary Artery Disease (CAD) from Stable Angina (SA) Towards Myocardial Infarction (MI): Role of Oxidative Stress."* J Clin Diagn Res **8**(2): 40-43.

van der Wulp, M. Y., Verkade, H. J. and Groen, A. K. (2013). *"Regulation of cholesterol homeostasis."* Mol Cell Endocrinol **368**(1-2): 1-16.

van Meer, G., Voelker, D. R. and Feigenson, G. W. (2008). *"Membrane lipids: where they are and how they behave."* Nat Rev Mol Cell Biol **9**(2): 112-124.

Van Rooyen, D. M. (2012). Cholesterol as a mediator of hepatic injury in non-alcoholic steatohepatitis. *College of Medicine, Biology and Environment* Canberra, Australian National University. **Doctor of Philosophy degree:** 304.

Van Rooyen, D. M. and Farrell, G. C. (2011). *"SREBP-2: a link between insulin resistance, hepatic cholesterol, and inflammation in NASH."* J Gastroenterol Hepatol **26**(5): 789-792.

Van Rooyen, D. M., Gan, L. T., Yeh, M. M., Haigh, W. G., Larter, C. Z., Ioannou, G., Teoh, N. C. and Farrell, G. C. (2013). *"Pharmacological cholesterol lowering reverses fibrotic NASH in obese, diabetic mice with metabolic syndrome."* J Hepatol **59**(1): 144-152.

Van Rooyen, D. M., Larter, C. Z., Haigh, W. G., Yeh, M. M., Ioannou, G., Kuver, R., Lee, S. P., Teoh, N. C. and Farrell, G. C. (2011). *"Hepatic free cholesterol accumulates in obese, diabetic mice and causes nonalcoholic steatohepatitis."* Gastroenterology **141**(4): 1393-1403, 1403 e1391-1395.

van Velzen, J. F., Laros-van Gorkom, B. A., Pop, G. A. and van Heerde, W. L. (2012). *"Multicolor flow cytometry for evaluation of platelet surface antigens and activation markers."* Thromb Res **130**(1): 92-98.

Vanier, M. T. (2010). *"Niemann-Pick disease type C."* Orphanet J Rare Dis **5**: 16.

Vanier, M. T. and Millat, G. (2004). *"Structure and function of the NPC2 protein."* Biochimica et Biophysica Acta (BBA) - Molecular and Cell Biology of Lipids **1685**(1–3): 14-21.

Vartanian, R., Masri, J., Martin, J., Cloninger, C., Holmes, B., Artinian, N., Funk, A., Ruegg, T. and Gera, J. (2011). *"AP-1 regulates cyclin D1 and c-MYC transcription in an AKT-dependent manner in response to mTOR inhibition: role of AIP4/Itch-mediated JUNB degradation."* Mol Cancer Res **9**(1): 115-130.

Vasina, E. M., Cauwenberghs, S., Staudt, M., Feijge, M. A., Weber, C., Koenen, R. R. and Heemskerk, J. W. (2013). *"Aging- and activation-induced platelet microparticles suppress apoptosis in monocytic cells and differentially signal to proinflammatory mediator release."* Am J Blood Res **3**(2): 107-123.

Vedhachalam, C., Duong, P. T., Nickel, M., Nguyen, D., Dhanasekaran, P., Saito, H., Rothblat, G. H., Lund-Katz, S. and Phillips, M. C. (2007). *"Mechanism of ATP-binding cassette transporter A1-mediated cellular lipid efflux to apolipoprotein A-I and formation of high density lipoprotein particles."* J Biol Chem **282**(34): 25123-25130.

Verhoef, P. A., Kertesy, S. B., Estacion, M., Schilling, W. P. and Dubyak, G. R. (2004). *"Maitotoxin induces biphasic interleukin-1beta secretion and membrane blebbing in murine macrophages."* Mol Pharmacol **66**(4): 909-920.

Videla, L. A., Tapia, G., Rodrigo, R., Pettinelli, P., Haim, D., Santibanez, C., Araya, A. V., Smok, G., Csendes, A., Gutierrez, L., Rojas, J., Castillo, J., Korn, O., Maluenda, F., Diaz, J. C., Rencoret, G. and Poniachik, J. (2009). *"Liver NF-kappaB and AP-1 DNA binding in obese patients."* Obesity (Silver Spring) **17**(5): 973-979.

Vine, D. F., Glimm, D. R. and Proctor, S. D. (2008). *"Intestinal lipid transport and chylomicron production: possible links to exacerbated atherogenesis in a rodent model of the metabolic syndrome."* Atheroscler Suppl **9**: 69-76.

Vlahopoulos, S. and Zoumpourlis, V. C. (2004). *"JNK: a key modulator of intracellular signaling."* Biochem **69**(8): 844-854.

Voet, D. and Voet, J. G. (2004). Lipids and membranes. *Biochemistry 3rd Edition*. New York, Wiley**:** 277-325.

Vonghia, L., Michielsen, P. and Francque, S. (2013). *"Immunological mechanisms in the pathophysiology of non-alcoholic steatohepatitis."* Int J Mol Sci **14**(10): 19867-19890.

Vreugdenhil, A. C., Snoek, A. M., van 't Veer, C., Greve, J. W. and Buurman, W. A. (2001). *"LPS-binding protein circulates in association with apoB-containing*

lipoproteins and enhances endotoxin-LDL/VLDL interaction." J Clin Invest **107**(2): 225-234.

Wagsater, D., Olofsson, P. S., Norgren, L., Stenberg, B. and Sirsjo, A. (2004). *"The chemokine and scavenger receptor CXCL16/SR-PSOX is expressed in human vascular smooth muscle cells and is induced by interferon gamma."* Biochem Biophys Res Commun **325**(4): 1187-1193.

Walenbergh, S. M. A., Koek, G. H., Bieghs, V. and Shiri-Sverdlov, R. (2013). *"Non-alcoholic steatohepatitis: The role of oxidized low-density lipoproteins."* J Hepatol **58**(4): 801-810.

Walker, J. M., Goodwin, G. H. and Johns, E. W. (1976). *"The similarity between the primary structures of two non-histone chromosomal proteins."* Eur J Biochem **62**(3): 461-469.

Walterfang, M., Chien, Y. H., Imrie, J., Rushton, D., Schubiger, D. and Patterson, M. C. (2012). *"Dysphagia as a risk factor for mortality in Niemann-Pick disease type C: systematic literature review and evidence from studies with miglustat."* Orphanet J Rare Dis **7**: 76.

Wang, F., Murrell, G. A. and Wang, M. X. (2007). *"Oxidative stress-induced c-Jun N-terminal kinase (JNK) activation in tendon cells upregulates MMP1 mRNA and protein expression."* J Orthop Res **25**(3): 378-389.

Wang, H., Yang, H. and Tracey, K. J. (2004). *"Extracellular role of HMGB1 in inflammation and sepsis."* J Intern Med **255**(3): 320-331.

Wang, J., Yin, Y., Hua, H., Li, M., Luo, T., Xu, L., Wang, R., Liu, D., Zhang, Y. and Jiang, Y. (2009). *"Blockade of GRP78 sensitizes breast cancer cells to microtubules-interfering agents that induce the unfolded protein response."* J Cell Mol Med **13**(9B): 3888-3897.

Wang, L., Zhang, J., Wang, B., Wang, G. and Xu, J. (2015). *"Blocking HMGB1 signal pathway protects early radiation-induced lung injury."* Int J Clin Exp Pathol **8**(5): 4815-4822.

Wang, M. E., Singh, B. K., Hsu, M. C., Huang, C., Yen, P. M., Wu, L. S., Jong, D. S. and Chiu, C. H. (2017). *"Increasing Dietary Medium-Chain Fatty Acid Ratio Mitigates High-fat Diet-Induced Non-Alcoholic Steatohepatitis by Regulating Autophagy."* Sci Rep **7**(1): 13999.

Wang, Q., Zhang, H., Zhao, B. and Fei, H. (2009). *"IL-1beta caused pancreatic beta-cells apoptosis is mediated in part by endoplasmic reticulum stress via the induction of endoplasmic reticulum Ca2+ release through the c-Jun N-terminal kinase pathway."* Mol Cell Biochem **324**(1-2): 183-190.

Wang, S. F., Yen, J. C., Yin, P. H., Chi, C. W. and Lee, H. C. (2008). *"Involvement of oxidative stress-activated JNK signaling in the methamphetamine-induced cell death of human SH-SY5Y cells."* Toxicology **246**(2-3): 234-241.

Wang, X., Sun, R., Wei, H. and Tian, Z. (2013). *"High-mobility group box 1 (HMGB1)-Toll-like receptor (TLR)4-interleukin (IL)-23-IL-17A axis in drug-induced damage-associated lethal hepatitis: Interaction of gammadelta T cells with macrophages."* Hepatol **57**(1): 373-384.

Watanabe, A. and Nagashima, H. (1983). *"Glutathione metabolism and glucose 6-phosphate dehydrogenase activity in experimental liver injury."* Acta Med Okayama **37**(6): 463-470.

Wei, J., Shi, M., Wu, W. Q., Xu, H., Wang, T., Wang, N., Ma, J. L. and Wang, Y. G. (2011). *"IkappaB kinase-beta inhibitor attenuates hepatic fibrosis in mice."* World J Gastroenterol **17**(47): 5203-5213.

Weidle, U. H., Scheuer, W., Eggle, D., Klostermann, S. and Stockinger, H. (2010). *"Cancer-related issues of CD147."* Cancer Genom Proteom **7**(3): 157-169.

Weltman, M. D., Farrell, G. C., Hall, P., Ingelman-Sundberg, M. and Liddle, C. (1998). *"Hepatic cytochrome P450 2E1 is increased in patients with nonalcoholic steatohepatitis."* Hepatol **27**(1): 128-133.

Wen, H., Ting, J. P. and O'Neill, L. A. (2012). *"A role for the NLRP3 inflammasome in metabolic diseases--did Warburg miss inflammation?"* Nat Immunol **13**(4): 352-357.

White, D. L., Kanwal, F. and El-Serag, H. B. (2012). *"Association between nonalcoholic fatty liver disease and risk for hepatocellular cancer, based on systematic review."* Clin Gastroenterol Hepatol **10**(12): 1342-1359.e1342.

Wigg, A. J., Roberts-Thomson, I. C., Dymock, R. B., McCarthy, P. J., Grose, R. H. and Cummins, A. G. (2001). *"The role of small intestinal bacterial overgrowth, intestinal permeability, endotoxaemia, and tumour necrosis factor alpha in the pathogenesis of non-alcoholic steatohepatitis."* Gut **48**(2): 206-211.

Will, O., Mahler, H. C., Arrigo, A. P. and Epe, B. (1999). *"Influence of glutathione levels and heat-shock on the steady-state levels of oxidative DNA base modifications in mammalian cells."* Carcinogenesis **20**(2): 333-337.

Willekens, F. L., Werre, J. M., Kruijt, J. K., Roerdinkholder-Stoelwinder, B., Groenen-Dopp, Y. A., van den Bos, A. G., Bosman, G. J. and van Berkel, T. J. (2005). *"Liver Kupffer cells rapidly remove red blood cell-derived vesicles from the circulation by scavenger receptors."* Blood **105**(5): 2141-2145.

Williams, C. D., Stengel, J., Asike, M. I., Torres, D. M., Shaw, J., Contreras, M., Landt, C. L. and Harrison, S. A. (2011). *"Prevalence of nonalcoholic fatty liver disease and nonalcoholic steatohepatitis among a largely middle-aged population utilizing ultrasound and liver biopsy: a prospective study."* Gastroenterology **140**(1): 124-131.

Willingham, S. B., Bergstralh, D. T., O'Connor, W., Morrison, A. C., Taxman, D. J., Duncan, J. A., Barnoy, S., Venkatesan, M. M., Flavell, R. A., Deshmukh, M., Hoffman, H. M. and Ting, J. P. (2007). *"Microbial pathogen-induced necrotic cell death mediated by the inflammasome components CIAS1/cryopyrin/NLRP3 and ASC."* Cell Host Microbe **2**(3): 147-159.

Windler, E., Greeve, J., Levkau, B., Kolb-Bachofen, V., Daerr, W. and Greten, H. (1991). *"The human asialoglycoprotein receptor is a possible binding site for low-density lipoproteins and chylomicron remnants."* Biochem J **276 (Pt 1)**: 79-87.

Winn, N. C., Liu, Y., Rector, R. S., Parks, E. J., Ibdah, J. A. and Kanaley, J. A. (2018). *"Energy-matched moderate and high intensity exercise training improves nonalcoholic fatty liver disease risk independent of changes in body mass or abdominal adiposity - A randomized trial."* Metabolism **78**: 128-140.

Wolfs, M. G. M., Gruben, N., Rensen, S. S., Verdam, F. J., Greve, J. W., Driessen, A., Wijmenga, C., Buurman, W. A., Franke, L., Scheja, L., Koonen, D. P. Y., Shiri-Sverdlov, R., van Haeften, T. W., Hofker, M. H. and Fu, J. (2015). *"Determining the association between adipokine expression in multiple tissues and phenotypic features of non-alcoholic fatty liver disease in obesity."* Nutr Diabetes **5**: e146.

Wong, R. J., Cheung, R. and Ahmed, A. (2014). *"Nonalcoholic steatohepatitis is the most rapidly growing indication for liver transplantation in patients with hepatocellular carcinoma in the U.S."* Hepatol **59**(6): 2188-2195.

Wong, V. W.-S., Chitturi, S., Wong, G. L.-H., Yu, J., Chan, H. L.-Y. and Farrell, G. C. *"Pathogenesis and novel treatment options for non-alcoholic steatohepatitis."* The Lancet **1**(1): 56-67.

World Gastroenterology Organisation Global Guidelines (2012). Nonalcoholic fatty liver disease and nonalcoholic steatohepatitis. *Global Guidelines*. Milwaukee, WI, World Gastroenterology Organisation.

World Health Organization (2015). "*Global obesity 2014*." Global burden of disease: 2014 update. Retrieved 2nd December 2015, 2015, from http://www.who.int/gho/ncd/risk_factors/overweight/en/.

Wree, A., McGeough, M. D., Pena, C. A., Schlattjan, M., Li, H., Inzaugarat, M. E., Messer, K., Canbay, A., Hoffman, H. M. and Feldstein, A. E. (2014). *"NLRP3 inflammasome activation is required for fibrosis development in NAFLD."* J Mol Med (Berl) **92**(10): 1069-1082.

Wu, S., Loke, H. N. and Rehemtulla, A. (2002). *"Ultraviolet Radiation-Induced Apoptosis is Mediated by Daxx."* Neoplasia (New York, NY) **4**(6): 486-492.

Xiang, Z., Chen, Y.-p., Ma, K.-f., Ye, Y.-f., Zheng, L., Yang, Y.-d., Li, Y.-m. and Jin, X. (2013). *"The role of Ursodeoxycholic acid in non-alcoholic steatohepatitis: a systematic review."* BMC Gastroenterol **13**(1): 140.

Xiao, X. and Song, B.-L. (2013). *"SREBP: a novel therapeutic target."* Acta Biochim Biophys Sin **45**(1): 2-10.

Xie, C., Zhou, Z.-S., Li , N., Bian, Y., Wang, Y.-J., Wang, L.-J., Li, B.-L. and Song, B.-L. (2012). *"Ezetimibe blocks the internalization of NPC1L1 and cholesterol in mouse small intestine."* J Lipid Res **53**(10): 2092-2101.

Xu, S., Benoff, B., Liou, H. L., Lobel, P. and Stock, A. M. (2007). *"Structural basis of sterol binding by NPC2, a lysosomal protein deficient in Niemann-Pick type C2 disease."* J Biol Chem **282**(32): 23525-23531.

Xu, Z., Chen, L., Leung, L., Yen, T. S., Lee, C. and Chan, J. Y. (2005). *"Liver-specific inactivation of the Nrf1 gene in adult mouse leads to nonalcoholic steatohepatitis and hepatic neoplasia."* Proc Natl Acad Sci U S A **102**(11): 4120-4125.

Xu, Z. J., Fan, J. G., Ding, X. D., Qiao, L. and Wang, G. L. (2010). *"Characterization of high-fat, diet-induced, non-alcoholic steatohepatitis with fibrosis in rats."* Dig Dis Sci **55**(4): 931-940.

Yamamoto, K., Hamada, H., Shinkai, H., Kohno, Y., Koseki, H. and Aoe, T. (2003). *"The KDEL receptor modulates the endoplasmic reticulum stress response through mitogen-activated protein kinase signaling cascades."* J Biol Chem **278**(36): 34525-34532.

Yamanaka, S., Katayama, E., Yoshioka, K., Nagaki, S., Yoshida, M. and Teraoka, H. (2002). *"Nucleosome linker proteins HMGB1 and histone H1 differentially enhance DNA ligation reactions."* Biochem Biophys Res Commun **292**(1): 268-273.

Yamaoka, S., Courtois, G., Bessia, C., Whiteside, S. T., Weil, R., Agou, F., Kirk, H. E., Kay, R. J. and Israel, A. (1998). *"Complementation cloning of NEMO, a component of the IkappaB kinase complex essential for NF-kappaB activation."* Cell **93**(7): 1231-1240.

Yan, D., Mayranpaa, M. I., Wong, J., Perttila, J., Lehto, M., Jauhiainen, M., Kovanen, P. T., Ehnholm, C., Brown, A. J. and Olkkonen, V. M. (2008). *"OSBP-related protein 8 (ORP8) suppresses ABCA1 expression and cholesterol efflux from macrophages."* J Biol Chem **283**(1): 332-340.

Yang, J., Bo, X. C., Ding, X. R., Dai, J. M., Zhang, M. L., Wang, X. H. and Wang, S. Q. (2006). *"Antisense oligonucleotides targeted against asialoglycoprotein receptor 1 block human hepatitis B virus replication."* J Viral Hepat **13**(3): 158-165.

Yang, L. and Seki, E. (2012). *"Toll-like receptors in liver fibrosis: cellular crosstalk and mechanisms."* Front Physiol **3**: 138.

Yang, R., Harada, T., Mollen, K. P., Prince, J. M., Levy, R. M., Englert, J. A., Gallowitsch-Puerta, M., Yang, L., Yang, H., Tracey, K. J., Harbrecht, B. G., Billiar, T. R. and Fink, M. P. (2006). *"Anti-HMGB1 neutralizing antibody ameliorates gut barrier dysfunction and improves survival after hemorrhagic shock."* Mol Med **12**(4-6): 105-114.

Ye, D., Li, F. Y., Lam, K. S., Li, H., Jia, W., Wang, Y., Man, K., Lo, C. M., Li, X. and Xu, A. (2012). *"Toll-like receptor-4 mediates obesity-induced non-alcoholic steatohepatitis through activation of X-box binding protein-1 in mice."* Gut **61**(7): 1058-1067.

Yoshida, H., Quehenberger, O., Kondratenko, N., Green, S. and Steinberg, D. (1998). *"Minimally oxidized low-density lipoprotein increases expression of scavenger receptor A, CD36, and macrosialin in resident mouse peritoneal macrophages."* Arterioscler Thromb Vasc Biol **18**(5): 794-802.

Yu, J., Shen, J., Sun, T. T., Zhang, X. and Wong, N. (2013). *"Obesity, insulin resistance, NASH and hepatocellular carcinoma."* Semin Cancer Biol **23**(6 Pt B): 483-491.

Yu, L., Simonson, O. E., Mohamed, A. J. and Smith, C. I. (2009). *"NF-kappaB regulates the transcription of protein tyrosine kinase Tec."* FEBS J **276**(22): 6714-6724.

Yu, M., Wang, H., Ding, A., Golenbock, D. T., Latz, E., Czura, C. J., Fenton, M. J., Tracey, K. J. and Yang, H. (2006). *"HMGB1 signals through toll-like receptor (TLR) 4 and TLR2."* Shock **26**(2): 174-179.

Yu, X. H., Jiang, N., Yao, P. B., Zheng, X. L., Cayabyab, F. S. and Tang, C. K. (2014). *"NPC1, intracellular cholesterol trafficking and atherosclerosis."* Clin Chim Acta **429**: 69-75.

Yu, Y. M. and Lin, H. C. (2010). *"Curcumin prevents human aortic smooth muscle cells migration by inhibiting of MMP-9 expression."* Nutr Metab Cardiovasc Dis **20**(2): 125-132.

Yuana, Y., Bertina, R. M. and Osanto, S. (2011). *"Pre-analytical and analytical issues in the analysis of blood microparticles."* Thromb Haemost **105**(3): 396-408.

Zarubica, A., Trompier, D. and Chimini, G. (2007). *"ABCA1, from pathology to membrane function."* Pfluegers Arch/Eur J Physiol **453**: 569-579.

Zeng, W., Shan, W., Gao, L., Gao, D., Hu, Y., Wang, G., Zhang, N., Li, Z., Tian, X., Xu, W., Peng, J., Ma, X. and Yao, J. (2015). *"Inhibition of HMGB1 release via salvianolic acid B-mediated SIRT1 up-regulation protects rats against non-alcoholic fatty liver disease."* Sci Rep **5**: 16013.

Zhan, Y. T. and An, W. (2010). *"Roles of liver innate immune cells in nonalcoholic fatty liver disease."* World J Gastroenterol **16**(37): 4652-4660.

Zhang, B., Zhang, Y., Bowerman, N. A., Schietinger, A., Fu, Y. X., Kranz, D. M., Rowley, D. A. and Schreiber, H. (2008). *"Equilibrium between host and cancer caused by effector T cells killing tumor stroma."* Cancer Res **68**(5): 1563-1571.

Zhang, J., Zhao, Y., Xu, C., Hong, Y., Lu, H., Wu, J. and Chen, Y. (2014). *"Association between serum free fatty acid levels and nonalcoholic fatty liver disease: a cross-sectional study."* Sci Rep **4**: 5832.

Zhang, J. R., Coleman, T., Langmade, S. J., Scherrer, D. E., Lane, L., Lanier, M. H., Feng, C., Sands, M. S., Schaffer, J. E., Semenkovich, C. F. and Ory, D. S. (2008). *"Niemann-Pick C1 protects against atherosclerosis in mice via*

regulation of macrophage intracellular cholesterol trafficking." J Clin Invest **118**(6): 2281-2290.

Zhang, M., Liu, P., Dwyer, N. K., Christenson, L. K., Fujimoto, T., Martinez, F., Comly, M., Hanover, J. A., Blanchette-Mackie, E. J. and Strauss, J. F. (2002). *"MLN64 Mediates Mobilization of Lysosomal Cholesterol to Steroidogenic Mitochondria."* J Biol Chem **277**(36): 33300-33310.

Zhang, M., Sun, M., Dwyer, N. K., Comly, M. E., Patel, S. C., Sundaram, R., Hanover, J. A. and Blanchette-Mackie, E. J. (2003). *"Differential trafficking of the Niemann-Pick C1 and 2 proteins highlights distinct roles in late endocytic lipid trafficking."* Acta Paediatr Suppl **92**(443): 63-73; discussion 45.

Zhang, X.-Q., Xu, C.-F., Yu, C.-H., Chen, W.-X. and Li, Y.-M. (2014). *"Role of endoplasmic reticulum stress in the pathogenesis of nonalcoholic fatty liver disease."* World J Gastroenterol **20**(7): 1768-1776.

Zhang, X., Wheeler, D., Tang, Y., Guo, L., Shapiro, R. A., Ribar, T. J., Means, A. R., Billiar, T. R., Angus, D. C. and Rosengart, M. R. (2008). *"Calcium/calmodulin-dependent protein kinase (CaMK) IV mediates nucleocytoplasmic shuttling and release of HMGB1 during lipopolysaccharide stimulation of macrophages."* J Immunol **181**(7): 5015-5023.

Zhang, Y., Dong, L., Yang, X., Shi, H. and Zhang, L. (2011). *"alpha-Linolenic acid prevents endoplasmic reticulum stress-mediated apoptosis of stearic acid lipotoxicity on primary rat hepatocytes."* Lipids Health Dis **10**: 81.

Zhang, Y. and Edwards, P. A. (2008). *"FXR signaling in metabolic disease."* FEBS Lett **582**(1): 10-18.

Zhang, Y., Karki, R. and Igwe, O. J. (2015). *"Toll-like receptor 4 signaling: A common pathway for interactions between prooxidants and extracellular disulfide high mobility group box 1 (HMGB1) protein-coupled activation."* Biochem Pharmacol **98**(1): 132-143.

Zhang, Y., Yang, X., Shi, H., Dong, L. and Bai, J. (2011). *"Effect of α-linolenic acid on endoplasmic reticulum stress-mediated apoptosis of palmitic acid lipotoxicity in primary rat hepatocytes."* Lipids Health Dis **10**: 122-122.

Zheng, S., Hoos, L., Cook, J., Tetzloff, G., Davis, H., Jr., van Heek, M. and Hwa, J. J. (2008). *"Ezetimibe improves high fat and cholesterol diet-induced non-alcoholic fatty liver disease in mice."* Eur J Pharmacol **584**(1): 118-124.

Zheng, Z., Xu, X., Zhang, X., Wang, A., Zhang, C., Huttemann, M., Grossman, L. I., Chen, L. C., Rajagopalan, S., Sun, Q. and Zhang, K. (2013). *"Exposure to ambient particulate matter induces a NASH-like phenotype and impairs hepatic glucose metabolism in an animal model."* J Hepatol **58**(1): 148-154.

Zhou, R., Yazdi, A. S., Menu, P. and Tschopp, J. (2011). *"A role for mitochondria in NLRP3 inflammasome activation."* Nature **469**(7329): 221-225.

Zhou, T., Li, S., Zhong, W., Vihervaara, T., Béaslas, O., Perttilä, J., Luo, W., Jiang, Y., Lehto, M., Olkkonen, V. M. and Yan, D. (2011). *"OSBP-Related Protein 8 (ORP8) Regulates Plasma and Liver Tissue Lipid Levels and Interacts with the Nucleoporin Nup62."* PLoS ONE **6**(6): e21078.

Zhu, L., Baker, R. D. and Baker, S. S. (2015). *"Gut microbiome and nonalcoholic fatty liver diseases."* Pediatr Res **77**(1-2): 245-251.

Zou, H., Henzel, W. J., Liu, X., Lutschg, A. and Wang, X. (1997). *"Apaf-1, a human protein homologous to C. elegans CED-4, participates in cytochrome c-dependent activation of caspase-3."* Cell **90**(3): 405-413.